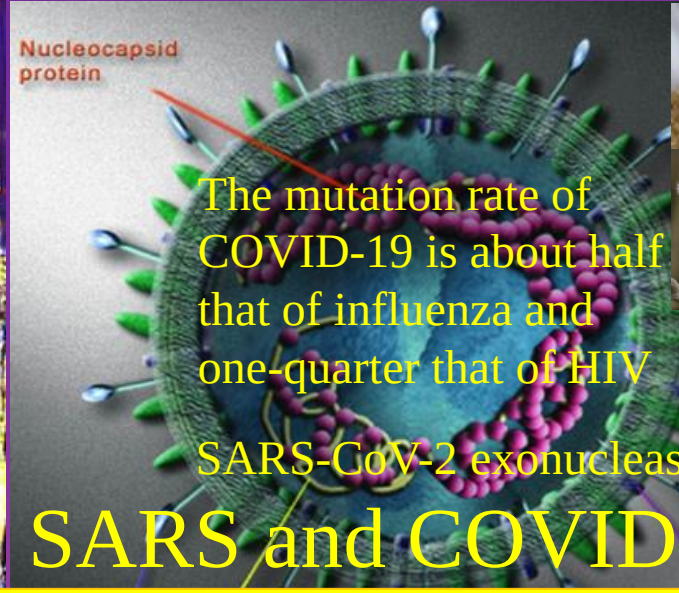

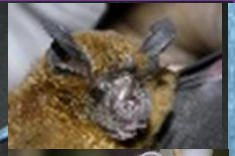

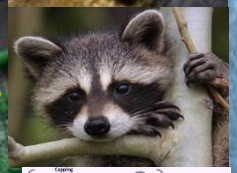

The mutation rate of COVID-19 is about half that of influenza and one-quarter that of HIV

SARS-CoV-2 exonuclease NSP14

SARS and COVID-19

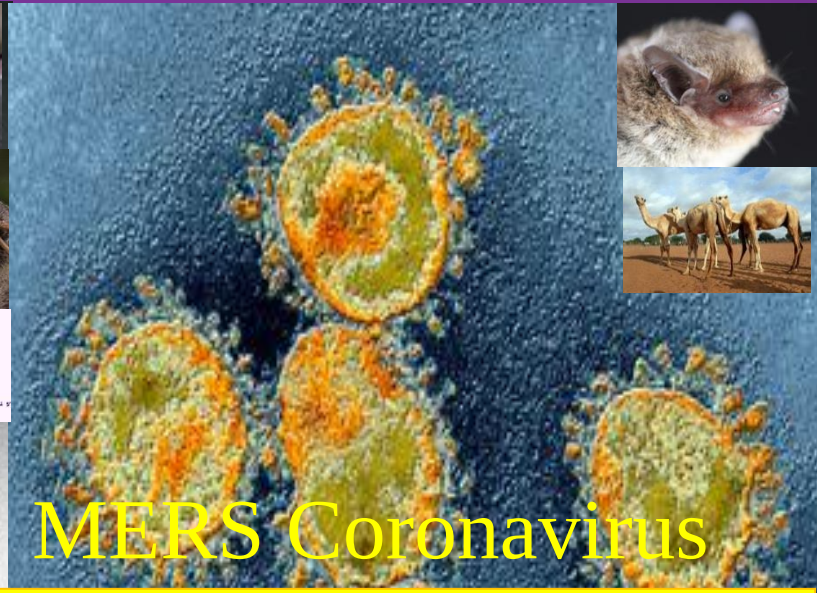

MERS Coronavirus

核糖核酸病毒如如不動的平等佛性

Therapeutic strategies against the non-mutable part of encapsulated RNA viruses

Avian Influenza Viruses

伊利沙伯醫院

Ebola Virus

黎鏡堯醫生

Dr. Lai Kang Yiu, Consultant Intensive Care Unit, Queen Elizabeth Hospital

Uprising RNA Virus Epidemic and Pandemic

MHV and SARS-CoV nsp14-ExoN mutants accumulated up to 20-fold more mutations than their wild-type counterparts.

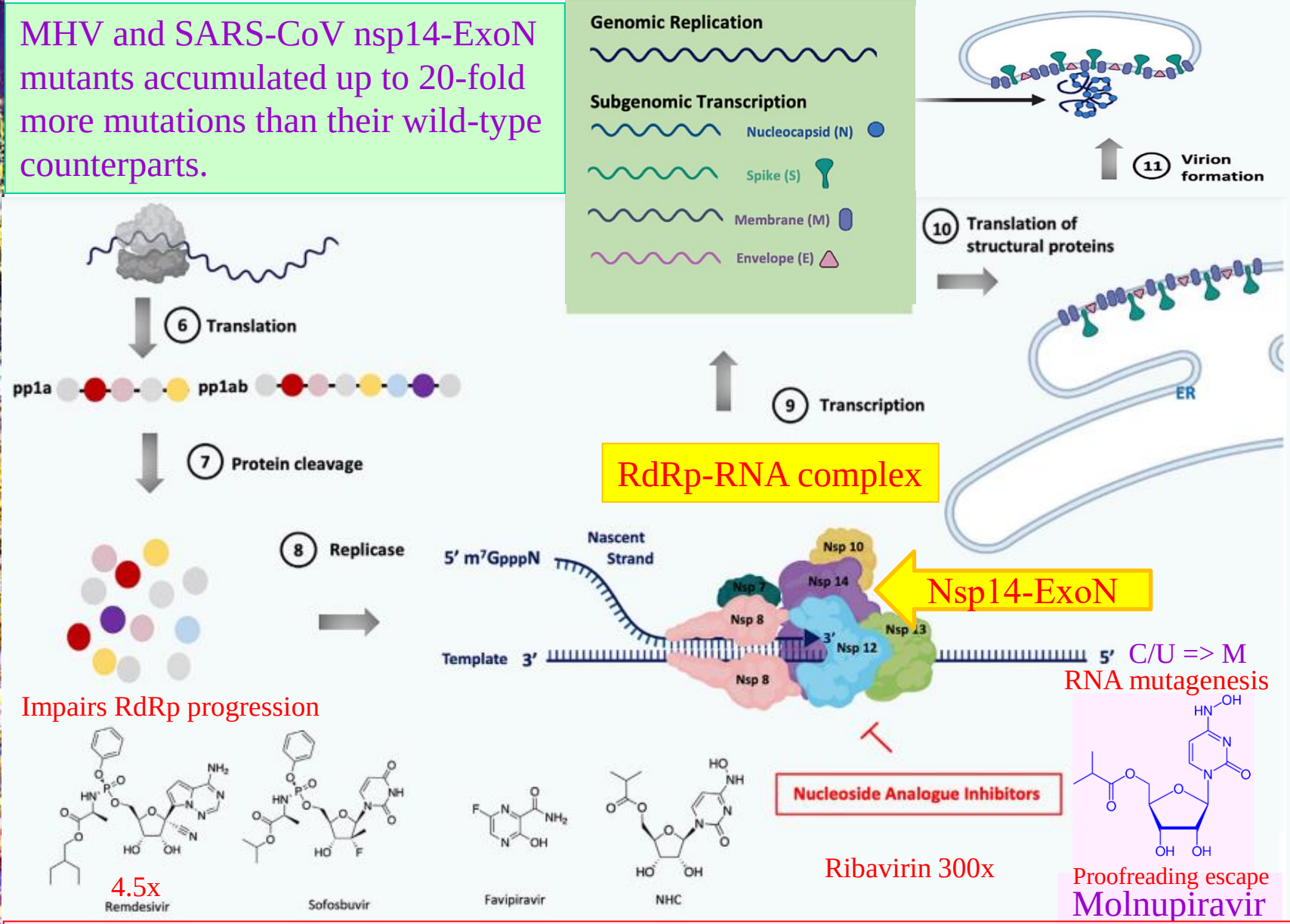

Like remdesivir, **molnupiravir escapes viral RNA proofreading** because M incorporation and M-directed misincorporation are apparently not recognized by the viral exonuclease Kabinger, F. et al. *Nat Struct Mol Biol* **28,** 740–746 (2021).

Robson F, et al. **Coronavirus RNA Proofreading: Molecular Basis and Therapeutic Targeting** Mol Cell. 2020 Sep 3;79(5):710-727.
Tahir M. Coronavirus genomic nsp14-ExoN, structure, role, mechanism, and potential application as a drug target. *J Med Virol.* 2021;93(7):4258-4264.

Therapeutic strategies against the non-mutable target of encapsulated RNA viruses

- 佛祖初成正覺:[奇哉!奇哉!一切眾生皆具如來智慧德相，但以妄想執著，不能得證。]
- 最初在華嚴會上為天人說法，講他自證完滿的境界。其後經歷四十九年為眾生說法，於法華涅槃會上大收與裙拾證他完滿，令眾生也能成佛，因眾生皆有佛性。
- 因此核糖核酸病毒當有佛性而佛性不二。 所以從了知核糖核酸病毒共通不二的佛性便可應對萬變的病毒。
- 中醫亦用近似理念殊途同歸治理了中國人2000多年。

核糖核酸病毒如如不動的平等佛性

WHO declared COVID-19 a pandemic

March 11, 2020 / as of 8:13 AM EST

1,016
U.S. cases

31
U.S. deaths

121,061
Worldwide cases

4,368
Worldwide deaths

No PCR kit before March 11

April 15 2021

(3 + 11) quarantine for airline crews

Hong Kong Vaccine Pass Starting from 24 February 2022 (311 days till end of year)

11 March 2021

Kumbh Mela Festival

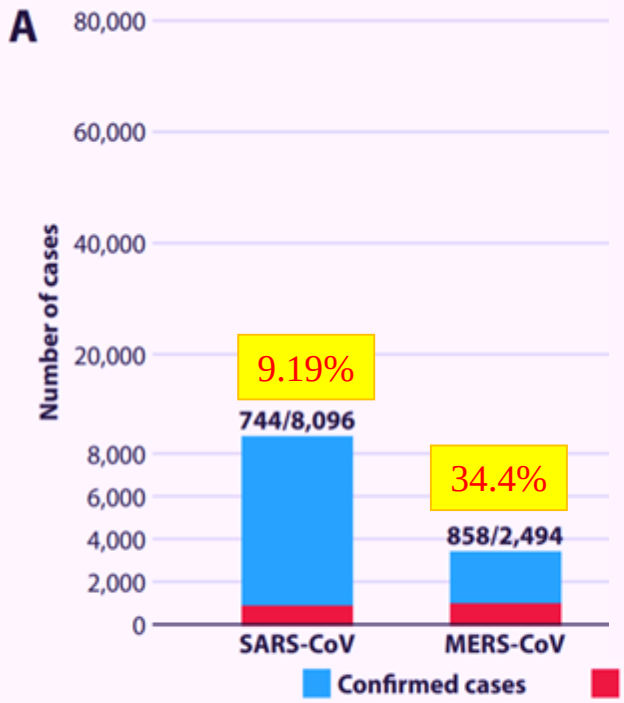

Cases	Deaths	
423M +1.54M	5.88M +8,348	1.39%

Location		Cases ↓	Deaths
United States	1.19%	78.4M +46,210	934K +692
India	1.19%	42.8M	512K
Brazil	2.28%	28.2M	644K
France	0.62%	21.6M	134K
United Kingdom	0.87%	18.6M	161K
Russia	2.25%	15M	338K

China (Mainland)

Cases		Deaths
108K	4.3%	4,654

HLA-B*46:01

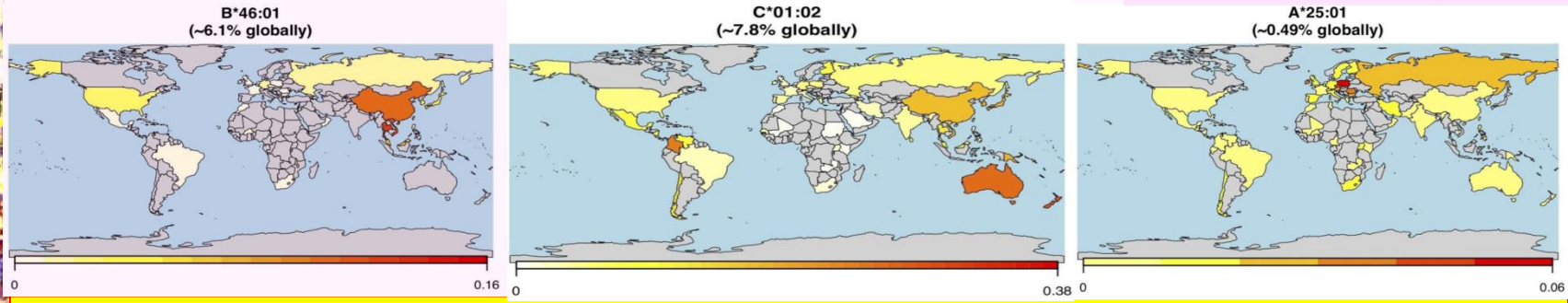

HLA-B*46:01 had the fewest predicted binding peptides for SARS-CoV-2, suggesting that individuals with this allele may be particularly vulnerable to COVID-19, and associated with severe disease (~ SARS).

Prompetchara E, Ketloy C, Palaga T. Immune responses in COVID-19 and potential vaccines: Lessons learned from SARS and MERS epidemic.
Nguyen A, David JK, Maden SK, et al. Human Leukocyte Antigen Susceptibility Map for Severe Acute Respiratory Syndrome Coronavirus 2. *J Virol*. 2020;94(13):e00510-20. Published 2020 Jun 16. doi:10.1128/JVI.00510-20

Covid-19, estimated vaccine effectiveness for ages 80+, %

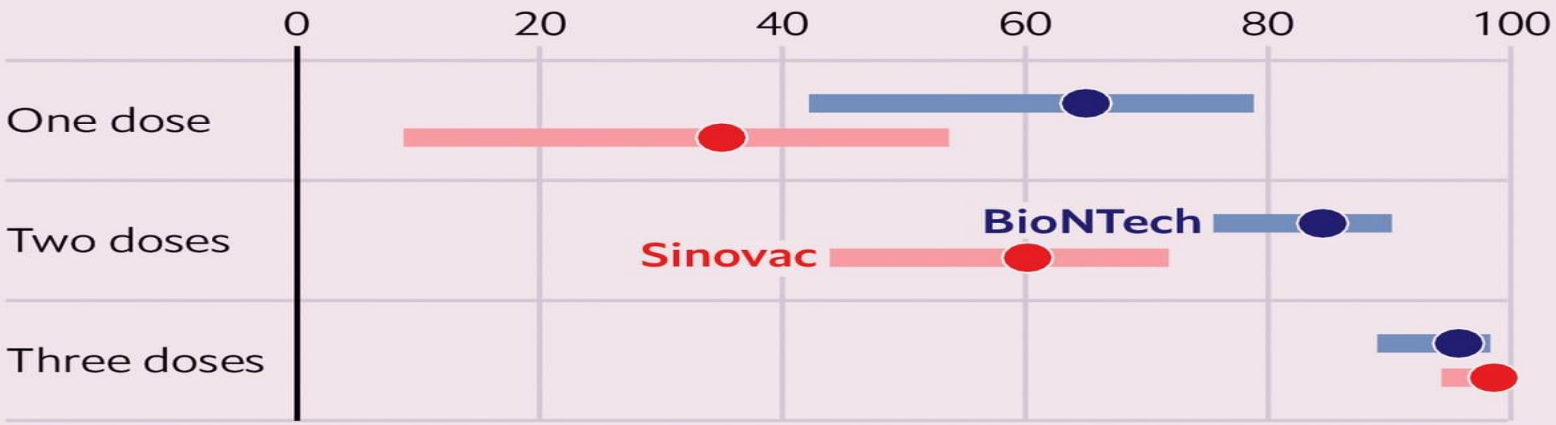

China, covid-19 vaccination status, 2022, %

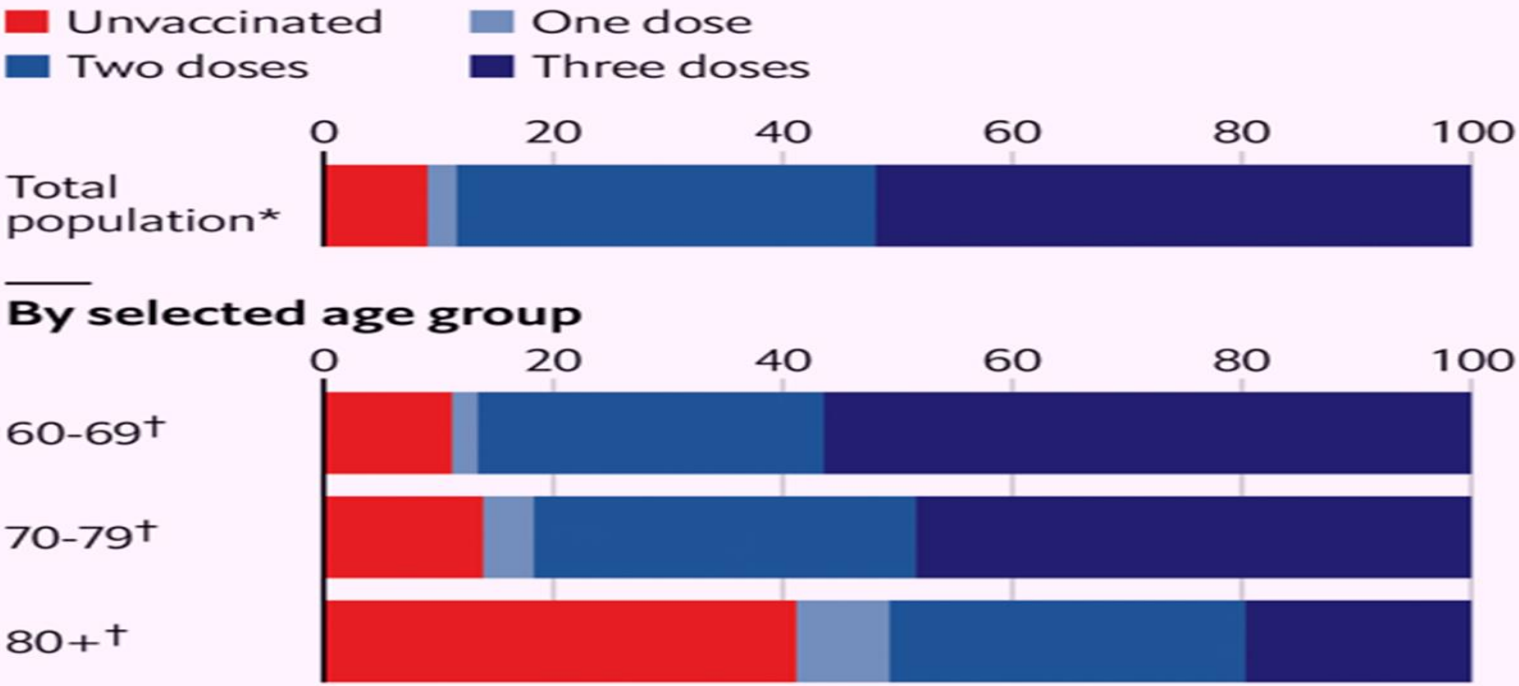

*To April 18th †To March 17th

Sources: National Health Commission of China; *The Economist*

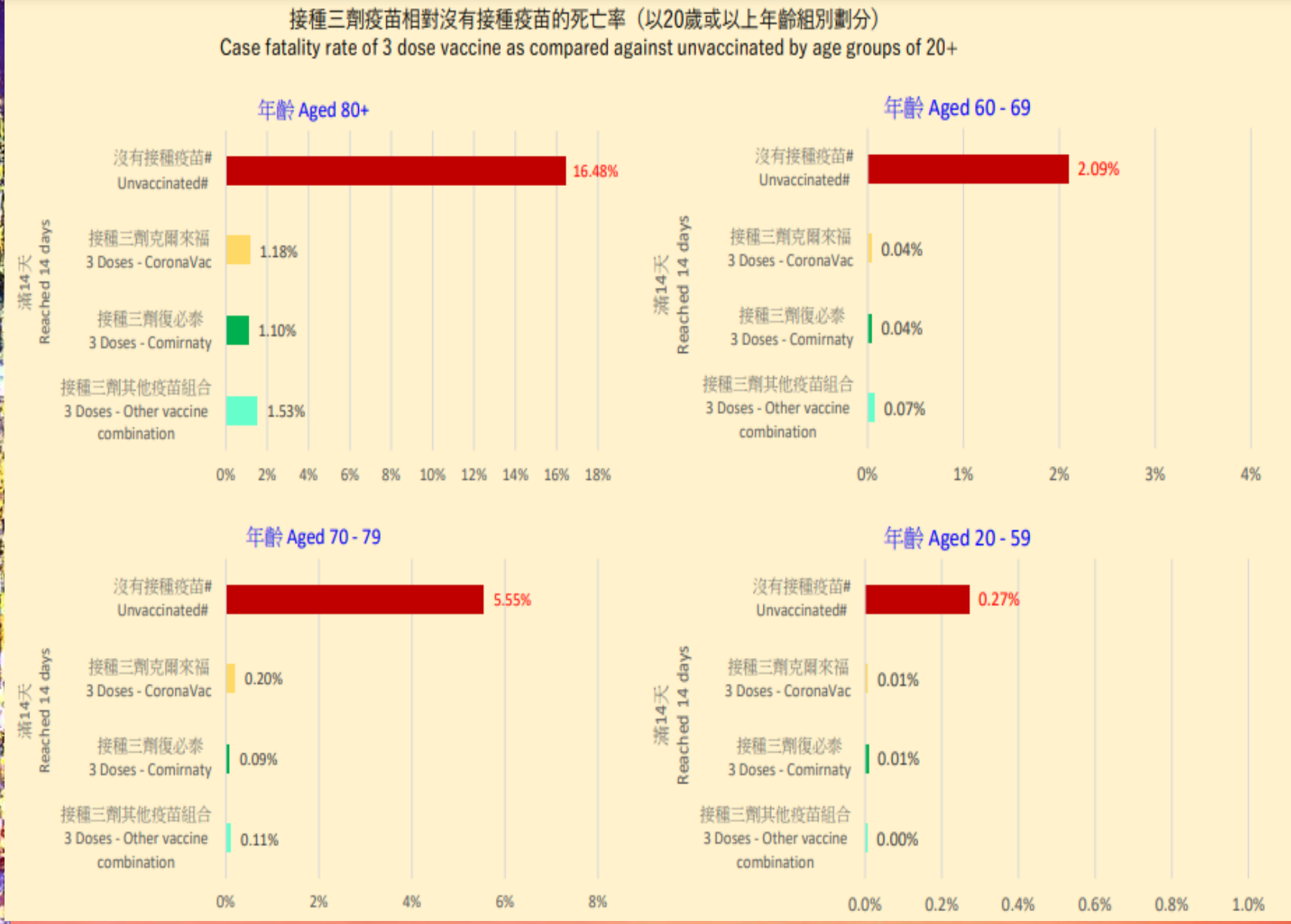

Hong Kong COVID Vaccination Status and Mortality

長者及兒童的疫苗接種率偏低 •

The vaccination rate among elderly and children is relatively low.

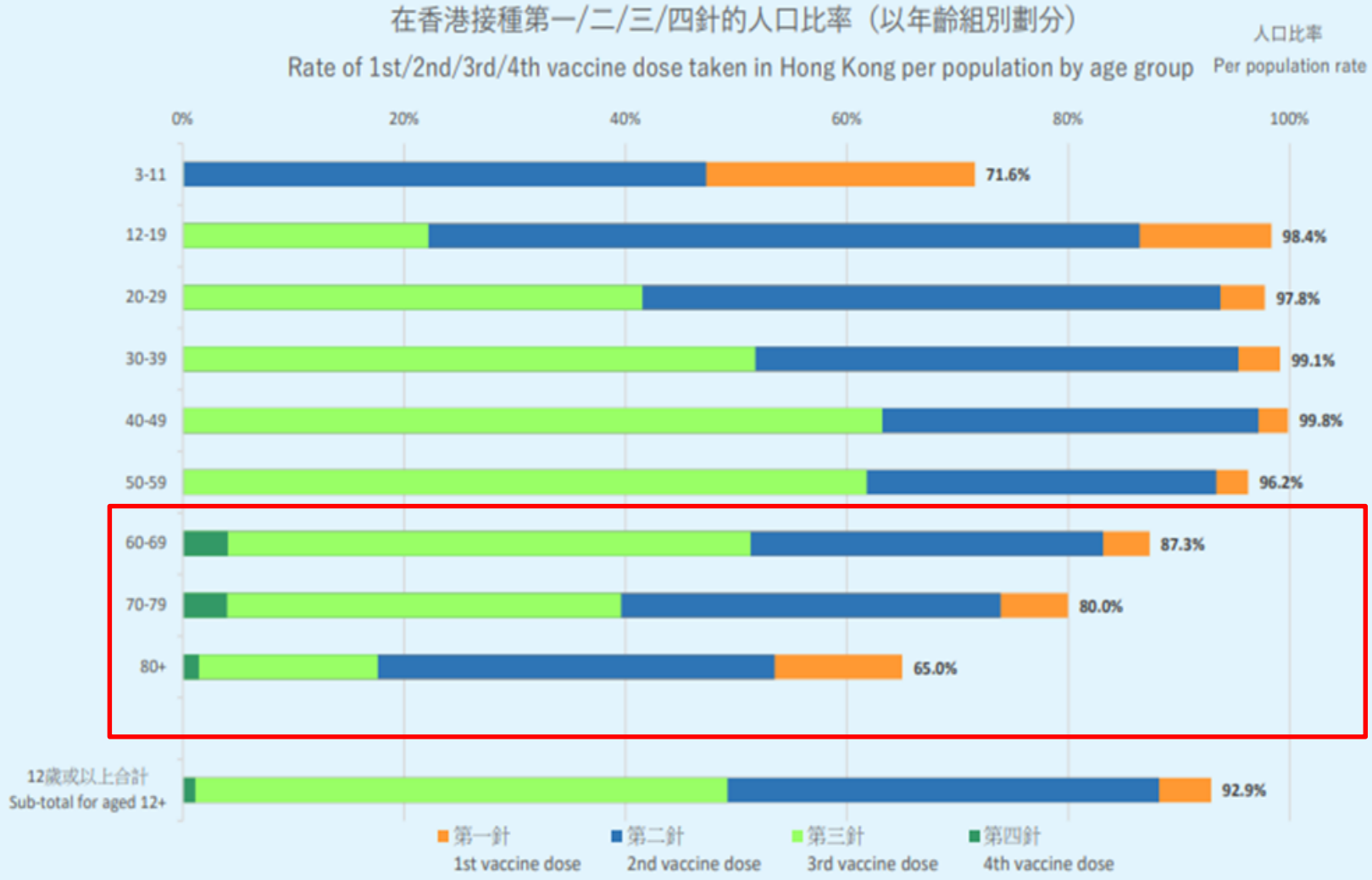

Unless these elderly population in Hong Kong has completed three doses of vaccination, zero-COVID policy is necessary to prevent our healthcare system being overwhelmed by COVID admission.

Any Questions ?

The HA announced on 9th March that QEH will be converted to COVID-19 hospital on 13th March 2022.

20th Apr 2022

Meeting with Guang Dong Health Official
(内地医疗救治专家组专会)
22nd February 2022
28th April 2022

宿主硫酸乙酰肝素蛋白聚糖与腺病毒载体 COVID-19 疫苗和 SARS-CoV-2 在脑静脉窦血栓形成发病机制中的相互作用

COVID-19感染的细胞因子失调及其管理

中西方醫藥醫治新冠肺炎相輔相成的基理

伊利沙伯醫院 黎鏡堯醫生

We are only chasing the ever-changing shadow of the moon !

Zoonotic origins

α

COVID

β

γ

SARS

δ

RNA viruses

o

MERS

H5N1
H7N9

1918PV
2009PV

229E
OC43
HL63
HKU1

Ebola

HIV

H2N2
H3N2

Poliovirus

HCV

Parainfluenza virus

Dengue

Mumps

Measles

Paramyxoviridae

Rinderpest virus

月有陰晴圓缺

如觀諸法生滅，悟世間無常。

In the past, we are chasing after the mutable viral determinant of influenza virus

HA NA

變幻原是永恆

Mutation and Reassortment
Antigenic drift and shift
Epidemic and Pandemic
Vaccination

Being an RNA virus, the RNA polymerase of influenza has no proofreading mechanism. ~1 error per replicated genome ➔ each cell can produce 10,000 new viral mutants to infect neighbouring cells. (300x than DNA virus)

XD, XE and XF – newly designated recombinant lineages

Variant XE is a mutant hybrid of the BA.1 and the more infectious BA.2 subvariant, also known as “stealth omicron.” According to Phylogenetic Assignment of Named Global Outbreak Lineages (Pangolin), there are two recombinants of Delta and BA.1, which are XD and XF, and there are six recombinants of BA.1 and BA.2, which are XE, XG, XH, XJ, XK and XL.


從月影的天魔萬相
窺破月影背後湛然不動的佛性
Unless we can understand the moon in a different perspective…

The eternal world behind the shadow of the moon was formed 4.4-4.6 billions years ago

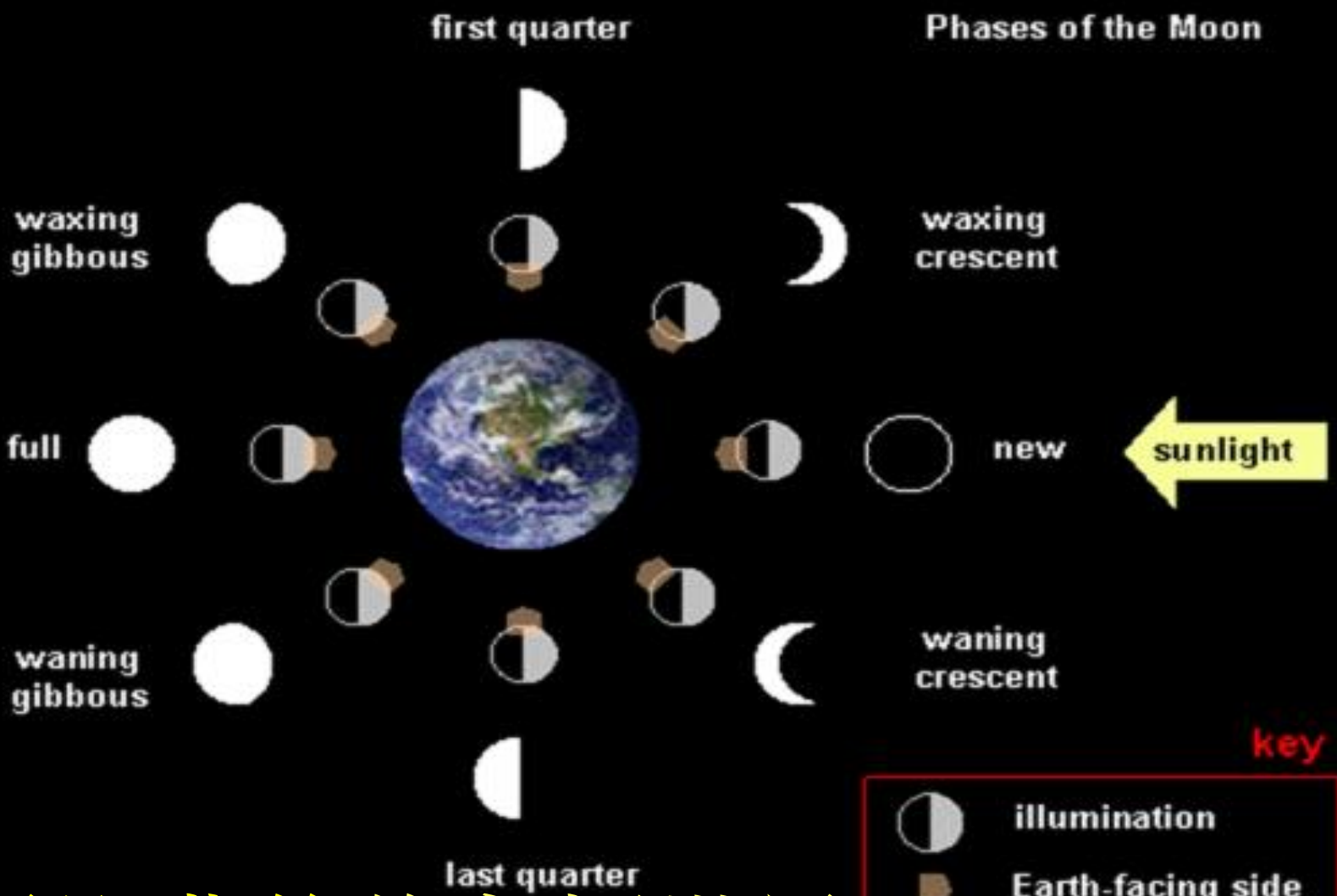

月影背後的永恆世界

無如是差別境界是名為不思議佛境界。
平等正覺諸佛境界當於眾生煩惱中求。
凡夫起貪瞋癡處便是如來所住平等法。
貪：Ebolavirus
瞋：Avian Influenza
癡：COVID-19, SARS-CoV-1, MERS-CoV

Current vaccination program, monoclonal antibodies and anti-viral medications are directed against the mutable part of the RNA viruses which is prone to rapid evolution within the host cells. **All viruses are obligatory parasite** that largely relies on host cell factors and physiological processes for its entry, replication, and egress. **Therapeutic agents directed against non-mutable targets of the host is independent of viral mutation.** They have a complementary role to those therapeutic agents under development that are directed against the mutable targets of the viruses.

文殊師利所說不思議佛境界經

Any Questions ?

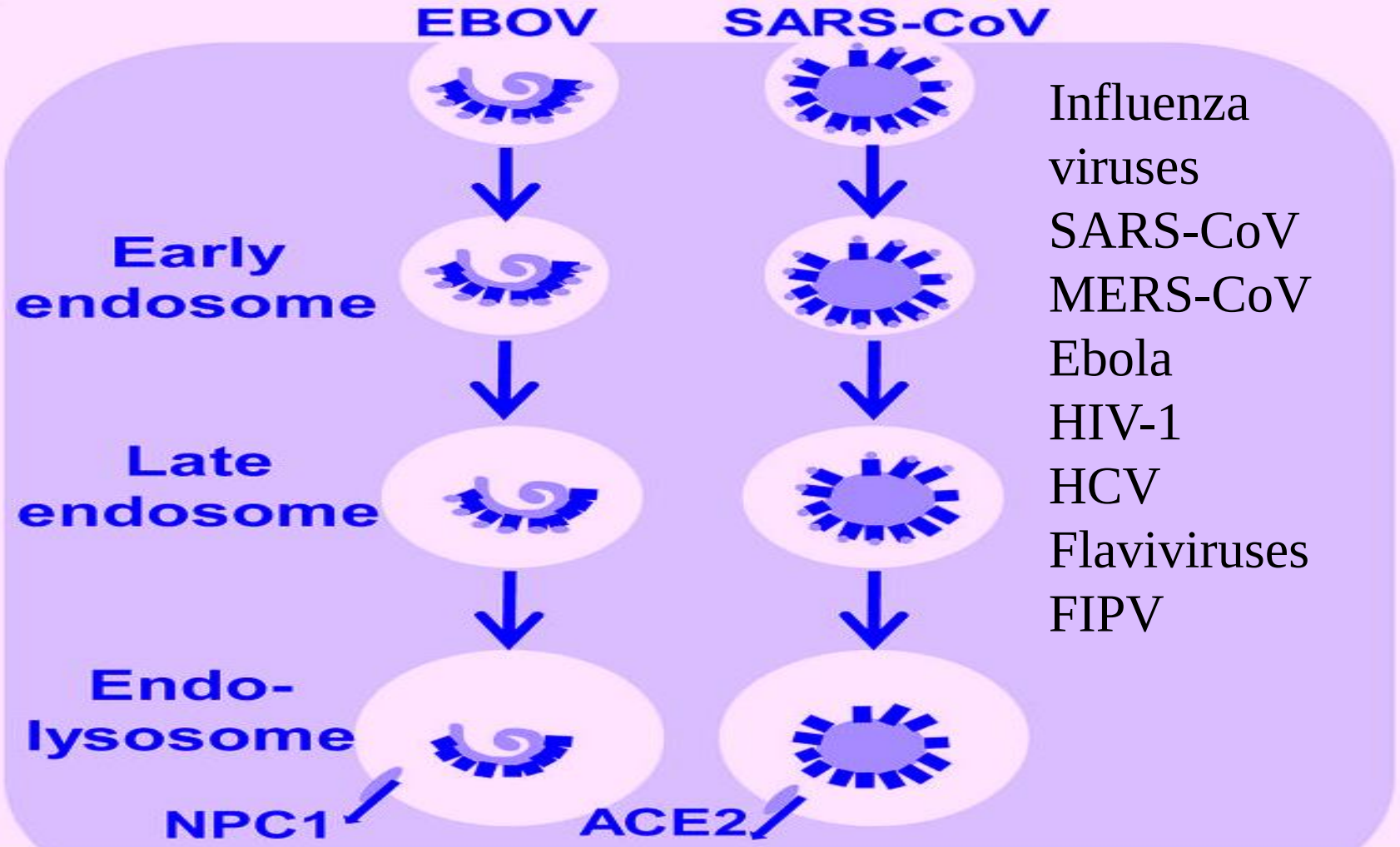

After the completion of the loading dose regimens for most Gram-positive bacterial infections, the serum concentrations of teicoplanin are at least 15 mg/liter (8.78 μm), which is ~27, 14, and 2 times higher than the IC50 values of teicoplanin against the entry of Ebola viruses, MERS-CoV/HIV-1, and SARS-CoV/HIV-1 pseudotyped viruses.

Zhou N, Pan T, Zhang J, et al. Glycopeptide Antibiotics Potently Inhibit Cathepsin L in the Late Endosome/Lysosome and Block the Entry of Ebola Virus, Middle East Respiratory Syndrome Coronavirus (MERS-CoV), and Severe Acute Respiratory Syndrome Coronavirus (SARS-CoV). *J Biol Chem*. 2016;291(17):9218-32.

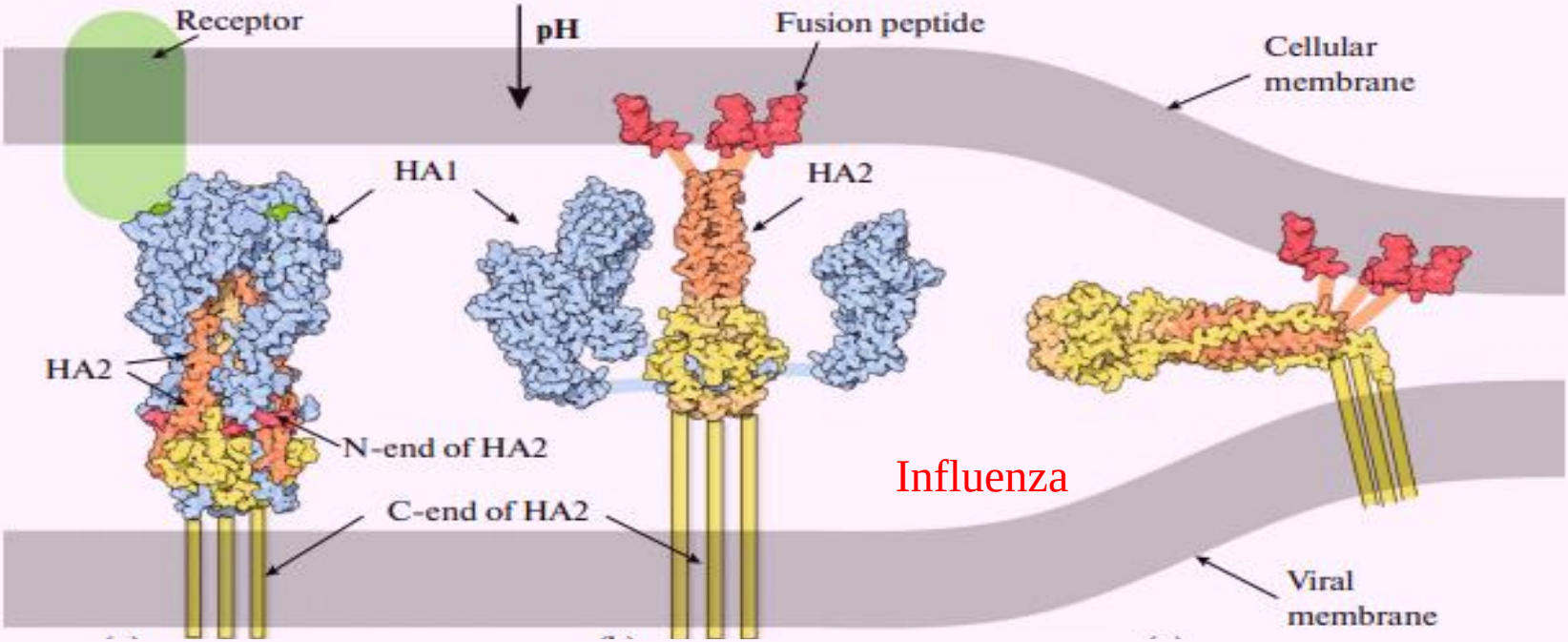

pH dependent conformational change and proteolysis in endosome induced by Cathepsin L/B for encapsulated RNA viruses

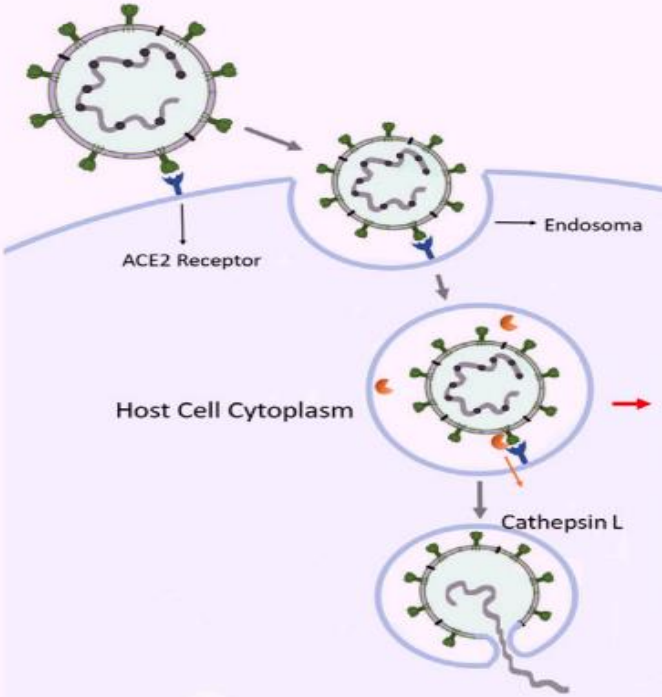

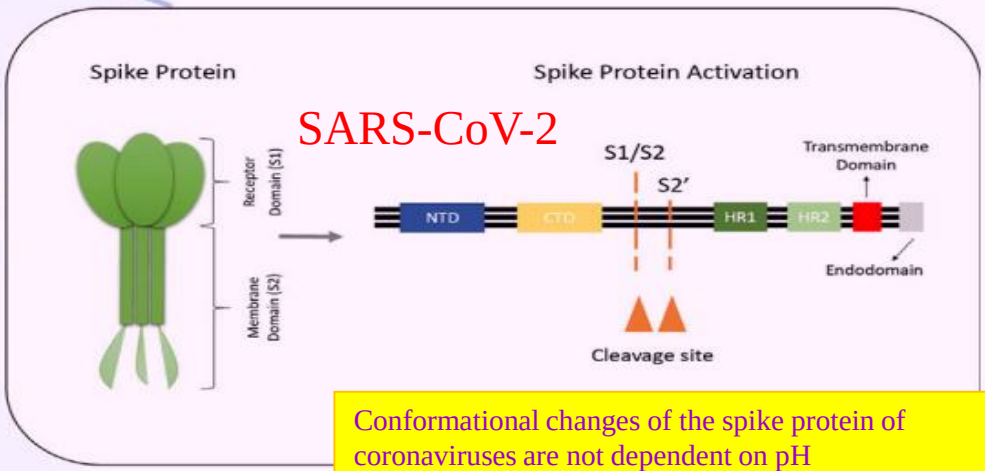

Conformational changes of the spike protein of coronaviruses are not dependent on pH

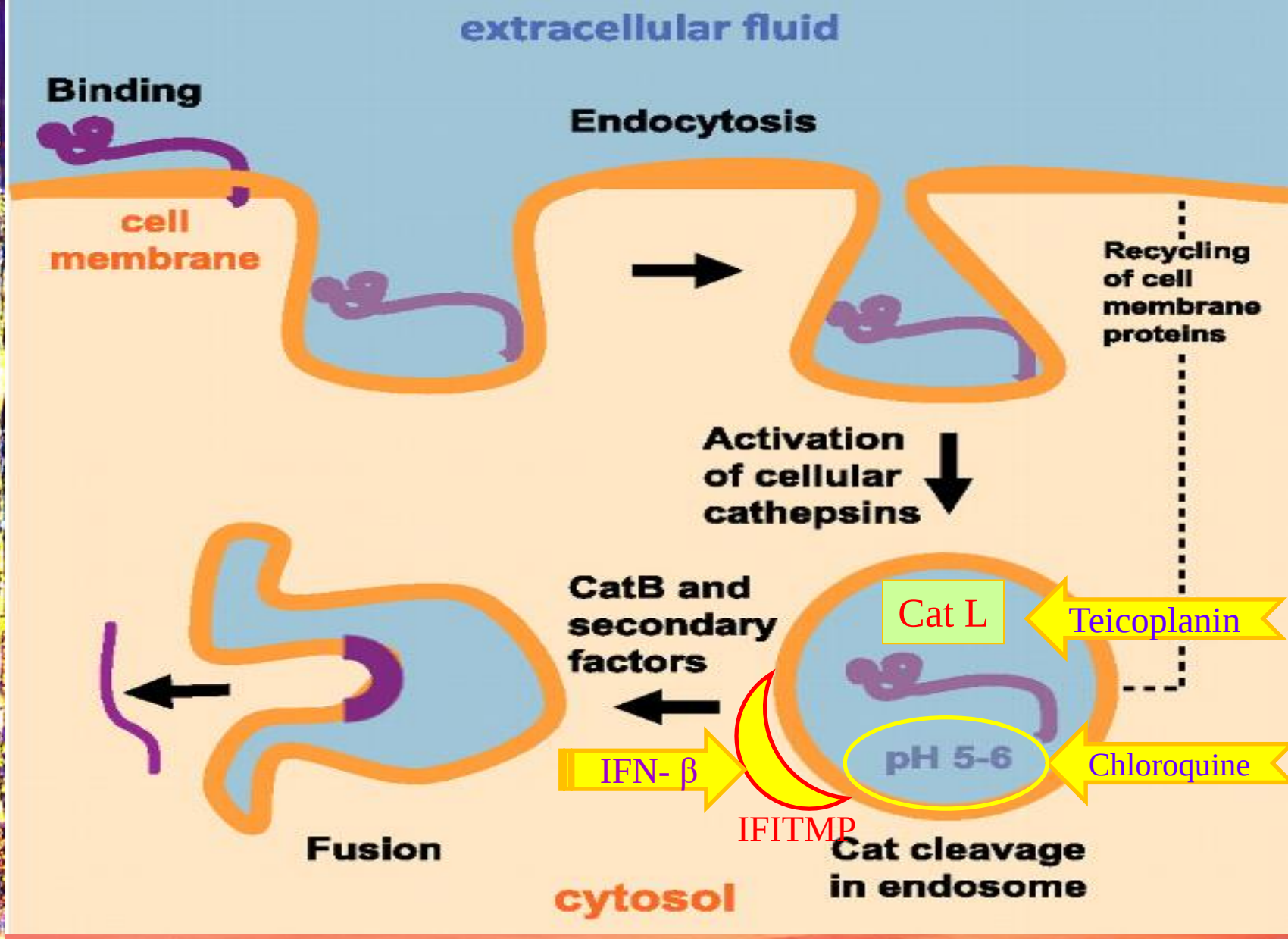

Hood CL, Abraham J, Boyington JC, Leung K, Kwong PD, Nabel GJ. Biochemical and structural characterization of cathepsin L-processed Ebola virus glycoprotein: implications for viral entry and immunogenicity. *J Virol*. 2010;84(6):2972-82

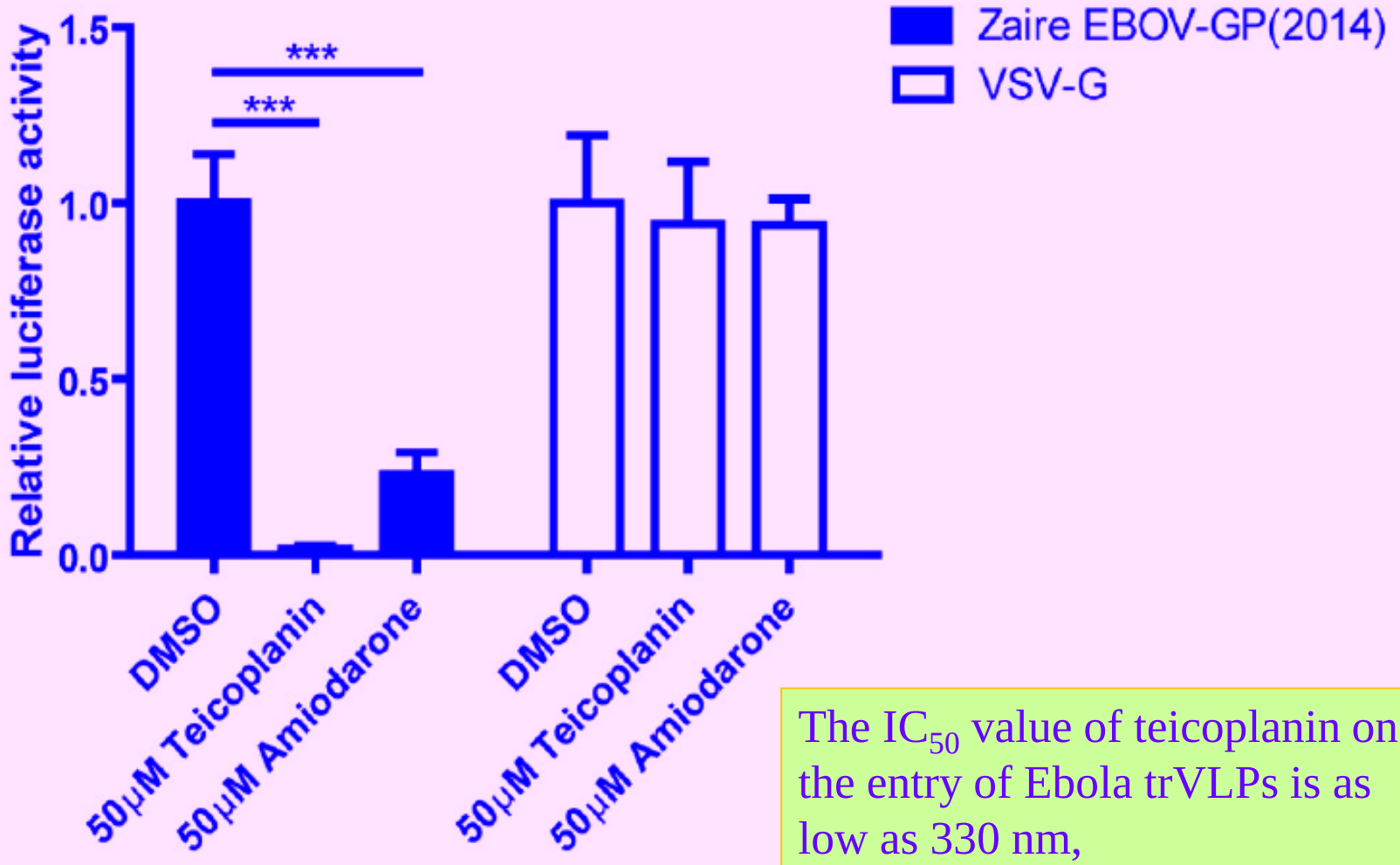

The IC_{50} value of teicoplanin on the entry of Ebola trVLPs is as low as 330 nm,

Trough concentration of Teicplanin at therapeutic dose 15 – 40 mg/L (8.78 μm – 23.4 μm)

Zhou N, Pan T, Zhang J, et al. Glycopeptide Antibiotics Potently Inhibit Cathepsin L in the Late Endosome/Lysosome and Block the Entry of Ebola Virus, Middle East Respiratory Syndrome Coronavirus (MERS-CoV), and Severe Acute Respiratory Syndrome Coronavirus (SARS-CoV). *J Biol Chem*. 2016;291(17):9218-32.

一真法界，諸法平等，萬相皆殊。

NS
(非結構性蛋白)

M
(子通道蛋白)

NP
(核蛋白質)

(雙鏈感應把關受體)
TLR3

dsRNA
雙股RNA

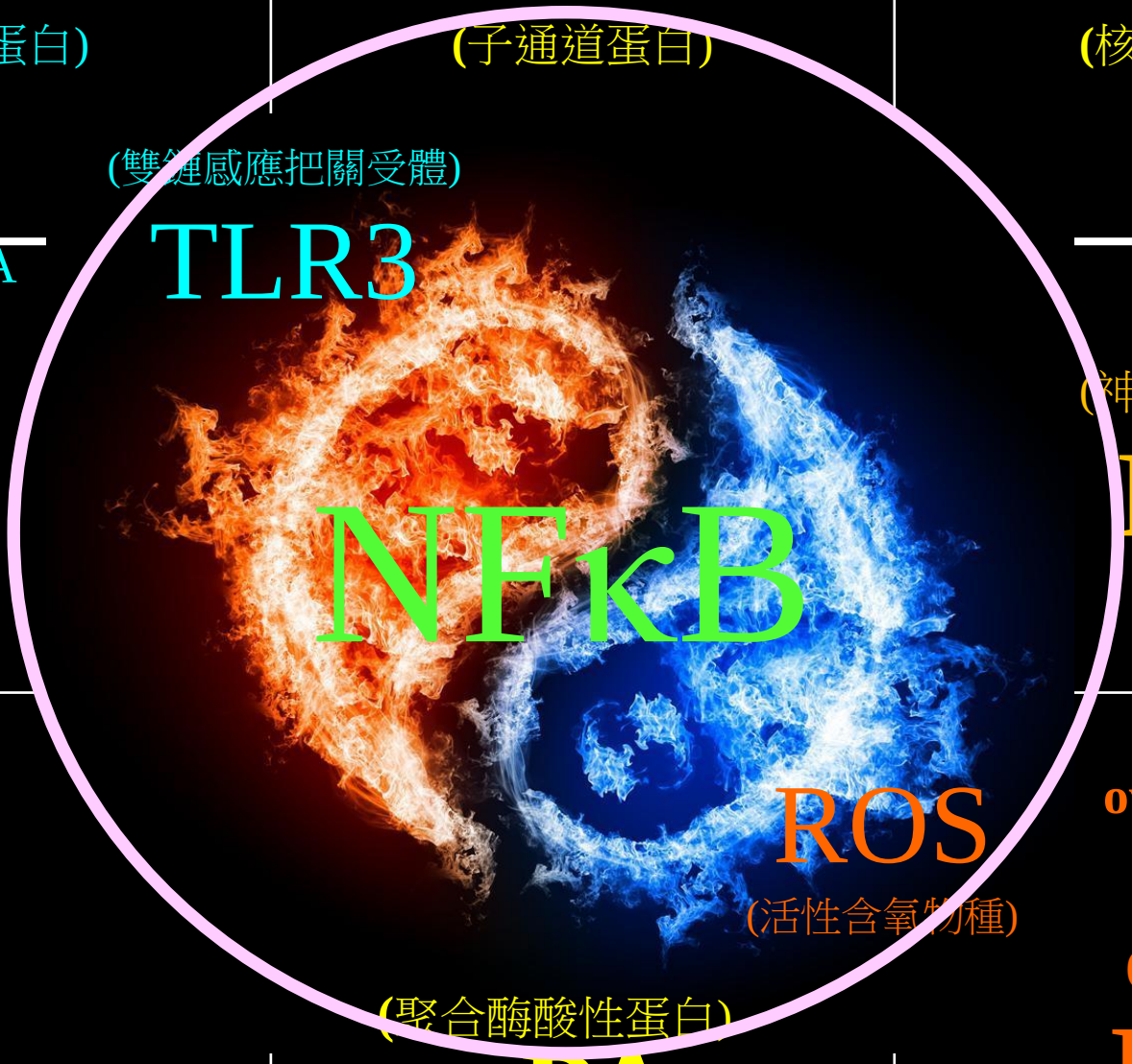

PB2
(聚合酶鹼性蛋白質)

(神經氨酸)
NA

ER-overlaod

(聚合酶鹼性蛋白)
PB1

PA

(血凝素)
HA

Bacterial Synergism in Influenza Infection

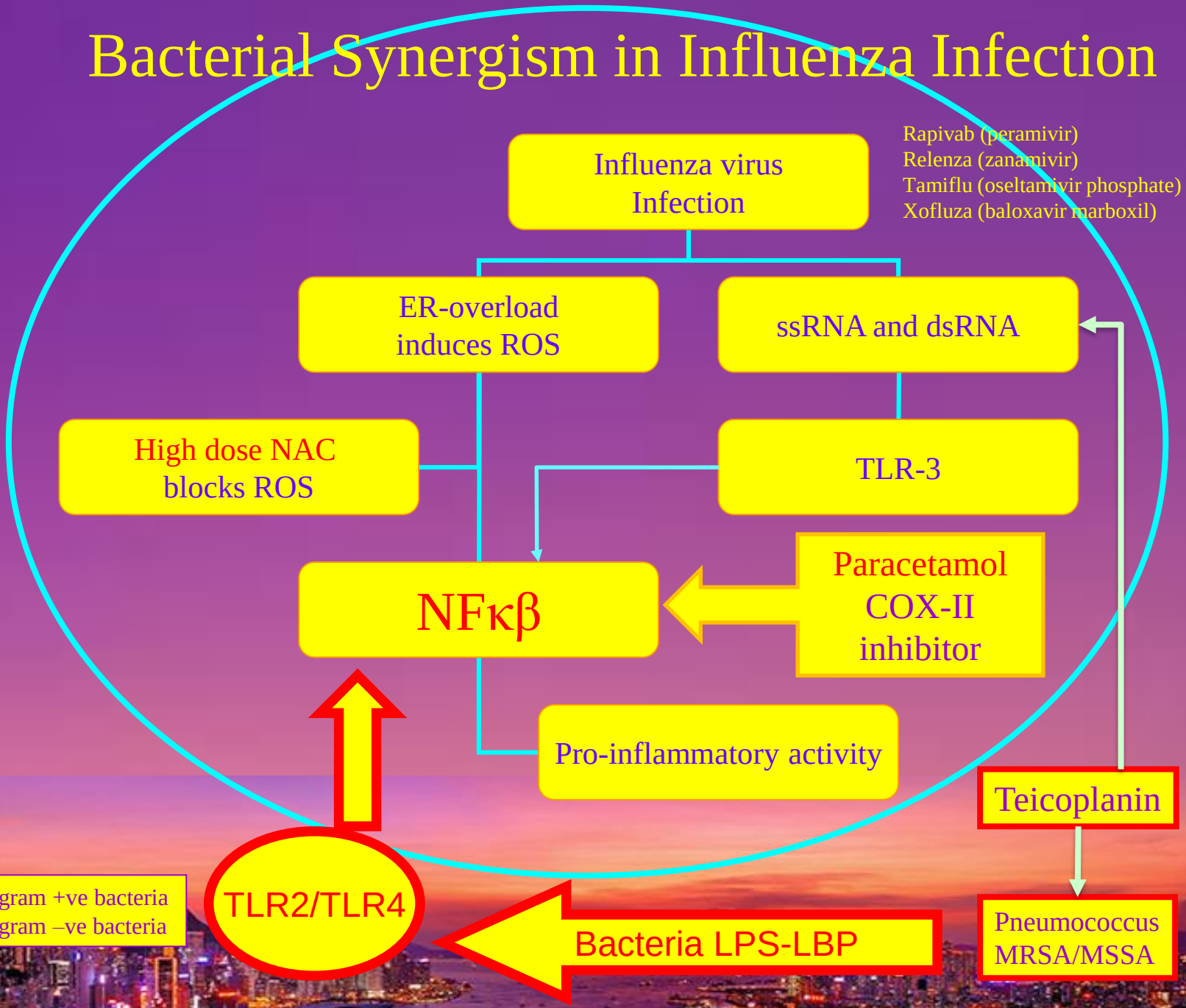

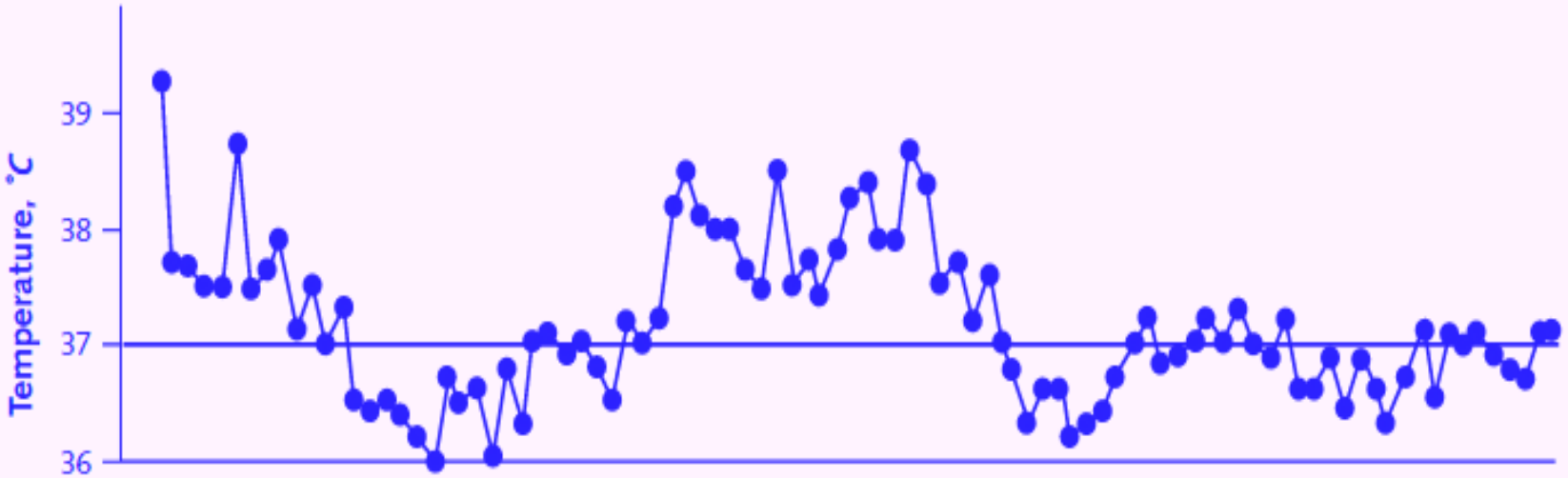

	7/15	7/16	7/17	7/18	7/19	7/20	7/21	7/22	7/23	7/24	7/25	7/26	7/27	7/28	7/29	7/30
CRP	183			38.8		11.7	11.3	11.5	132		101		27.4	20.0	16.5	15.0
H1	+							+	+	+	+	–	±	±	–	–
Mx	+							+	–	–	+	–	–	–	–	–
M	PCV	PCV	PCV	VC	VC	CPAP	CPAP	CPAP	PCV	PCV	PCV	VC	CPAP	CPAP	CPAP	NC
FIO_2	1.0	0.7	0.6	0.4	0.4	0.35	0.4	0.5	0.85	0.5	0.4	0.35	0.35	0.35	0.35	4L
PEEP	18	18	18	15	12	10	10	13	16	15	13	10	8	8	8	0
NO	20	20	0	0	0	0	0	0	0	0	0	0	0	0	0	0
			HDNAC								HDNAC					

Lai KY, Ng WY, Osburga Chan PK, Wong KF, Cheng F. High-dose N-acetylcysteine therapy for novel H1N1 influenza pneumonia. Ann Intern Med. 2010 May 18;152(10):687-8.

Novel H1N1 and Streptococcus Pneumoniae Pneumonia
CXR & CRP response to high-dose N-acetylcysteine (100mg/Kg/D infusion) and Teicoplanin

	20/2	21/2	22/2	23/2	24/2	25/2	26/2	27/2	28/2	6/3
CRP	190	149	85	73	62	42	41	26	29	11

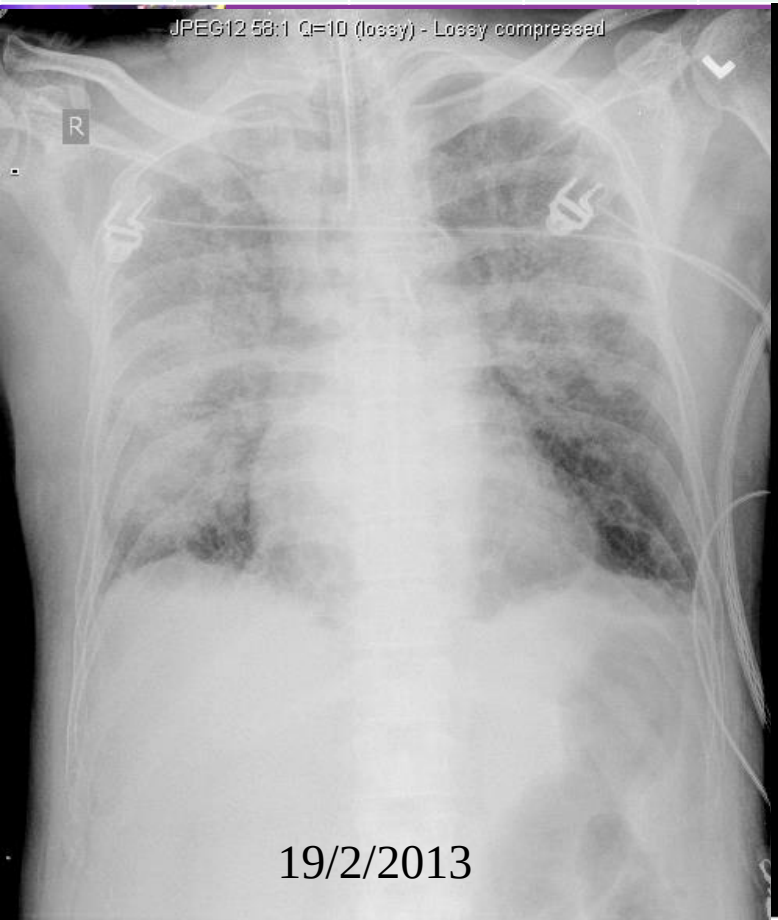

19/2/2013

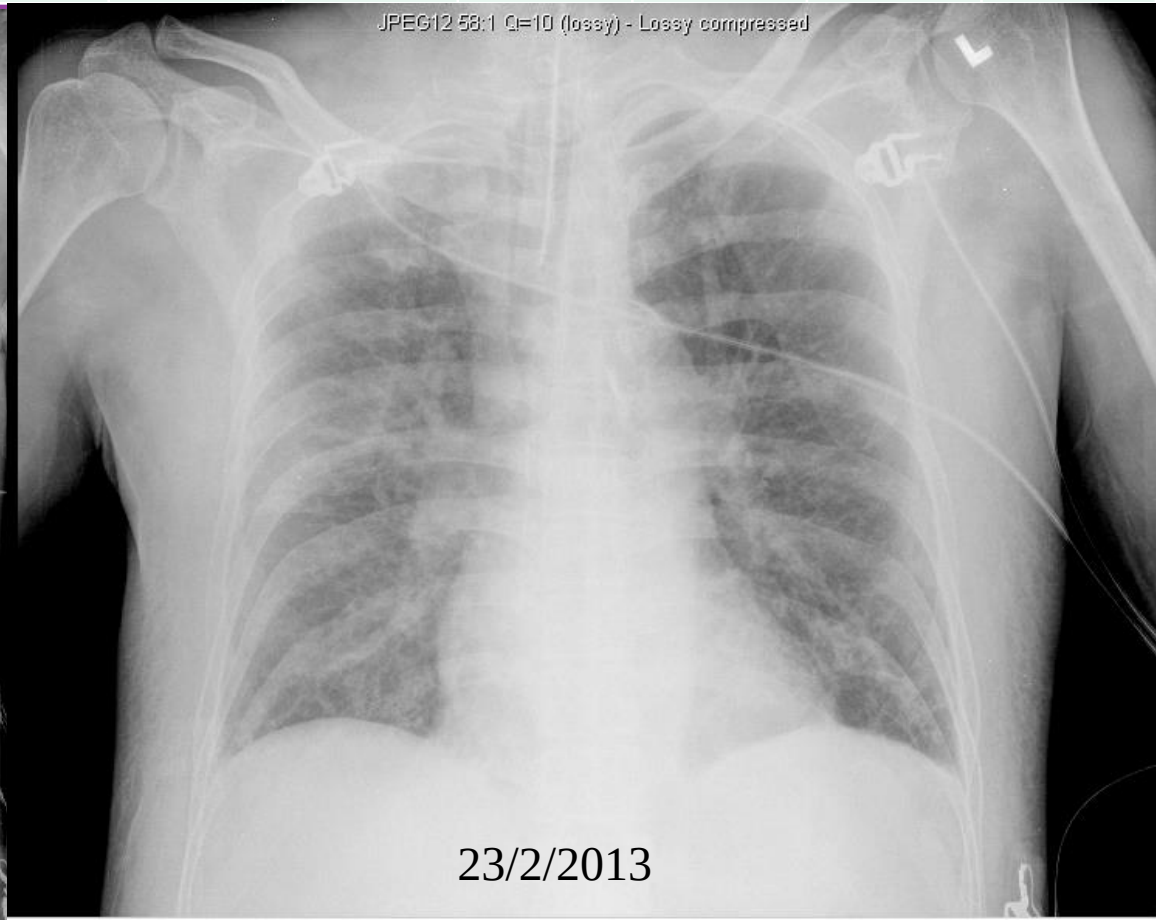

23/2/2013

Bacteria and Virus Synergism

Influenza virus

Neuraminidase facilitate bacterial adhesion and invasion

NS1 protein of H1N1 1918 & H5N1

Epithelial damage

Upregulation of PAFr
Fibrin and fibrinogen deposition facilitate adhesion

Cleavage activation of Haemagglutinin amplify viral proliferation

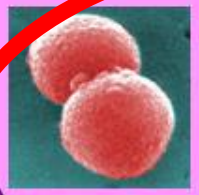

CA-MRSA
MSSA
Pneumococcus

Pneumococcal Neuraminidase, NanA and NanB !

Oseltamivir but not Zanamivir inhibit NanA

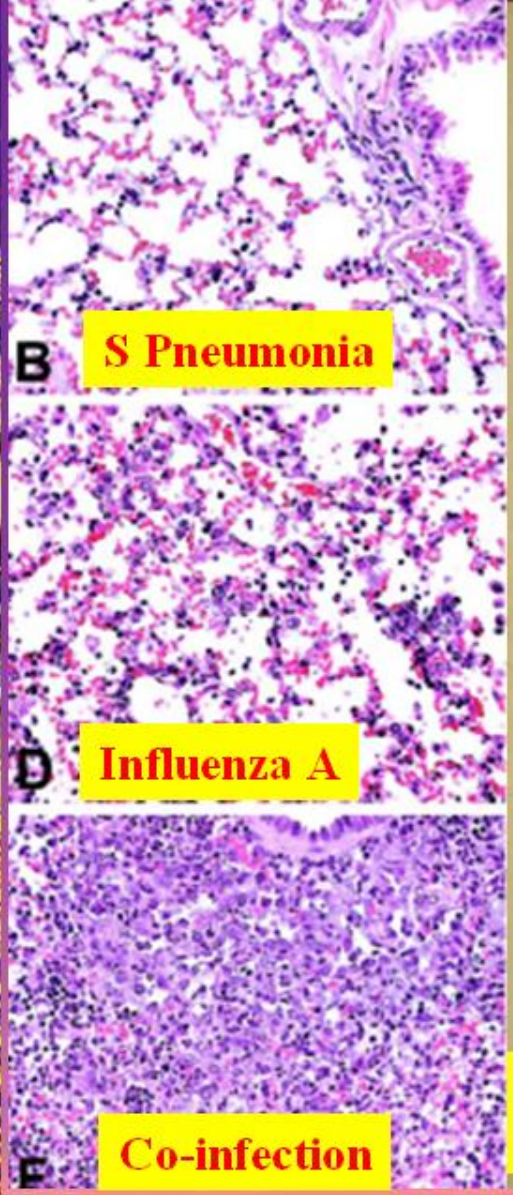
B
S Pneumonia
D
Influenza A
F
Co-infection

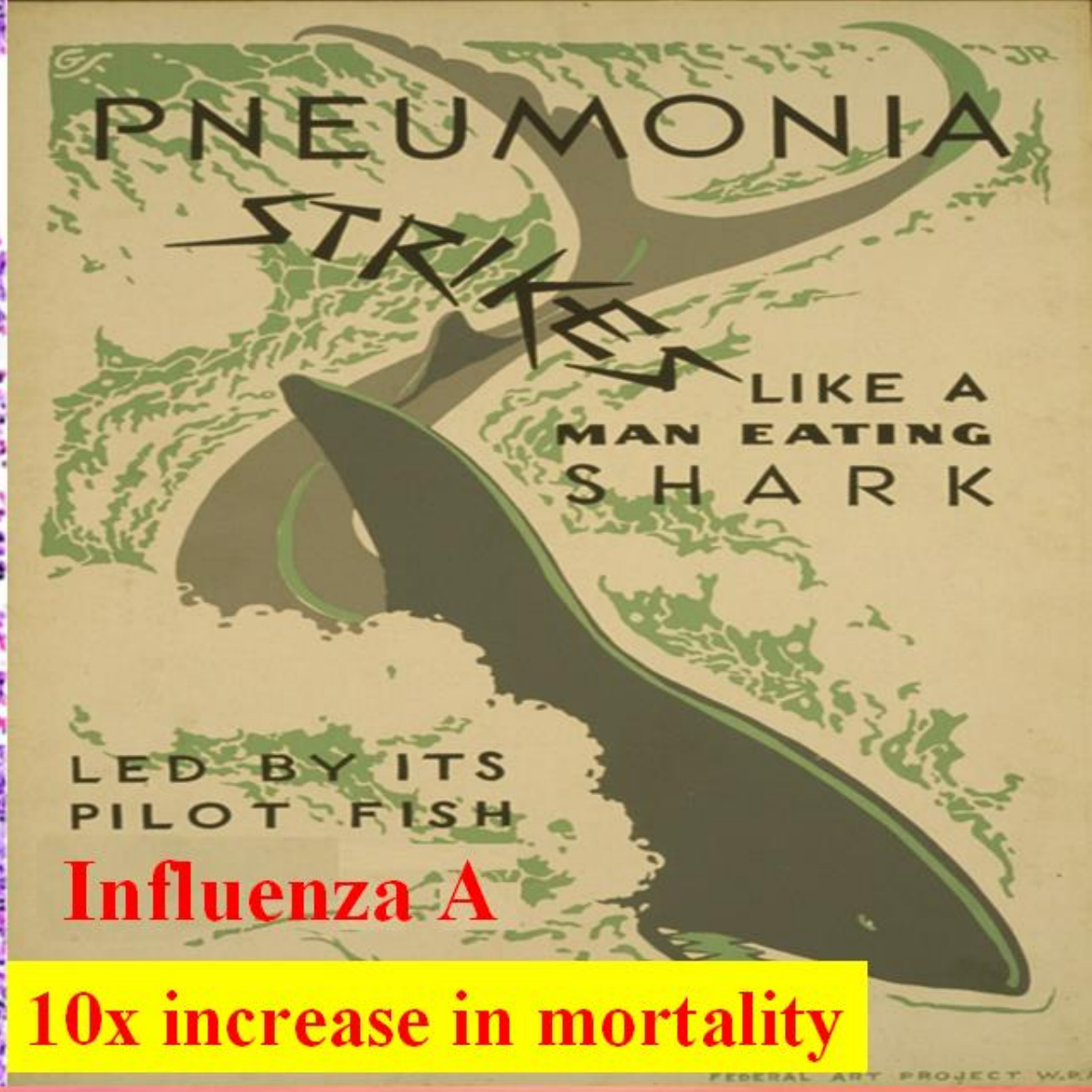
PNEUMONIA
STRIKES
LIKE A
MAN EATING
SHARK
LED BY ITS
PILOT FISH
Influenza A
10x increase in mortality
FEDERAL ART PROJECT W.P.A.

Predominant Role of Bacterial Pneumonia as a cause of death in pandemic influenza: implications for pandemic influenza preparedness

(Morens J infect Dis 2008:198:962-970)

Bacterial culture results in lung tissues from 5226 victims of the 1918-1919 influenza pandemic from 96 autopsy series	
Bacterial pathogens	**% of culture from which organism was recovered**
Streptococcus pneumoniae	**24%**
Streptococcus pyogenes	17%
Haemophilus influenza	**10%**
Staphylococcus aureus	8%
Mixed growth	21%
Others	16%
No growth	4%

Case-fatality ratio of 20-30% (10x) when there is secondary bacterial infection

Predominant pathogens responsible for bacterial co-infection during pandemic

Pandemic	Predominant pathogen for bacterial co-infection
1918	S pneumonia(24%), H. influenza (10%) and S pyogenes (17%)
1957	S. Aureus (69%)
1968	S. Pneumoniae (48%) S. Aureus (26%) H. Influenza (11%)

Pandemic outbreak of Panton-Valentine leukocidin (PVL)-positive penicillin resistant S. *aureus* (Phage Type 80/81) in 1954- 1957 causing a high frequency of skin and soft tissue infections, sepsis and pneumonia in healthy children and young adults.

In the three pandemic of the 20th century, bacterial pneumonia was estimated to develop in 15-20% of influenza patients.

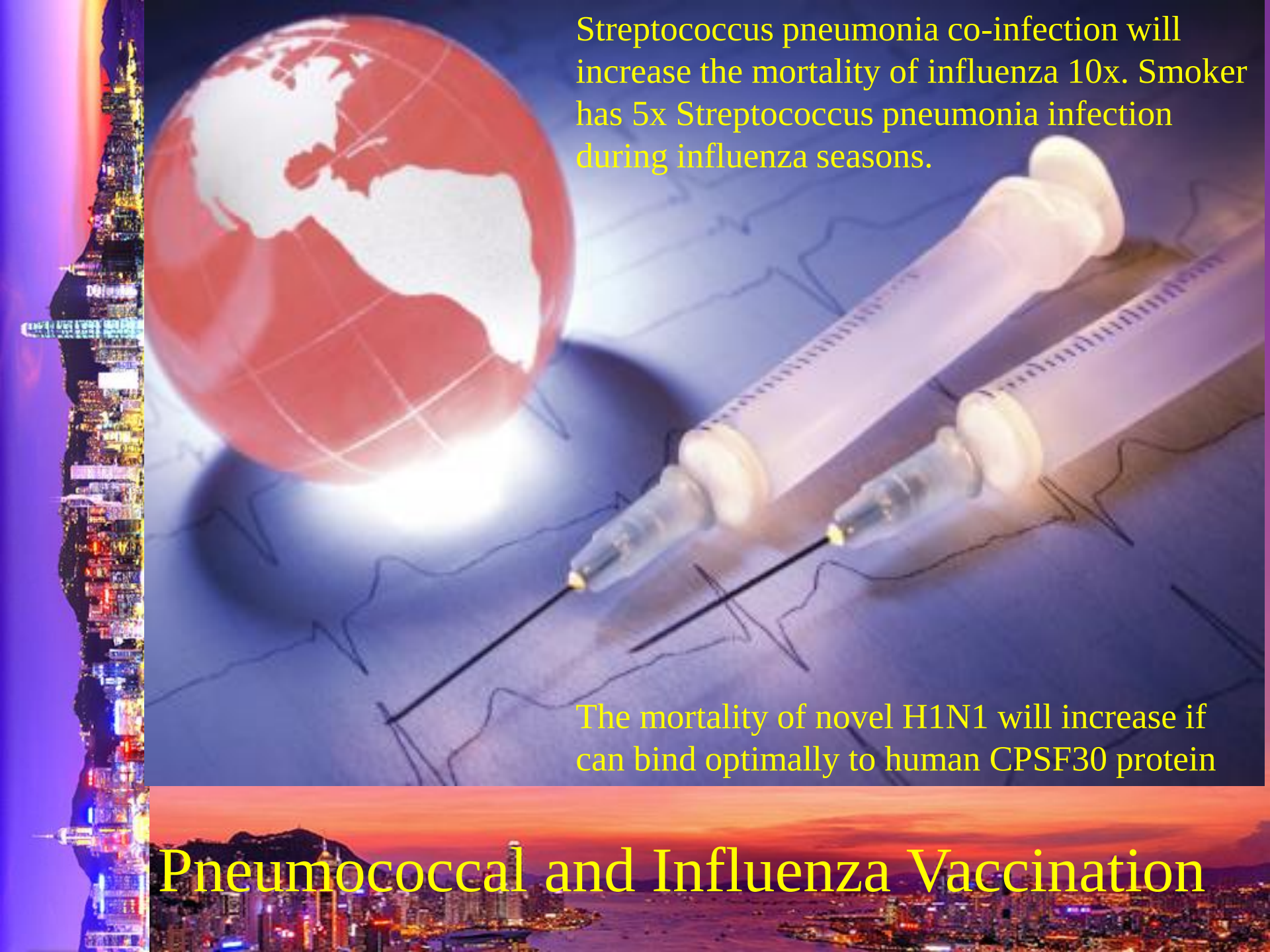

Streptococcus pneumonia co-infection will increase the mortality of influenza 10x. Smoker has 5x Streptococcus pneumonia infection during influenza seasons.

The mortality of novel H1N1 will increase if can bind optimally to human CPSF30 protein

Pneumococcal and Influenza Vaccination

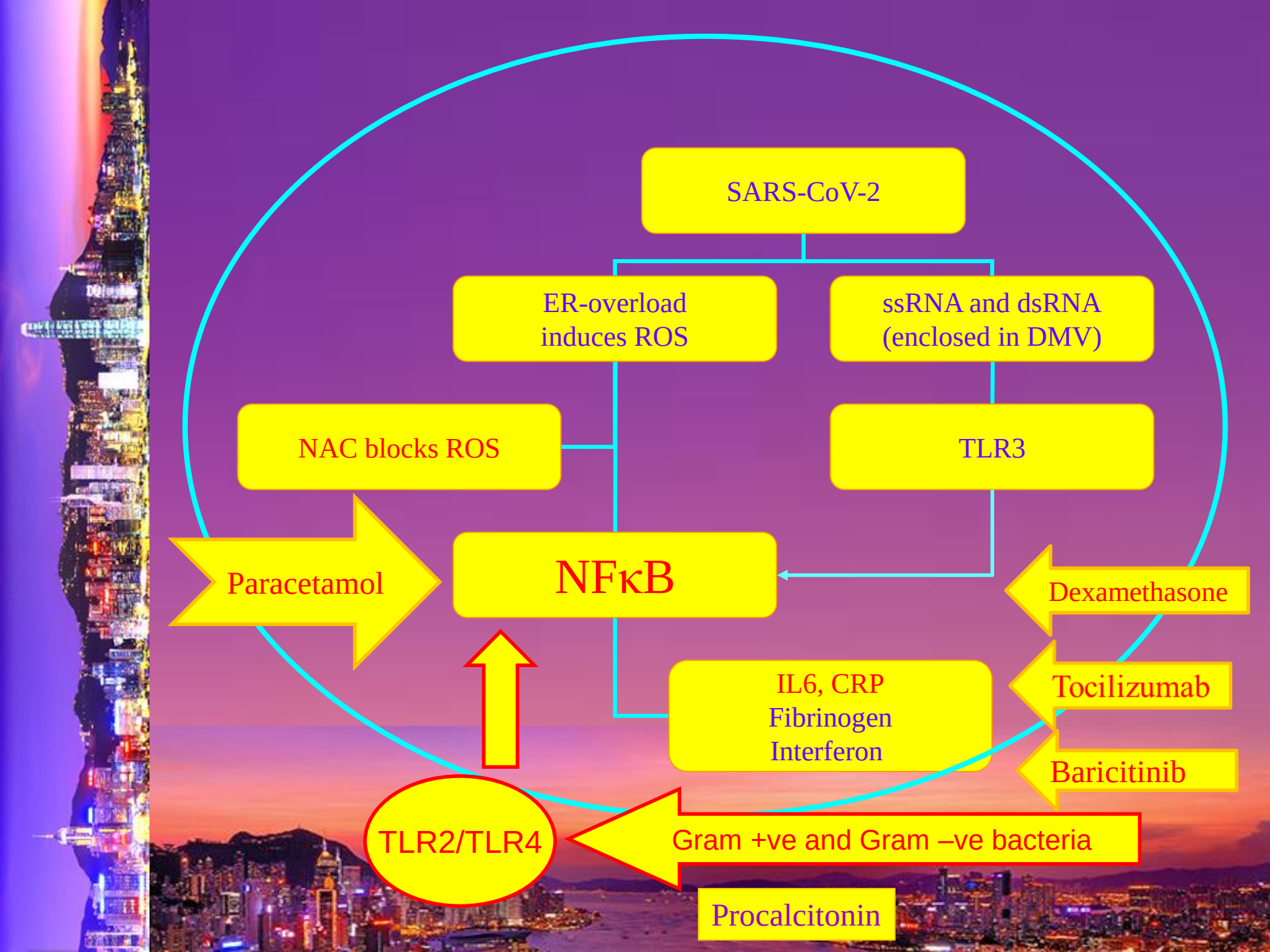
SARS-CoV-2
ER-overload
induces ROS
ssRNA and dsRNA
(enclosed in DMV)
NAC blocks ROS
TLR3
Paracetamol
NFκB
Dexamethasone
IL6, CRP
Fibrinogen
Interferon
Tocilizumab
Baricitinib
TLR2/TLR4
Gram +ve and Gram –ve bacteria
Procalcitonin

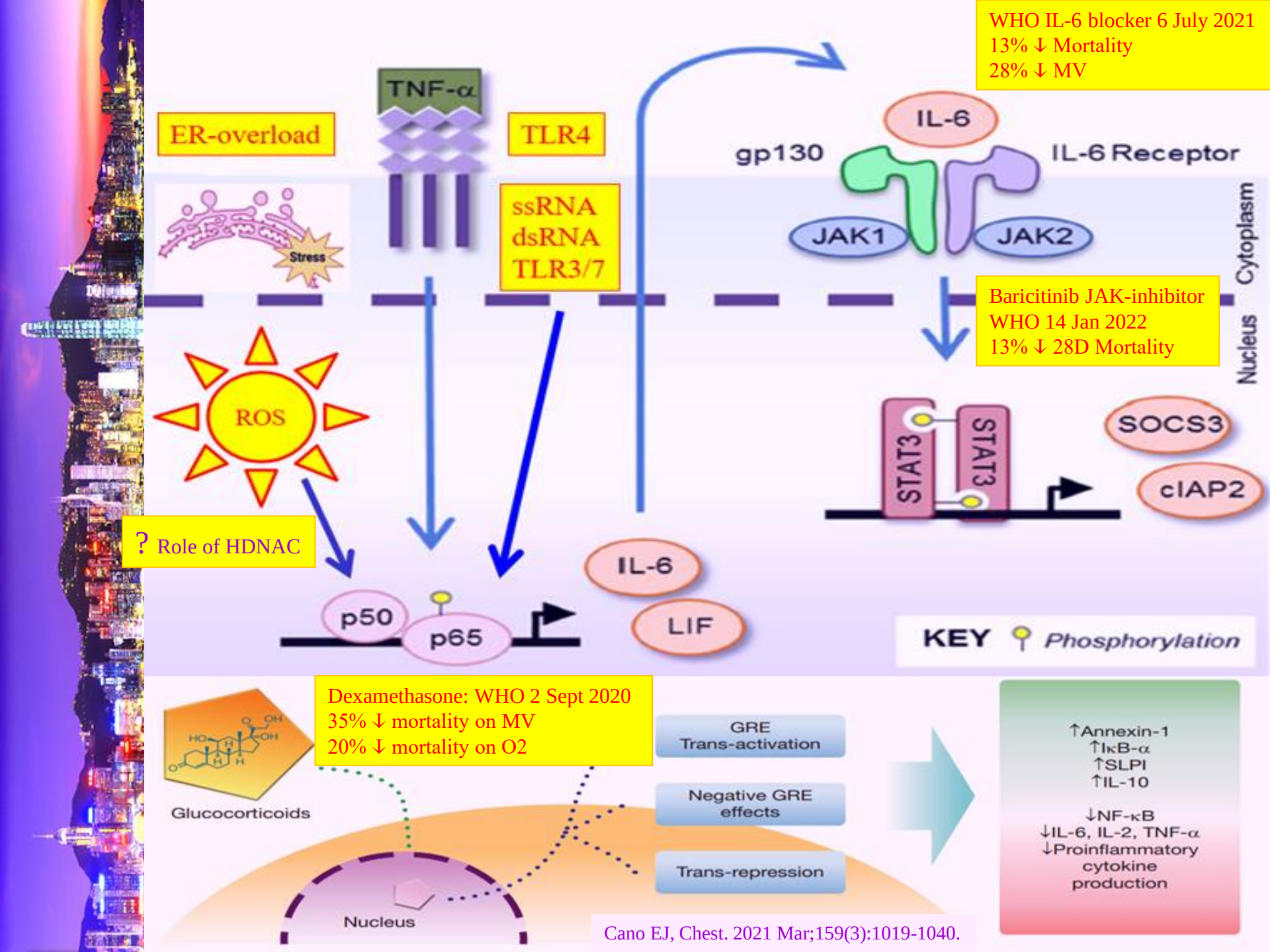
WHO IL-6 blocker 6 July 2021
13% ↓ Mortality
28% ↓ MV
TNF-α
ER-overload
TLR4
IL-6
gp130
IL-6 Receptor
Stress
ssRNA
dsRNA
TLR3/7
JAK1
JAK2
Cytoplasm
Nucleus
Baricitinib JAK-inhibitor
WHO 14 Jan 2022
13% ↓ 28D Mortality
ROS
STAT3
STAT3
SOCS3
cIAP2
? Role of HDNAC
IL-6
p50
p65
LIF
KEY
Phosphorylation
Dexamethasone: WHO 2 Sept 2020
35% ↓ mortality on MV
20% ↓ mortality on O2
Glucocorticoids
GRE
Trans-activation
Negative GRE
effects
Trans-repression
Nucleus
↑Annexin-1
↑IκB-α
↑SLPI
↑IL-10
↓NF-κB
↓IL-6, IL-2, TNF-α
↓Proinflammatory
cytokine
production
Cano EJ, Chest. 2021 Mar;159(3):1019-1040.

Demographic and clinical characteristics of hospitalized COVID-19 patients, by NAC use.

Izquierdo JL, Sci Prog. 2022 Jan-Mar;105(1):368504221074574.

	Total COVID19	without NAC	with NAC	*P* value OR (CI95%)
N	19.208	17.137	2071	
Age. Years (SD)	66.6 (20.9)	65.9 (21.4)	70.1 (15.6)	*P* < 0.001
Sex. Male (%)	53.6	52.6	60.1	*P* < 0.001

Association of drugs with mortality in hospitalized COVID-19 patients.

	Total COVID19	COVID19 No dead	COVID19 Dead	OR (CI95%)
N	19.208	17.162	2046	
NAC	2071	1935	136	0.56 (0.47–0.67)
%		11.3	(6.6)	
Corticosteroids	7479	6898	581	0.59 (0.53–0.65)
%		40.2	28.4	
Enoxaparin	6649	6213	436	0.47 (0.43–0.53)
%		36.2	21.3	
Acenocoumarin	1917	1624	293	1.60 (1.40–1.83)
%		9.5	14.3	

Despite greater baseline risk, use of NAC (600 mg every 8 h) in COVID-19 patients was associated with significantly lower mortality (OR 0.56; 95%CI 0.47-0.67), a finding that remained significant in a multivariate analysis adjusting by baseline characteristics and concomitant use of corticosteroids.

Thank you for your attention

Influenza's Achilles' Heel?

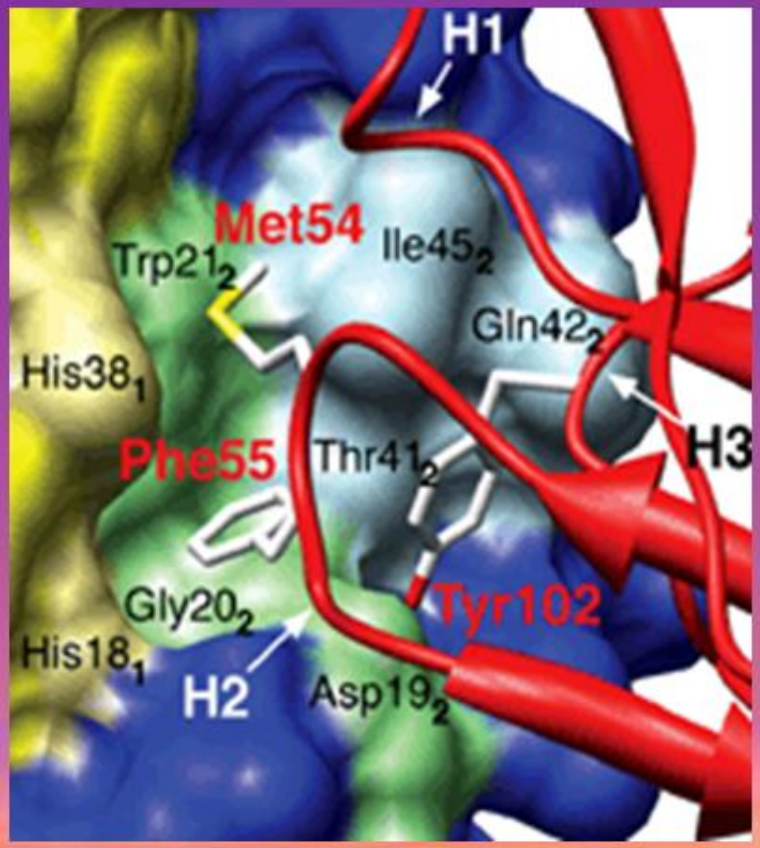

- Two research teams identify a highly conserved epitope that could be key to developing broad-spectrum prophylactic and therapeutic strategies that target influenza, including H5N1 strains.
- Both groups find that the antibodies bind a relatively concealed hydrophobic pocket in the conserved stem region of HA, which is normally shielded by the variable mushroom-shaped head of the protein but plays a critical role in viral entry by means of membrane fusion.

(*Nat. Struct. Mol. Biol.* 16, 265–273, 2009; *Science*, 26 February 2009)

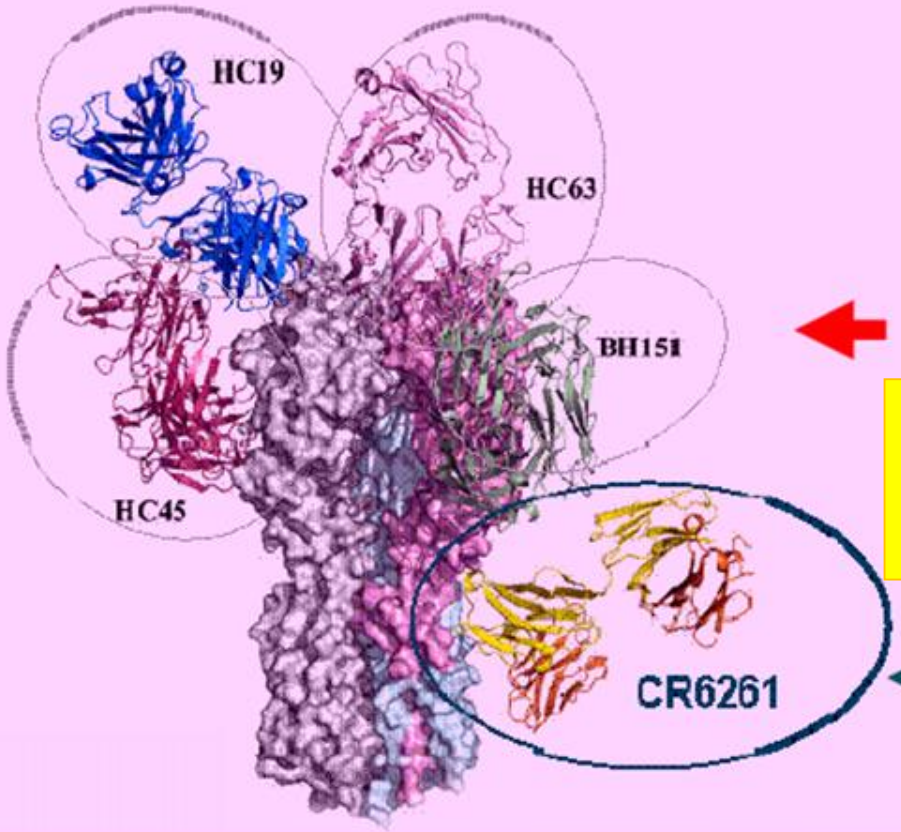

Globular head domain

Receptor binding site

Variable structures binding antibodies generated by seasonal vaccines

Stalk/stem domain

Blocks conformational arrangement associated with membrane fusion

The highly conserved structure recognized by mAb CR 6261

Towards An Universal Influenza A Antibody ?

- Effective for most influenza A virus
- Effective in reducing mortality during influenza A infection

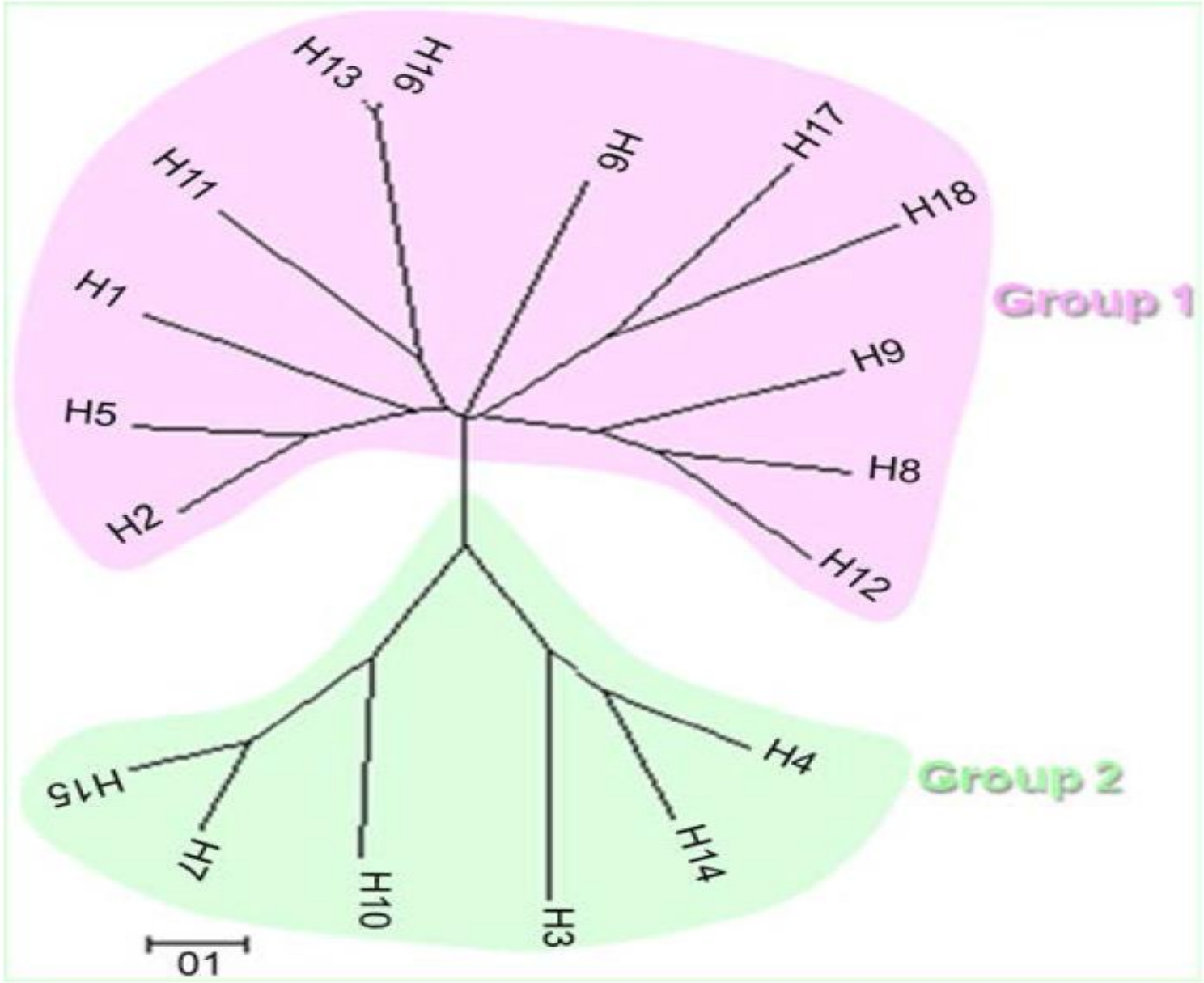
H13
H16
H6
H17
H11
H18
H1
Group 1
H9
H5
H8
H2
H12
H4
H15
Group 2
H7
H14
H10
H3
01

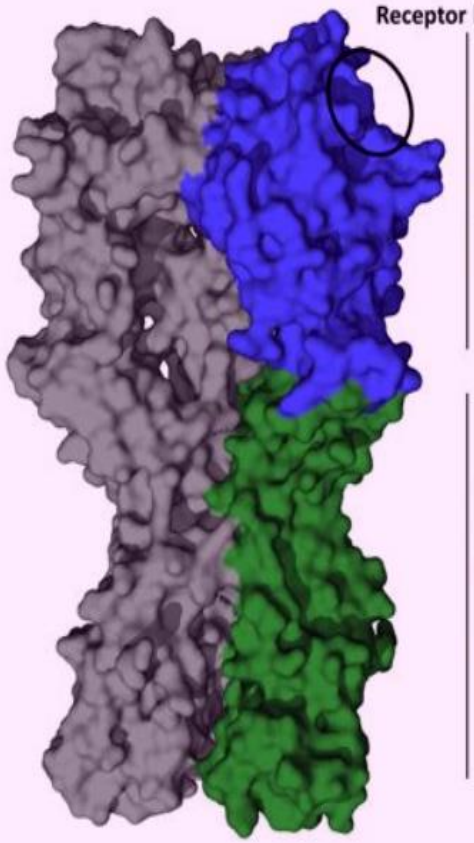

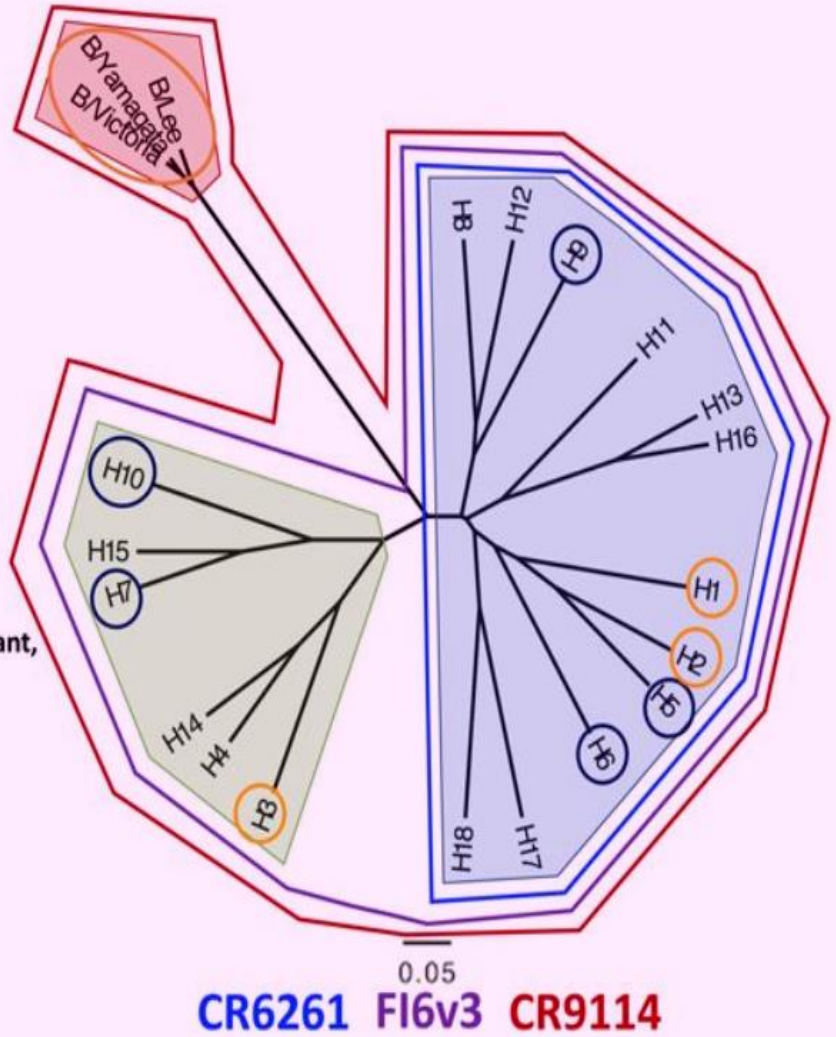

Influenza A	**Group 1**	**H1**, **H2**, **H5**, H6,H8,H9,H11, H12, H13, H16,H17
	Group 2	**H3**, H4, **H7**, H10,H14,H15
Influenza B		

Kirkpatrick E, Qiu X, Wilson PC, Bahl J, Krammer F. The influenza virus hemagglutinin head evolves faster than the stalk domain. *Sci Rep*. 2018;8(1):10432. Published 2018 Jul 11. doi:10.1038/s41598-018-28706-1

The Tetherin Antagonism of the Ebola Virus Glycoprotein Requires an Intact Receptor-Binding Domain and Can Be Blocked by GP1-Specific Antibodies.

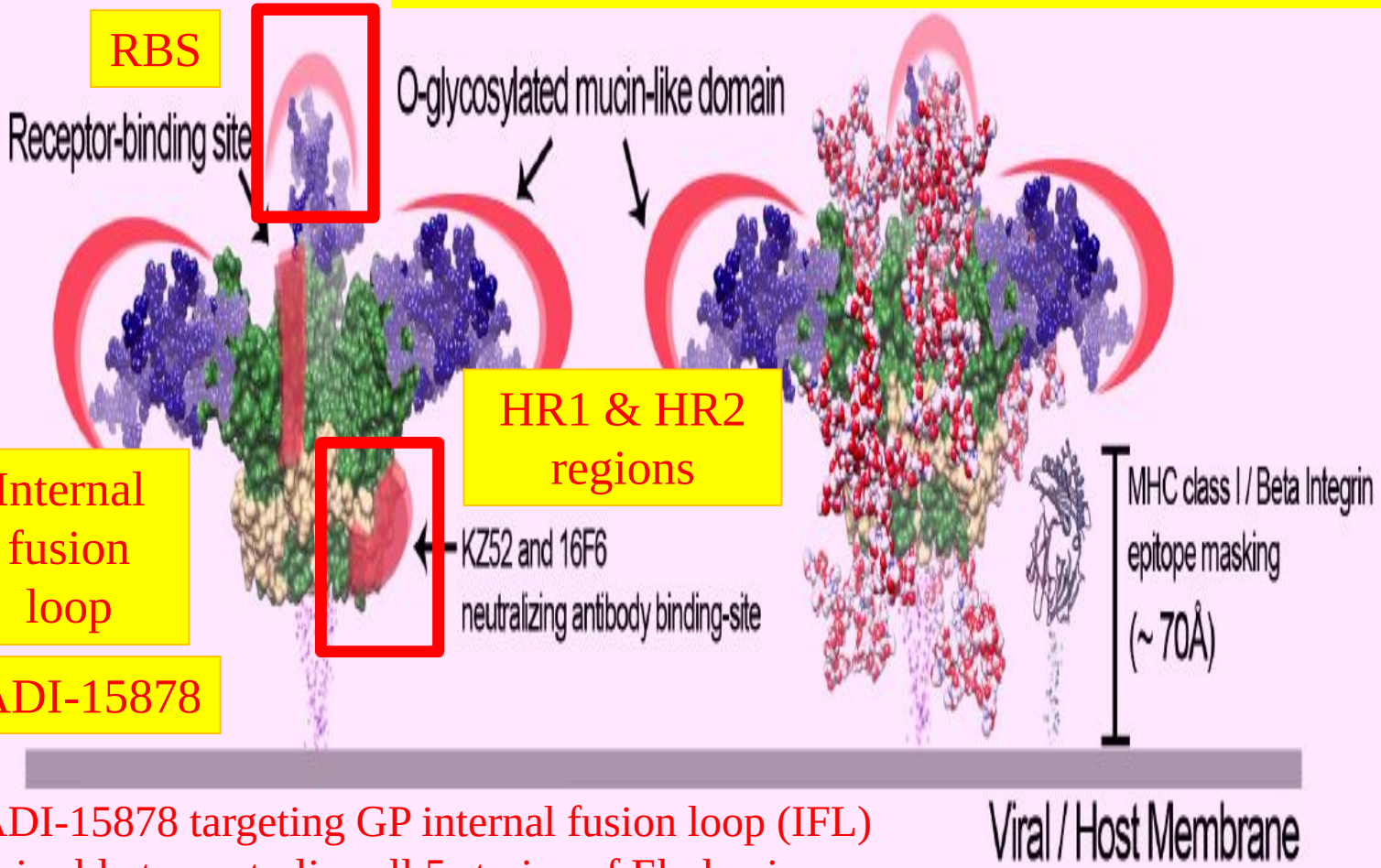

ADI-15878 targeting GP internal fusion loop (IFL) is able to neutralize all 5 strains of Ebola virus

"Base-binding" and fusion loop-binding epitope antibodies

PLoS Pathog. 2013;9(5):e1003258.

West BR, Moyer CL, King LB, et al. Structural Basis of Pan-Ebolavirus Neutralization by a Human Antibody against a Conserved, yet Cryptic Epitope. *MBio*. 2018;9(5):e01674-18. Published 2018 Sep 11. doi:10.1128/mBio.01674-18

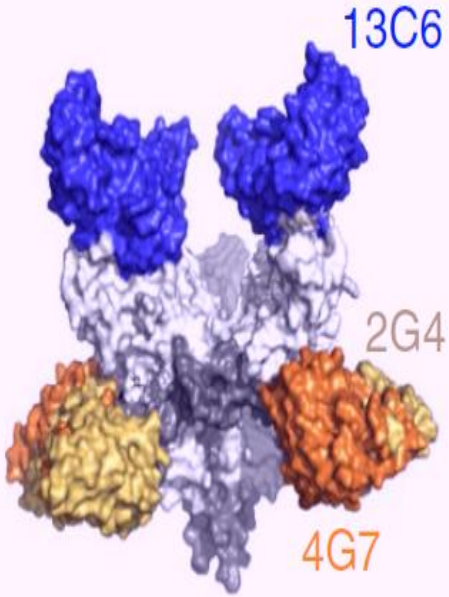

ZMapp cocktail
Chimeric
Nicotiana
50 mg/kg days 5,8,11
100% survival, rhesus

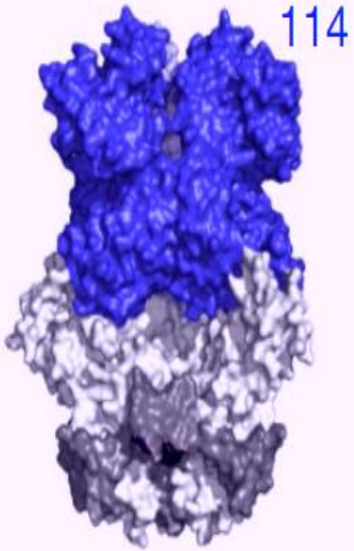

mAb 114 monotherapy
Human
293F
50 mg/kg days 5,6,7
100% survival, rhesus

REGN-EB3 cocktail
Human
Modified CHO
50 mg/kg days 5,8
100% survival, rhesus
(Single dose day 5, 100 or 50 mg/kg,
89% or 78% survival)

Saphire, E.O., Schendel, S.L., Gunn, B.M. *et al.* Antibody-mediated protection against Ebola virus. *Nat Immunol* **19,** 1169–1178 (2018).

The preliminary PALM data showed a 29% mortality rate for participants treated with REGN-EB3 and 34% with mAb114, versus 53% with remdesivir and 49% with ZMapp.
https://www.nature.com/articles/s41587-019-0284-y

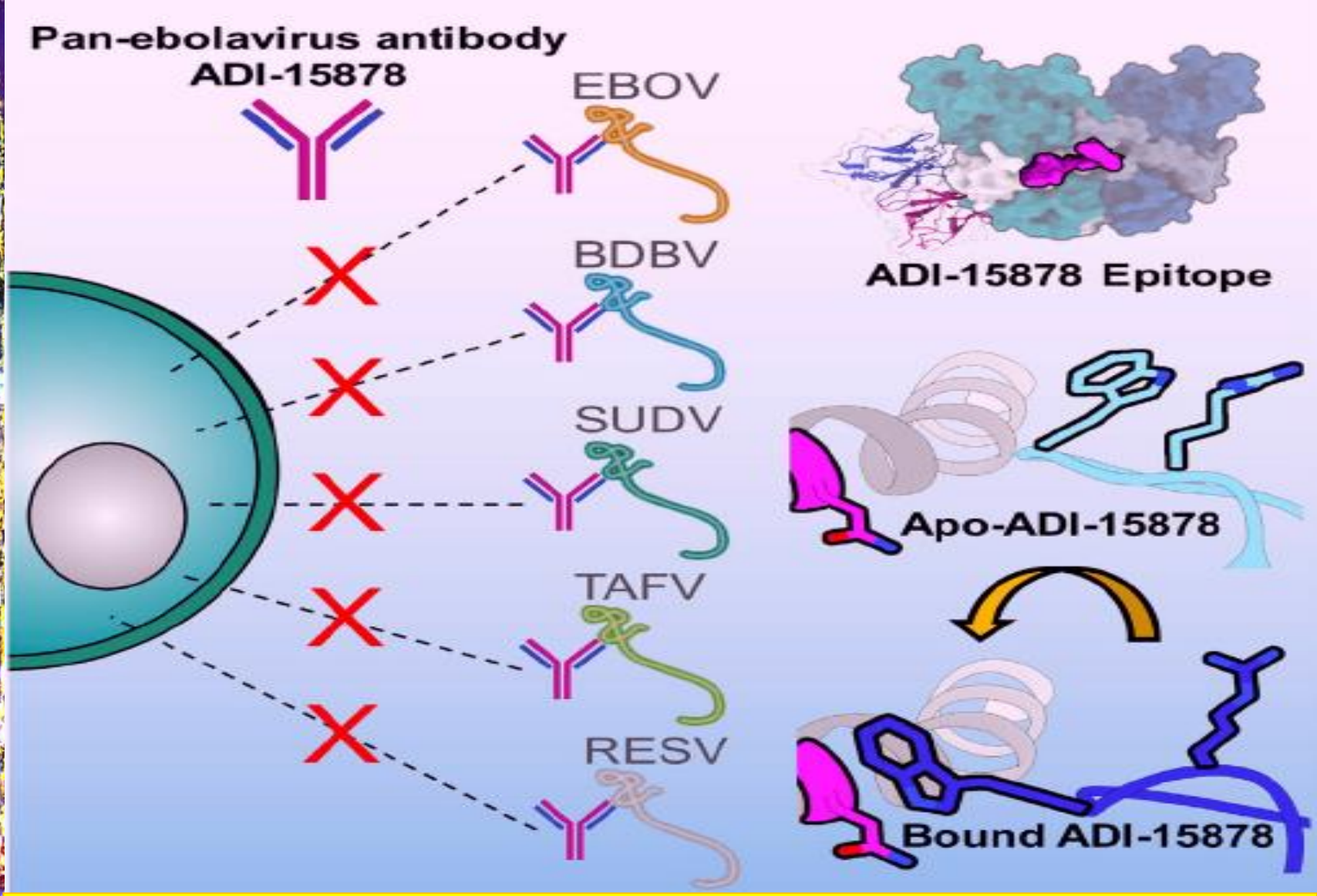

The HR1 and IFL on filoviral GPs are highly conserved in sequence and structure across genera
ADI-15878 targeting GP internal fusion loop is able to neutralize all 5 strains of Ebola virus

Murin CD, Bruhn JF, Bornholdt ZA, Copps J, Stanfield R, Ward AB. Structural Basis of Pan-Ebolavirus Neutralization by an Antibody Targeting the Glycoprotein Fusion Loop. *Cell Rep*. 2018;24(10):2723-2732.e4.

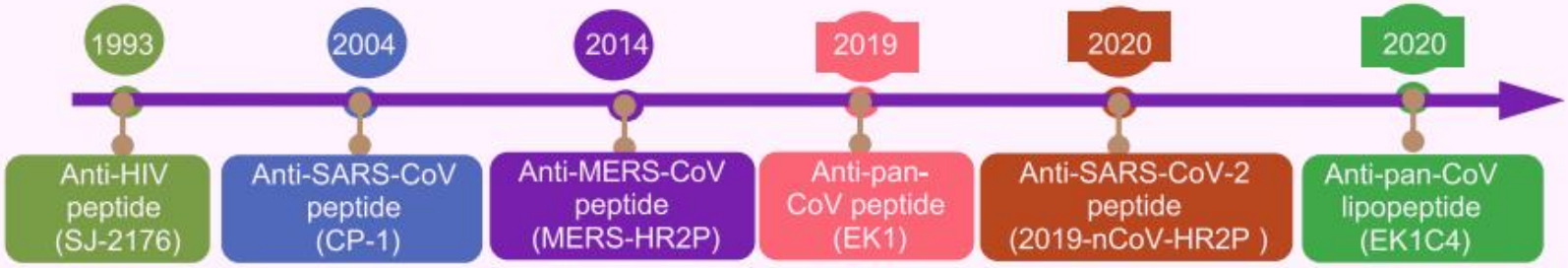

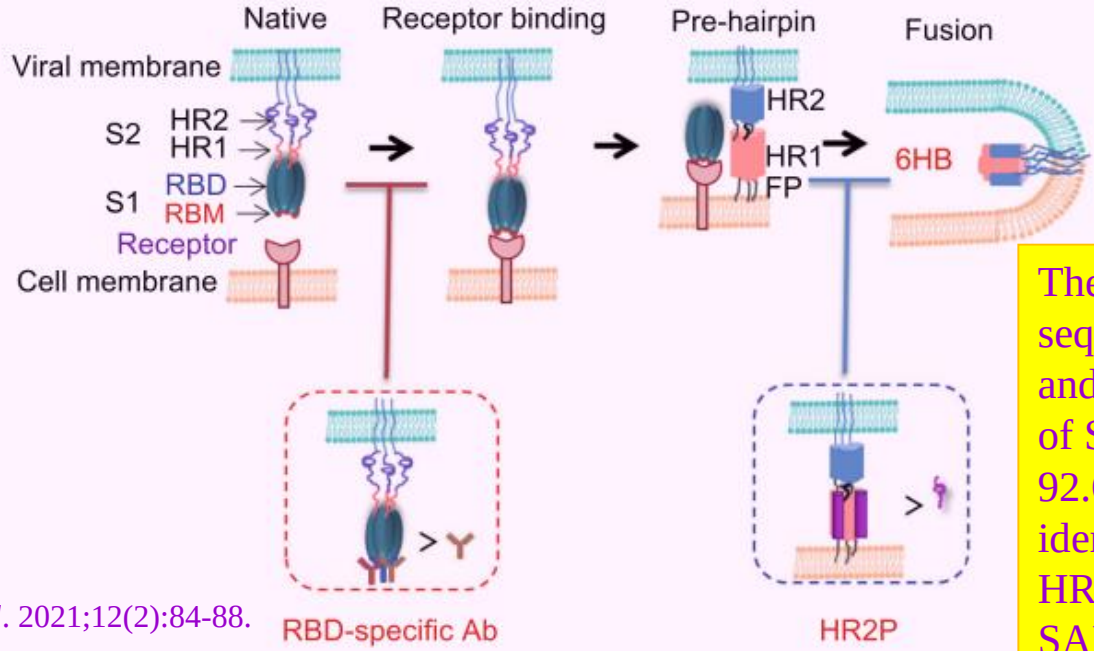

Wang X, *Protein Cell*. 2021;12(2):84-88.

The amino acid sequences of HR1 and HR2 domains of SARS-CoV-2 are 92.6% and 100% identical to those of HR1 and HR2 of SARS-CoV, respectively

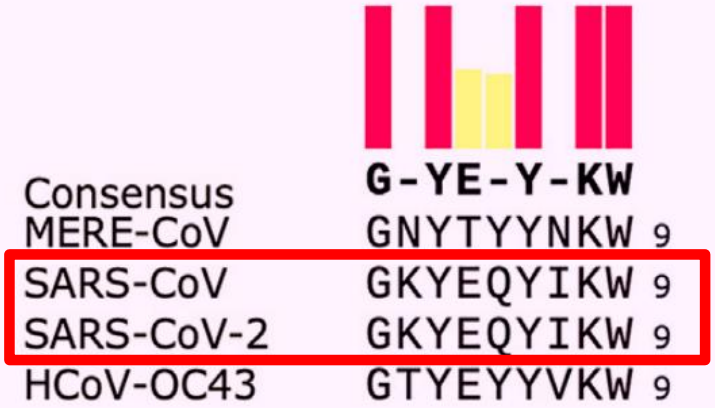

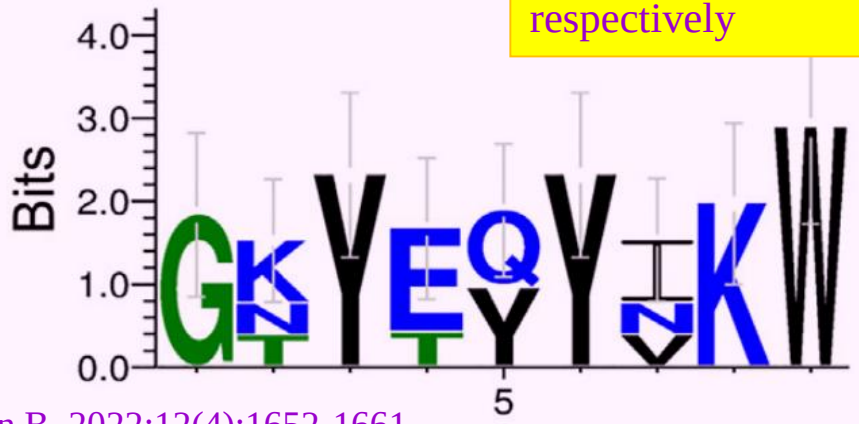

Zhou J, Acta Pharm Sin B. 2022;12(4):1652-1661

Authentic SARS-CoV-2 Omicron infection

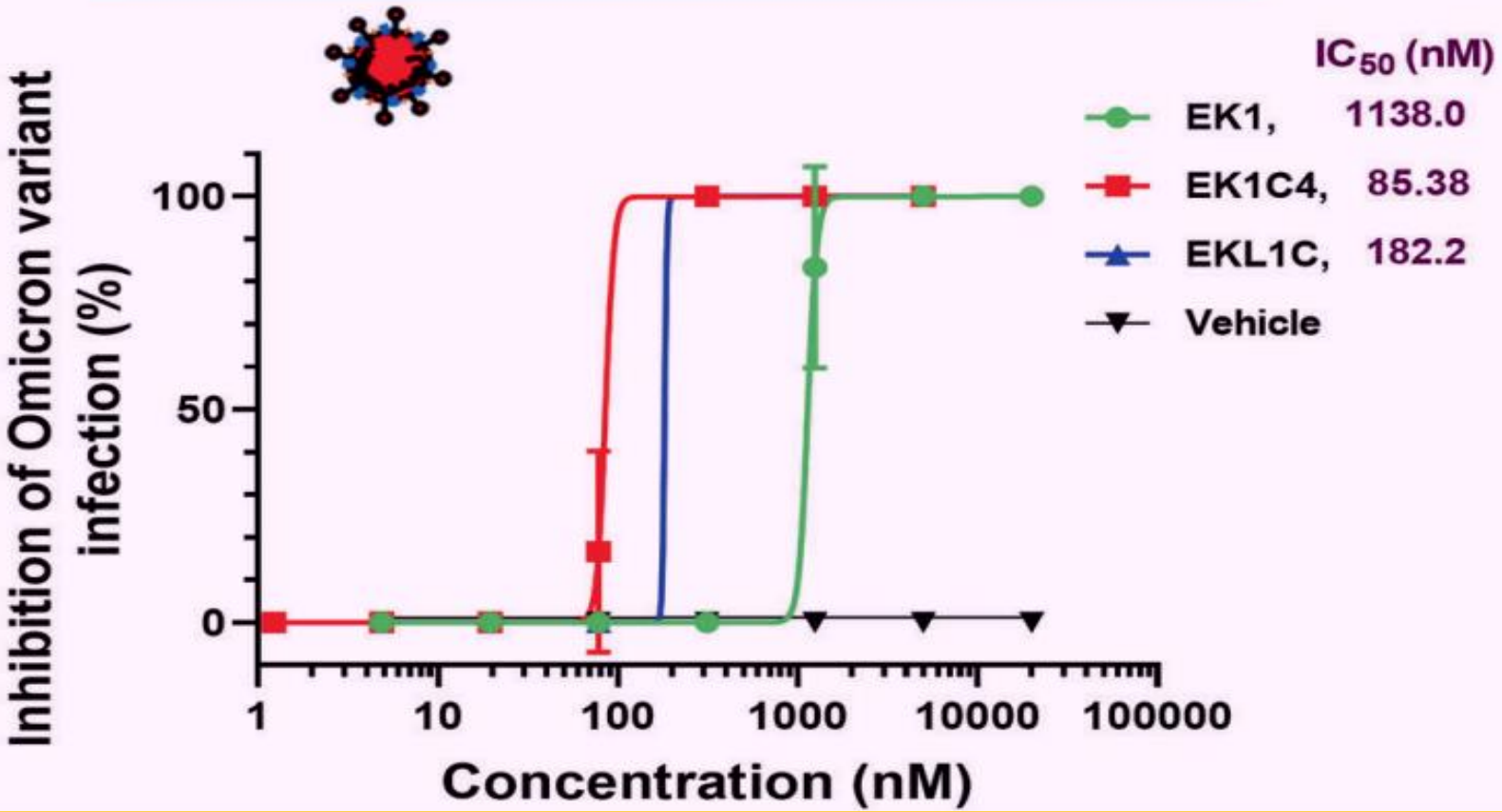

EK1, EK1C4, and EKL1C are peptide-based pan-coronavirus (CoV) fusion inhibitors, exhibiting potent and broad-spectrum inhibitory activity against multiple human CoVs by targeting the conserved HR1 region in the S2 subunit of S protein. EK1C4, a lipopeptide of EK1 was 226-fold and 149-fold more potent against SARS-CoV2 S protein-mediated membrane fusion and PsV infection, respectively, than EK1.

Xia S, Chan JF, Wang L, Jiao F, Chik KK, Chu H, Lan Q, Xu W, Wang Q, Wang C, Yuen KY, Lu L, Jiang S. Peptide-based pan-CoV fusion inhibitors maintain high potency against SARS-CoV-2 Omicron variant. Cell Res. 2022 Apr;32(4):404-406.

Memory B cell repertoire from triple vaccinees against diverse SARS-CoV-2 variants

95 (57/60) have neutralizing Ab after 3rd dose

Kang Wang, Zijing Jia, ... Xiangxi Wang

Nature **603**, 919–925 (2022)

The researchers isolated 323 human monoclonal antibodies (mAbs) derived from memory B cells in three-dose recipients, half of which recognized the receptor binding domain. A subset of them (24/163) neutralize all SARS-CoV-2 variants of concern (VOCs), including Omicron, potently.

CoronaVac elicited significantly higher structural protein-specific $CD4^+$ and $CD8^+$ T-cell responses than BNT162b2 vaccine. Mok CKP, Respirology. 2022 Apr;27(4):301-310.

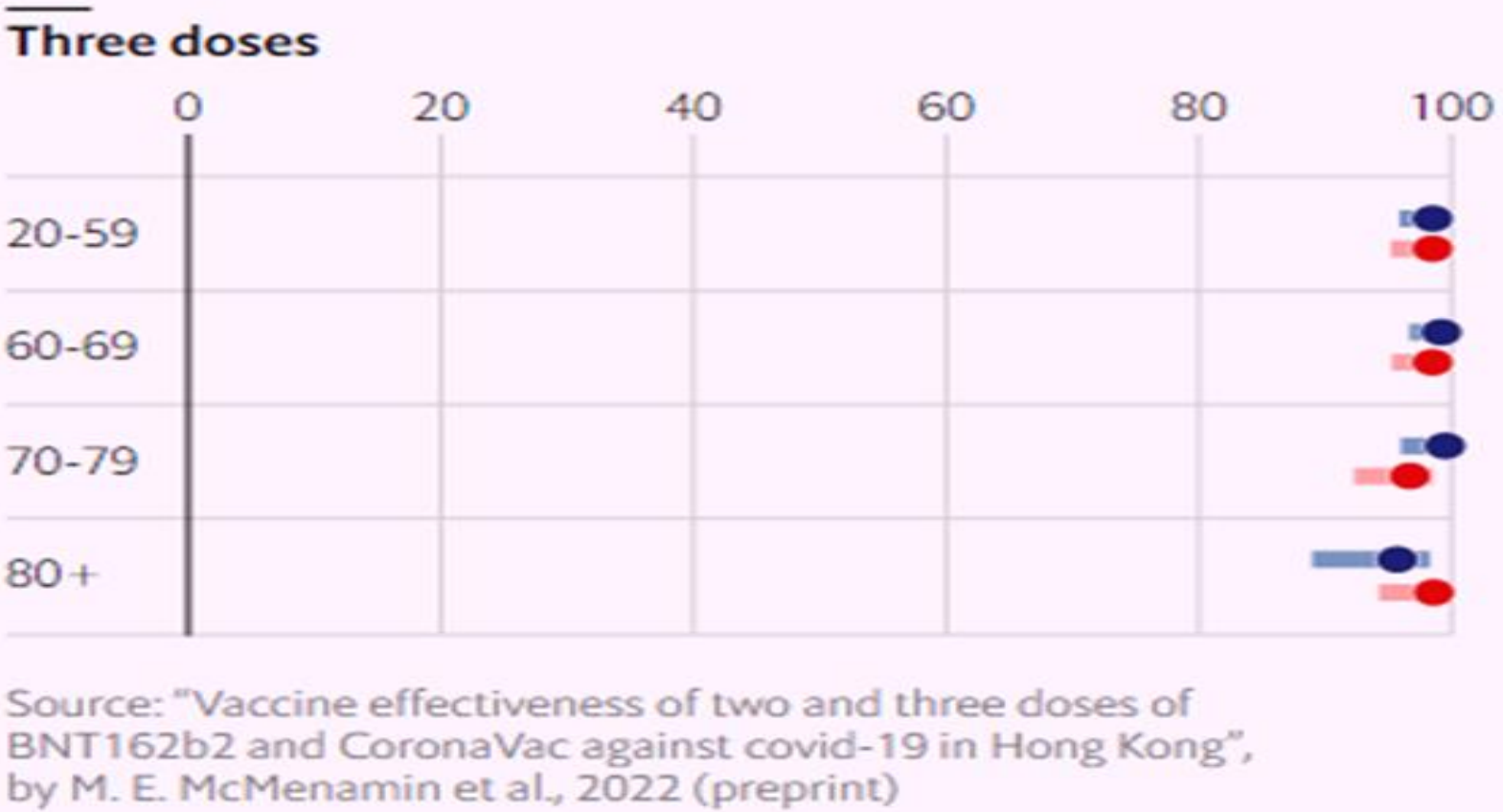

Source: "Vaccine effectiveness of two and three doses of BNT162b2 and CoronaVac against covid-19 in Hong Kong", by M. E. McMenamin et al., 2022 (preprint)

Omicron-specific COVID-19 vaccine

- A raft of early animal studies suggest that Omicron-specific boosters offer no advantage over a third dose of current vaccines
- Omicron-specific mRNA vaccine induced potent neutralizing antibody against Omicron but not other SARS-CoV-2 variants.
- Bivalent vaccine composed of both Omicron and Delta RBD-LNP generated antibody with broadly neutralizing activity against the wild-type virus and all variants.
- During preclinical studies, animals vaccinated with Omicron-specific inactivated vaccine can generate a high level of neutralizing antibodies against the variant. The vaccine also boosted protection against the original strain and other mutations, including the Beta and Delta strains. China will perform “sequential trial” on fully vaccinated individual.
- Vaccine under trial
  - BioNTech: mRNA vaccine
  - Moderna: bivalent mRNA vaccine
  - Sinovac: inactivated vaccine
  - Sinopharm (China National Biotech Group) : inactivated vaccine
  - China's Suzhou Abogen Biosciences Co: mRNA vaccine

Thank you for your attention

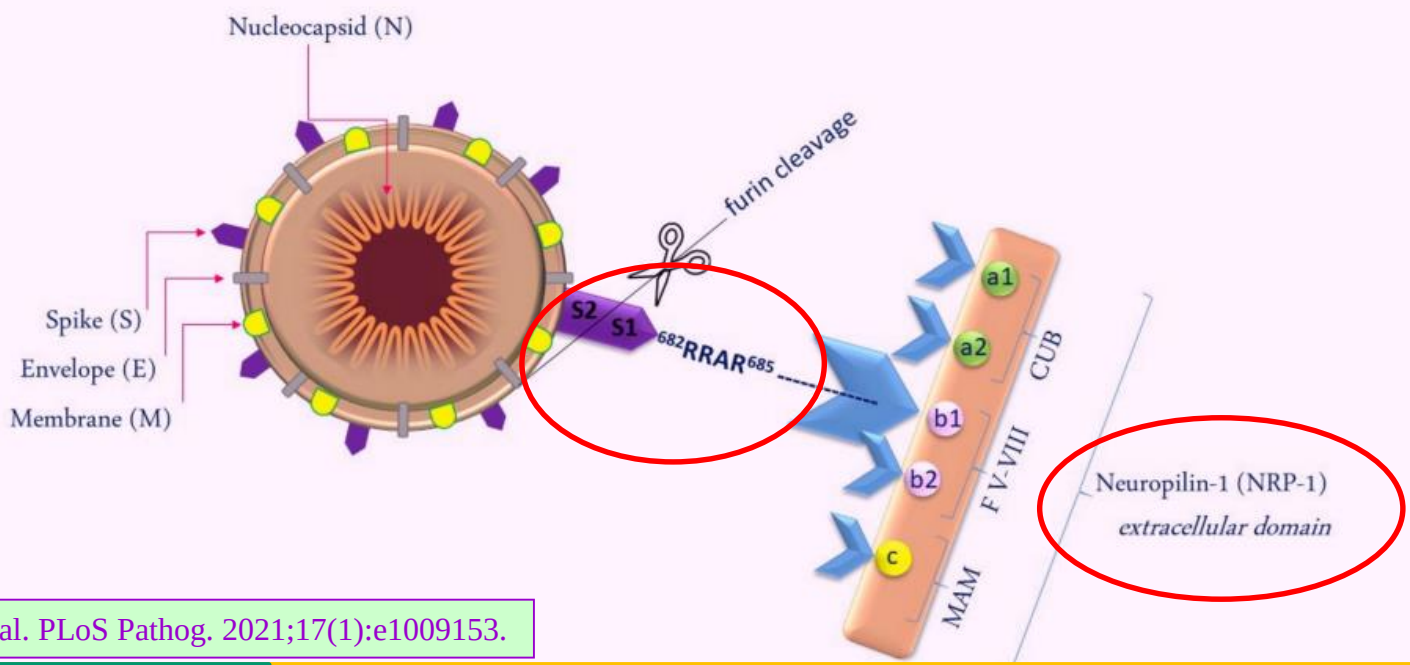

Mayi BS, et al. PLoS Pathog. 2021;17(1):e1009153.

Co-receptors

Epithelium

Endothelium

De Pasquale V, Int J Mol Sci. 2021 Jun 18;22(12):6574.

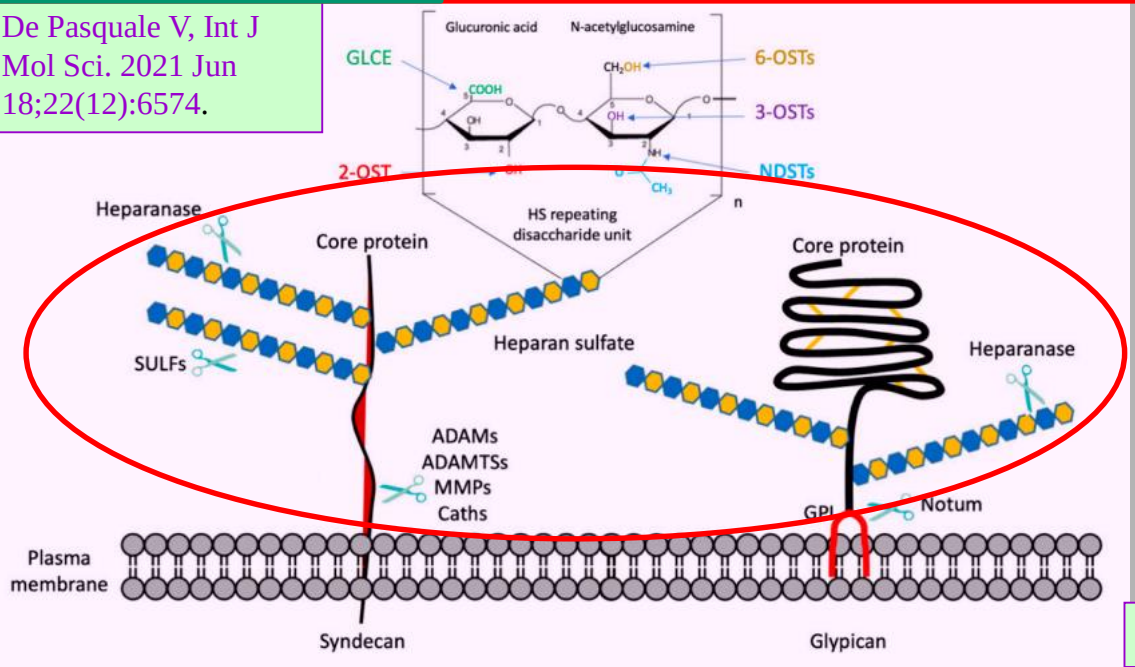

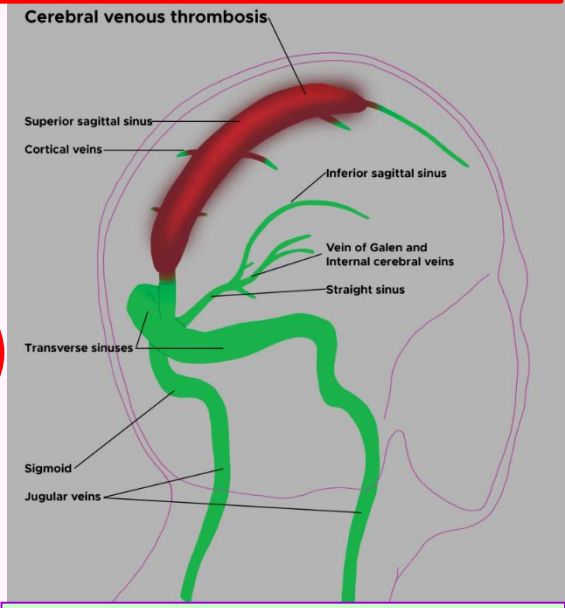

Prasanna Tadi, StatPearls

Hong Kong does not want to take any chances

BIRD-FLU SCARE SWEEPS HONG KONG!

MILLION CHICKEN MASSACRE

Highly Pathogenic H5N1 Avian Influenza 1997

Multiple basic amino acids adjacent to the HA cleavage site allow cleavage by furin

–RRRKK– insertion at the cleavage loop of the hemagglutinin H5

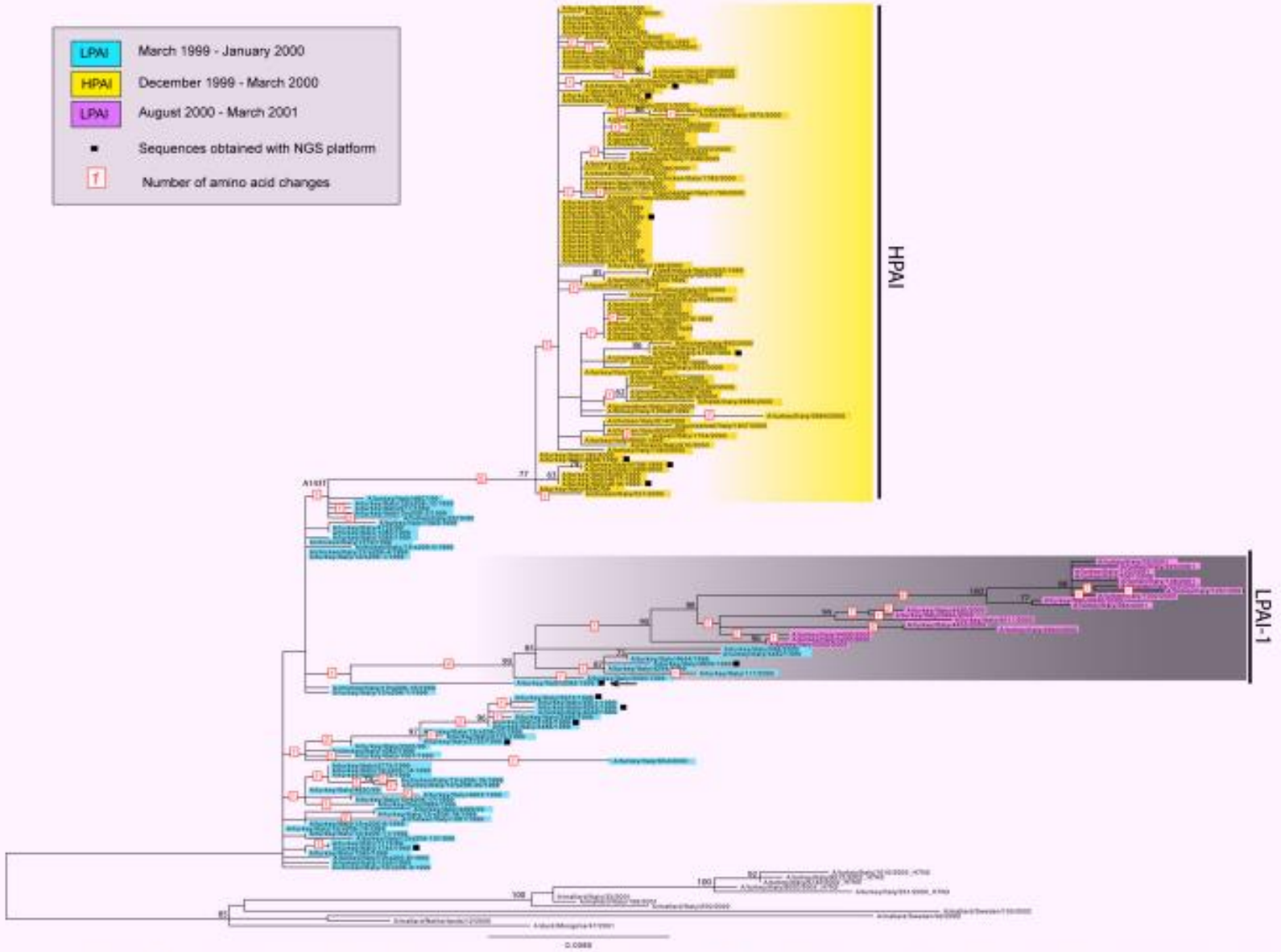

ML tree of the HA gene segment of H7N1 avian influenza virus. Viruses are colored blue for LPAI viruses collected from March 1999 to January 2000, pink

Monne I, et al. Emergence of a highly pathogenic avian influenza virus from a low-pathogenic progenitor. J Virol. 2014;88(8):4375-4388.

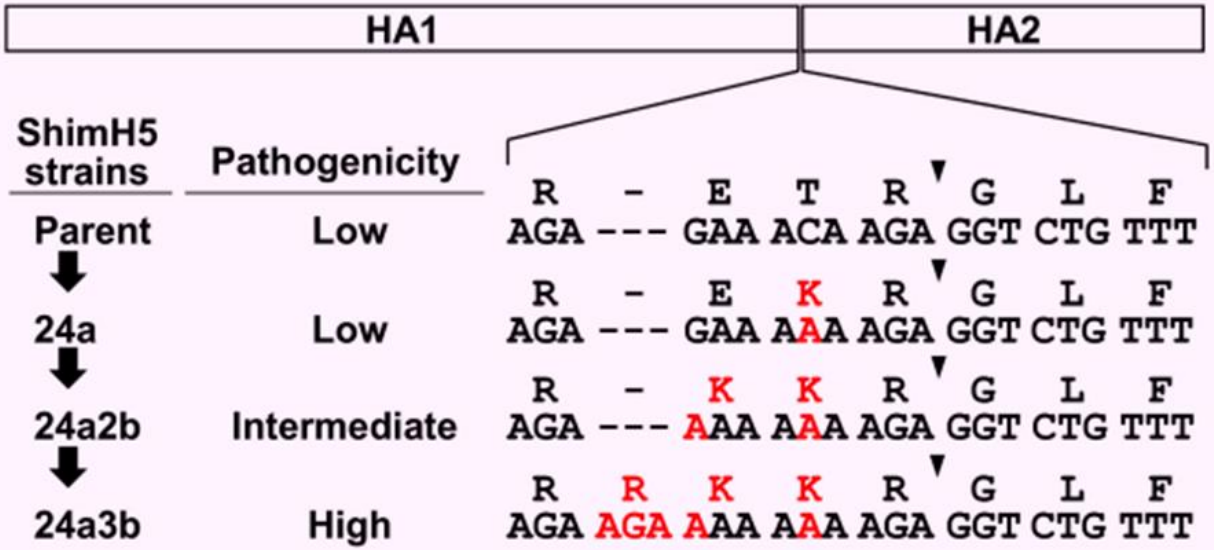

HA cleavage site sequences of ShimH5 and its variants passaged in chickens. HA was synthesized as a single polypeptide and then cleaved into HA1 and HA2 subunits at the cleavage site (indicated by arrowheads). ShimH5 and its variants (parent, 24a, 24a2b, and 24a3b) strains have different nucleotide and amino acid sequences at their HA cleavage sites and different pathogenicities for chickens (26). Nucleotide sequences at positions 1043 to 1063 (ShimH5 parent, 24a, and 24a2b) and 1043 to 1066 (24a3b) and the corresponding amino acid sequences are shown. Dashes are included to adjust the sequence alignment, and nucleotides and amino acids different from those of the parental ShimH5 sequence are shown in red.

Nao N, et al mBio. 2017 Feb 14;8(1):e02298-16.

RNA editing-like activity is the key mechanism for nucleotide insertions. Consecutive adenine residues and a stem-loop structure are important for nucleotide insertions into this RNA region around the cleavage site. These are frequently found in the viral RNA region encoding amino acids around the cleavage site of low-pathogenic H5 and H7 avian influenza viruses isolated from waterfowl reservoirs but not H1, H2, H3, and H4 avian influenza viruses. This provide a clue as to why the acquisition of the polybasic HA cleavage site is restricted to the particular HA subtypes.

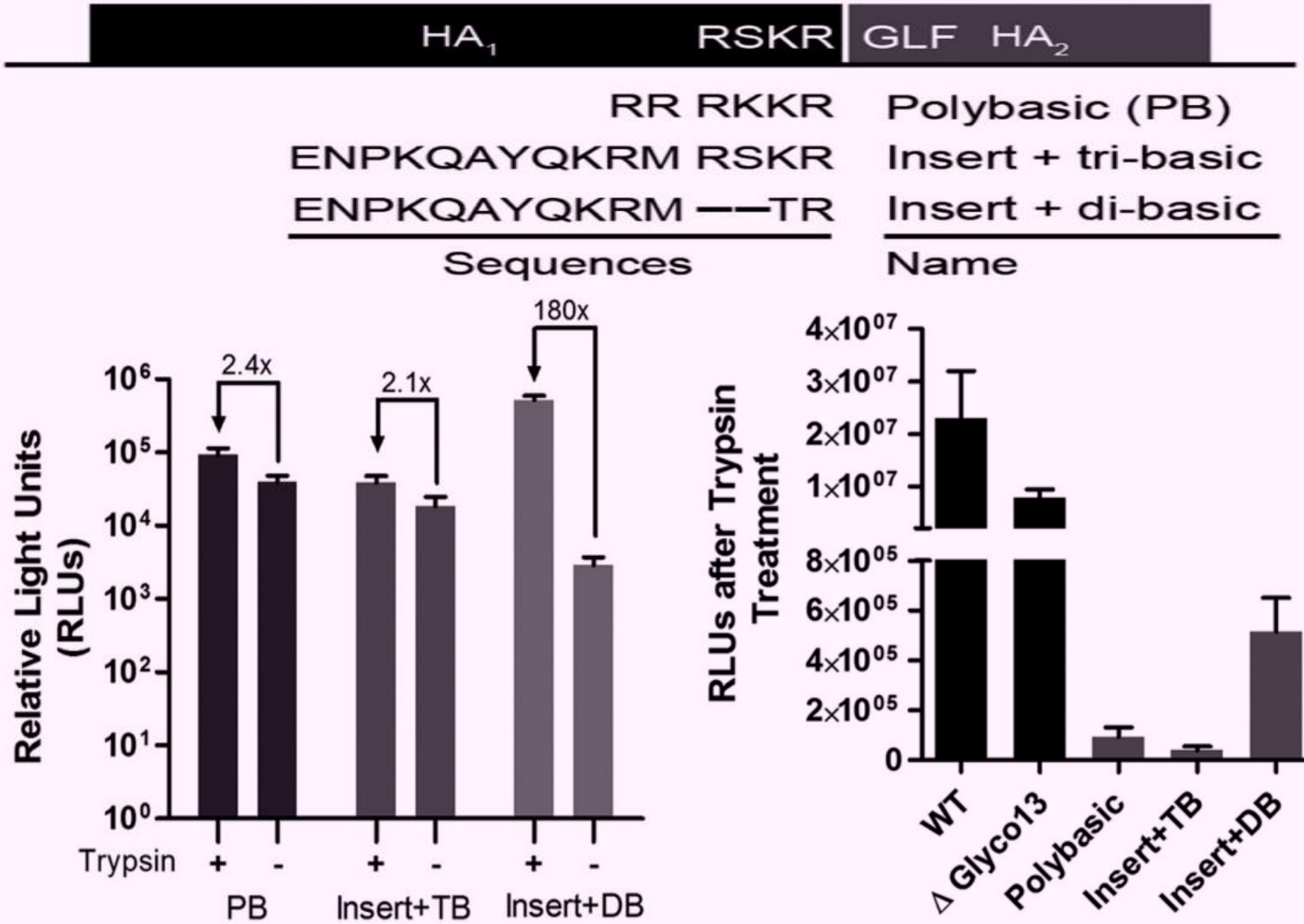

Efficient cleavage activation of an H9 HA by endogenous furin can be achieved by a combination of a tribasic cleavage site (R-S-K-R) and a loss of a glycosylation site at HA_1 residue 13.

Tse LV, Hamilton AM, Friling T, Whittaker GR. A novel activation mechanism of avian influenza virus H9N2 by furin. *J Virol*. 2014;88(3):1673-1683.

Reassortant H5N1

21/6/2012

H5N1

22/6/2012

Species Specificity of NS of Influenza !!!!

No experiment on human cell lines !

Furin

TMPRSS2 pathway

Camostat mesylate
Nafamostat

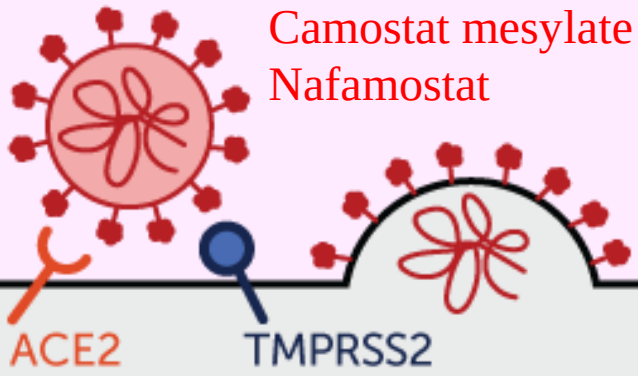

Ciliated and secretary cells
Type I alveolar epithelial cells (AT1)
Increased with aging
Androgen dependent
Increased by IL-13 (atopic asthma)
(decrease ACE2)

Cell-cell fusion

Chloroquine
Hydroxychloroquine

Teicoplanin

Cathepsin pathway

The IC50 of hydroxychloroquine against SARS-CoV-2 was increased by 5- to 60-fold for low and high TMPRSS2-expressing cells, respectively

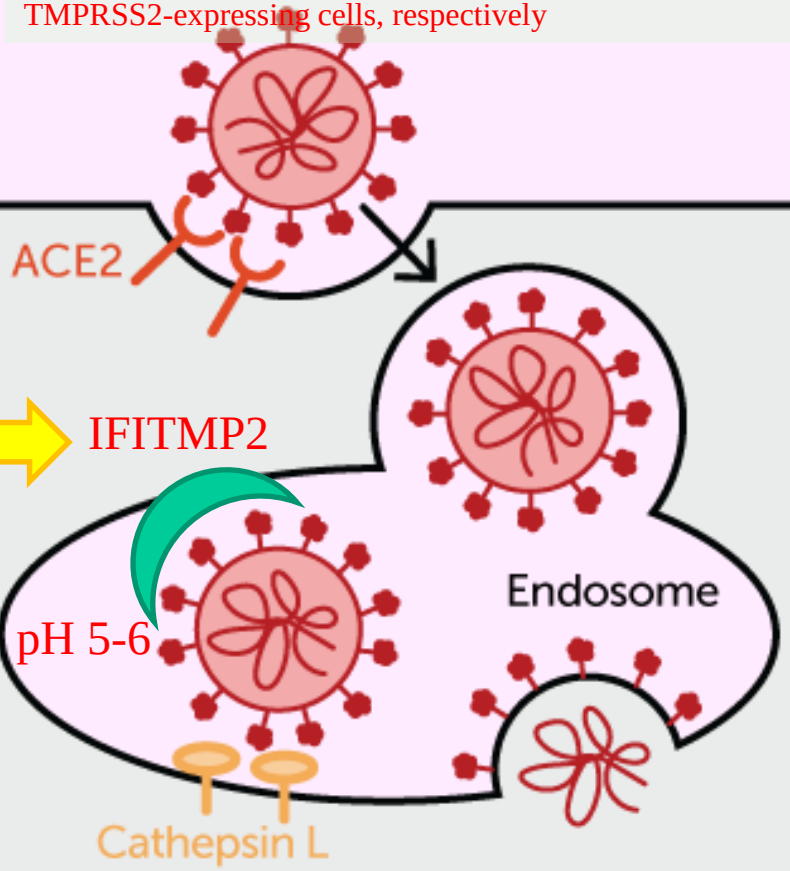

Presence of a furin cleavage site at the S1/S2 junction is not uncommon in human coronaviruses; while half of human seasonal coronaviruses as well as MERS-CoV contain furin cleavage site, the remaining strains and SARS-CoV do not

https://www.sciencenews.org/article/covid-coronavirus-omicron-variant-mutation-infectious

Comparative sequences of envelope protein cleavage site(s) in coronaviruses (above) and in other RNA viruses (below). Empty boxes: no consensus motif detected..

Coronavirus	S1/S2, site 1	S1/S2, site 2	S2'
2019-nCoV	SPRRAR↓SVAS	IAY↓TMS	SKPSKR↓SF
CoV-ZX21	TASILR↓STGQ	IAY↓TMS	SKPSKR↓SF
Bat-AC45	TASILR↓STGQ	IAY↓TMS	SKPSKR↓SF
SARS-CoV	TVSLLR↓STGQ	IAY↓TMS	LKPTKR↓SF
BM48-31	SSTLVR↓SGGH	LAY↓TMS	LKPTKR↓SF
HKU9-1	ADSLPR↓LQLV	VNY↓DPL	GATTYR↓SA
MERS-CoV	TPRSCR↓SVPG		GSRSAR↓SA
HKU1	SRRKRR↓SISA		CGSSSR↓SF
HCoV-OC43	KNRRSR↓GAITT		SKASSR↓SA
HCoV-229E	IAVQPR↓NVSYD		SRVAGR↓SA
HCoV-NL63	IPVRPR↓NSSDN		SRIAGR↓SA

Virus	Envelope Protein	Cleavage site
HIV	Gp160	VQREKR↓AV
Influenza Virus H5	HA	RKRKKR↓GL
Avian H5N1 A/HK/98	HA	RERKRKKR↓GL
Avian H5N1 TKY/ENG	HA	NTPQRKKR↓GL
Human CMV	gB	HKRTKR↓ST
Human RSV	F protein	KKRKRR↓FL
Yellow Fever Virus	PrM	SRRSRR↓AI
Zika Virus	PrM	ARRSRR↓AV
Ebola virus	GP	GRRTRR↓EA
2019-nCoV (S1/S2) site	Spike Protein	TNSPRRAR↓SV
2019-nCoV (S2') site	Spike Protein	SKPSKR↓SF

Furin promoter can be upregulated by 3- to 400-fold under hypoxia and iron depletion conditions. Viral , Staphylococcus and Pseudomonas infection can induce hypoxia-inducible factor 1 (HIF-1) leading to upregulation of furin. Tse LV, et al. *J Virol*. 2014;88(3):1673-1683

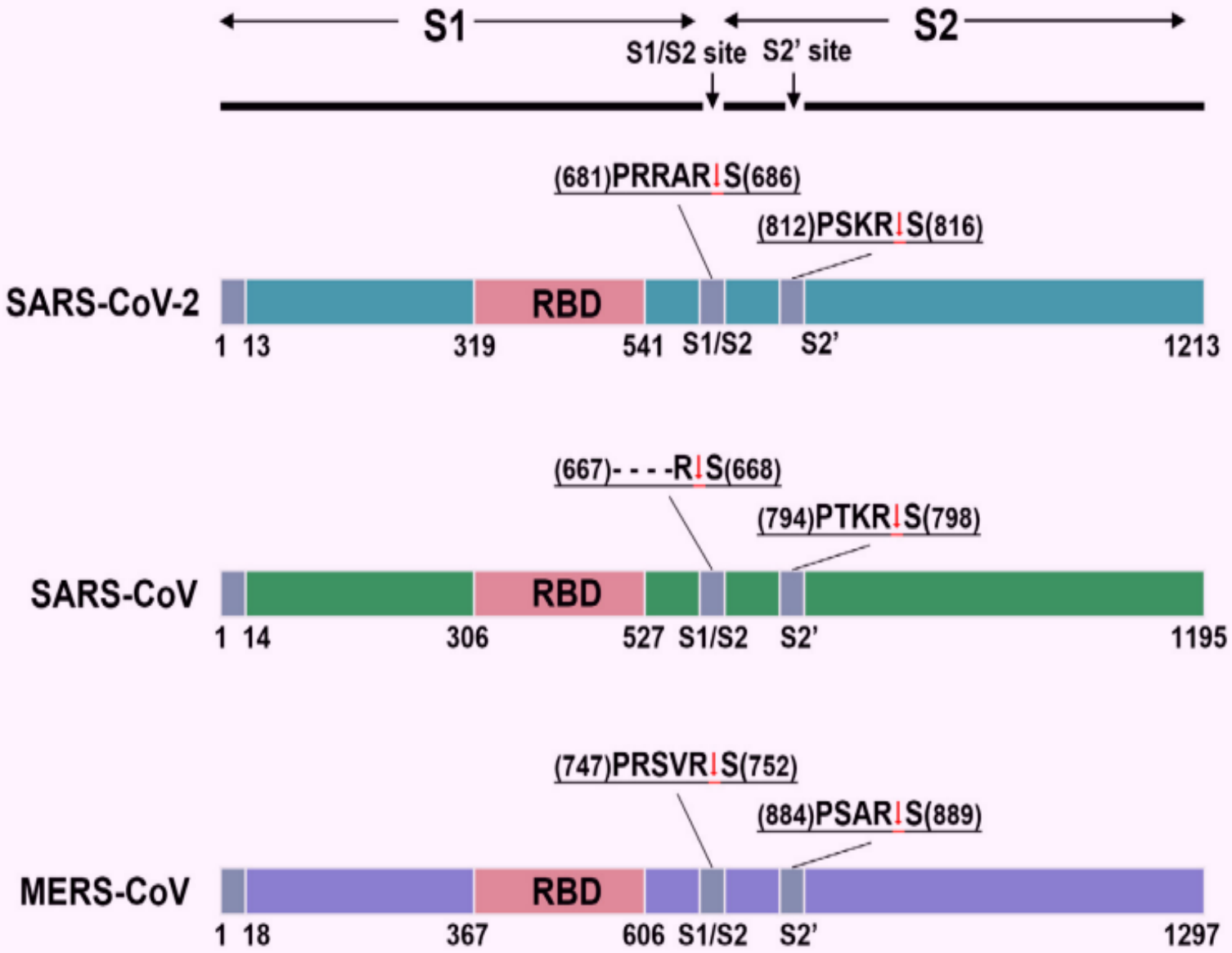

Hao W, Ma B, Li Z, Wang X, Gao X, Li Y, Qin B, Shang S, Cui S, Tan Z. Binding of the SARS-CoV-2 spike protein to glycans. Sci Bull (Beijing). 2021 Jun 30;66(12):1205-1214.

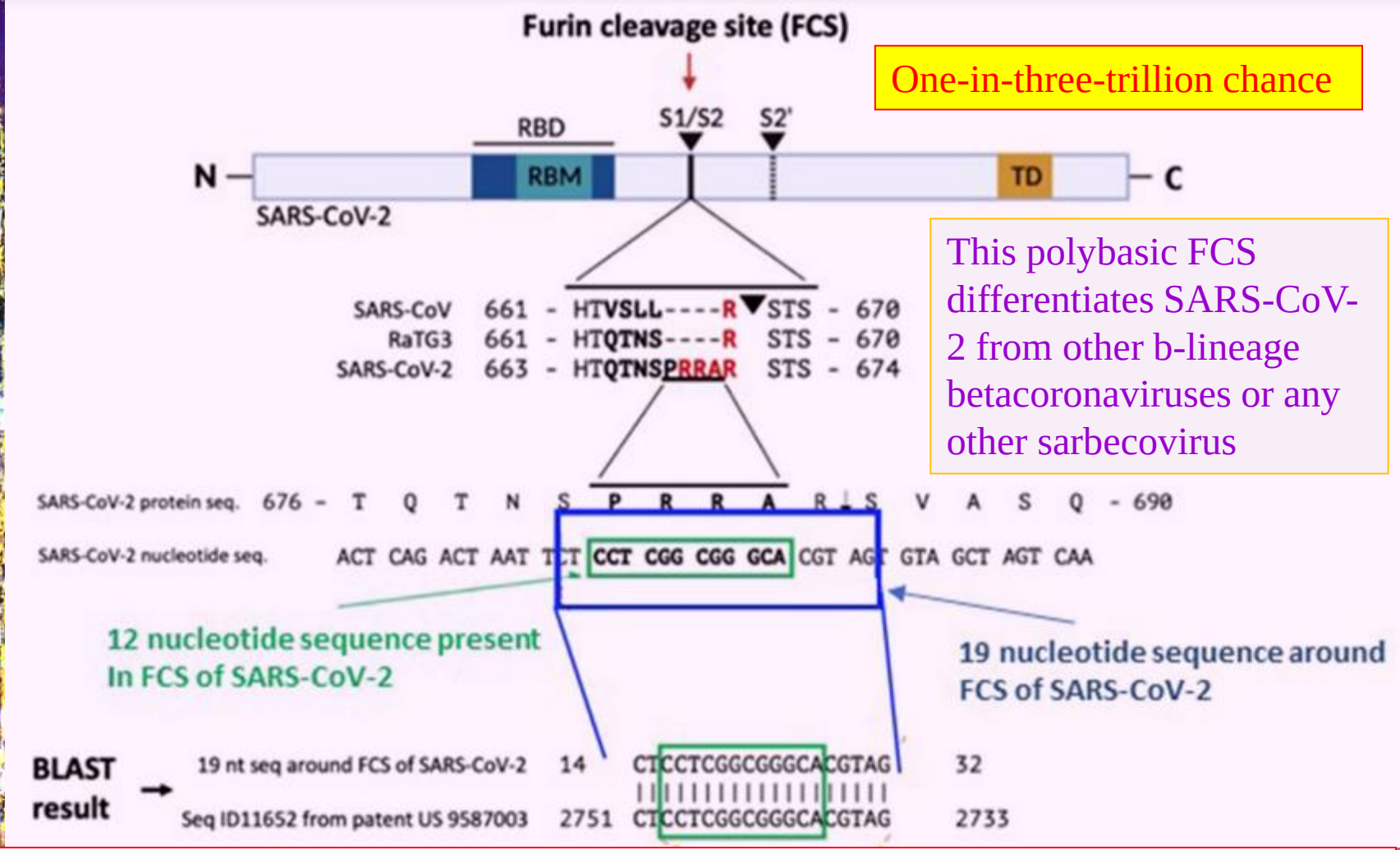

The 19-nucleotide sequence including 12 nucleotides coding for the FCS PRRA is a 100% complementary match to a codon-optimized proprietary sequence (Seq ID11652) that is the reverse complement of the human mutS homolog (MSH3). Seq ID11652 is patented (US 958 7003) by Moderna in February 2016. SEQ ID11652 is transcribed to a MSH3 mRNA that appears to be codon optimized for humans. This 19-nucleotide sequence CTCCTCGGCGGGCACGTAG is not found in any eukaryotic or viral genomes except SARS-CoV-2.

The chance occurrence of such mutation through natural evolution is 1 in 3.21×10^{-11}

Ambati BK, Varshney A, Lundstrom K, Palú G, Uhal BD, Uversky VN and Brufsky AM (2022) MSH3 Homology and Potential Recombination Link to SARS-CoV-2 Furin Cleavage Site. *Front. Virol.* 2:834808.

Cleavage of S protein by furin generates a **polybasic Arg-Arg-Ala-Arg** carboxyl-terminal sequence on S1 that binds to cell surface **neuropilin-1 (NRP1) receptors**

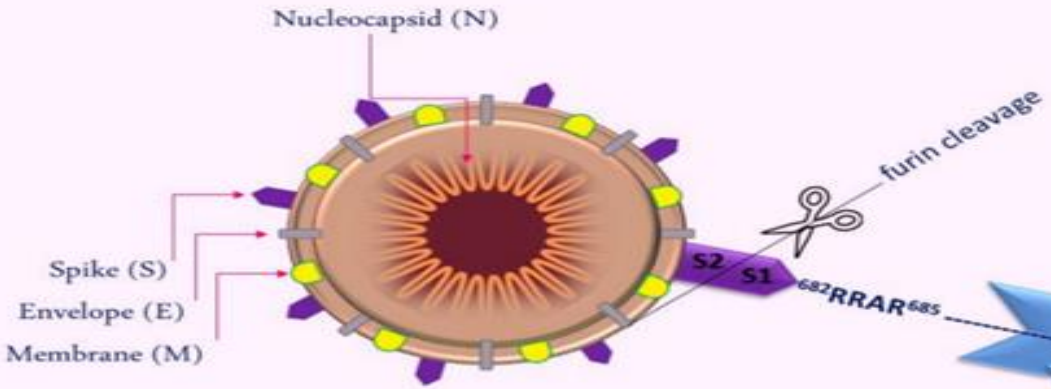

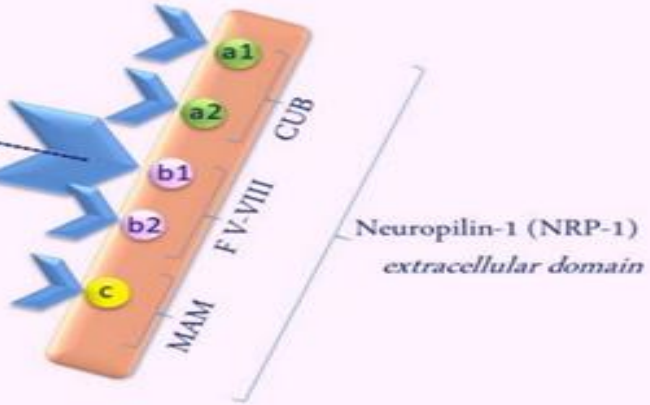

Neuropilin-1 (NRP1), which is known to bind furin-cleaved substrates, potentiates SARS-CoV-2 infectivity. NRP1 is abundantly expressed in the respiratory and olfactory epithelium, with highest expression in endothelial cells and in the epithelial cells facing the nasal cavity.

SARS-CoV-2 entry into host cells depends on NRP-1.

Human airway epithelial cell

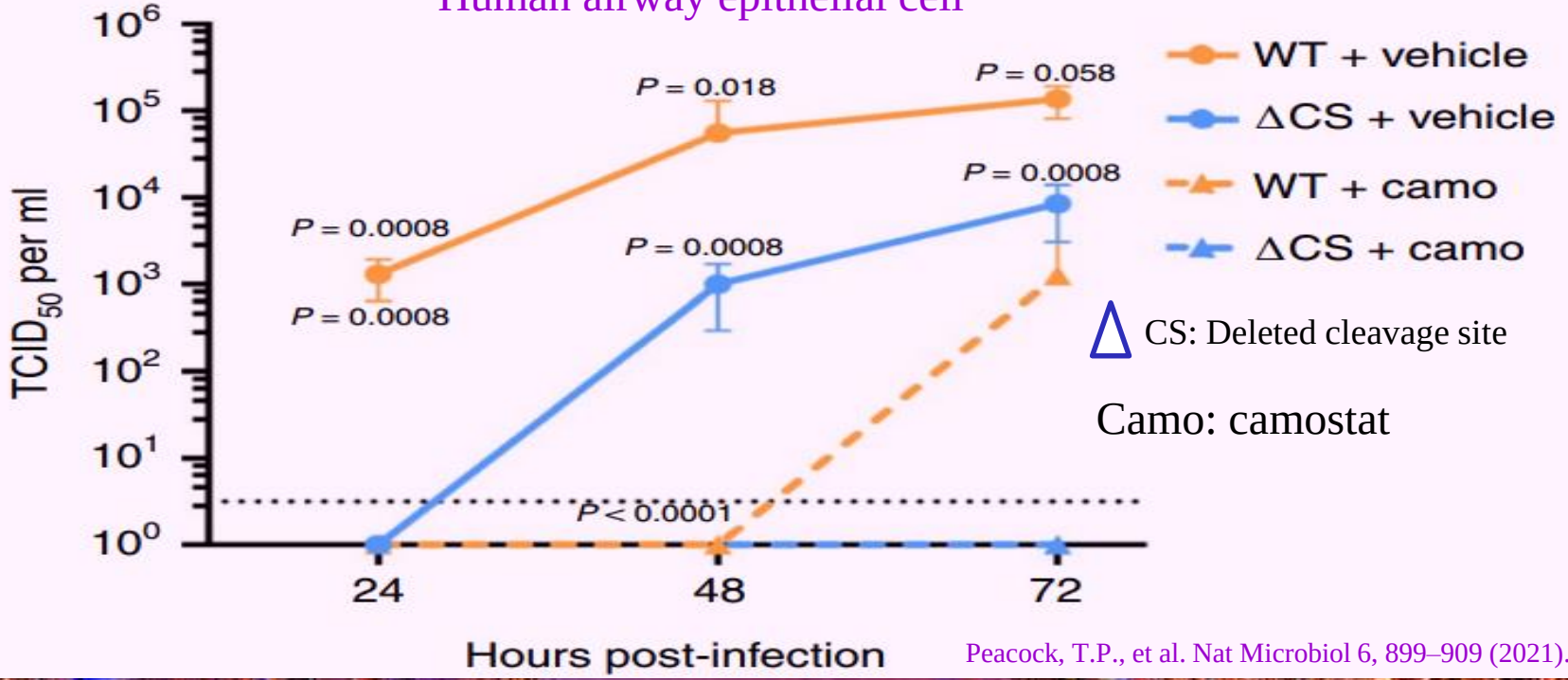

Δ CS: Deleted cleavage site

Camo: camostat

Peacock, T.P., et al. Nat Microbiol 6, 899–909 (2021).

The furin cleavage site in the SARS-CoV-2 spike protein is required for transmission in ferrets

Peacock TP, et al. Nat Microbiol. 2021 Jul;6(7):899-909.

The disruption of the furin cleavage site in the SARS-CoV-2 spike protein was identified as the most promising strategy to produce live-attenuated SARS-CoV-2 vaccines

Lewandowski, P. etal. The Reassessed Potential of SARS-CoV-2 Attenuation for COVID-19 Vaccine Development—A Systematic Review. Viruses 2022, 14, 991.

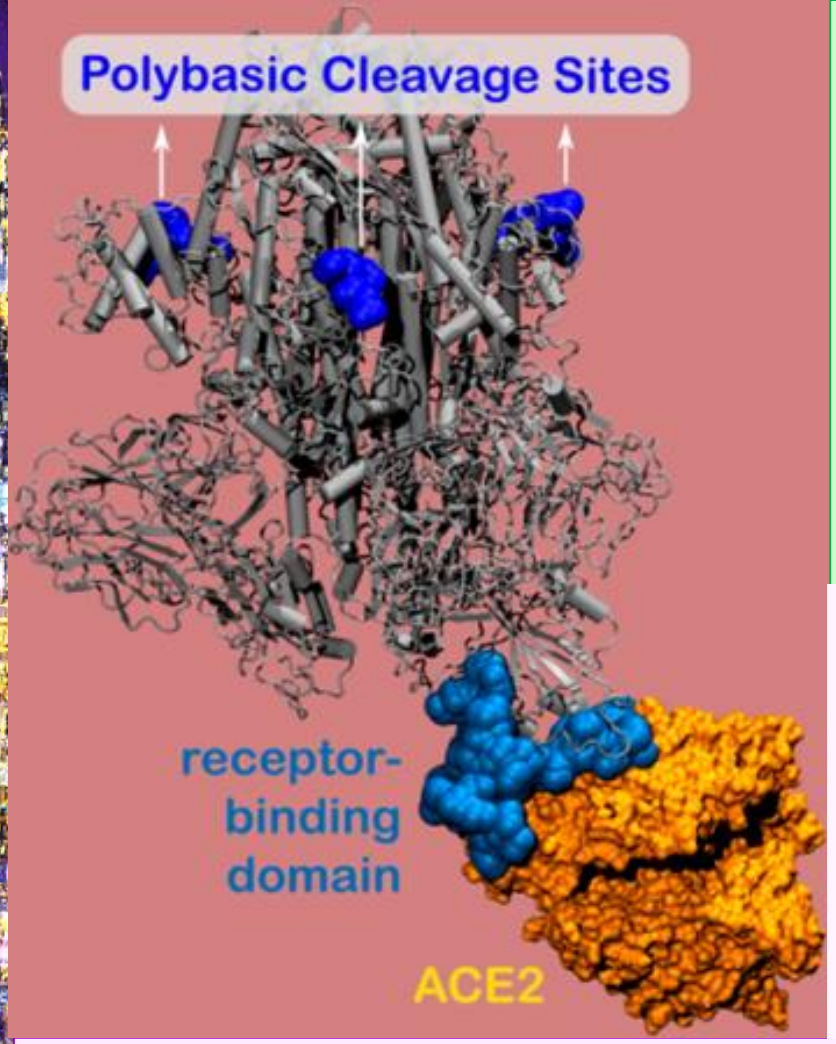

The affinity constant for the receptor binding domain (RBD) of SARS-CoV-2 to ACE2 is greater than that of SARS-CoV by as much as a factor of 10 to 15, and the furin recognition sequence “RRAR” at the S1–S2 cleaving site of SARS-CoV-2 represents a near-optimal match for the cellular serine protease TMPRSS2. Both factors contribute to the efficiency of virus transmission, making COVID-19 more contagious than infections by SARS-CoV and the influenza virus.

Wang Y, et al.Proc Natl Acad Sci U S A. 2020 Jun 23;117(25):13967-13974.

A stable salt bridge between Lys417 of SARS-CoV-2 S protein andAsp30 ofACE2 as well as three stable hydrogen bonds betweenTyr449,Gln493 and Gln498 of SARS-CoV-2 andAsp38,Glu35 and Lys353 ofACE2, which were absent in the ACE2–SARS-CoV interface enhance binding. Ali, A., et al. Sci Rep 10, 14214 (2020).

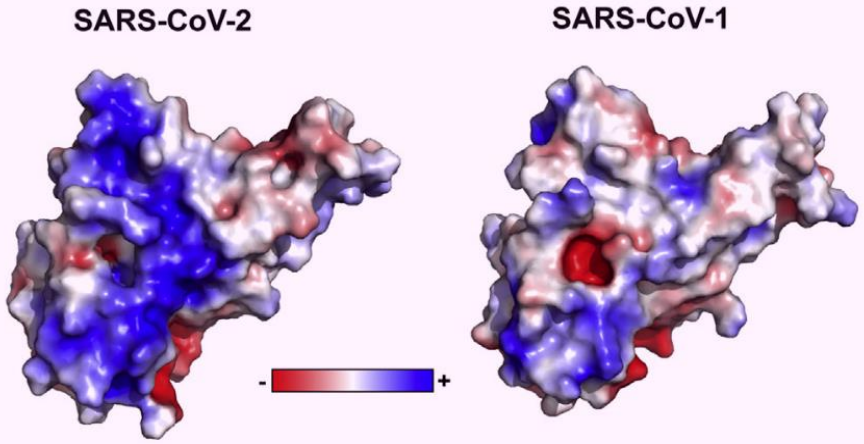

SARS-CoV and SARS-CoV-2 S proteins are both attractive to the negatively charged ACE2 by electrostatic force. Though distributed approximately 10 nm away from the RBD, the positively charged SARS-CoV-2 polybasic cleavage sites enhance, via electrostatic interactions and hydration, the RBD−ACE2 binding affinity.

Qiao B, et al.. Enhanced Binding of SARS-CoV-2 Spike Protein to Receptor by Distal Polybasic Cleavage Sites. *ACS Nano*. 2020;14(8):10616-10623.

Vaccination Status	Infection per 100,000 people (C.D.C)
Delta	
Unvaccinated	699.12
2 doses	104.8
Omicron	
Unvaccinated	3230.1
2 doses	1467.31
3 doses	1053.6

Changing charge

Mutations in the omicron spike protein (right) have made it more positively charged (blue) than the delta variant's spike (left). The charge attracts omicron toward the negatively charged ACE2 protein on human cells even across relatively large distances. Negative charges are shown in red and neutral parts of the protein in white.

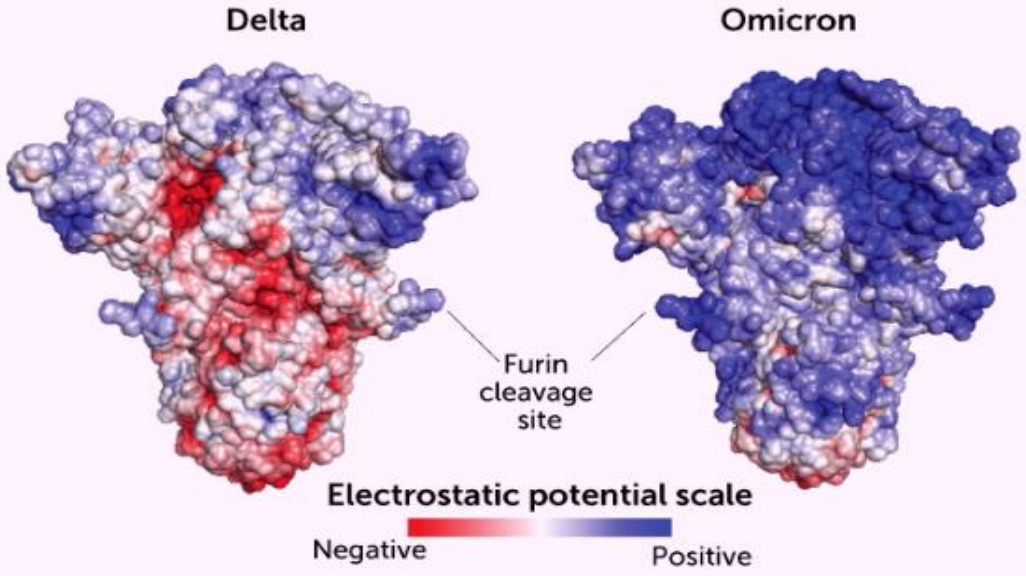

Omicron doesn't use the TMPRSS2 pathway efficiently and relies more on cathepsin L to get into cells
https://www.sciencenews.org/article/covid-coronavirus-omicron-variant-mutation-infectious

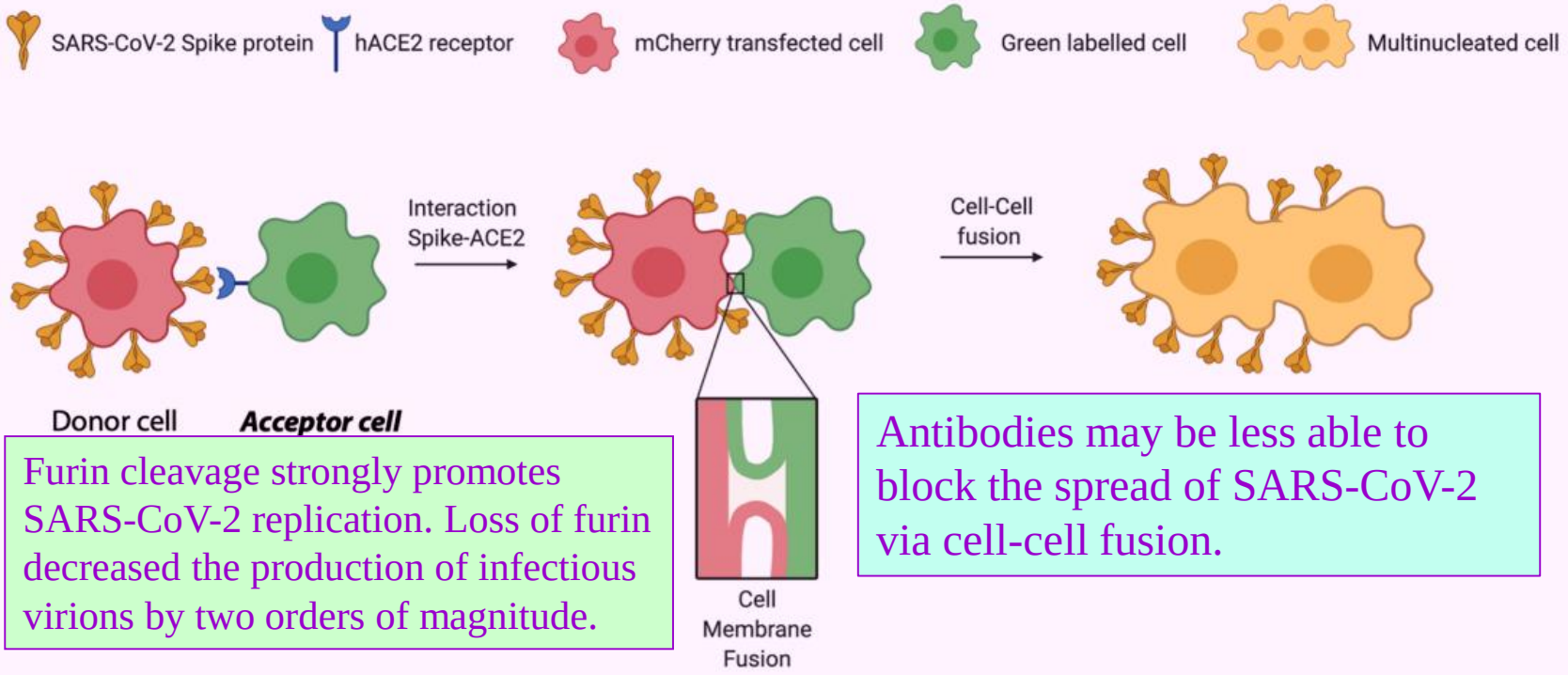

Furin cleavage strongly promotes SARS-CoV-2 replication. Loss of furin decreased the production of infectious virions by two orders of magnitude.

Antibodies may be less able to block the spread of SARS-CoV-2 via cell-cell fusion.

SARS-CoV-2 S protein possesses high fusogenic activity and is able to trigger large syncytia formation in vitro and in vivo, contrary to the S protein of two related coronaviruses SARS-CoV and MERS-CoV. SARS-CoV-2 S-mediated syncytia formation between uninfected and infected cells and between different cell types. TMPRSS2 may be rate limiting for cell-cell fusion and overexpression of TMPRSS2 promotes cell to cell fusion. TMPRSS2 protease is required on acceptor cells to trigger cell-cell fusion. TMPRSS2 processing of S at the S2' site is important in triggering cell-cell fusion. C**leavage at the multibasic site by furin or other proteases is essential for cell-cell fusion.**

Papa G, et al. Furin cleavage of SARS-CoV-2 Spike promotes but is not essential for infection and cell-cell fusion. PLoS Pathog. 2021 Jan 25;17(1):e1009246.

Thank you for your attention

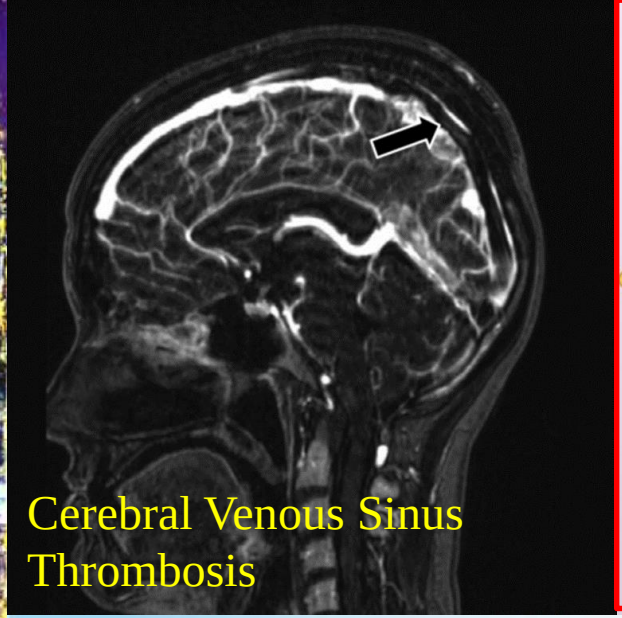

Cerebral Venous Sinus Thrombosis

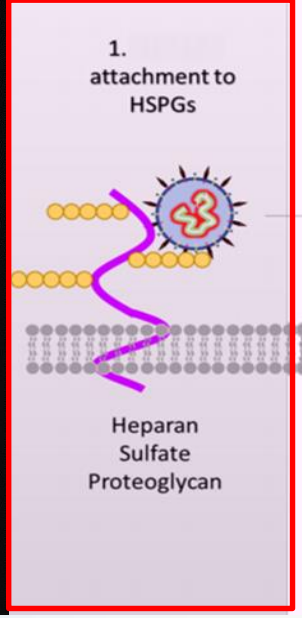

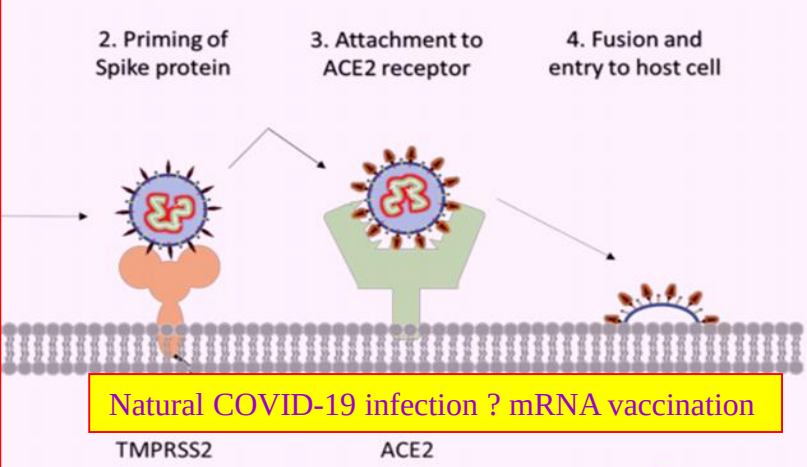

Natural COVID-19 infection ? mRNA vaccination

Vaccine-induced immune thrombotic thrombocytopenia
Adenovirus Vectored COVID-19 vaccine

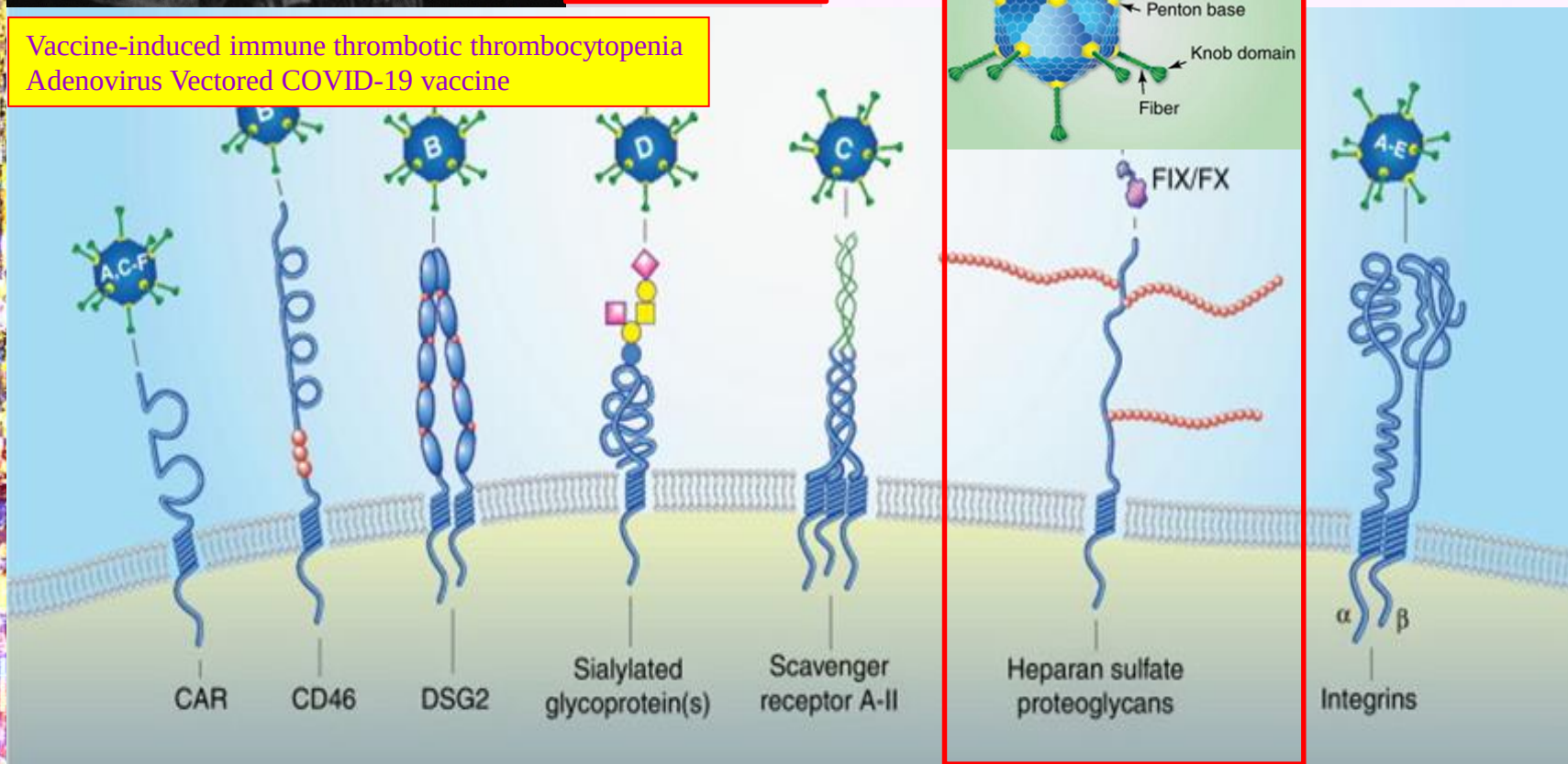

Cerebral Venous Sinus Thrombosis
(Within 2 week period after COVID-19 infection or vaccination)

	Incidence (per million population)
Background Rate	0.53-0.77
COVID-19 infection * (Patient with prior CVST excluded)	42.8 (35.3*)
Influenza infection	0
mRNA vaccination (BNT162b2 or mRNA-1273)	4.1
ChAdOx1 nCoV-19 ('Oxford-AstraZeneca') vaccination	5 (4-10)
Ad26.COV2.S ("Janssen") vaccination	1.7

Taquet M, Husain M, Geddes JR, Luciano S, Harrison PJ. Cerebral venous thrombosis and portal vein thrombosis: A retrospective cohort study of 537,913 COVID-19 cases. EClinicalMedicine. 2021 Sep;39:101061.

The Interplay of Host Heparan Sulfate Proteoglycans With Adenovirus Vectored COVID-19 Vaccine and SARS-CoV-2 In The Pathogenesis Of Cerebral Venous Sinus Thrombosis (脑静脉窦血栓)

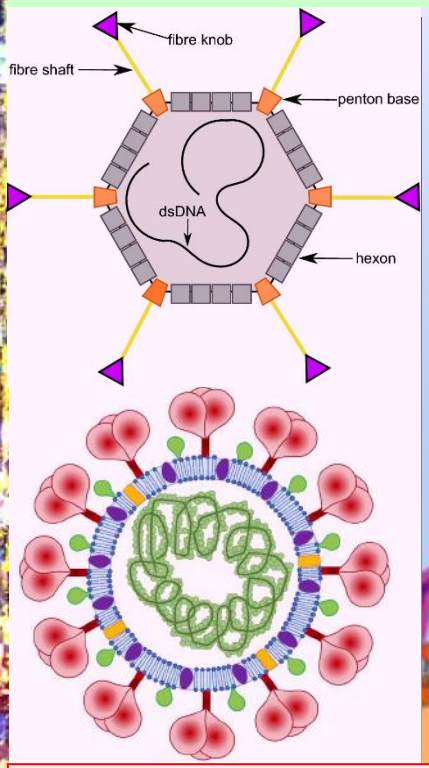

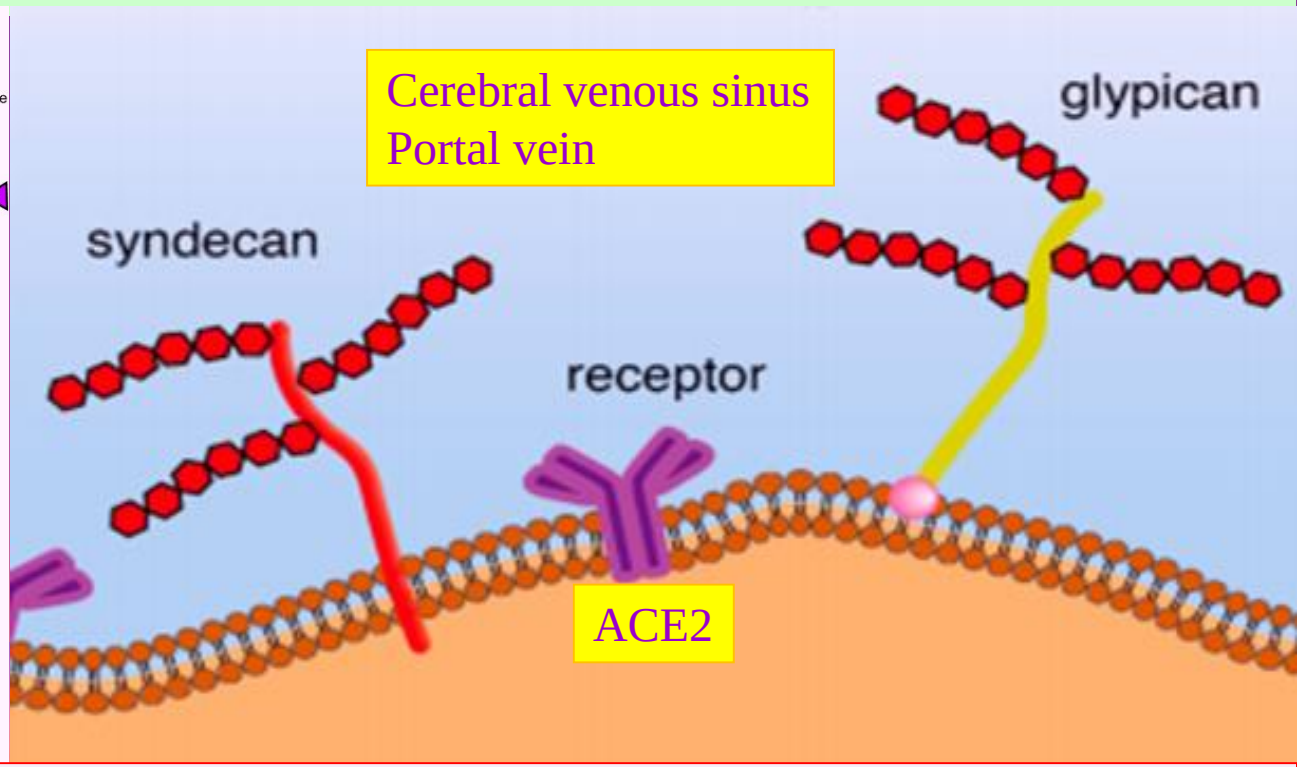

Angiotensin-converting enzyme 2 (ACE2) and heparan sulfate proteoglycans (HSPGs) are abundantly expressed on brain microvascular endothelial cells (BMECs). Chen R, et al. Front Neurol. 2021 Jan 20;11:573095. Bobardt et al. J Virol. 2004 Jun;78(12):6567-84.

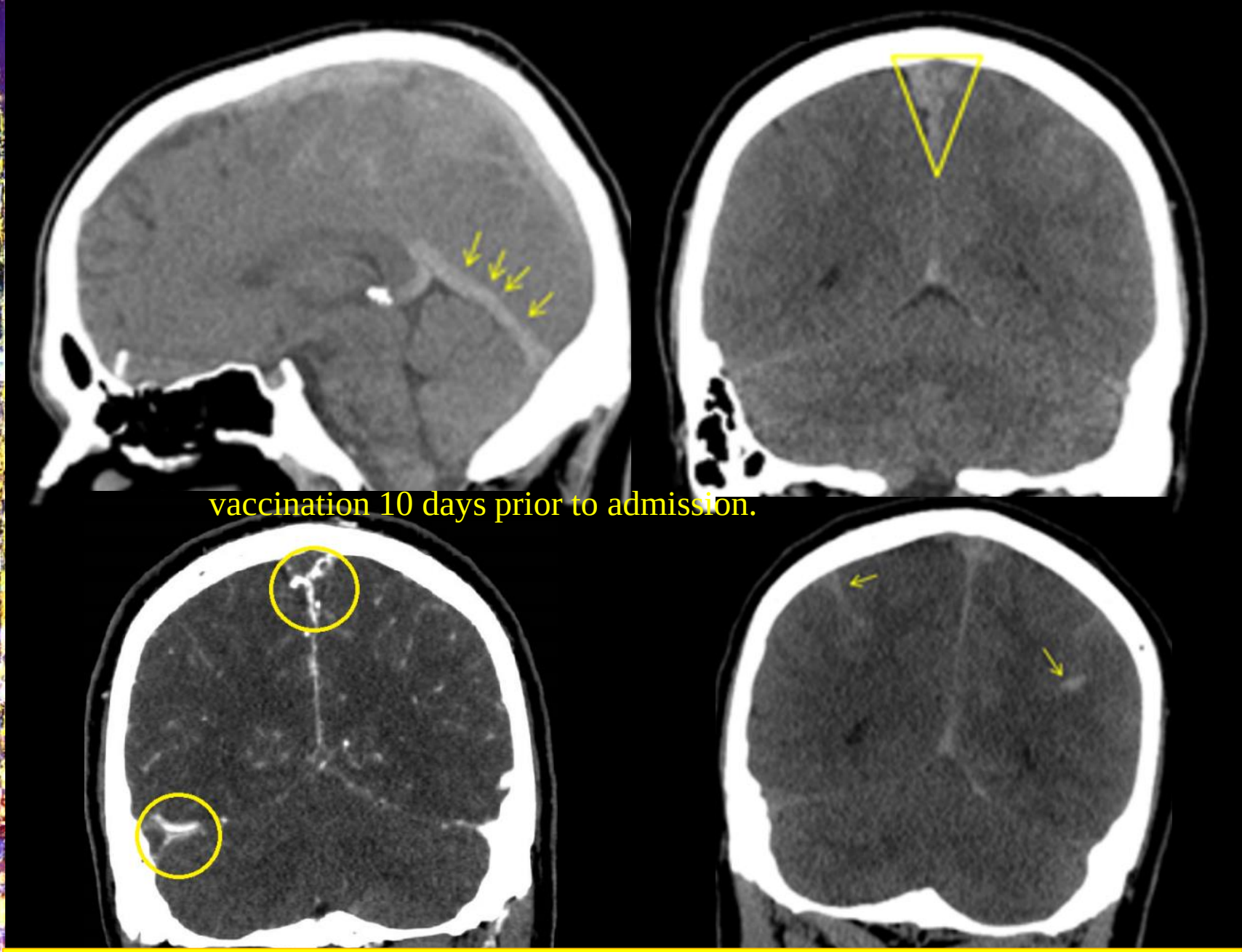

vaccination 10 days prior to admission.

Unchartered territory: Cerebral venous sinus and portal vein thrombosis (VITT) post ChAdOx1 nCoV-19 vaccination (10 days) Honida Mansour et al. Neuroradiology

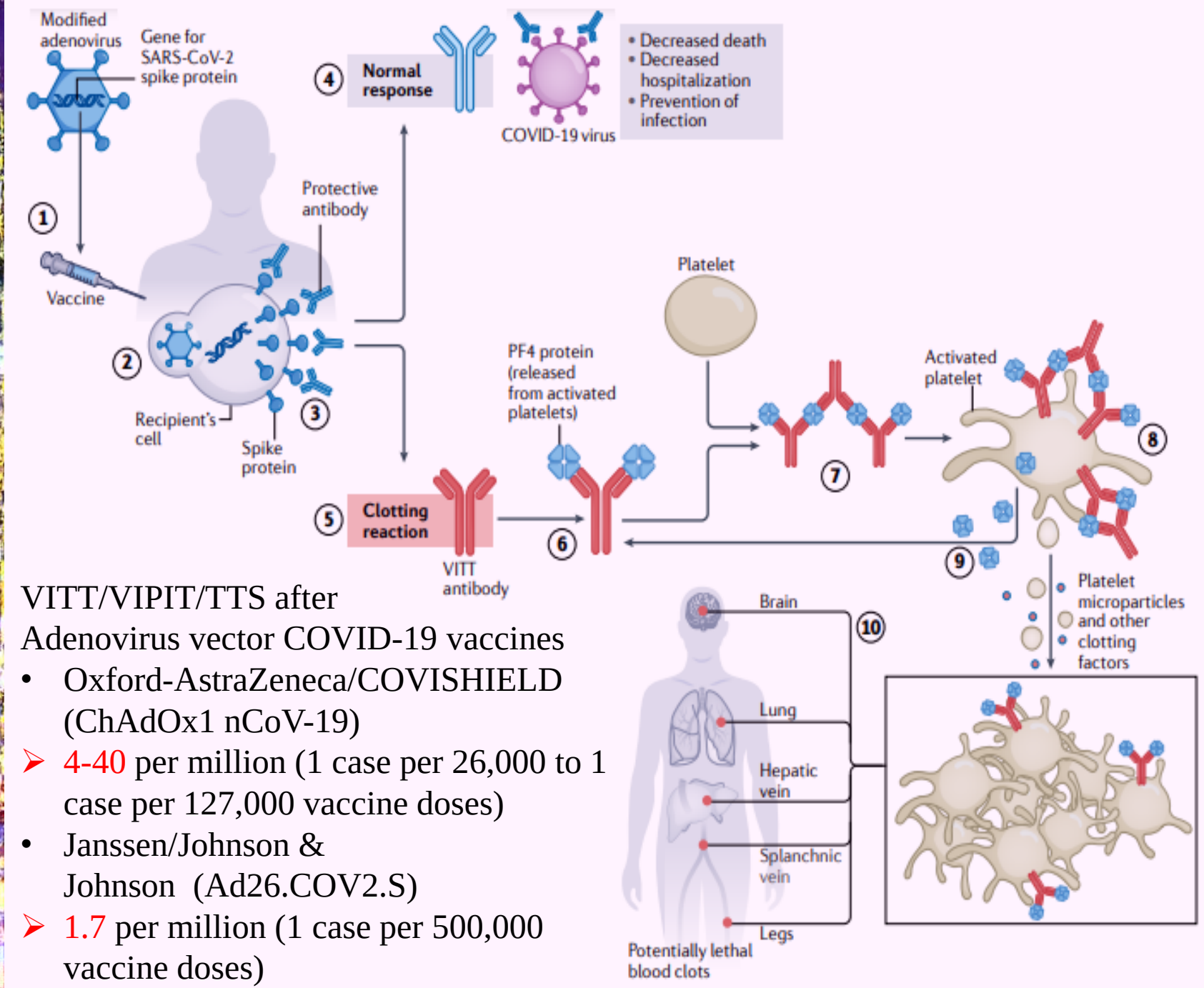

VITT/VIPIT/TTS after Adenovirus vector COVID-19 vaccines

- Oxford-AstraZeneca/COVISHIELD (ChAdOx1 nCoV-19)
  - ➢ 4-40 per million (1 case per 26,000 to 1 case per 127,000 vaccine doses)
- Janssen/Johnson & Johnson (Ad26.COV2.S)
  - ➢ 1.7 per million (1 case per 500,000 vaccine doses)

Overview of vaccine-induced immune thrombotic thrombocytopenia. In most people, administration of an

Autoimmune heparin-induced thrombocytopenia

- Can activate platelet strongly in the absence of heparin
- Platelet activation is inhibited at high heparin concentrations (10-100 IU mL^{-1} heparin)

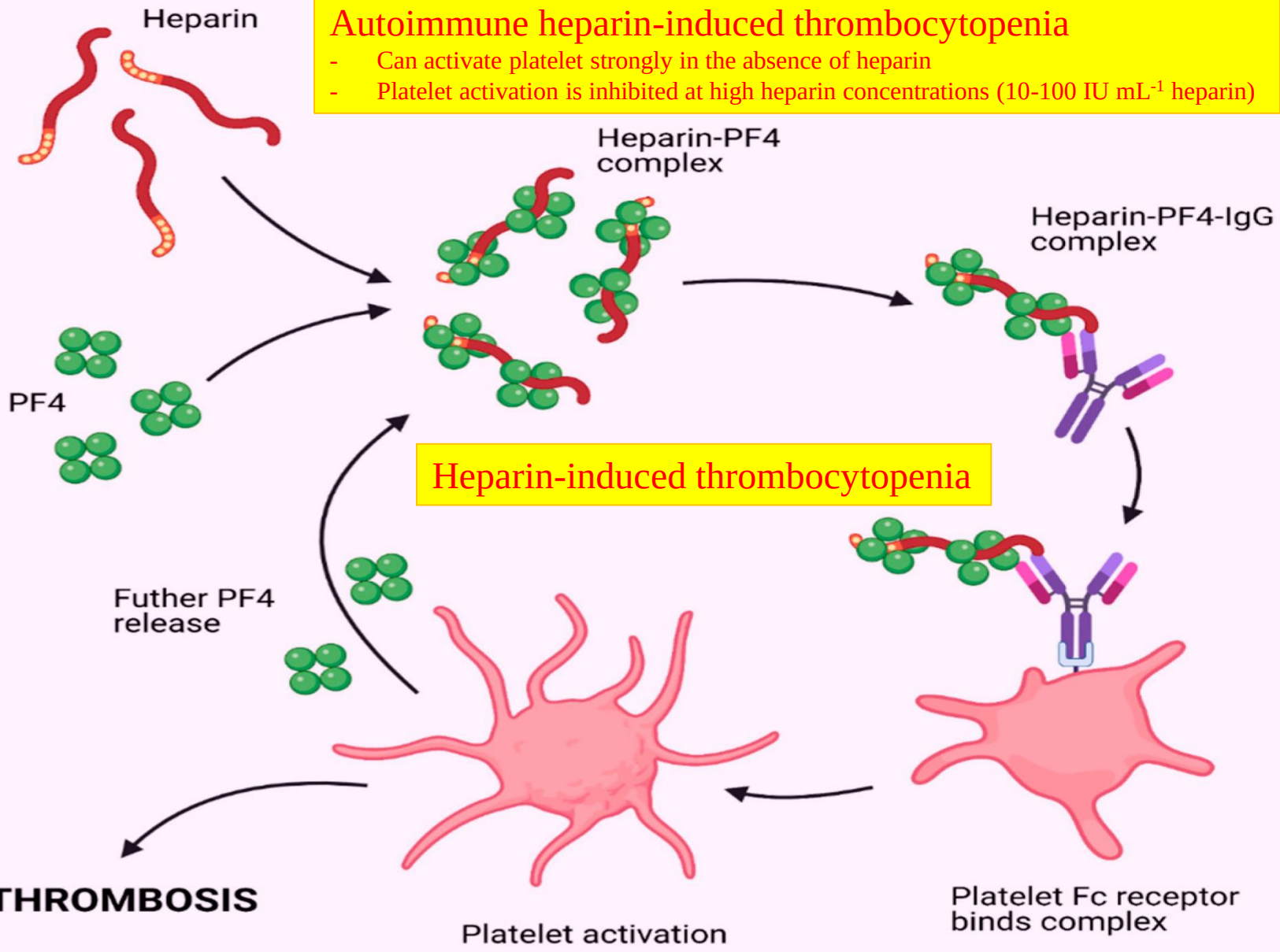

Vaccine-Induced Immune Thrombotic Thrombocytopenia (VITT)

Vaccine-Induced Prothrombotic Immune Thrombocytopenia (VIPIT)

Thrombotic Thrombocytopenia Syndrome (TTS).

Greinacher A, Thiele T, Warkentin TE, Weisser K, Kyrle PA, Eichinger S. Thrombotic Thrombocytopenia after ChAdOx1 nCov-19 Vaccination. N Engl J Med. 2021 Apr 9.

- Platelet-activating antibodies against platelet factor 4 in patients without previous exposure to heparin after ChAdOx1 nCov-19 vaccination.
- Clinical features mimicking autoimmune heparin-induced thrombocytopenia.
  - Serum from these patients activated platelets in the absence of heparin.
  - Platelet activation was inhibited by high levels of heparin.

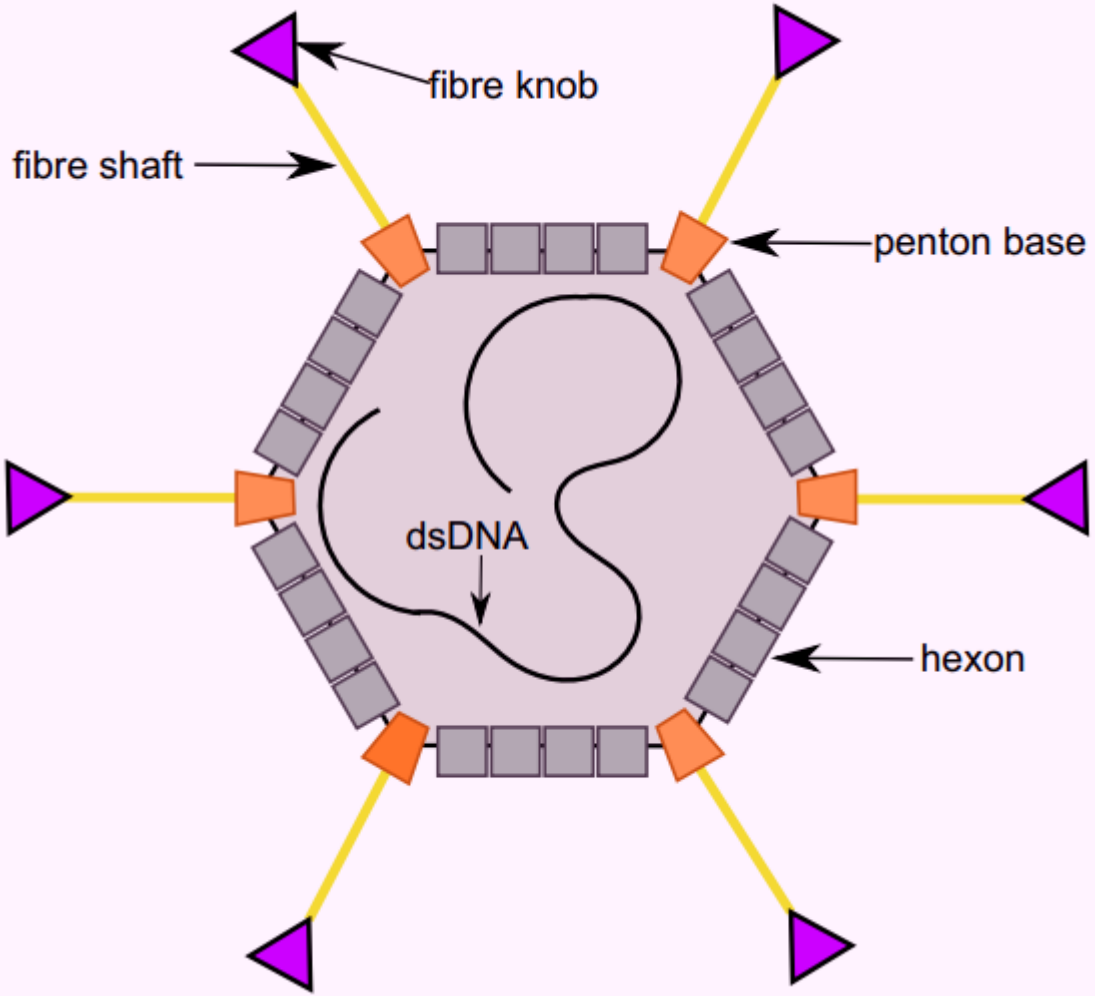

HAdVs engage two types of receptors: first, an attachment receptor that is bound by the fibre knob protein protruding from the icosahedral capsid, and next, an integrin entry receptor bound by the pentameric penton base at the capsid vertices.

Stasiak AC, Stehle T. Human adenovirus binding to host cell receptors: a structural view. *Med Microbiol Immunol*. 2020;209(3):325-333.

The diversity of HAdV receptors contributes to the broad tropism of these viruses

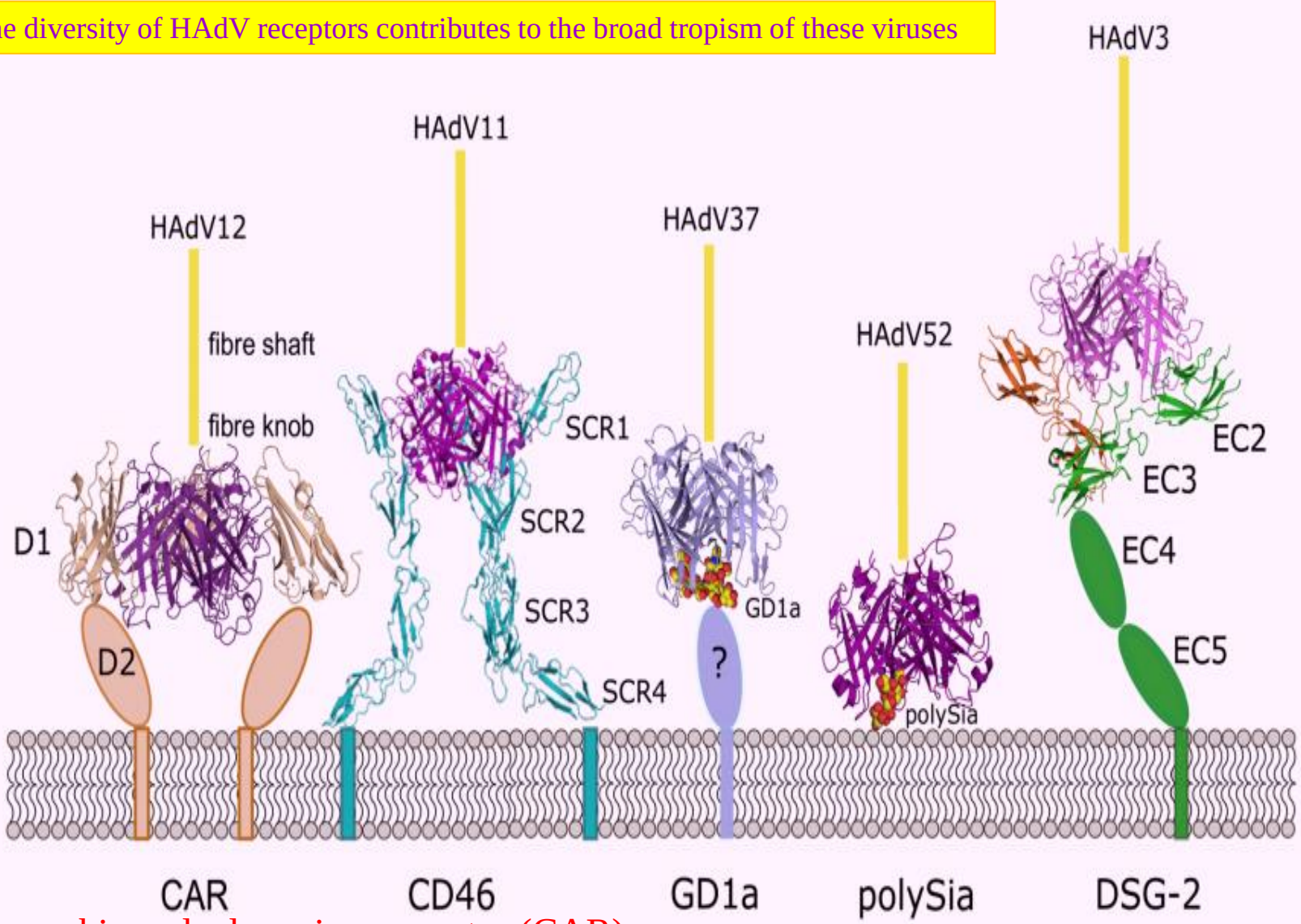

Coxsackie and adenovirus receptor (CAR)

Stasiak AC, Stehle T. Human adenovirus binding to host cell receptors: a structural view. *Med Microbiol Immunol*. 2020;209(3):325-333.

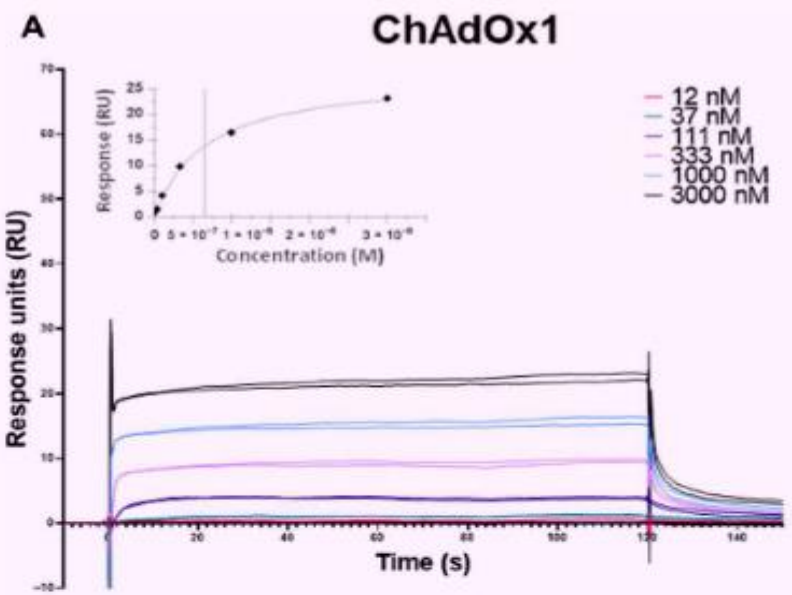

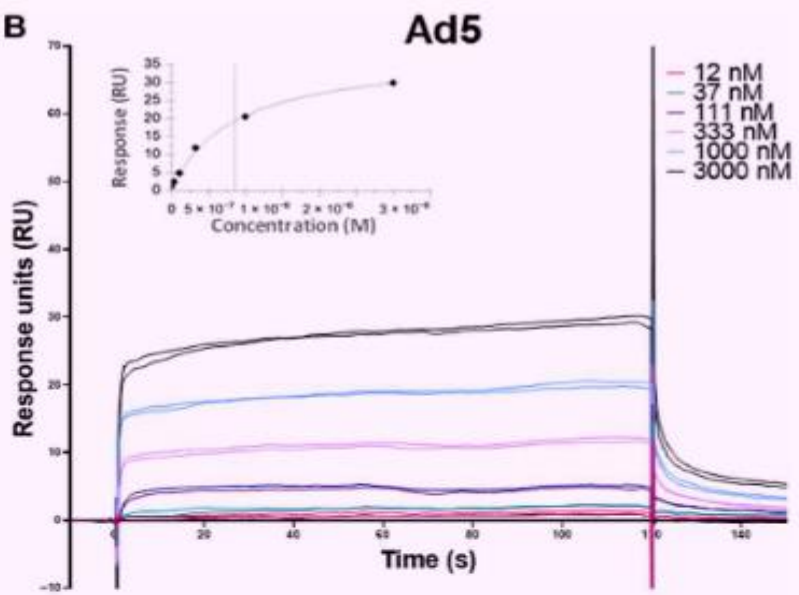

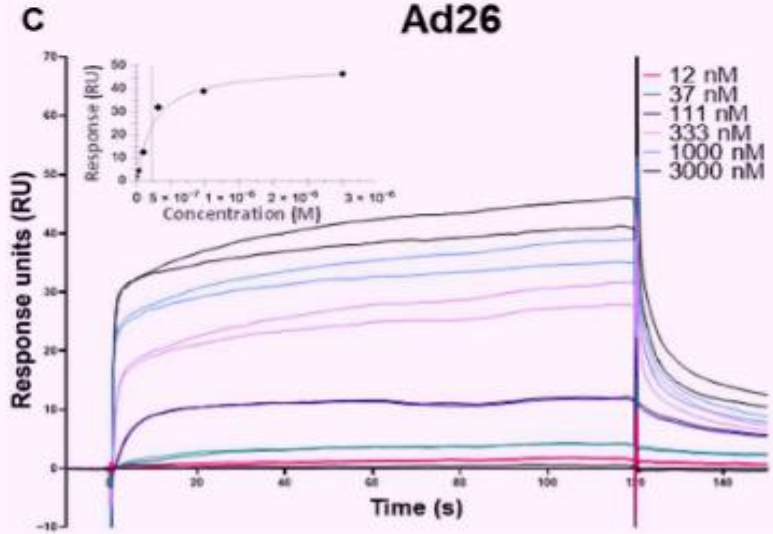

D

Virus	Average K_D (nM)
ChAdOx1	661 ± 53
Ad5	789 ± 137
Ad26	301 ± 67

Clinical adenoviruses bind to PF4 with nanomolar affinity.

Baker AT, ChAdOx1 interacts with CAR and PF4 with implications for thrombosis with thrombocytopenia syndrome. Sci Adv. 2021 Dec 3;7(49):eabl8213

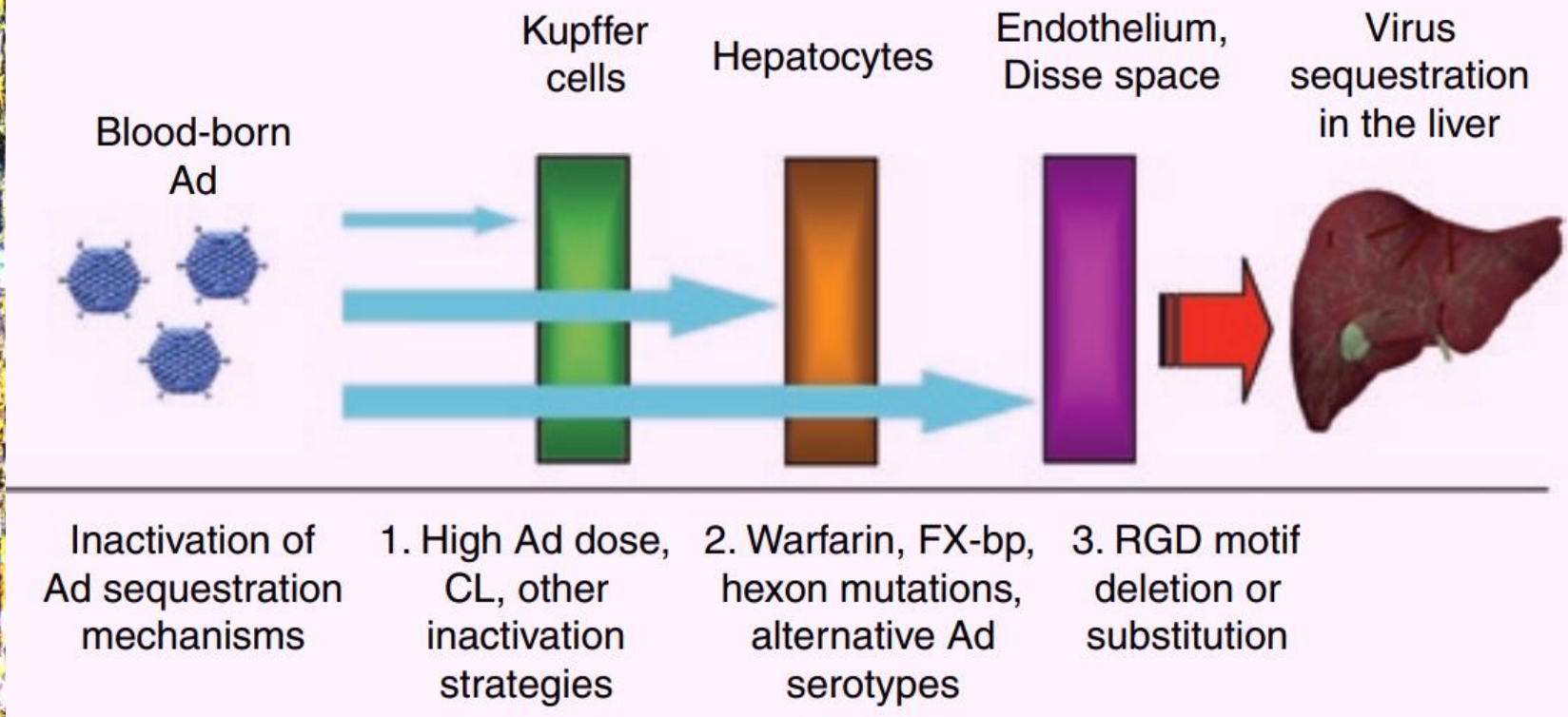

Di Paolo NC, van Rooijen N, Shayakhmetov DM. Redundant and synergistic mechanisms control the sequestration of blood-born adenovirus in the liver. Mol Ther. 2009 Apr;17(4):675-84.

The majority of intravenously injected Ad particles are sequestered by the liver, which in turn causes an inflammatory response characterized by acute transaminitis and vascular damage.

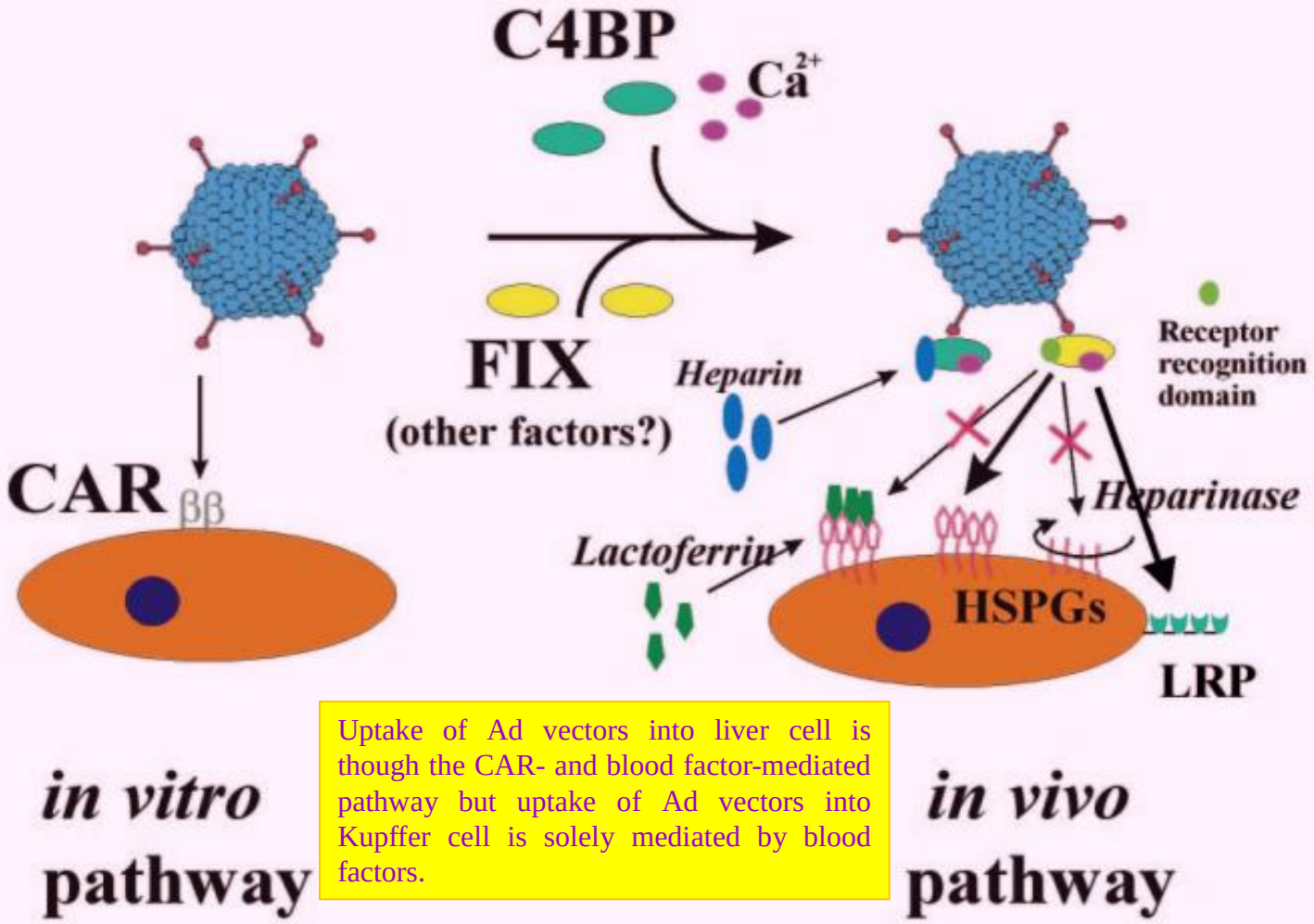

Uptake of Ad vectors into liver cell is though the CAR- and blood factor-mediated pathway but uptake of Ad vectors into Kupffer cell is solely mediated by blood factors.

Schematic representation of CAR-dependent and blood factor-dependent pathways of Ad infection and action of competitors (lactoferrin, heparin, and heparinase).

Shayakhmetov DM, Gaggar A, Ni S, Li ZY, Lieber A. Adenovirus binding to blood factors results in liver cell infection and hepatotoxicity. J Virol. 2005 Jun;79(12):7478-91.

Thank you for your attention

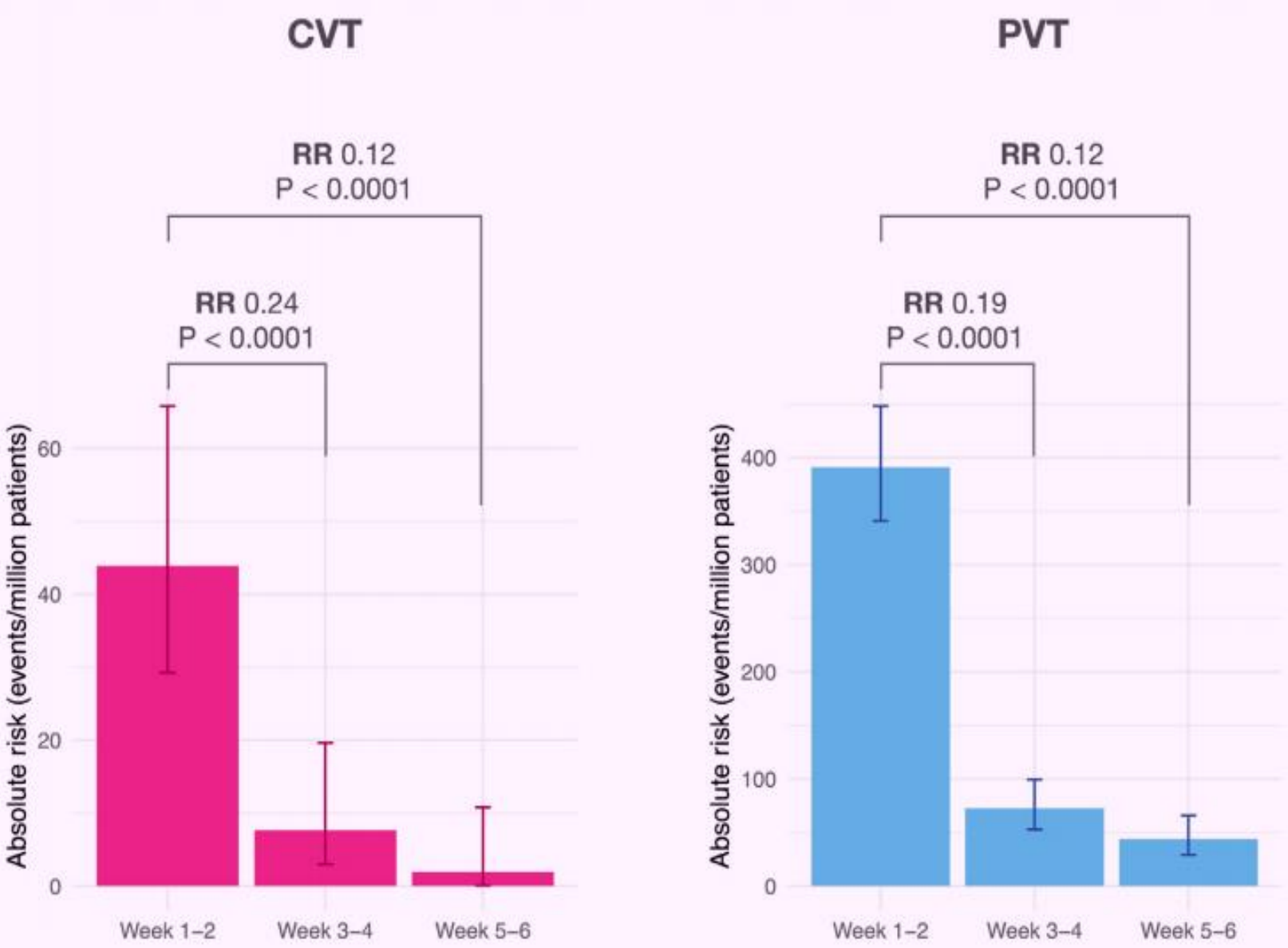

Taquet M, Husain M, Geddes JR, Luciano S, Harrison PJ. Cerebral venous thrombosis and portal vein thrombosis: A retrospective cohort study of 537,913 COVID-19 cases. EClinicalMedicine. 2021 Sep;39:101061.

Cerebral venous thrombosis (CVT)
(events/mln people in 2 weeks)

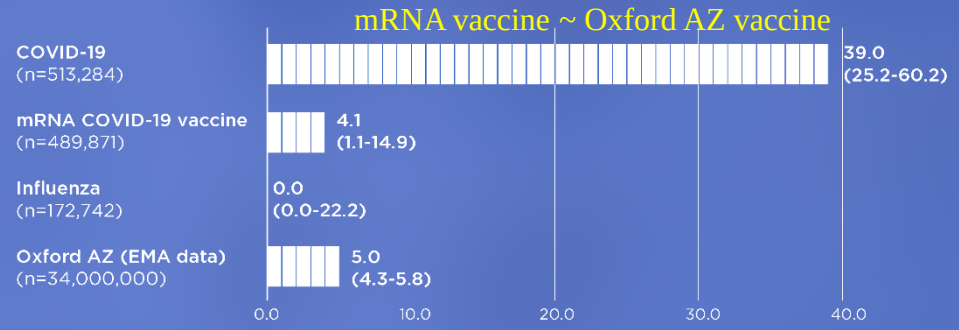

Incidence of CVT per million people in the two weeks after different health events. The numbers in parentheses on the right of each bar represent the 95% confidence intervals. Data for the ChAdOx1 nCoV-19 vaccine are presented for reference and inferred from the European Medicines Agency data (posted 7 April 2021).

Source: «Cerebral venous thrombosis: a retrospective cohort study». University of Oxford, UK, April 15, 2021.

Portal vein thrombosis (PVT)
(events/mln people in 2 weeks)

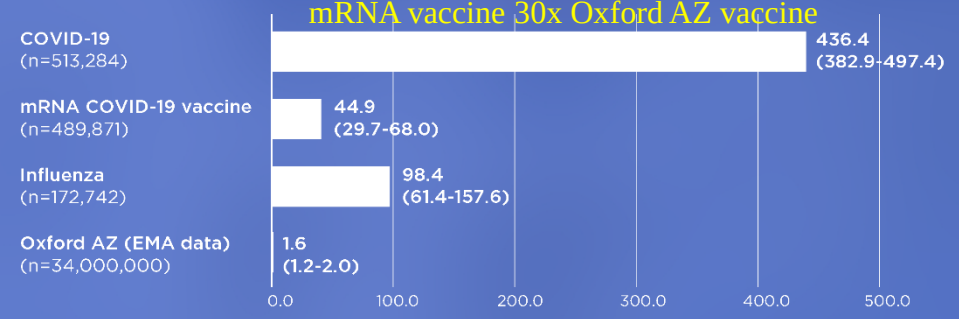

Incidence of PVT per million people in the two weeks after different health events. The numbers in parentheses on the right of each bar represent the 95% confidence intervals. Data for the ChAdOx1 nCoV-19 vaccine are presented for reference and inferred from the European Medicines Agency data (posted 7 April 2021).

Source: «Cerebral venous thrombosis: a retrospective cohort study». University of Oxford, UK, April 15, 2021.

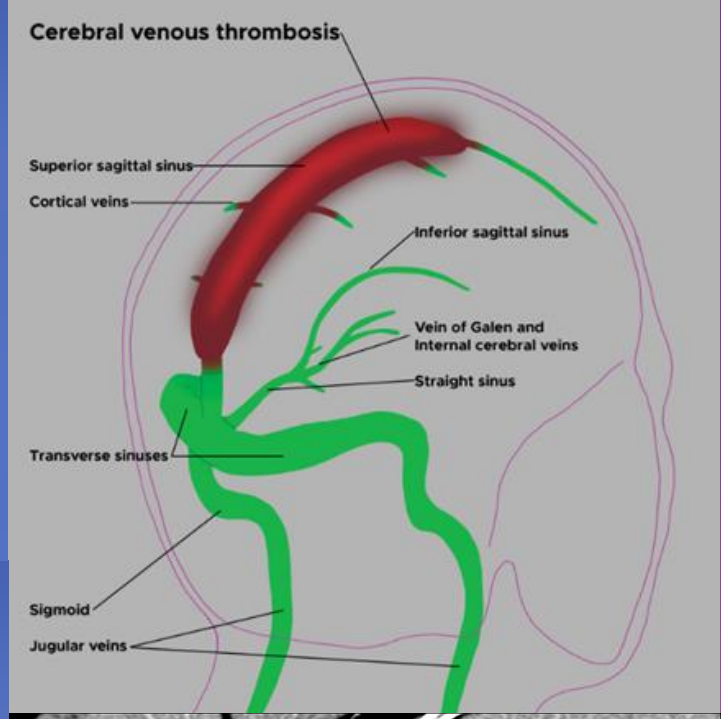

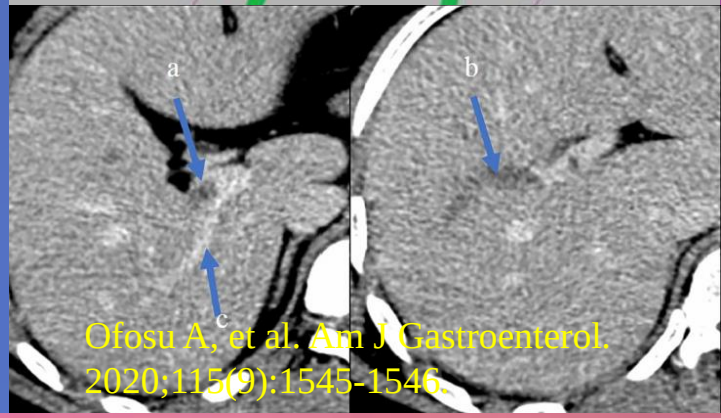

Ofosu A, et al. Am J Gastroenterol. 2020;115(9):1545-1546.

Taquet M, Husain M, Geddes JR, Luciano S, Harrison PJ. Cerebral venous thrombosis and portal vein thrombosis: A retrospective cohort study of 537,913 COVID-19 cases. EClinicalMedicine. 2021;39:101061.

In people <70 years, rates of hospitalisation due to intracranial venous thrombosis (ICVT) or due to thrombocytopenia were higher after vaccination with ChAdOx1-S but not BNT162b2, although the absolute increase in the risk of these events was very small.

From electronic health records on 46 million adults, of whom 21 million were vaccinated during the study, and compared the incidence of venous and arterial events before and after the first vaccination with ChAdOx1-S and BNT162b2 COVID-19 vaccines, overall rates of major arterial and venous events were lower after vaccination with both ChAdOx1-S and BNT162b2, after adjusting for potential confounding factors.

In adults ≥70 years, a first vaccination with either ChAdOx1-S and BNT162b2 was not associated with an increase in rates major arterial or venous thrombotic events.

Whiteley WN, et al. Association of COVID-19 vaccines ChAdOx1 and BNT162b2 with major venous, arterial, or thrombocytopenic events: A population-based cohort study of 46 million adults in England. PLoS Med 19(2): e1003926

Numbers and incidence rates pre- and post-first ChAdOx1-S. Incidence rate per 100,000 person years. Disclosure control prevents presentation of $n > 5$.

	Prevaccination or unvaccinated		Postvaccination ≤28 days		Postvaccination >28 days	
Outcome	**N (events)**	**Incidence rate (95% CI)**	**N (events)**	**Incidence rate (95% CI)**	**N (events)**	**Incidence rate (95% CI)**
All venous	14,769	139.8 (137.6–142.1)	2,006	293.6 (281.0–306.7)	995	359.3 (337.6–382.3)
ICVT	207	1.96 (1.71–2.25)	27	3.95 (2.71–5.76)	9	3.25 (1.69–6.24)
Portal vein thrombosis	121	1.15 (0.96–1.37)	14	2.05 (1.21–3.46)	9	3.25 (1.69–6.24)
PE	8,473	80.2 (78.5–81.9)	1,203	176.0 (166.4–186.3)	587	211.9 (195.4–229.7)
DVT	5,664	53.6 (52.2–55.0)	739	108.1 (100.6–116.2)	374	135.0 (122.0–149.4)
Other	459	4.35 (3.97–4.76)	51	7.46 (5.67–9.82)	30	10.8 (7.6–15.5)
All arterial	57,602	545.6 (541.1–550.0)	8,256	1,210.6 (1184.8–1237.0)	4,634	1,677.8 (1630.2–1726.8)
MI	28,134	266.4 (263.3–269.5)	3,814	558.5 (541.1–576.5)	2,050	740.7 (709.4–773.5)
Ischaemic stroke (ischaemic, unknown, spinal)	28,639	271.2 (268.1–274.3)	4,334	634.8 (616.1–654.0)	2,539	917.9 (882.9–954.3)
Other arterial	1,308	12.4 (11.7–13.1)	189	27.6 (24.0–31.9)	98	35.4 (29.0–43.1)
Haematological						
DIC	13	0.12 (0.07–0.21)	<5	0.44 (0.14–1.36)	<5	-
TTP	70	0.66 (0.52–0.84)	<5	0.59 (0.22–1.56)	<5	0.72 (0.18–2.89)
Any thrombocytopenia	1,357	12.8 (12.2–13.5)	200	29.3 (25.5–33.6)	89	32.1 (26.1–39.5)
Other						
Haemorrhagic stroke (intracerebral or subarachnoid)	3,747	35.5 (34.4–36.6)	487	71.2 (65.2–77.9)	289	104.3 (92.9–117.0)
Mesenteric thrombosis	1,170	11.1 (10.5–11.7)	171	25.0 (21.5–29.1)	109	39.3 (32.6–47.5)
Lower limb fracture	18,347	173.7 (171.2–176.3)	2,657	389.0 (374.5–404.0)	1,632	589.7 (561.7–619.0)
Death	123,580	1,169.9 (1163.4–1176.4)	16,192	2,368.5 (2332.3–2405.2)	11,738	4,235.1 (4159.2–4312.4)

Whiteley WN, et al. Association of COVID-19 vaccines ChAdOx1 and BNT162b2 with major venous, arterial, or thrombocytopenic events: A population-based cohort study of 46 million adults in England. PLoS Med 19(2): e1003926

Numbers and incidence rates pre- and post-first BNT162b2. Incidence rate per 100,000 person years. Disclosure control prevents presentation of $n > 5$.

	Prevaccination or unvaccinated		Postvaccination ≤28 days		Postvaccination >28 days	
Outcome	**N (events)**	**Incidence rate (95% CI)**	**N (events)**	**Incidence rate (95% CI)**	**N (events)**	**Incidence rate (95% CI)**
All venous	14,769	139.8 (137.6–142.1)	1,546	240.8 (229.1–253.1)	1,587	277.1 (263.8–291.0)
ICVT	207	1.96 (1.71–2.25)	13	2.02 (1.18–3.49)	6	1.05 (0.47–2.33)
Portal vein thrombosis	121	1.15 (0.96–1.37)	5	0.78 (0.32–1.87)	12	2.09 (1.19–3.69)
PE	8,473	80.2 (78.5–81.9)	928	144.5 (135.5–154.1)	955	166.7 (156.5–177.6)
DVT	5,664	53.6 (52.2–55.0)	555	86.4 (79.5–93.9)	590	103.0 (95.0–111.6)
Other	459	4.35 (3.97–4.76)	55	8.56 (6.58–11.15)	39	6.81 (4.97–9.31)
All arterial	57,602	545.6 (541.1–550.0)	7,960	1,241.8 (1214.9–1269.4)	8,799	1,539.7 (1507.8–1572.2)
MI	28,134	266.4 (263.3–269.5)	3,722	580.1 (561.8–599.0)	4,023	702.9 (681.5–724.9)
Ischaemic stroke (ischaemic, unknown, spinal)	28,639	271.2 (268.1–274.3)	4,143	645.7 (626.4–665.7)	4,702	821.8 (798.6–845.6)
Other arterial	1,308	12.4 (11.7–13.1)	156	24.3 (20.8–28.4)	167	29.1 (25.0–33.9)
Haematological						
DIC	13	0.12 (0.07–0.21)	<5	0.31 (0.08–1.25)	<5	0.35 (0.09–1.40)
TTP	70	0.66 (0.52–0.84)	<5	0.62 (0.23–1.66)	<5	0.35 (0.09–1.40)
Any thrombocytopenia	1,357	12.8 (12.2–13.5)	136	21.2 (17.9–25.1)	144	25.1 (21.3–29.6)
Other						
Haemorrhagic stroke (intracerebral or subarachnoid)	3,747	35.5 (34.4–36.6)	440	68.5 (62.4–75.2)	579	101.0 (93.1–109.6)
Mesenteric thrombosis	1,170	11.1 (10.5–11.7)	161	25.1 (21.5–29.3)	217	37.9 (33.2–43.3)
Lower limb fracture	18,347	173.7 (171.2–176.3)	2,573	400.8 (385.6–416.6)	3,176	554.7 (535.8–574.4)
Death	123,580	1,169.9 (1163.4–1176.4)	9,117	1,419.6 (1390.8–1449.0)	13,935	2,431.7 (2391.7–2472.4)

Whiteley WN, et al. Association of COVID-19 vaccines ChAdOx1 and BNT162b2 with major venous, arterial, or thrombocytopenic events: A population-based cohort study of 46 million adults in England. PLoS Med 19(2): e1003926.

Spike protein can cross human brain endothelial cell barrier effectively but less in intestinal barrier. Petrovszki D, et al. Biomedicines. 2022 Jan 17;10(1):188.

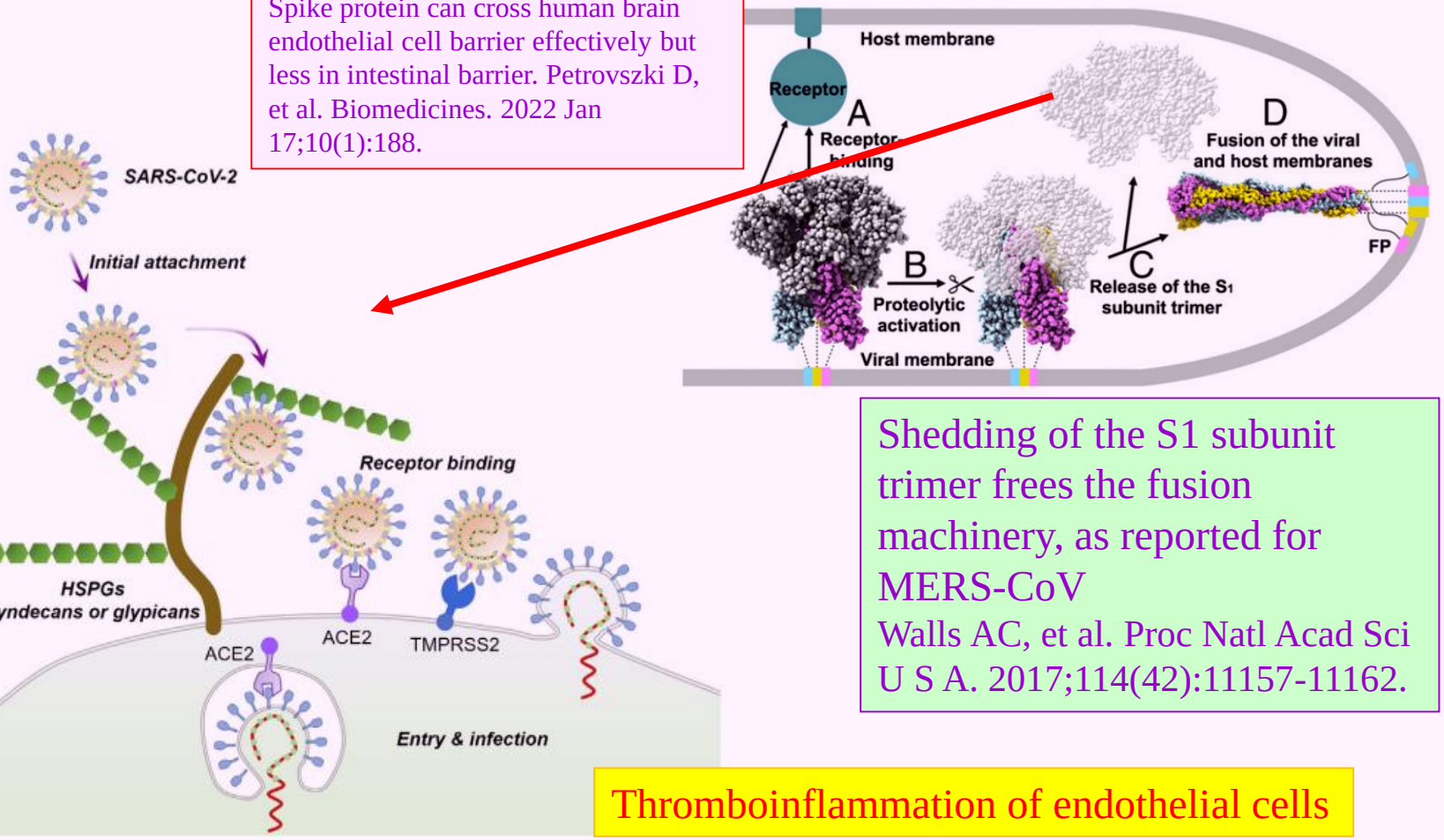

Shedding of the S1 subunit trimer frees the fusion machinery, as reported for MERS-CoV
Walls AC, et al. Proc Natl Acad Sci U S A. 2017;114(42):11157-11162.

Thromboinflammation of endothelial cells

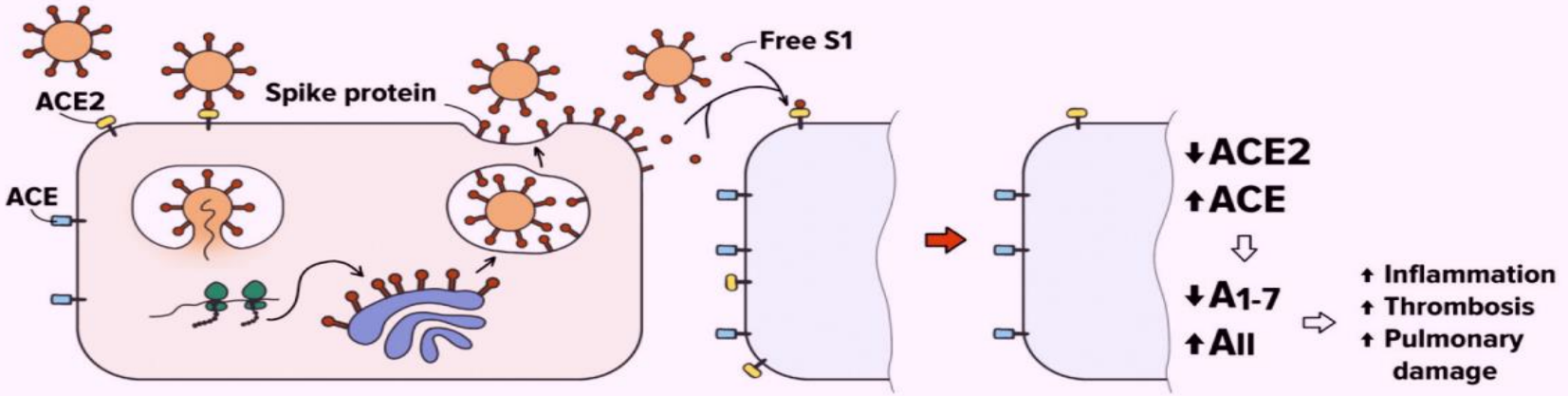

Letarov, A.V., *Biochemistry Moscow* **86,** 257–261 (2021).

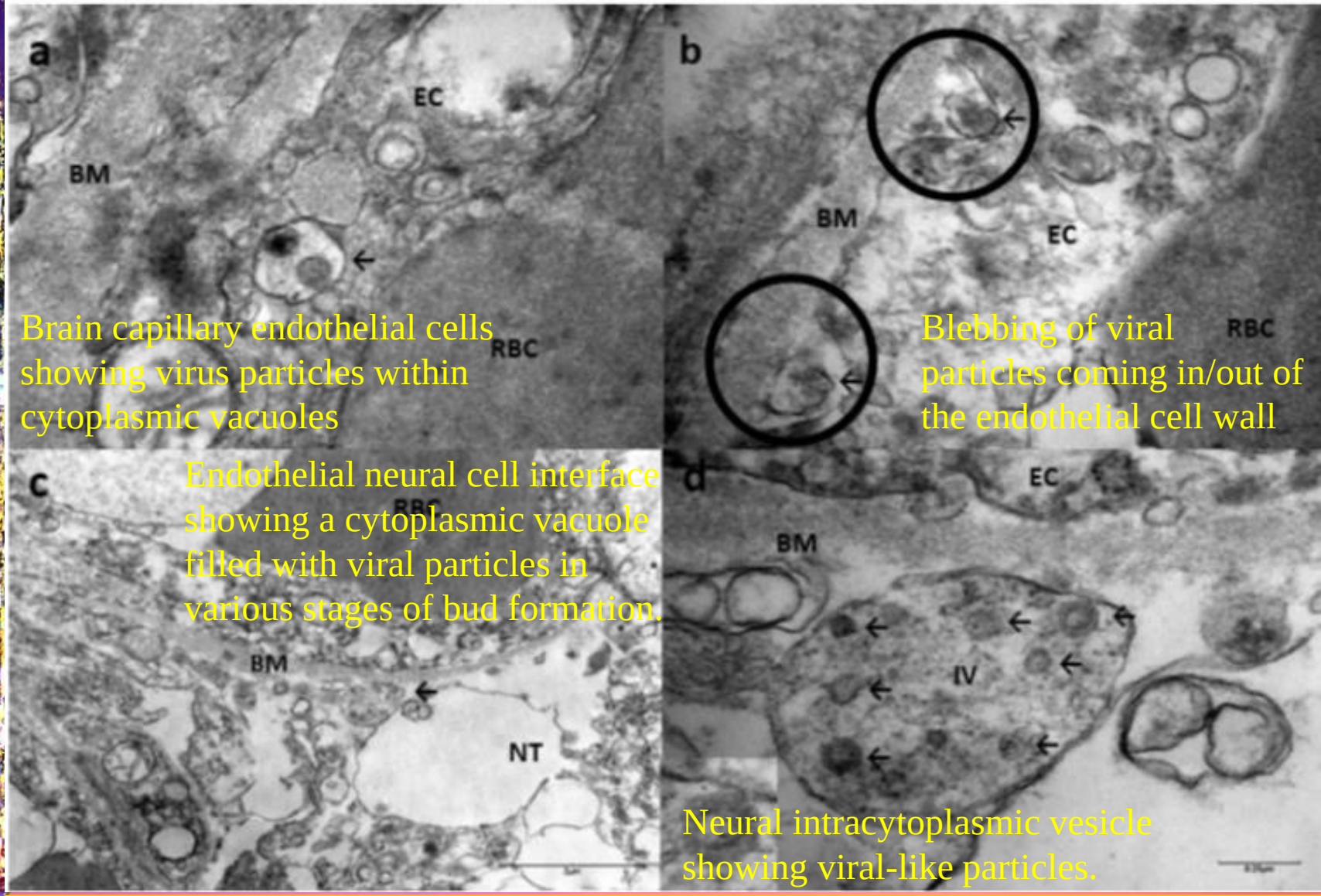

Brain capillary endothelial cells showing virus particles within cytoplasmic vacuoles

Blebbing of viral particles coming in/out of the endothelial cell wall

Endothelial neural cell interface showing a cytoplasmic vacuole filled with viral particles in various stages of bud formation.

Neural intracytoplasmic vesicle showing viral-like particles.

Viral-like particles in brain capillary endothelium and actively budding across endothelial cells in patient died of COVID-19.

Paniz-Mondolfi A, Bryce C, Grimes Z, et al. Central nervous system involvement by severe acute respiratory syndrome coronavirus-2 (SARS-CoV-2). *J Med Virol*. 2020;92(7):699-702.

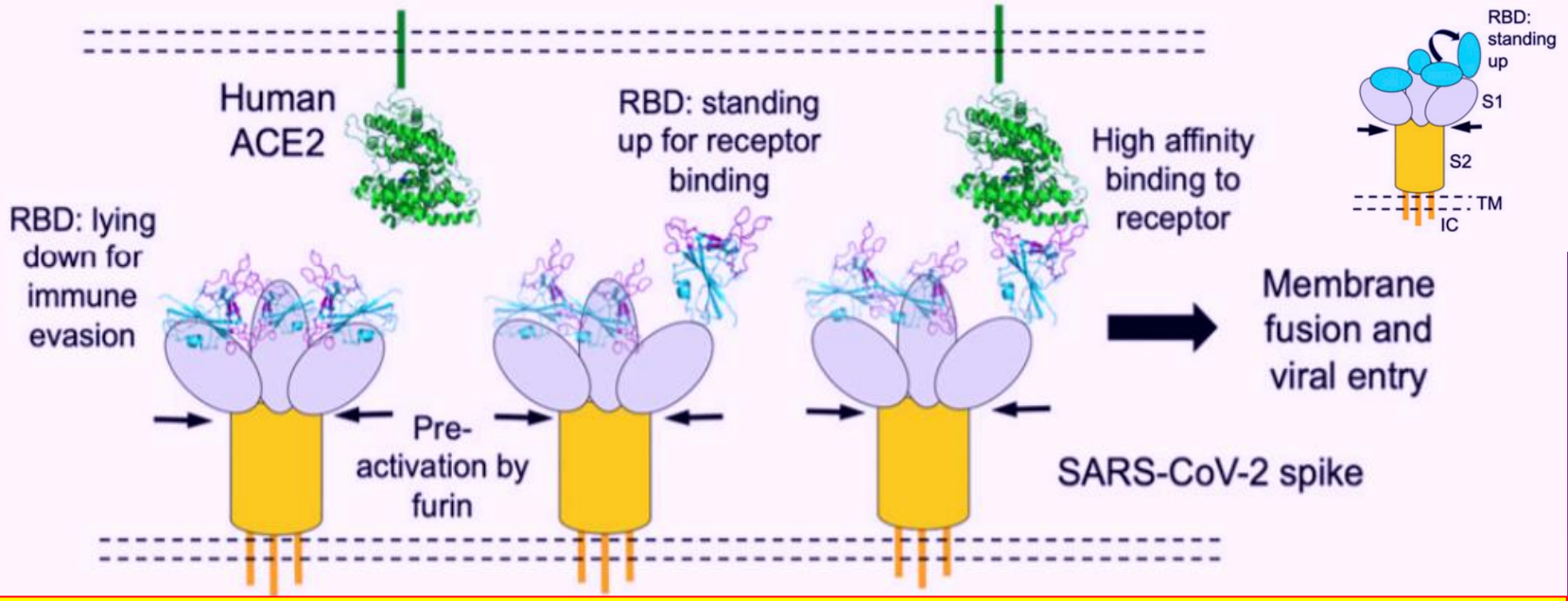

The high hACE2 binding affinity of the RBD, furin preactivation of the spike, and hidden RBD in the spike potentially allow SARS-CoV-2 to maintain efficient cell entry while evading immune surveillance

Features of viral entry	SARS-CoV	SARS-CoV-2	Implications for SARS-CoV-2
Frequency of RBD standing up	High	Low	Immune evasion (hidden RBD)
Human ACE2-binding affinity by RBD	Low	High	Enhanced entry (compensation for hidden RBD)
Pre-activation by furin	No	Yes	Enhanced entry into some types of cells (compensation for hidden RBD)

Cell entry mechanisms of SARS-CoV-2 Jian Shang, Yushun Wan, Chuming Luo, Gang Ye, Qibin Geng, Ashley Auerbach, and Fang Li PNAS May 26, 2020 117 (21) 11727-11734;

Negatively charged HS strongly interacts with positively charged Arg346, Arg355, Lys444, Arg466, and probably Arg509 amino acid residues of the S-protein RBD

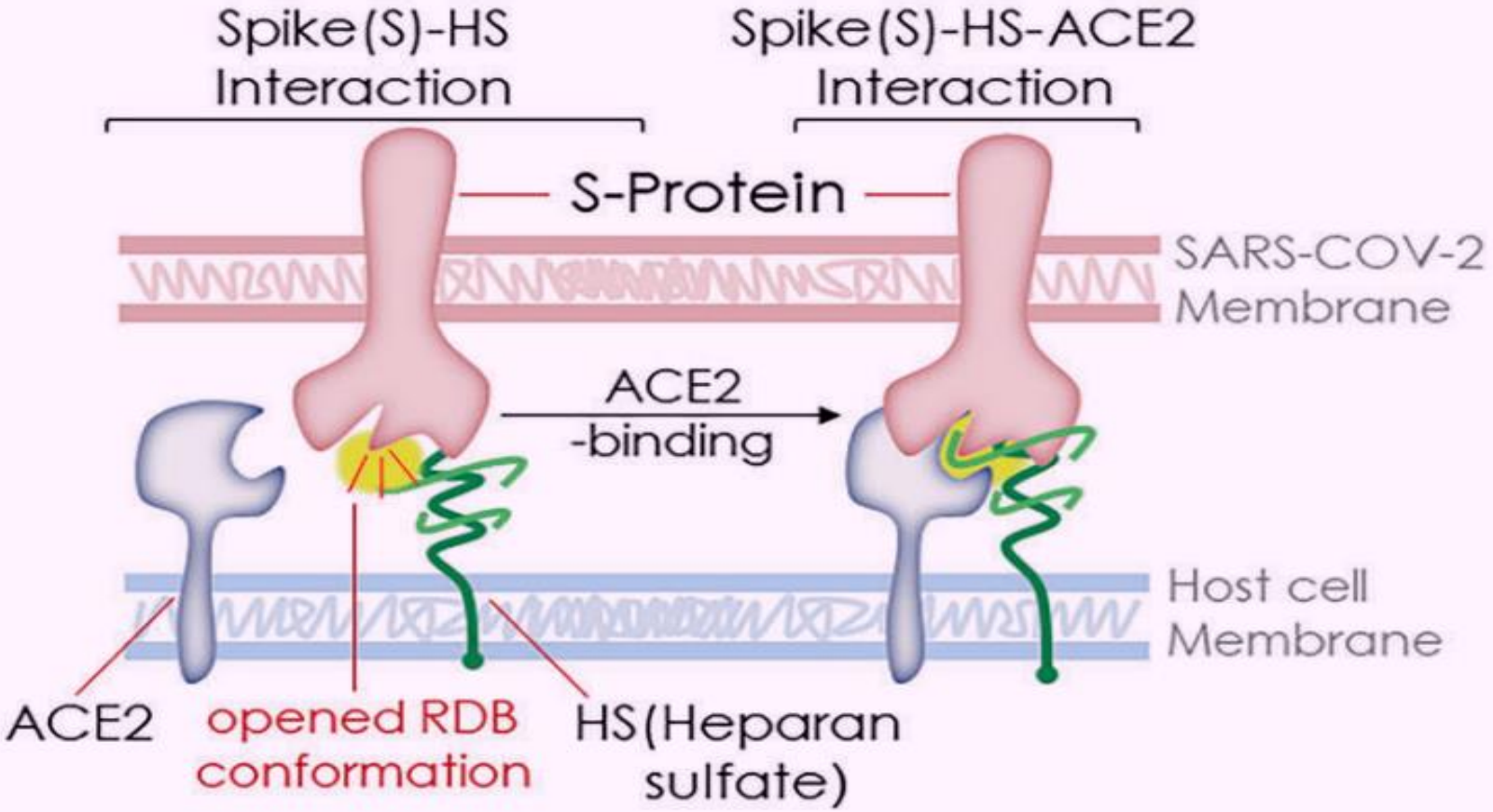

Heparan sulfate (HS) functions as a necessary cofactor for SARS-CoV-2 binding to the ACE2 at the host cell membrane. HS interacts with RBD at the S1 subunit of the SARS-CoV-2 trimeric S-protein, which facilitates the opening of S-protein conformation from for ACE2 binding.

Clausen TM, et al. SARS-CoV-2 infection depends on cellular heparan sulfate and ACE2. *Cell*. 2020;183:1–15.

Kalra RS, Kandimalla R. Engaging the spikes: heparan sulfate facilitates SARS-CoV-2 spike protein binding to ACE2 and potentiates viral infection. *Signal Transduct Target Ther*. 2021;6(1):39.

THE MUTATION THAT LOOSENS THE SPIKE PROTEIN

Spike proteins on SARS-CoV-2 bind to receptors on human cells, helping the virus to enter. A spike protein is made up of three smaller peptides in 'open' or 'closed' orientations; when more are open, it's easier for the protein to bind. The D614G mutation — the result of a single-letter change to the viral RNA code — seems to relax connections between peptides. This makes open conformations more likely and might increase the chance of infection.

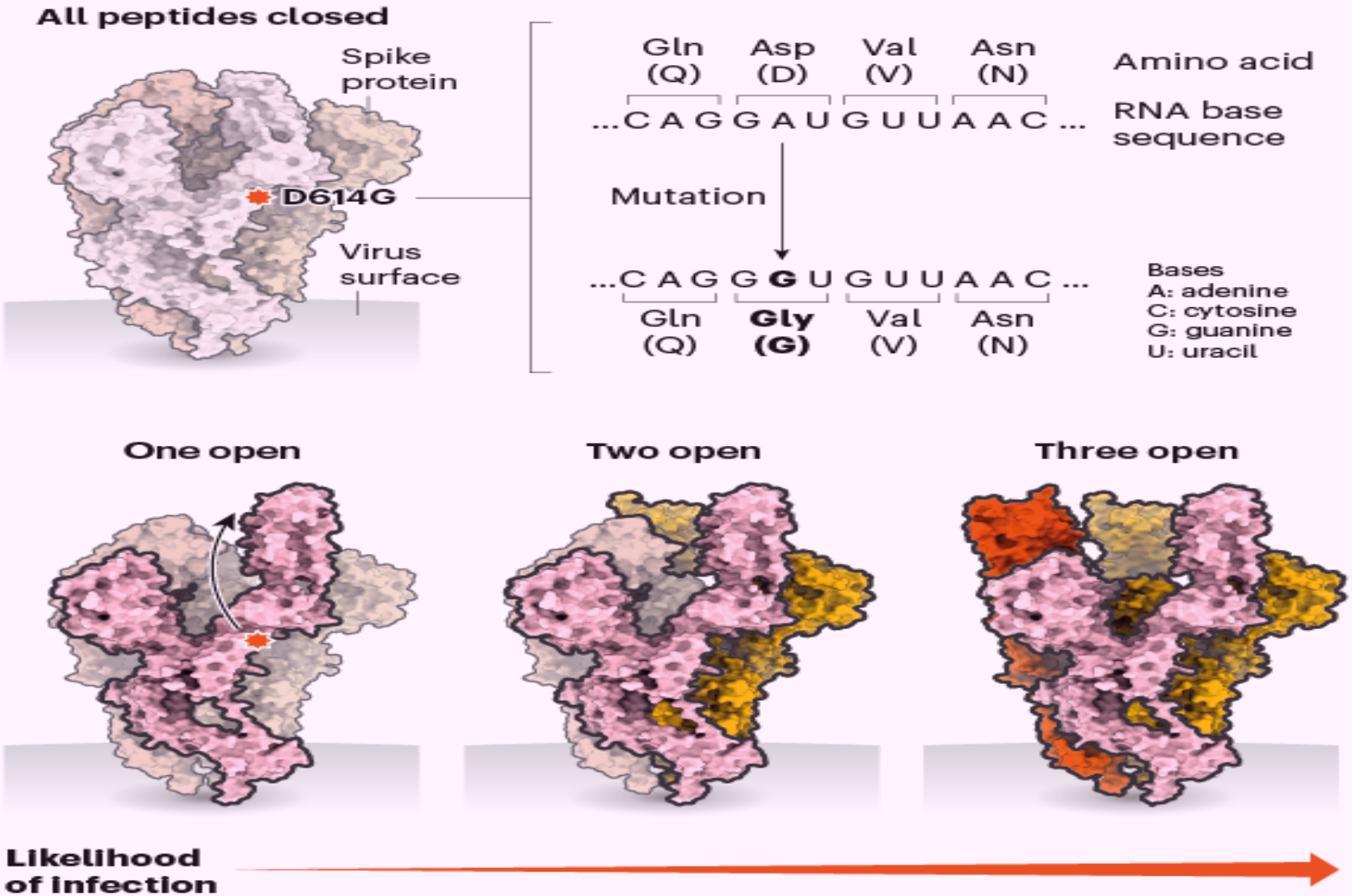

Callaway E. The coronavirus is mutating - does it matter? Nature. 2020 Sep;585(7824):174-177.

- Host cell surface SARS-CoV-2 spike protein (SV2-S) binding depends on and correlates with host cell surface HS expression.
- This binding is required for SARS-Cov-2 virus to infect host cells and can be blocked by heparin lyase, HS antagonist surfen, heparin, and heparin derivatives.
- The binding of heparin/HS to SV2-S is mainly determined by its overall sulfation with potential, minor contribution of specific SV2-S binding motifs.
- The higher binding affinity of SV2-S G614 mutant to heparin and upregulated HS expression may be one of the mechanisms underlying the higher infectivity of the SARS-CoV-2 G614 variant and the high vulnerability of lung cancer patients to SARSCoV-2 infection, respectively

Yue J, et al. Heparan Sulfate Facilitates Spike Protein-Mediated SARS-CoV-2 Host Cell Invasion and Contributes to Increased Infection of SARS-CoV-2 G614 Mutant and in Lung Cancer. *Front Mol Biosci*. 2021;8:649575.

Summary of IC_{50} calculations for SARS-CoV-2 inhibitors[a]

Inhibitor	IC_{50} (per liter)		Bottom limit (per cell)[b]	
	Value	95% CI	Value	95% CI
UFH	5.99 μg	2.90–11.96 μg	74.38†	64.28–84.36
UFH-de6S	1.77 μg	61.4–4,903 ng	80.76†	68.46–92.97
Enoxaparin	1.08 mg	247–4,164 μg	73.64†	45.44–99.54
Enoxaparin-de6S	5.86 mg	0.374–59.49 mg	99.71†	53.15–132.00
L. variegatus sulfated fucan	33.2 μg	15.5–68.7 μg	20.42‡	9.45–31.23
B. occidentalis sulfated galactan	54.0 μg	26.3–103.4 μg	24.75‡	15.43–33.95
Enoxaparin-deNS	No activity			
Enoxaparin-fully-deS	No activity			

Tandon R, et al.. *J Virol*. 2021;95(3):e01987-20.

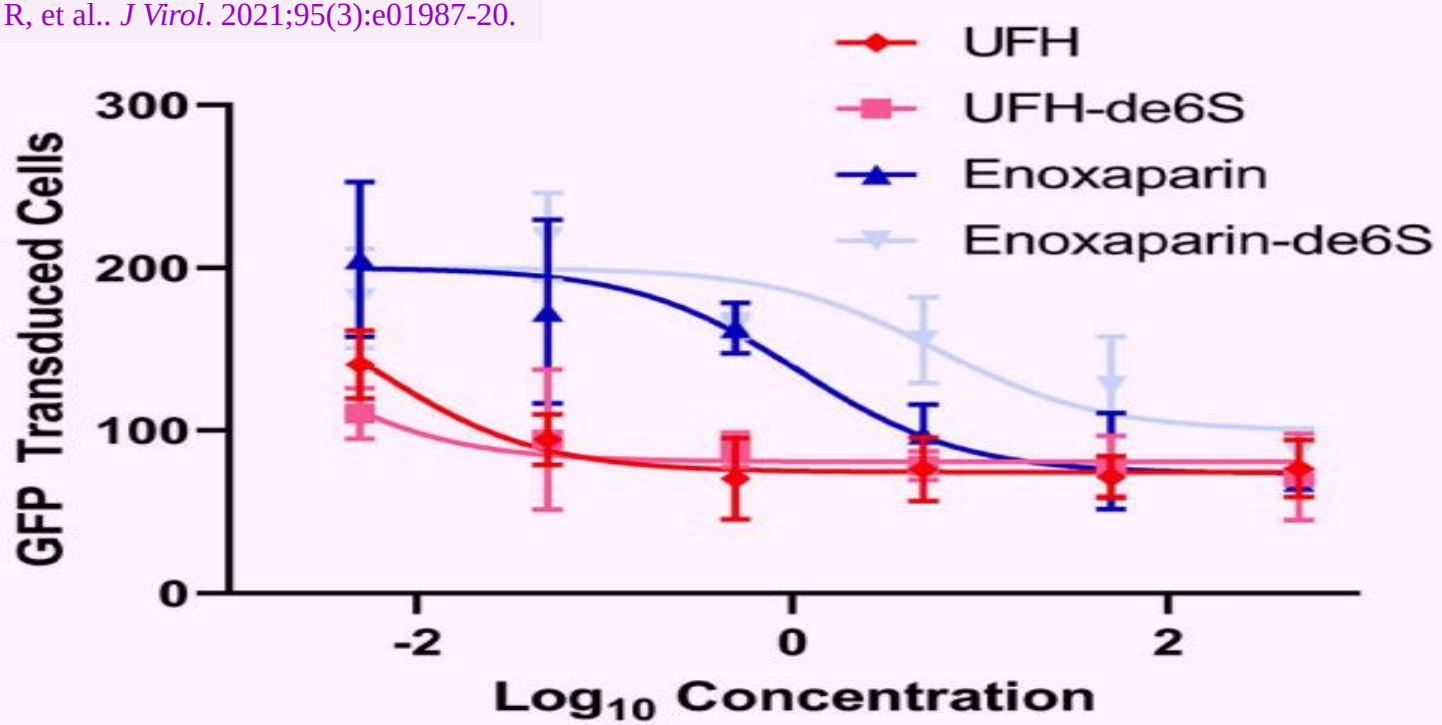

LMWH was associated with reduced mortality, improved markers of cell death, and curtailed viral persistence in COVID-19 infection.

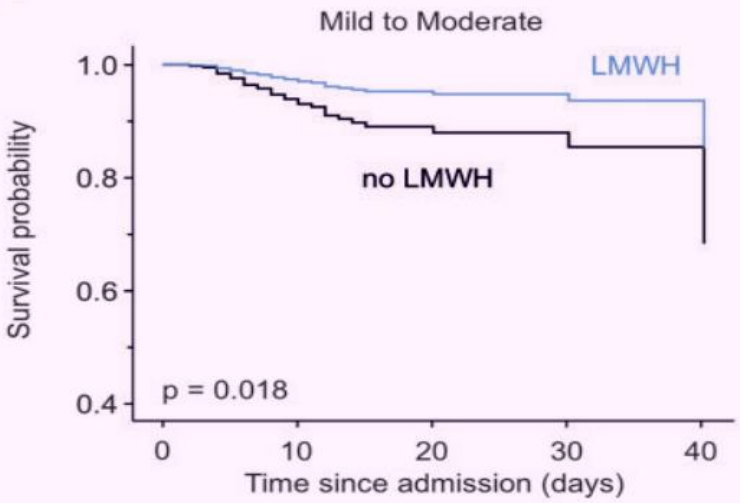

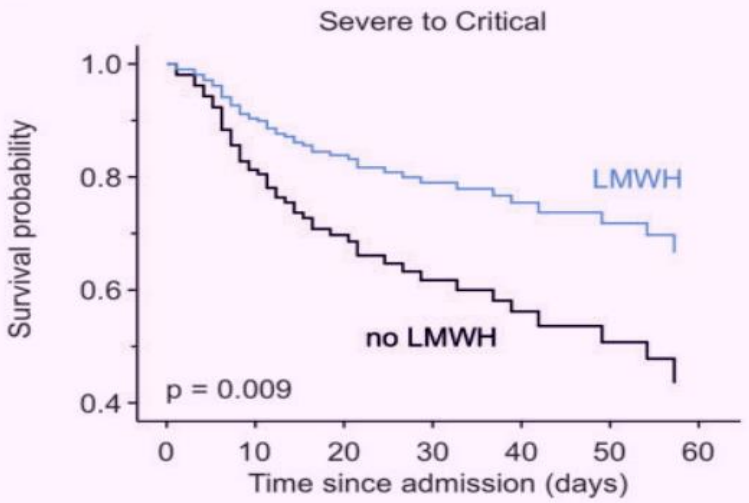

Anticoagulation with LMWH is associated with improved survival in COVID-19. Kaplan–Meier curve showing survival for patients

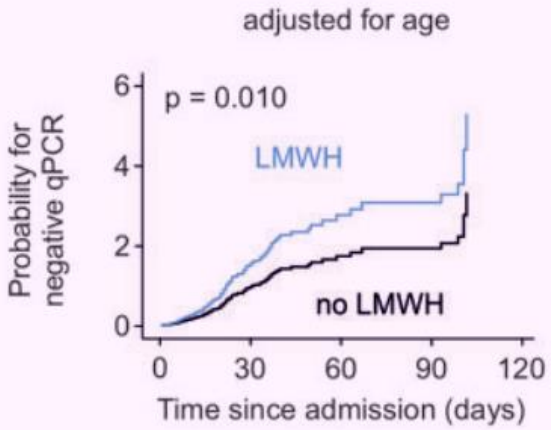

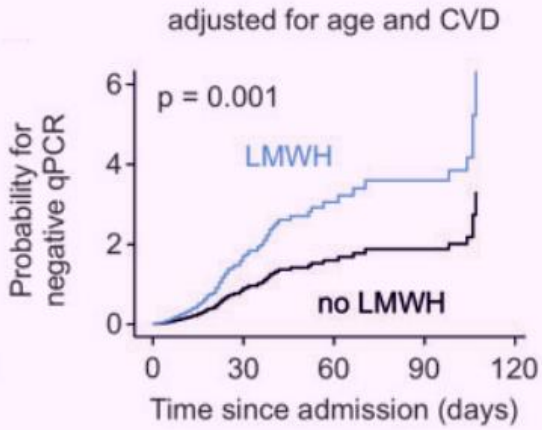

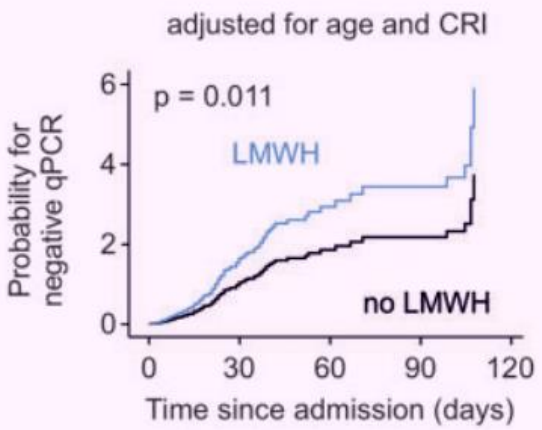

Anticoagulation has no effect on development of CAC and thromboinflammation while impacting viral persistence.

Pereyra D, Cardiovasc Res. 2021;cvab308. doi:10.1093/cvr/cvab308

Thank you for your attention

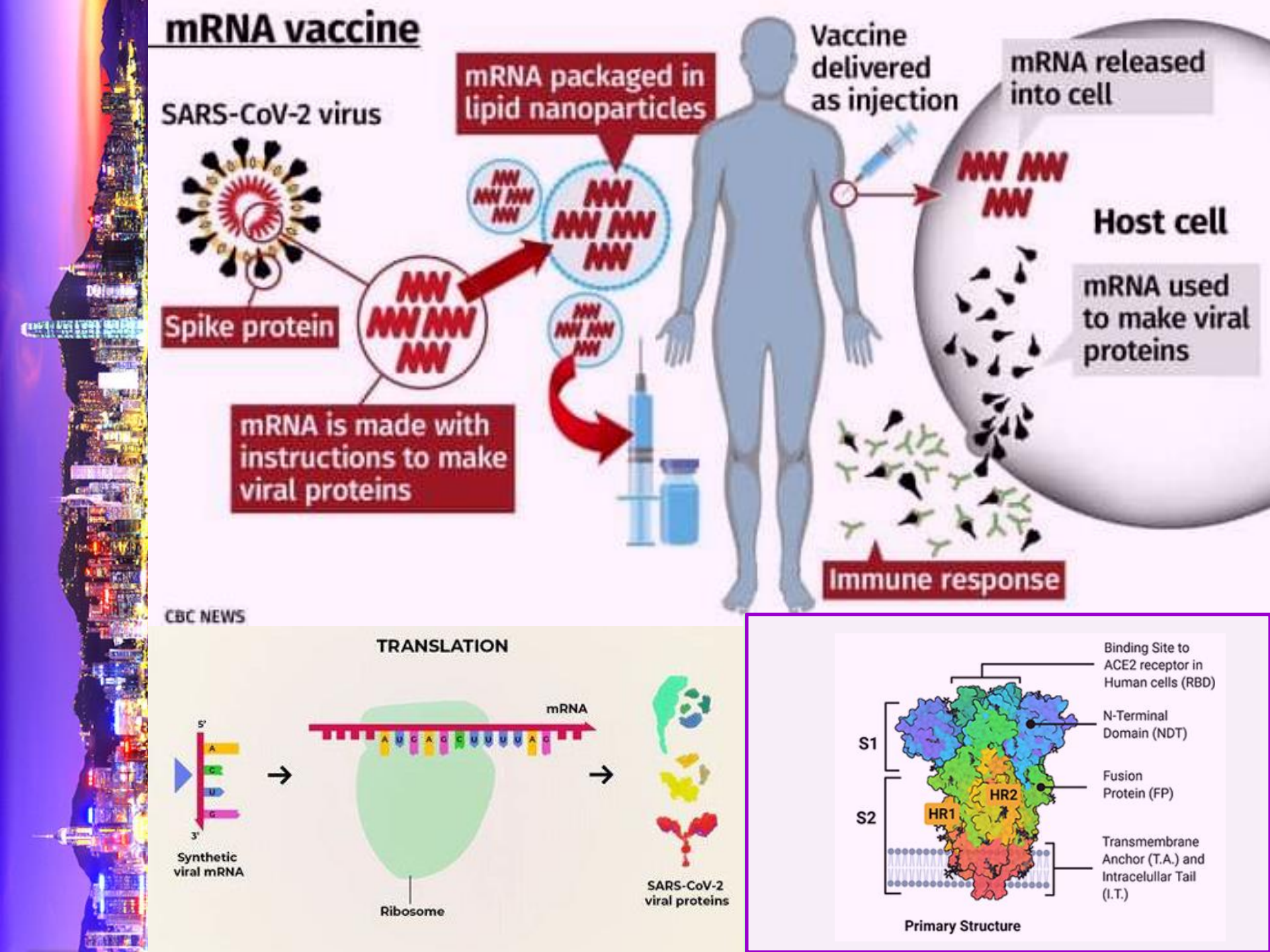
mRNA vaccine
SARS-CoV-2 virus
Spike protein
mRNA is made with instructions to make viral proteins
mRNA packaged in lipid nanoparticles
Vaccine delivered as injection
mRNA released into cell
Host cell
mRNA used to make viral proteins
Immune response
CBC NEWS
TRANSLATION
mRNA
Synthetic viral mRNA
Ribosome
SARS-CoV-2 viral proteins
Binding Site to ACE2 receptor in Human cells (RBD)
N-Terminal Domain (NDT)
Fusion Protein (FP)
Transmembrane Anchor (T.A.) and Intracelullar Tail (I.T.)
S1
S2
HR1
HR2
Primary Structure

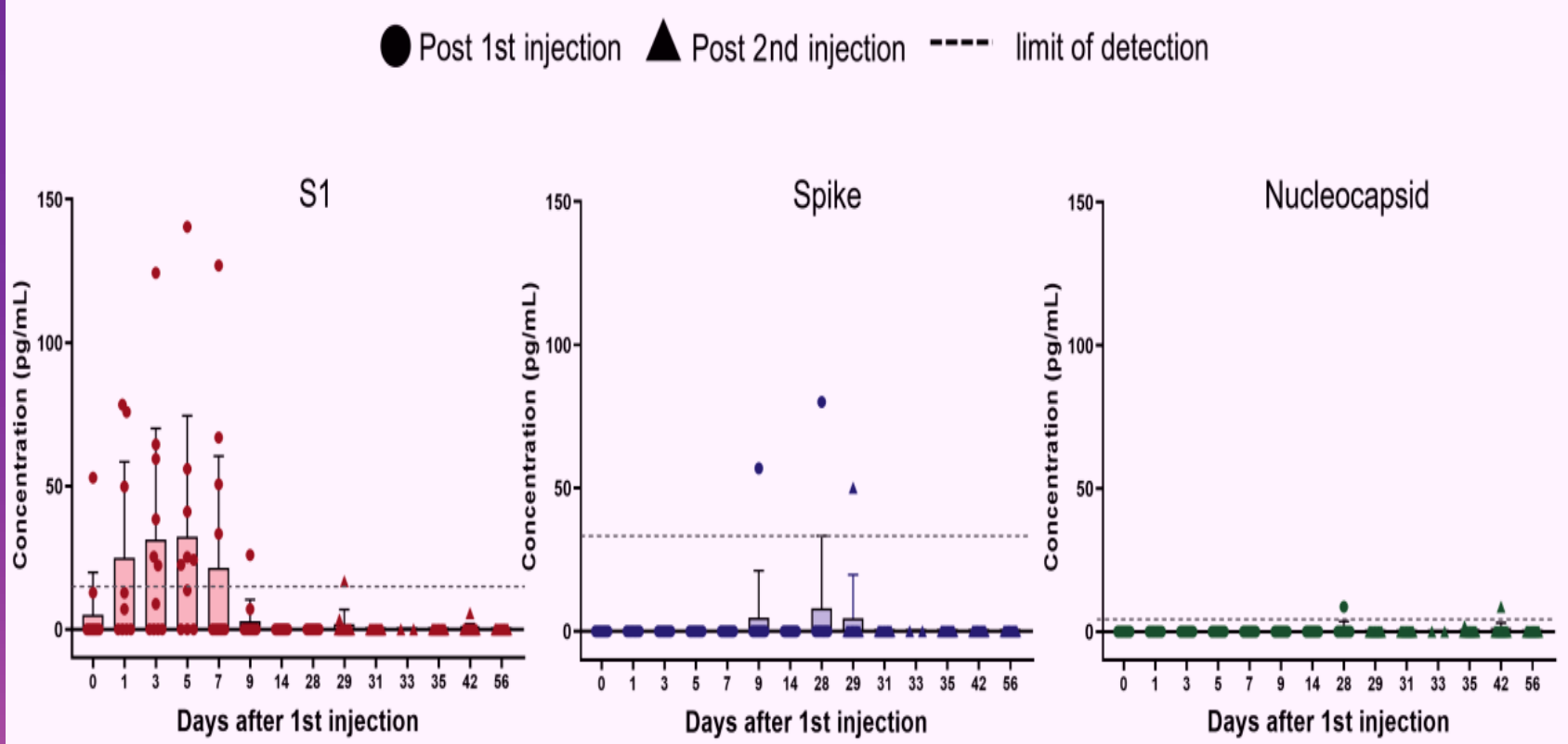

S1 antigen was detected as early as day 1 postvaccination, and peak levels were detected on average 5 days after the first injection. The mean S1 peak level was 68 pg/mL ± 21 pg/mL. S1 in all participants declined and became undetectable by day 14. Spike protein was detectable in 3 of 13 participants an average of 15 days after the first injection. The mean spike peak level was 62 pg/mL ± 13 pg/mL.

Ogata AF, et al. Circulating Severe Acute Respiratory Syndrome Coronavirus 2 (SARS-CoV-2) Vaccine Antigen Detected in the Plasma of mRNA-1273 Vaccine Recipients. *Clin Infect Dis*. 2022;74(4):715-718.

SARS-CoV-2 Spike Protein S1

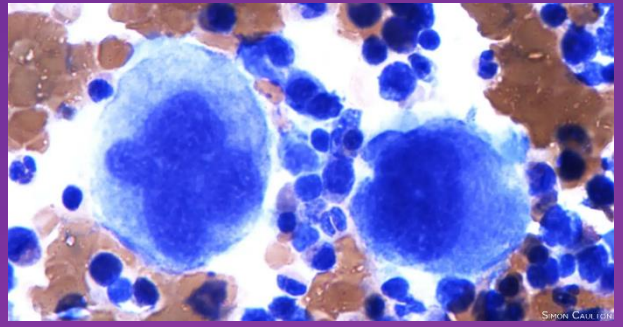

Megakaryocytes were found in cortical capillaries of 33% PM who died with severe COVID-19

Nauen DW, et al. JAMA Neurol. 2021;78(6):760–762.

Platelet hyperactivation

Anomalous clotting with amyloid signal (resistant to fibrinolysis)

Spontaneous fibrin fiber formation (even in the absence of thrombin)

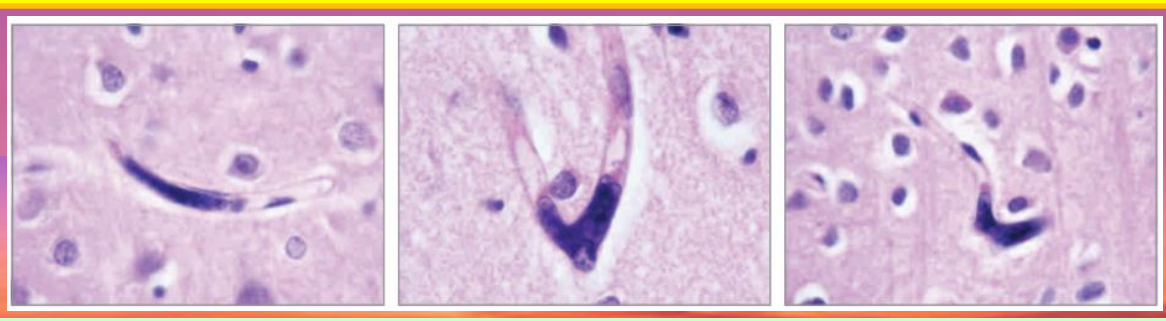

The spike protein S1 can induce hypercoagulopathy and endothelial damage directly, without being taken up by cells.

Grobbelaar LM, Venter C, Vlok M, et al. SARS-CoV-2 spike protein S1 induces fibrin(ogen) resistant to fibrinolysis: implications for microclot formation in COVID-19. Biosci Rep. 2021;41(8):BSR20210611.

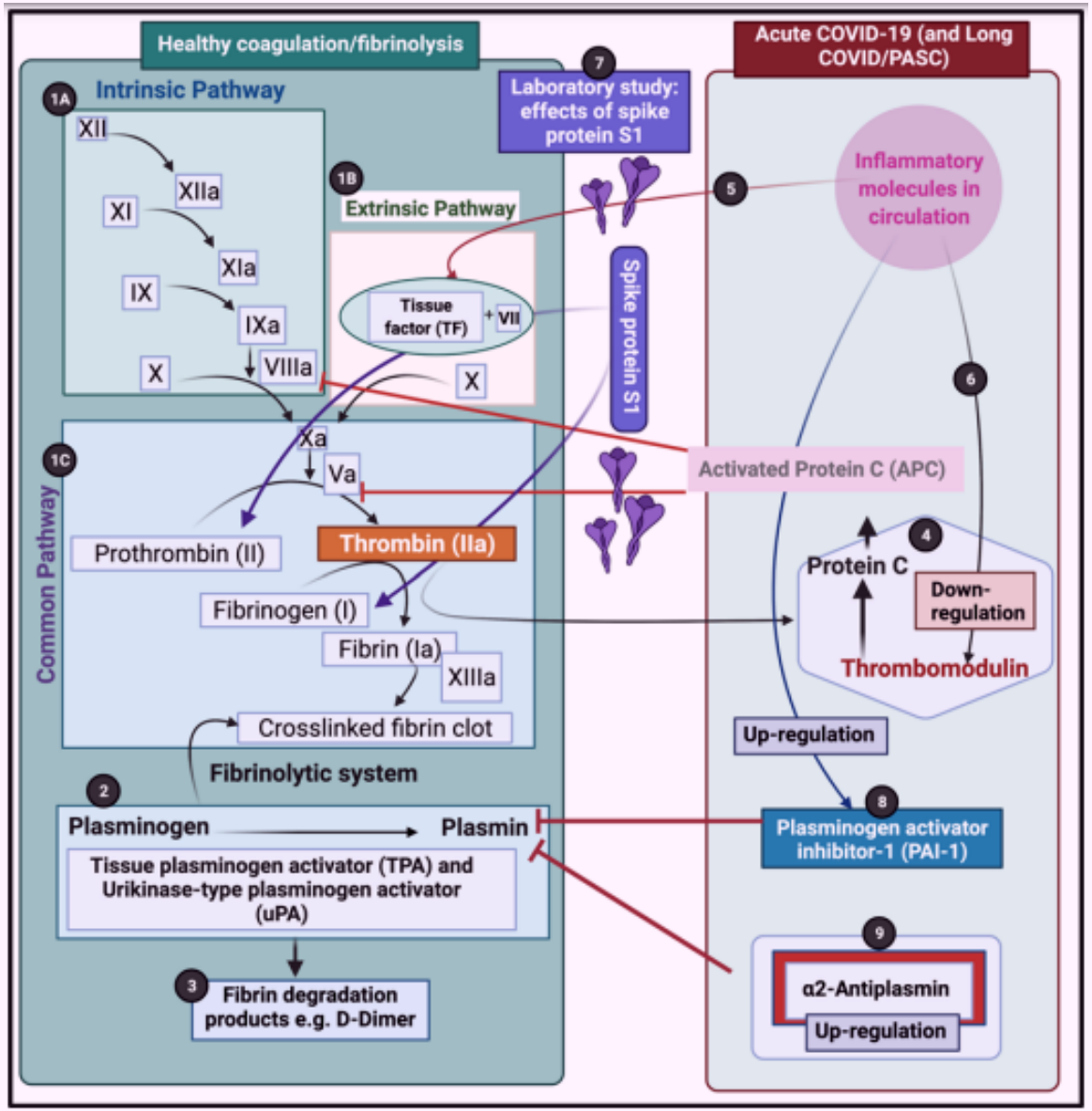

Grobbelaar LM, Venter C, Vlok M, et al. SARS-CoV-2 spike protein S1 induces fibrin(ogen) resistant to fibrinolysis: implications for microclot formation in COVID-19. Biosci Rep. 2021;41(8):BSR20210611.

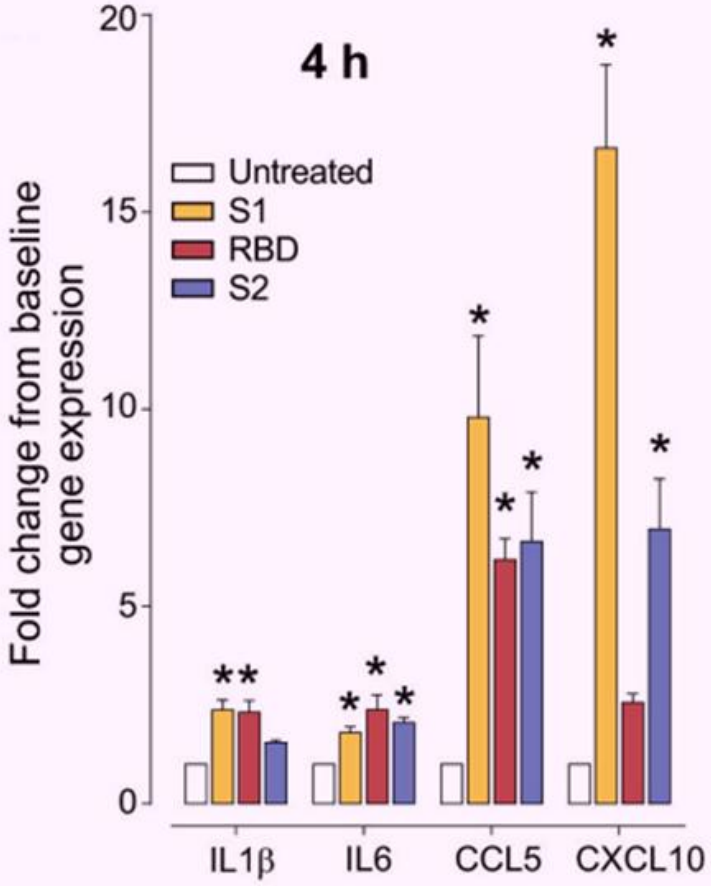

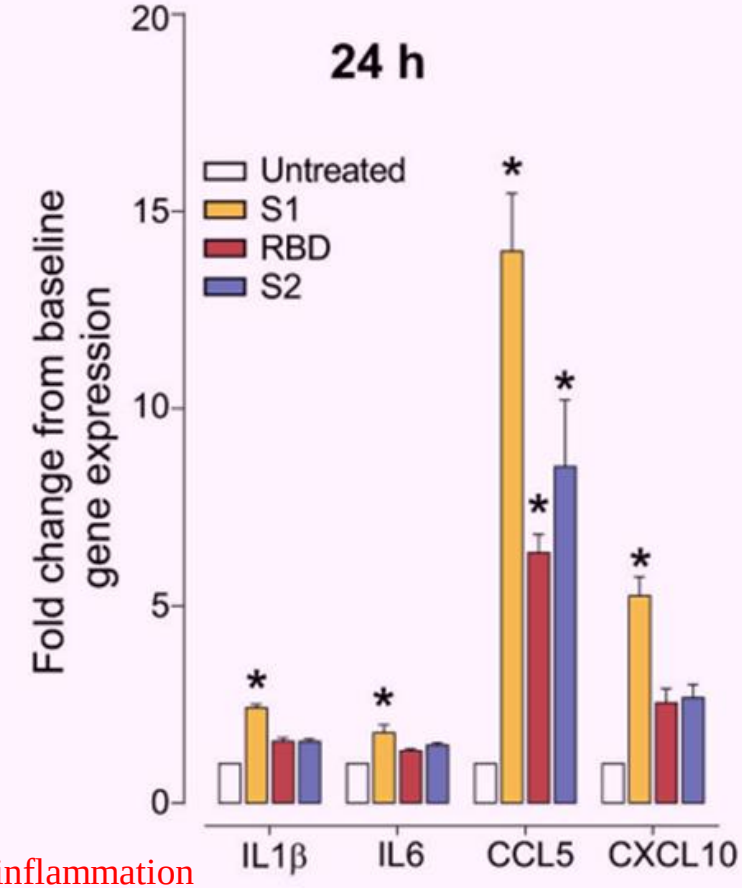

Thromboinflammation

SARS-CoV-2 spike protein S1 subunit alone can lead to pro-inflammatory responses through TLR4 signaling in murine and human macrophages and induce endothelial damage. SARS-CoV-2 spike protein induces inflammation via TLR2-dependent activation of the NF-κB pathway. SARS-CoV-2 spike proteins trigger a proinflammatory response on brain endothelial cells that may contribute to an altered state of BBB function.

Buzhdygan TP, et al. The SARS-CoV-2 spike protein alters barrier function in 2D static and 3D microfluidic in-vitro models of the human blood-brain barrier. *Neurobiol Dis.* 2020;146:105131.

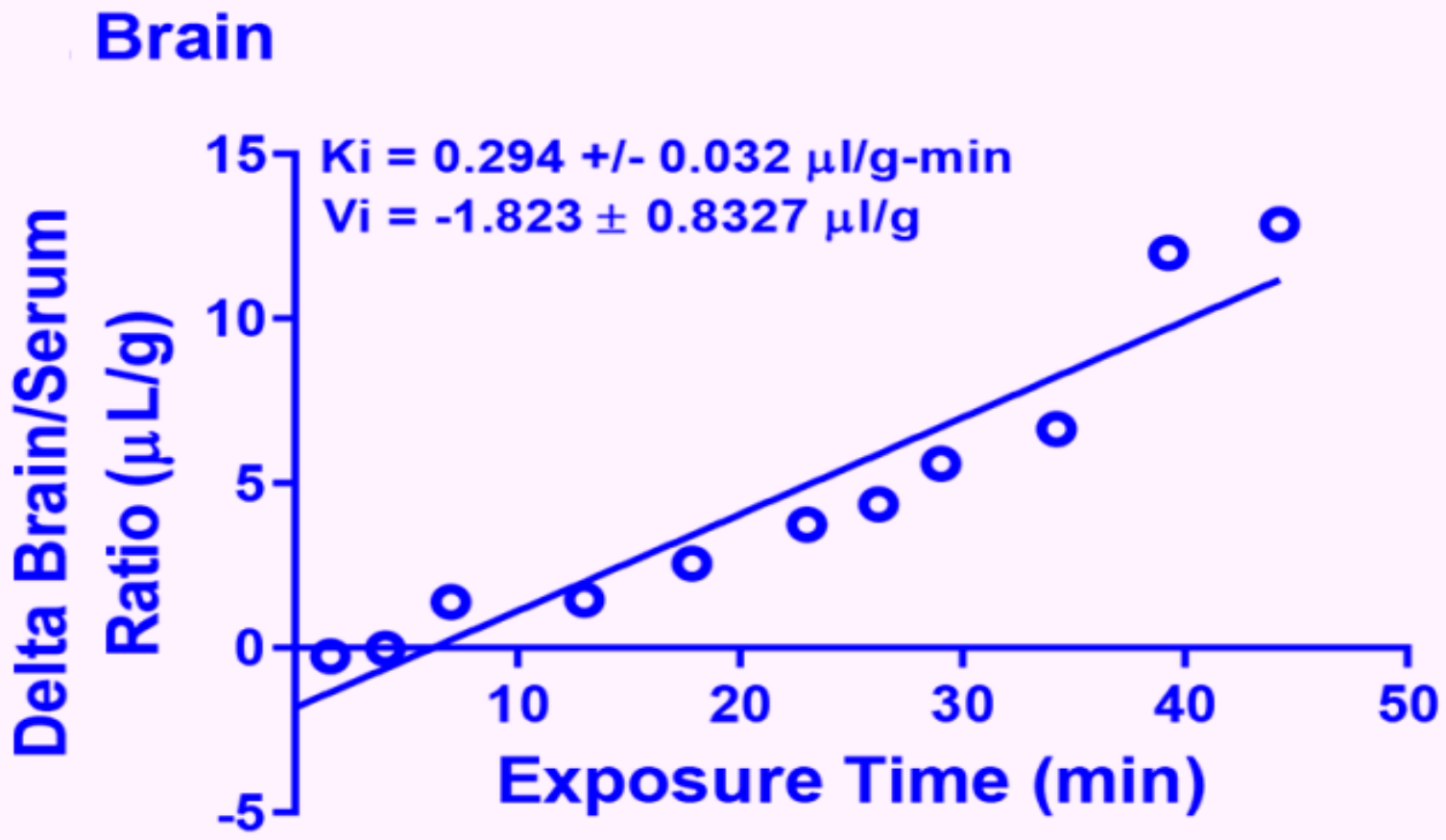

Intravenously injected radioiodinated S1 (I-S1) readily crossed the blood-brain barrier in male mice, was taken up by brain regions and entered the parenchymal brain space. I-S1 was also taken up by the lung, spleen, kidney and liver. Mechanistic studies indicated that I-S1 crosses the blood-brain barrier by adsorptive transcytosis.

Rhea EM, et al. The S1 protein of SARS-CoV-2 crosses the blood-brain barrier in mice. Nat Neurosci. 2021 Mar;24(3):368-378.

Any Questions ?

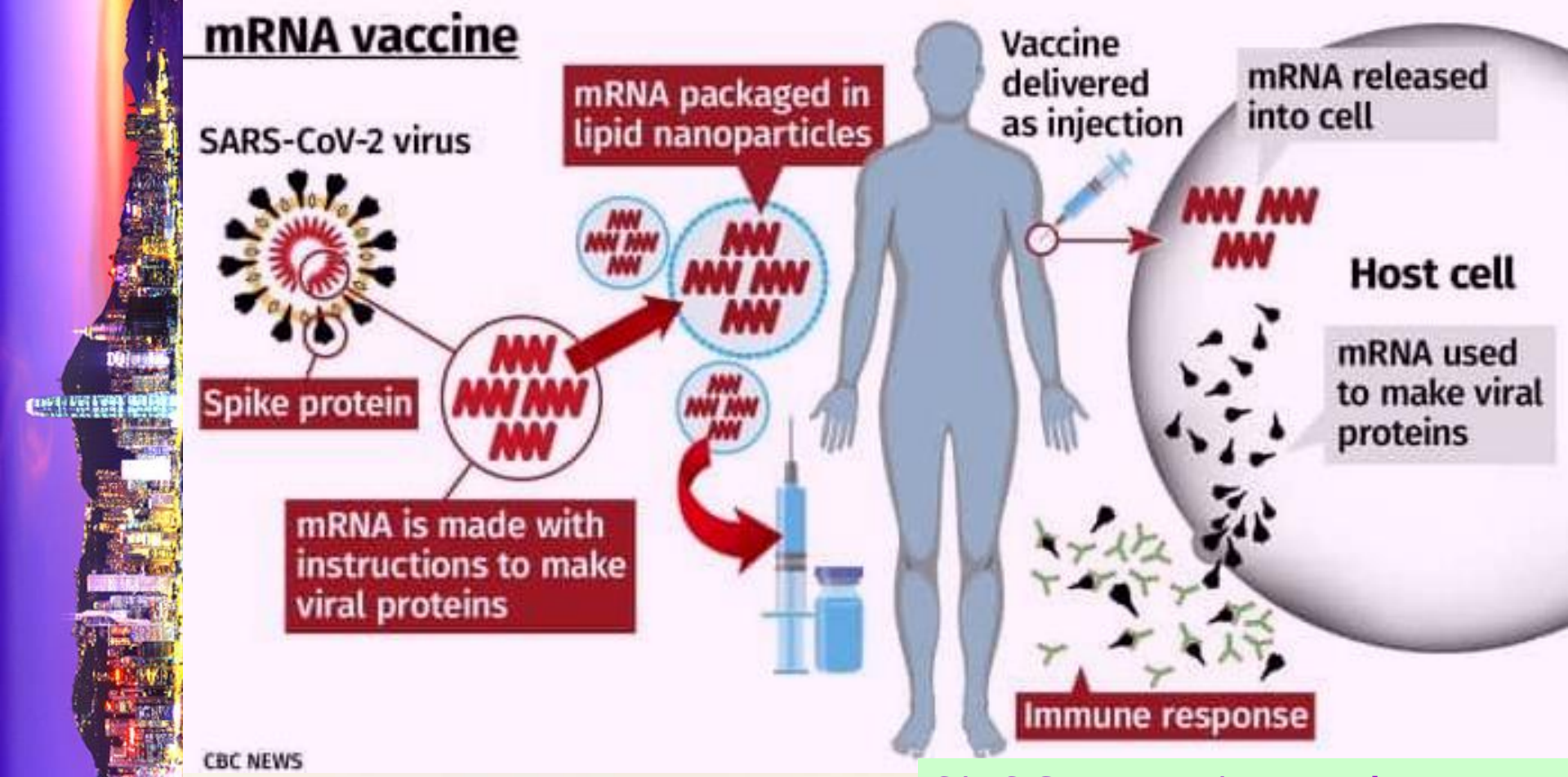

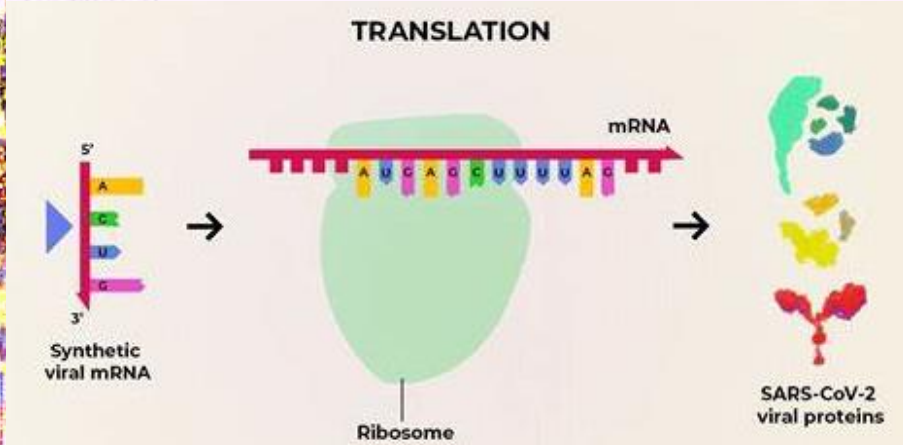

SARS-CoV-2 RNAs can be reverse-transcribed and integrated into the DNA of human cells during COVID-19 infection

Zhang L, et al. Proc Natl Acad Sci U S A. 2021 May 25;118(21):e2105968118.

BNT162b2 mRNA is reverse transcribed intracellularly into DNA in human liver tumour cell (Huh7 cell line) in as fast as 6 h upon BNT162b2 exposure.

Markus Aldén, et al. Mol. Biol. 2022, 44(3), 1115-1126

Thank you for your attention

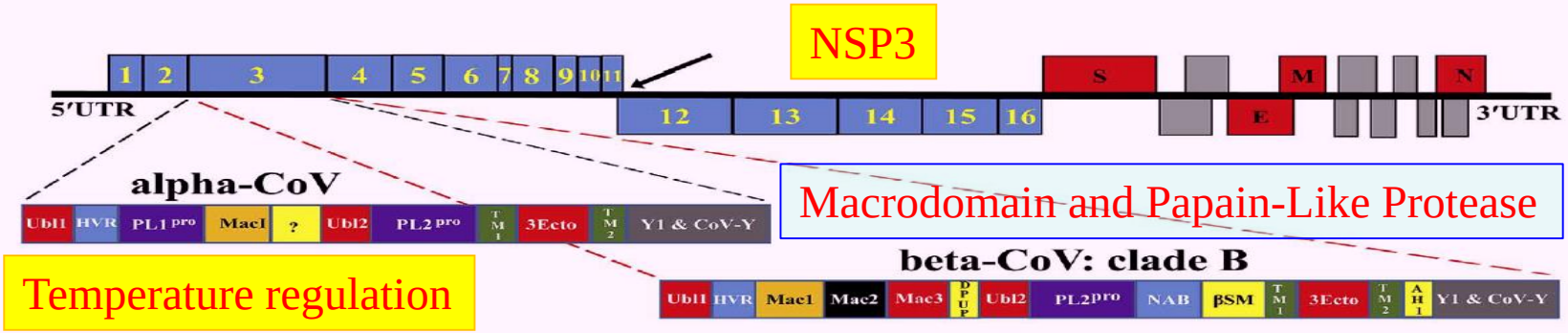

Deng X, Mettelman RC, et al.. Analysis of Coronavirus Temperature-Sensitive Mutants Reveals an Interplay between the Macrodomain and Papain-Like Protease Impacting Replication and Pathogenesis. *J Virol*. 2019;93(12):e02140-18.

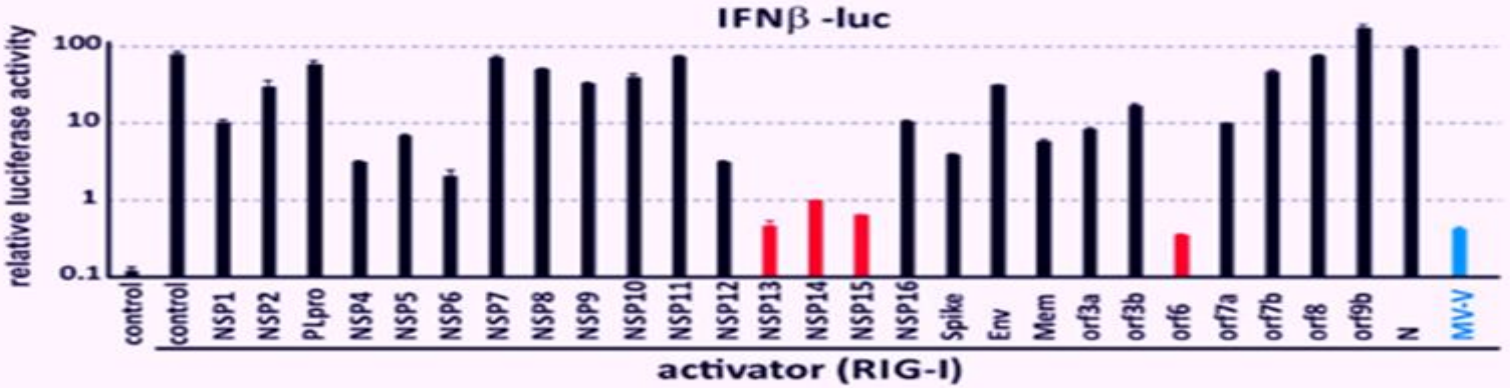

Yuen CK, Lam JY, Wong WM, et al. SARS-CoV-2 nsp13, nsp14, nsp15 and orf6 function as potent interferon antagonists. *Emerg Microbes Infect*. 2020;9(1):1418-1428.

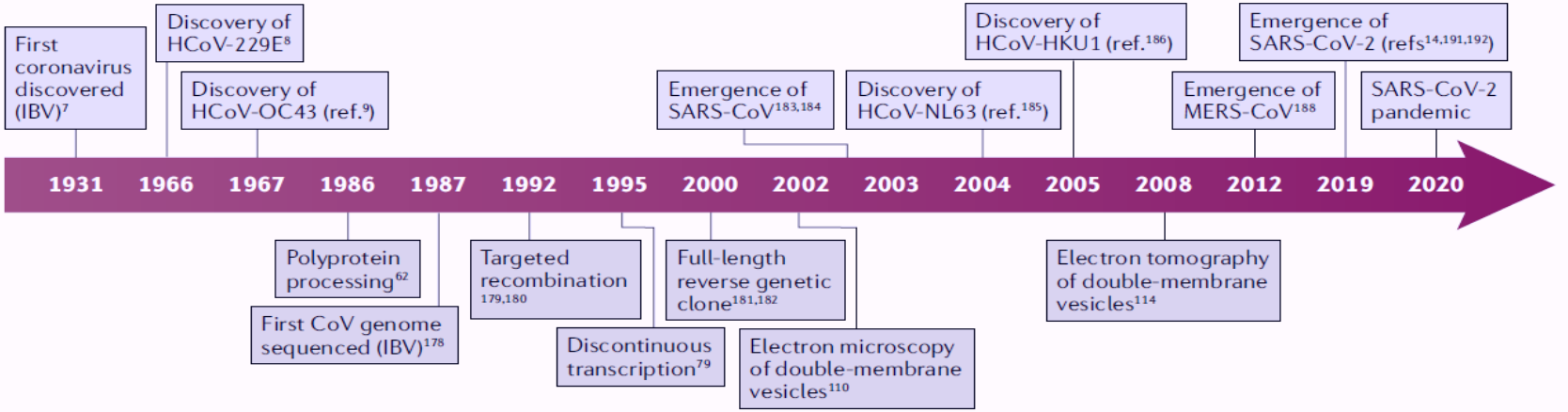

V'kovski, P., Kratzel, A., Steiner, S. *et al.* Coronavirus biology and replication: implications for SARS-CoV-2. *Nat Rev Microbiol* (2020).

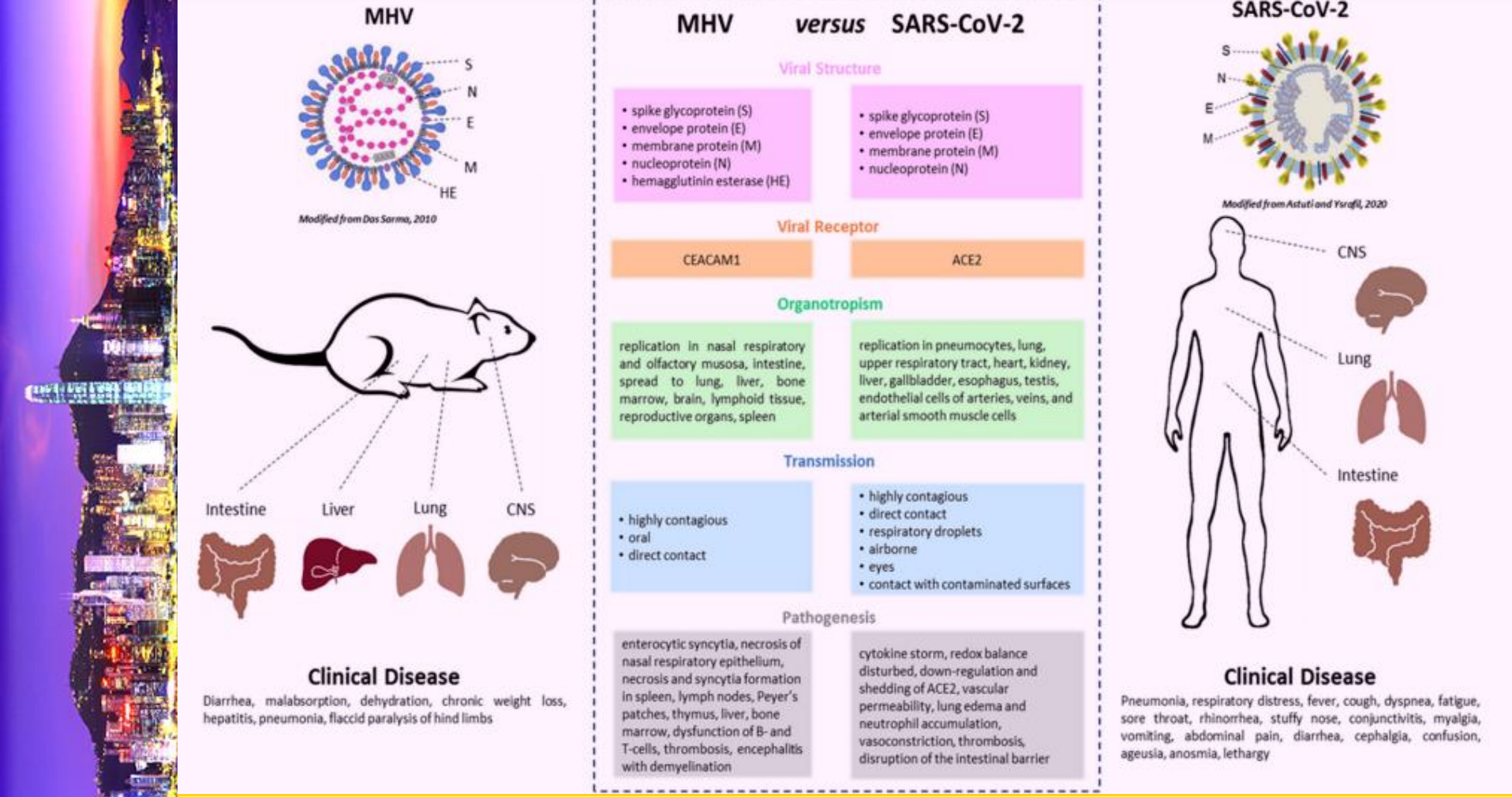

Temperature-sensitive (ts) coronavirus mutants of mouse hepatitis virus (MHV) (tsNC11) could offer mechanistic insights into the understanding of SARS-CoV-2. Whereas a dose of 100 p.f.u. of wild-type virus killed mice within a week, a 1000-fold higher dose of *ts* mutants did not. The growth defect in tsNC11 was attributed to a coding mutation within the macrodomain and papain-like protease 2 domain of the nonstructural protein 3

Deng X, Mettelman RC, O'Brien A, Thompson JA, O'Brien TE, Baker SC. Analysis of Coronavirus Temperature-Sensitive Mutants Reveals an Interplay between the Macrodomain and Papain-Like Protease Impacting Replication and Pathogenesis. J Virol. 2019 May 29;93(12):e02140-18.

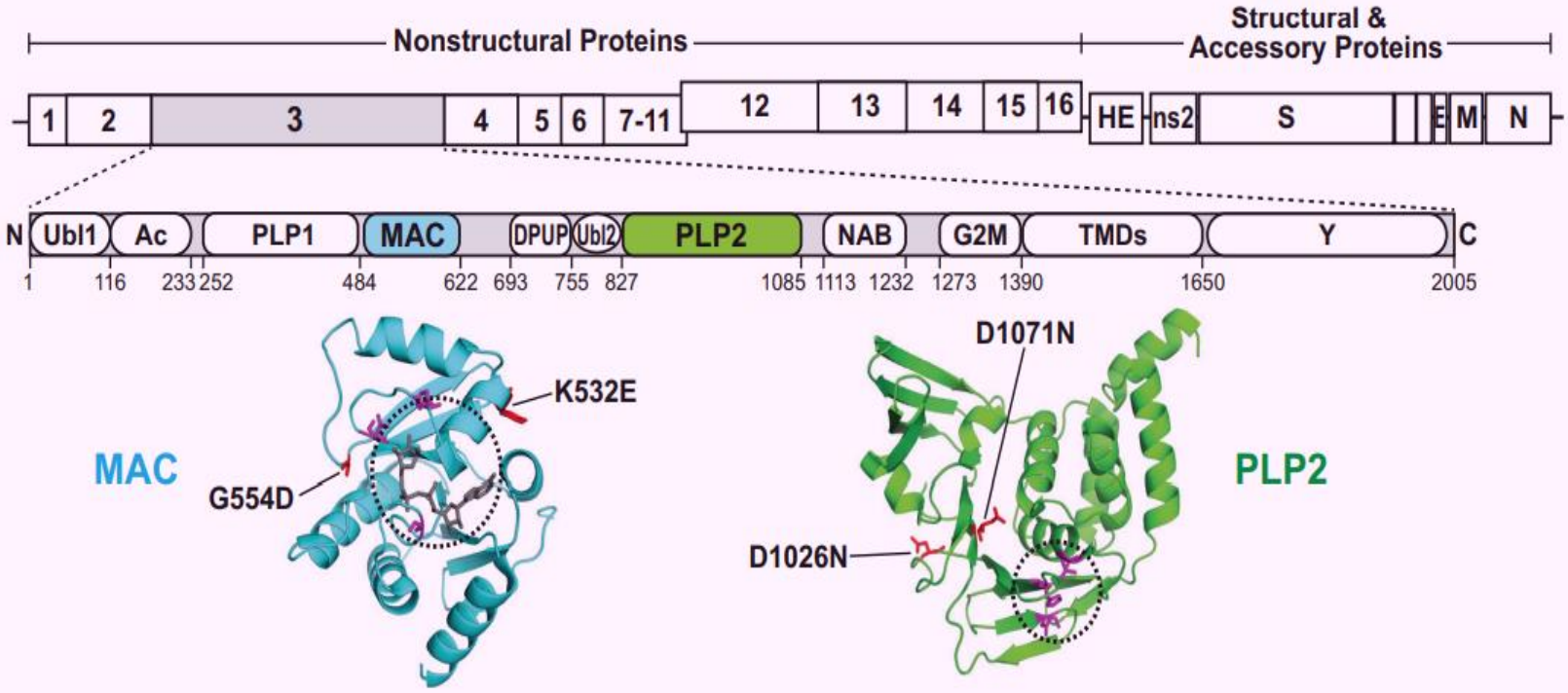

Produce temperature sensitive mutants

Both lead to post-translational block in IFN response

Prevent reversal to wide type

CoV replication induces profound rearrangement of the host ER and generates viral dsRNA intermediates, processes that can be sensed by the host to activate the innate immune response. CoV encodes highly conserved nonstructural proteins to serve as interferon (IFN) antagonists, and sequesters viral RNA in DMVs to prevent detection by host pattern recognition receptors. A key component in the assembly of the DMVs is nsp3, in particular the the macrodomain (MAC) and papain-like protease 2 (PLP2).

Deng X, Mettelman RC, O'Brien A, Thompson JA, O'Brien TE, Baker SC. Analysis of Coronavirus Temperature-Sensitive Mutants Reveals an Interplay between the Macrodomain and Papain-Like Protease Impacting Replication and Pathogenesis. J Virol. 2019 May 29;93(12):e02140-18.

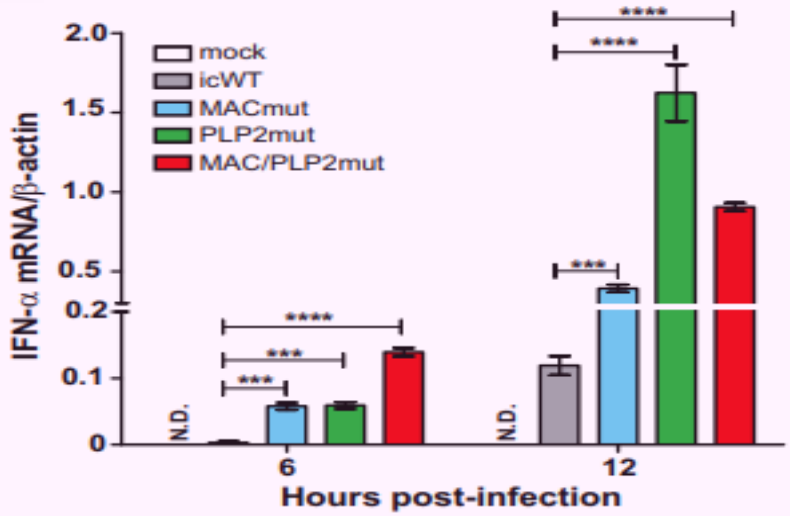

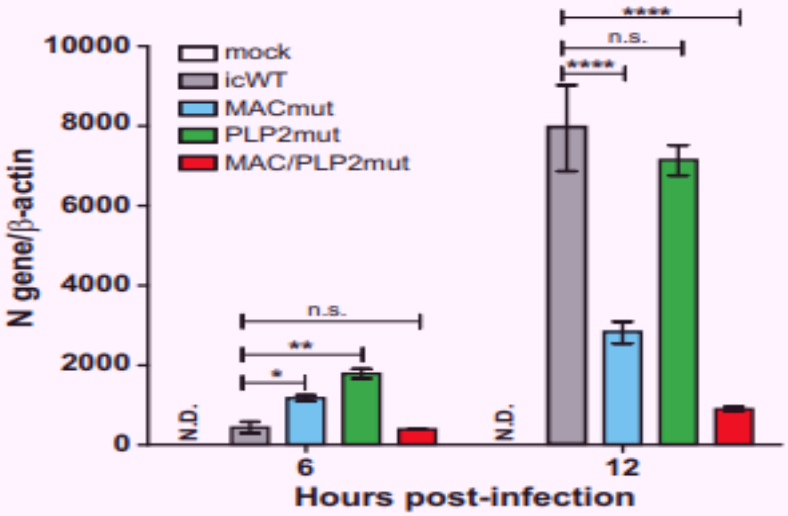

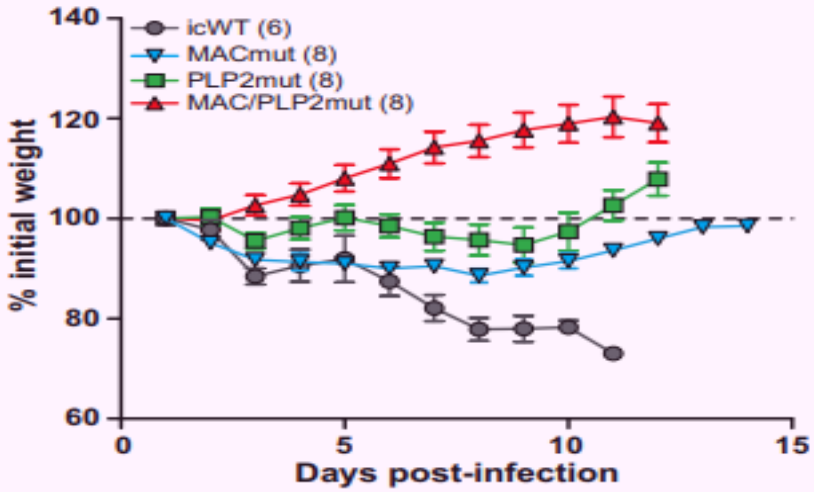

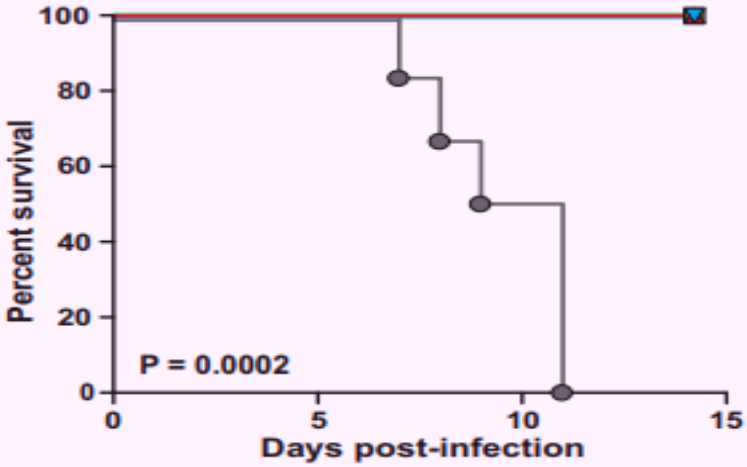

The interplay of macrodomains, enzymes that remove posttranslational ADP-ribosylation of proteins, and viral multifunctional papain-like proteases (PLP2 domain), enzymes that cleave polyproteins and remove polyubiquitin chains via deubiquitinating activity, are important for replication and antagonizing the host innate immune response. The replicase proteins containing the MAC and PLP2 mutations were more rapidly degraded at the nonpermissive temperature than were the wild-type proteins.

Deng X, Mettelman RC, O'Brien A, Thompson JA, O'Brien TE, Baker SC. Analysis of Coronavirus Temperature-Sensitive Mutants Reveals an Interplay between the Macrodomain and Papain-Like Protease Impacting Replication and Pathogenesis. J Virol. 2019 May 29;93(12):e02140-18.

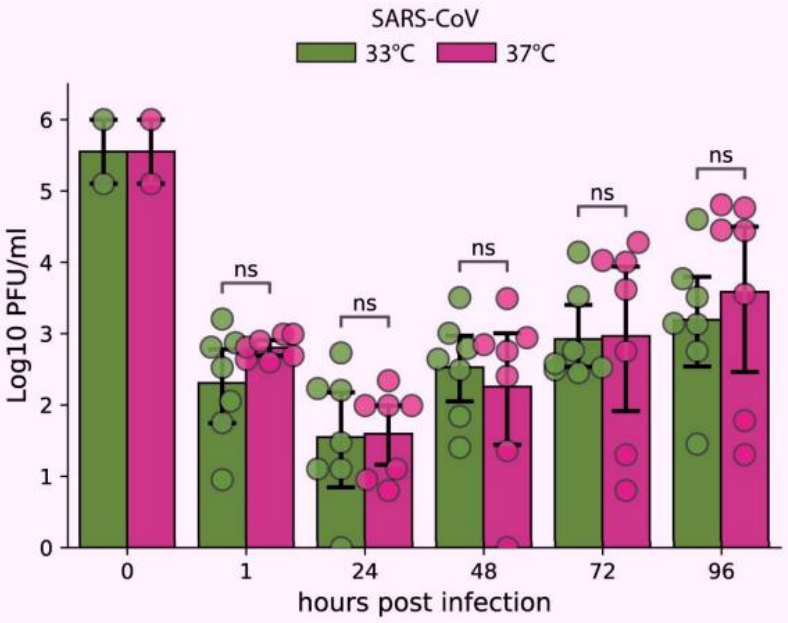

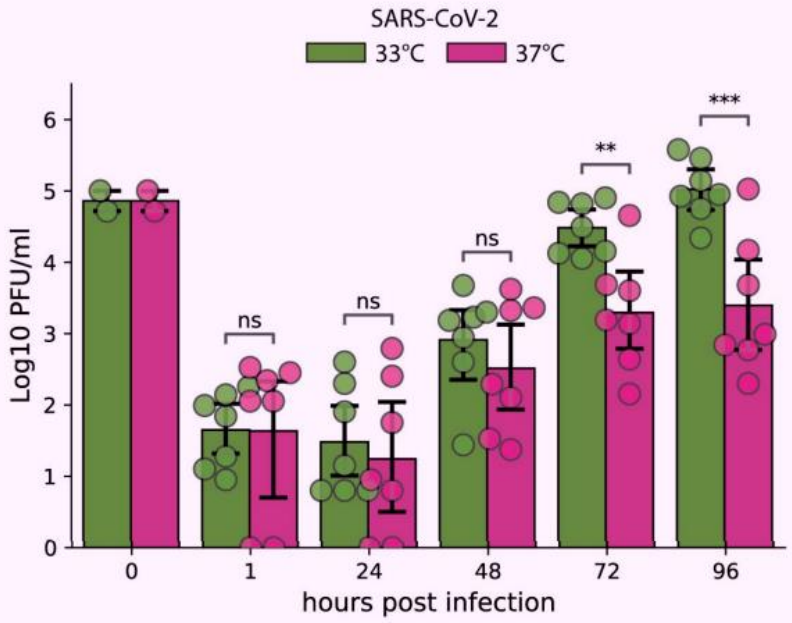

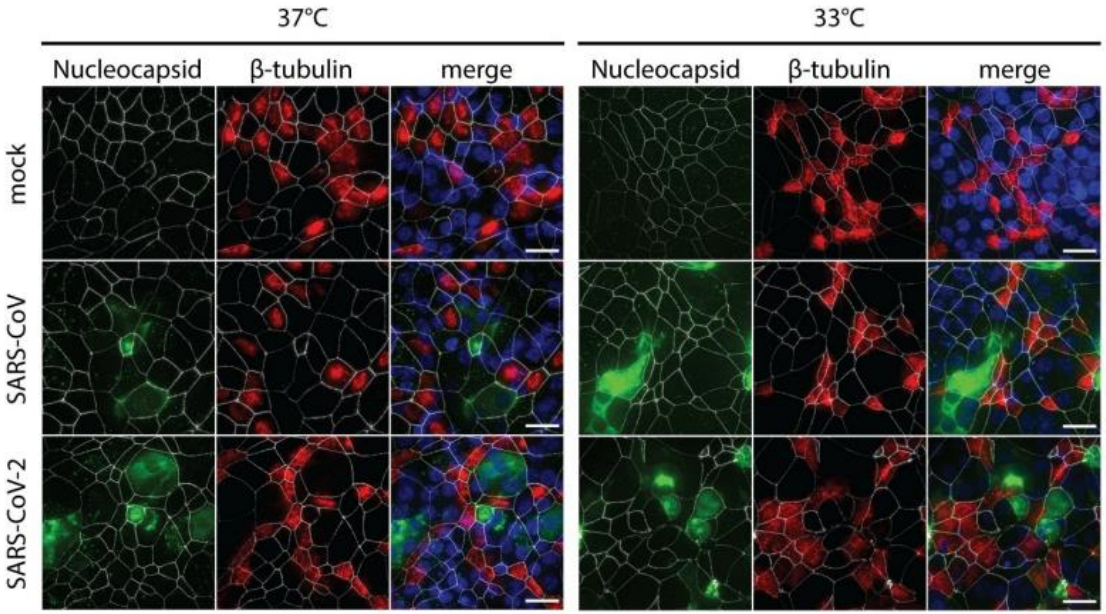

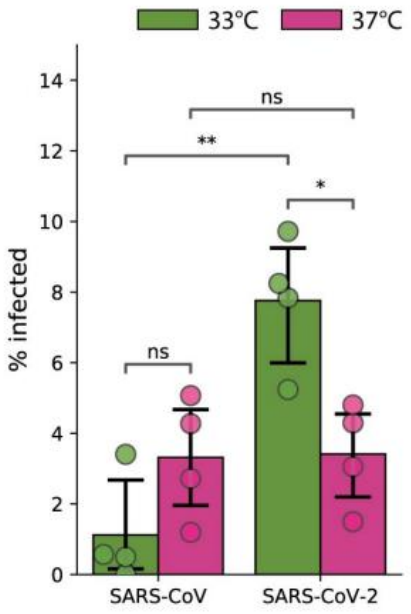

SARS-CoV and SARS-CoV-2 replication kinetics in hAEC cultures. Well-differentiated hAEC cultures

V'kovski P, Gultom M, Kelly JN, et al. *PLoS Biol*. 2021;19(3):e3001158.

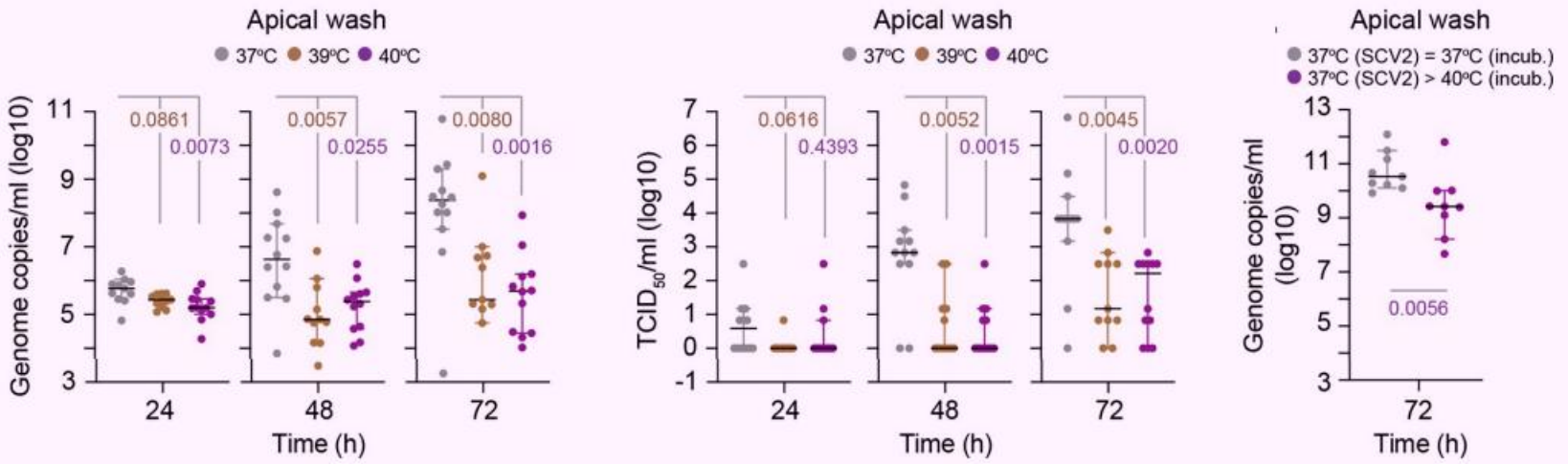

Elevated temperature restricts SARS-CoV-2 replication in respiratory airway cultures. Ciliated respiratory cultures

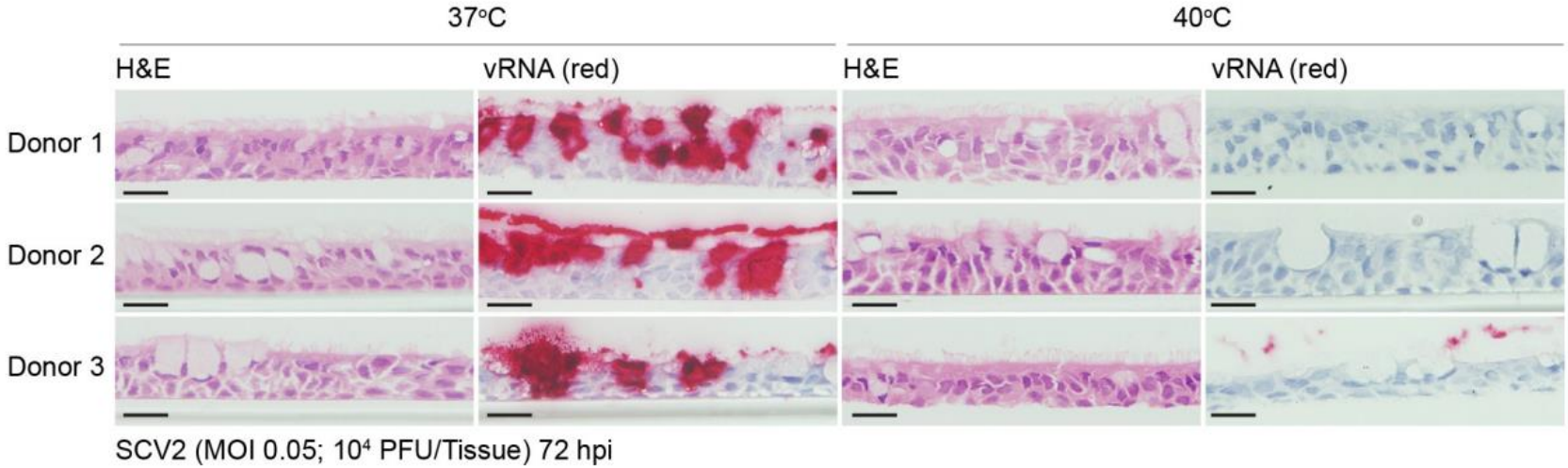

Elevated temperature restricts SARS-CoV-2 replication in respiratory airway cultures in a donor-independent manner.

Herder V, Dee K, Wojtus JK, et al. Elevated temperature inhibits SARS-CoV-2 replication in respiratory epithelium independently of IFN-mediated innate immune defenses. *PLoS Biol*. 2021;19(12):e3001065.

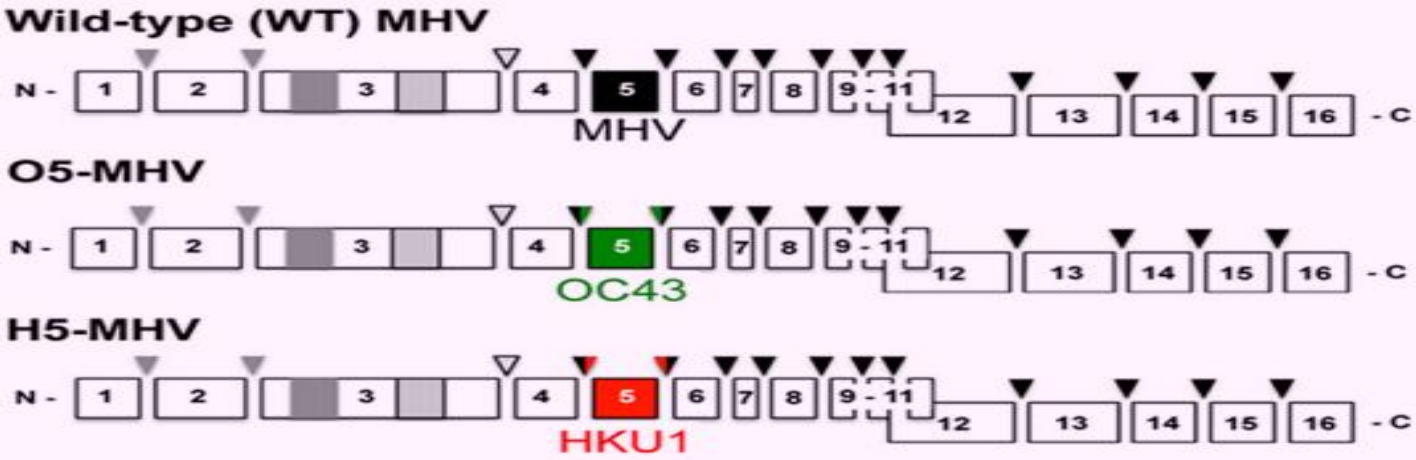

Virus	Virus Titers (PFU / mL)*		EOP
	32°C	40°C	Titer 40°/ Titer 32°
WT-MHV	5.1×10^7	7.2×10^7	1.4
H5-MHV	2.0×10^7	1.1×10^8	5.7
O5-MHV	1.1×10^7	2.0×10^7	1.7
H5-V148A	3.1×10^6	8.7×10^6	2.8
O5-V148A	1.2×10^7	2.1×10^7	1.7
O5-S133A	1.5×10^7	8.8×10^4	6×10^{-3}
O5-V148A / Y134H	2.0×10^5	5.0×10^1	3×10^{-4}

Unique sequences of amino acids in cold-adapted live attenuated SARS-CoV-2 vaccine strain (SARS-CoV-2/human/Korea/CNUHV03-CA22°C/2020).

Protein Name			Difference of Amino Acid Sequences	The Number of Changed Sequence
ORF1ab polyprotein	ORF1a polyprotein	nsp2	Deletion: GHV(82~84), M85V	4/641
		nsp6	N3609K, D3671T	2/290
		nsp7	D3926A	1/83
	ORF1b	helicase	L5604F	1/601
	S protein		T95I, N185K, S968A	3/1274
	Total amino acids			11/9755 (including nonchanged ORFs)

vaccines

MDPI

Article

Cold-Adapted Live Attenuated SARS-Cov-2 Vaccine Completely Protects Human ACE2 Transgenic Mice from SARS-Cov-2 Infection

Sang Heui Seo [1,2,*] and Yunyueng Jang [1,2]

1 Laboratory of Influenza Research, College of Veterinary Medicine, Daejeon 34134, Korea; jyy1915@naver.com
2 Institute of Influenza Virus, Chungnam National University, Daejeon 34134, Korea
* Correspondence: seos@cnu.ac.kr; Tel.: +82-42-821-7819; Fax: +82-42-821-6762

Received: 28 August 2020; Accepted: 1 October 2020; Published: 3 October 2020

Virulence marker and pathogenic determinant	Pandemic virus				HPAI virus		Contemporary seasonal virus	
	1918 H1N1	1957 H2N2	1968 H3N2	2009 H1N1	H5N1	H7N7	H1N1	H3N2
HA (binding and fusing with the host cell; antigenic determinant)								
Sialic acid linkage specificity	α-2,6*	α-2,6‡	α-2,6‡	α-2,6 and α-2,3§	α-2,3	α-2,3‖	α-2,6	α-2,6
Residues involved in binding specificity¶	D190 and D225	Q226 and N186, or 226 and S228	L226 and S228	D190 and D225§;K133#, K145# and K222#	G143, T160, N186, Q196, Q226 and G228	Q226**	D190 and D225	L226‡‡ and S228
Multibasic cleavage site	No	No	No	No	Yes	Yes	No	No
PB1–F2 (induction of apoptosis; promotion of secondary bacterial infection)								
S66 (associated with increased virulence), N66 or truncation	S66	N66	N66	Truncation	S66 or N66‡‡	N66	Truncation	N66
PB2 (temperature-dependent replication competence)								
Adaptation to mammalian hosts	K627	K627	K627	R591	K627 or N701‖‖	K627 or N701‖‖	K627	K627
NS1 (host antiviral response antagonist)								
PDZ domain-binding motif¶¶	KSEV	RSKV	RSKV	Truncated	ESEV or EPEV; ~3.3% of H5N1 isolates in 2003 were truncated	ESEV	RSEV	RSKV
CPSF30 binding	Yes	Yes##	Yes##	No	Yes##	Yes***	Yes	Yes
E91 associated with virulence	No	No	No	No	Yes‡‡‡	No	No	No
M2 (ion channel)								
Resistant to adamantanes (presence of N31)	No	No	No	Yes	Yes and no§§§	No	No	Yes
NA (receptor-destroying enzyme)								
Resistant to oseltamavir (presence of Y275 and S294)	No	No	No	No‖‖‖	No‖‖‖	No	Yes	No

CPSF30, cleavage and polyadenylation specificity factor 30 kDa subunit; HA, haemagglutinin; HPAI, highly pathogenic avian influenza; NA, neuraminidase; NS1, non-structural protein 1.

*Some 1918 virus variants have differential receptor binding, allowing dual α-2,6-linked sialic acid (α-2,6-SA) and α-2,3-SA specificity (see main text for details).

LPAI virus

H7N9

A-2,3

Q226L

No

Unknown

E627K/ D701N

truncated

Unknown

Unknown

Yes

5aa stalk deletion

2 patients on steroid

	Human (ZJ/DTID-ZJU01*)	Chicken (CK/ZJ/DTID-ZJU01*)	Human (Shanghai/1†)	Human (Shanghai/2†)	Human (Anhui/1†)	Function
Haemagglutinin‡						
186	Val	Val	Gly	Val	Val	Gly186Val increases binding affinity for α-2,6-linked sialic acid receptor
226	Leu	Gln	Gln	Leu	Leu	Gln226Leu increases binding affinity for α-2,6-linked sialic acid receptor
Neuraminidase§						
292	Arg	Arg	Lys	Arg	Arg	Arg292Lys reduces susceptibility to oseltamivir and zanamivir
M2						
31	Asn	Asn	Asn	Asn	Asn	Ser31Asn causes resistance to adamantanes
PB2						
627	Glu	Glu	Lys	Lys	Lys	Glu627Lys results in mammalian host adaptation for viral RNA replication at 33°C
701	Asn	Asp	Asp	Asp	Asp	Asp701Asn enhances transmission in guinea pigs

*Described in our study. †Described in another report.[14] ‡H3 numbering. §N2 numbering.

PB2-E627K (Glutamic acid627Lysine) and PB2-D701N(Aspartic acid701Asparagine) mutants are absents in poultry (chicken, duck, quail, pigeon) isolated in the live poultry market !

聚合酶鹼性蛋白質 2 (Polymerase basic 2, *PB2*)

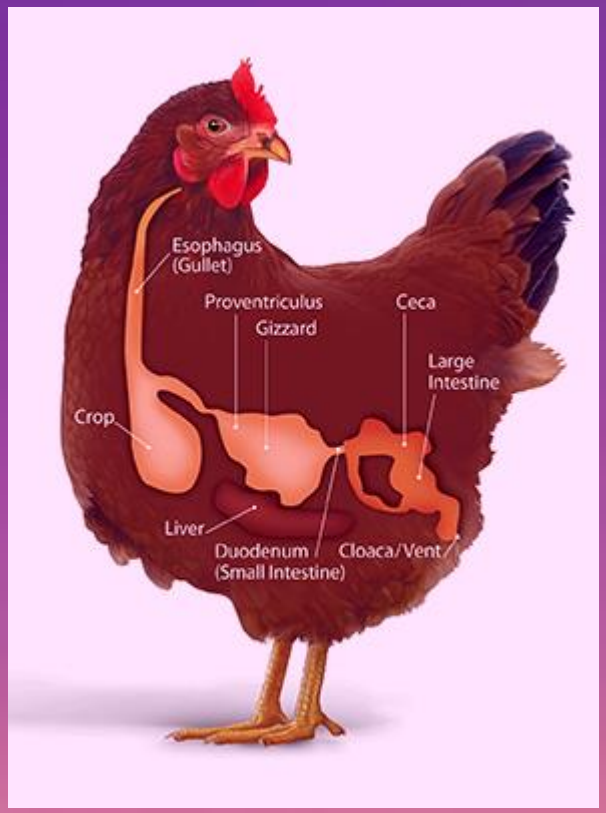

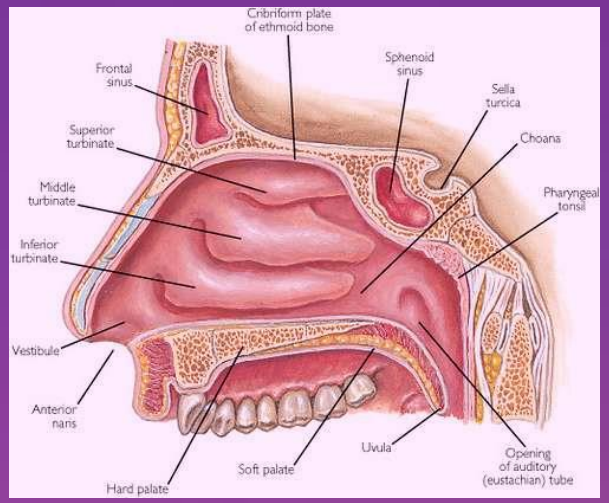

PB2

E627K

33°C

37°C

D701N

44°C

Mammals

PB2 627 amino acid composition for H5N1, H9N2, and H7N9 viruses.

Residue	Avian H5N1	Human H5N1	Avian/Human H9N2	Human H7N9
E	805	128	245	0
K	**242**	**49**	**4**	**3**
V	0	0	51	0
G	0	0	1	0
Total	1047	177	301	3
K Percentage	23.11%	27.68%	1.33%	100.00%

Chen GW, Lai MM, Wu SC, Chang SC, Huang LM, Shih SR. Is avian influenza A (H7N9) virus staggering its way to humans? J Formos Med Assoc. 2013 Jun;112(6):312-8. doi: 10.1016/j.jfma.2013.04.015.

文匯網:鸵鸟蛋是上海静安寺下沉广场举办的新年食品节上的年货“新宠”。

上海野生動物園

鸵鸟养殖

“High disease resistant” species of ostrich and emu chicks are available for sale in Beijing

Delicacies in Shanghai

青海湖

2005 H5N1
PB2-627Lys
(E627K)
33°C and 37°C
H7N7 only
human death is
associated with
E627K mutant

Struthio asiaticus was an ostrich of the Pliocene and Pleistocene

In China, ostriches are known to have become extinct only around or even after the end of the last ice age; images of ostriches have been found there on prehistoric pottery and as petroglyphs indicating that they were around at the same time as humans first reached China.

Number of avian virus isolates encoding mammalian-type amino acids at positions 627 and 701 in PB2 in the Influenza Virus Resource database[a]

Avian species	No. of viruses possessing:		Total no. of viruses
	PB2-627Lys	PB2-701Asn	
Duck	1	1	375
Chicken	2	0	426
Ratitae			
Ostrich	2	0	6
Emu	2	1	4
Rhea	1	0	2

[a] Numbers of viruses isolated prior to 2005 from duck, chicken, and three *Ratitae* species (ostrich, emu, and rhea) are shown.

Shinya, K. et al. Ostrich involvement in the selection of H5N1 influenza virus possessing mammalian-type amino acids in the PB2 protein. J Virol. 83, 13015-8 (2009).

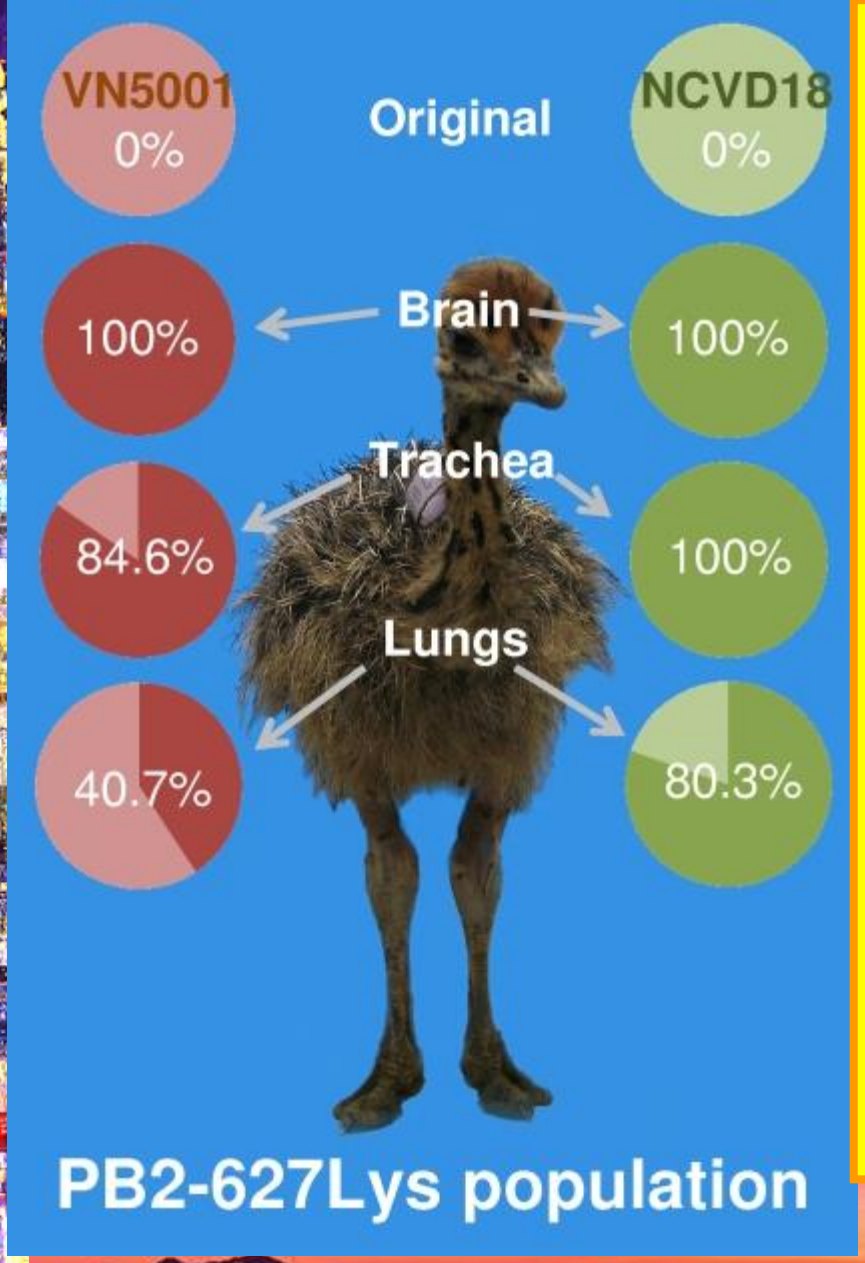

PB2, 627Lys and 701Asn mutation in human H5N1 infection

(1) 701Asn mutation + in patient (Lancet Yu Chen 25/4/13)

(2) 627Lys(K) mutation 3/3 patients (NEJM Gao 11/4/2013)

➔ Simultaneous 627Lys and 701Asn mutation may allow efficient transmission among humans

Infection of Ostrich by H5N1 can lead to the selection of these mutants.

China start ostrich farming since 1992 and becomes the largest ostrich raiser in Asia in 2004 and now ranks the fifth ostrich raiser in the world

South Africa ostrich flock drop from a million ↓to 250 000 due to outbreak of H5N2.in 2012.and H7N1 in 2013.

Shinya, K. et al. Ostrich involvement in the selection of H5N1 influenza virus possessing mammalian-type amino acids in the PB2 protein. J Virol. 83, 13015-8 (2009).

1992 China started to import and artificially breed ostriches
1997 Outbreak of H5N1 in Hong Kong
2004 China becomes largest ostrich raiser in Asia
2005 Outbreak of E267K mutation of H5N1 in Lake Qinghai

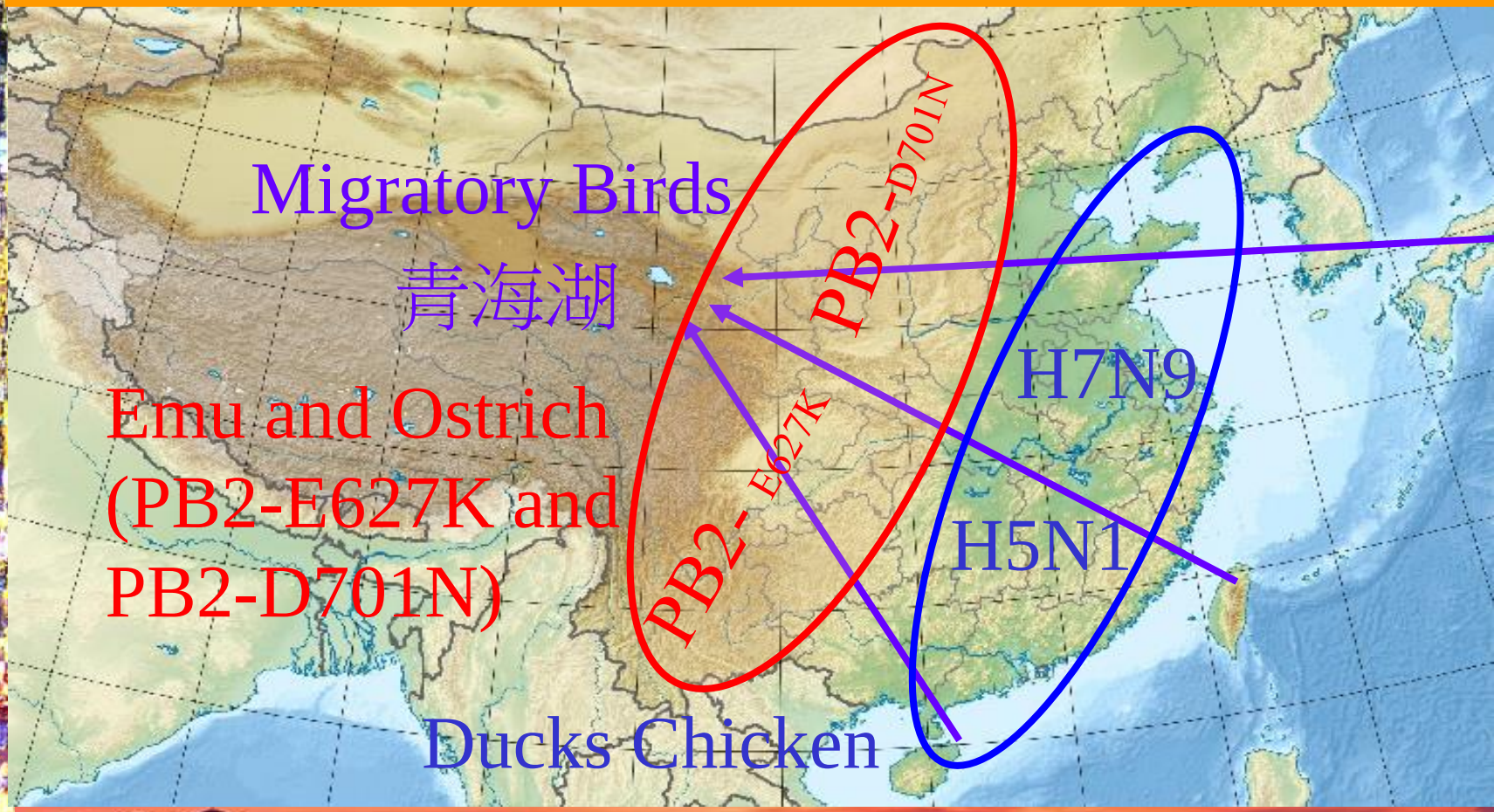

Hypothesis : PB2 E267K Mutation in 2005 in Lake Qinghai and the current situation of H7N9 in China

NFκB activation (活化) is a prerequisite for influenza infection and cytokine dysregulation

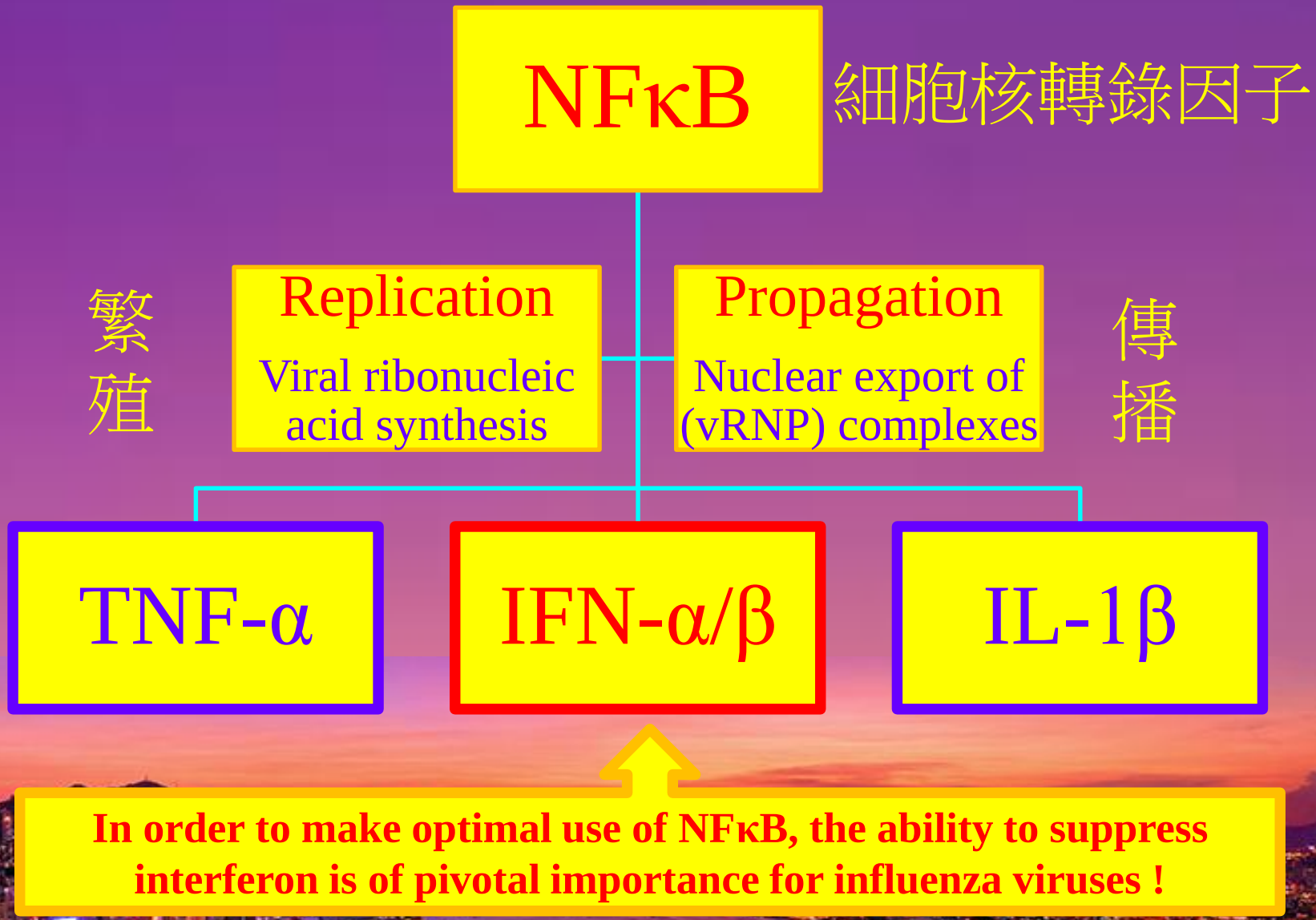

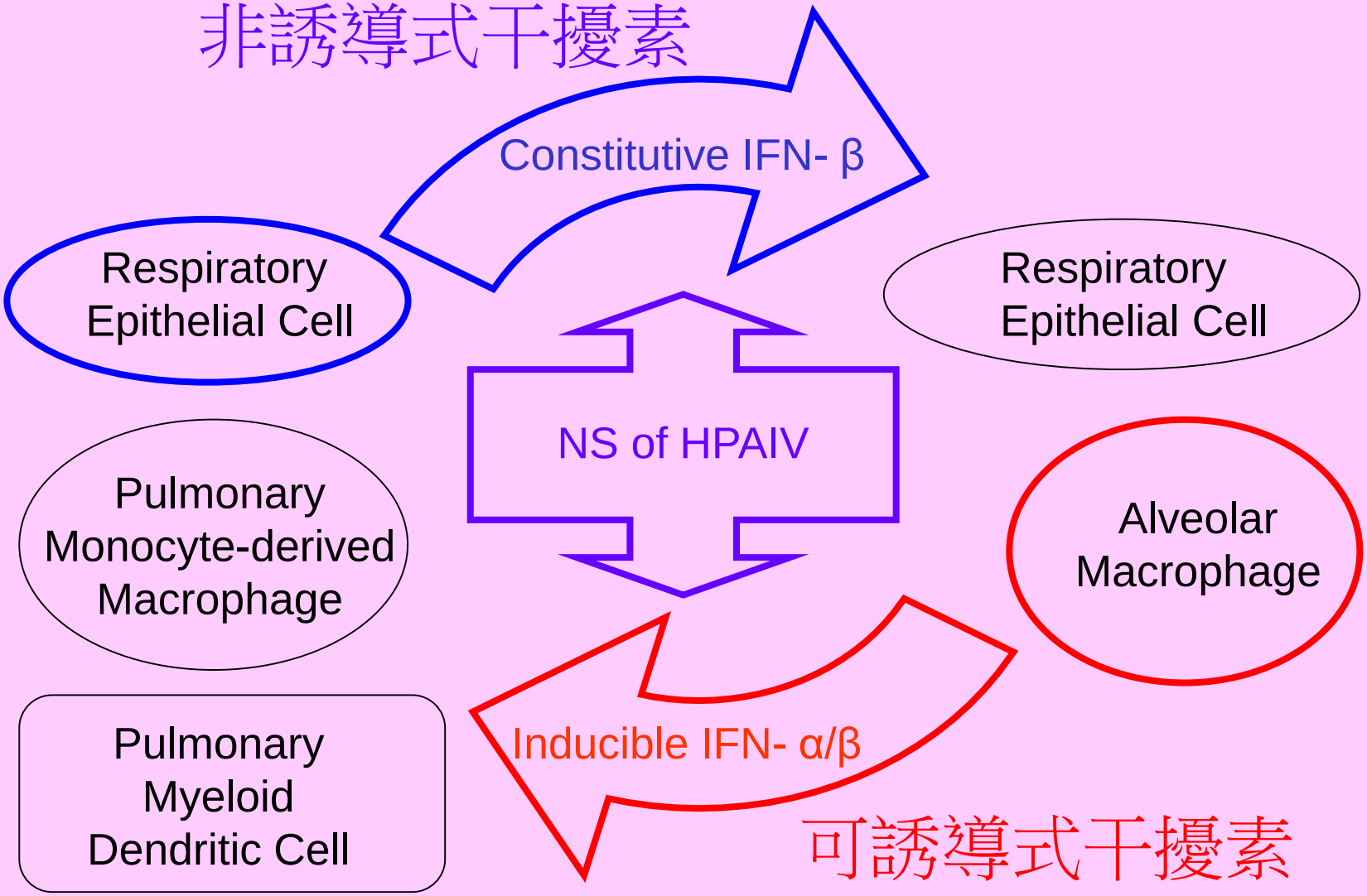

IFN-β plays an important role in the defense against influenza A virus that cannot be compensated for by IFN-α.

Constitutive and Inducible IFN-β

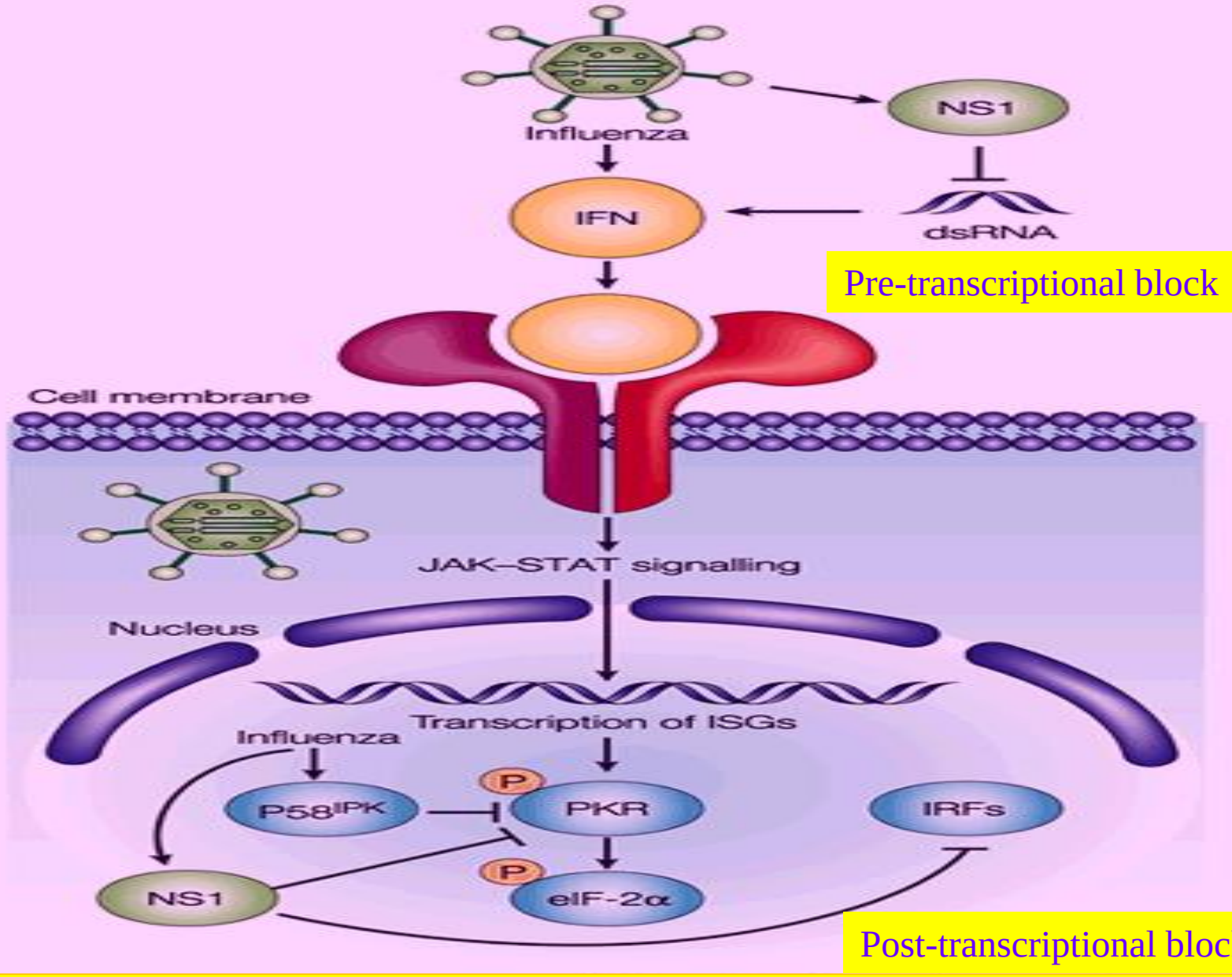

The inducible Type I interferon can be blocked at the pre-transcriptional and post-transcriptional level.

IFN-β	Constitutive IFN-β inhibition	Inducible IFN-β inhibition		Mortality
		Pre-transcriptional	Post-transcriptional (Optimal human CPSF30 binding)	
H2N2 or H3N2	×	×	✓	<0.1%
2009PV	?	✓	×	<0.1%
1918PV	?	✓	✓	~2.5%
H5N1 (1997)	✓	✓	×	33%
H7N9 (2013)	?	✓	×	33%
H5N1 (2003-	✓	✓	✓	~60%

IFN-β is encoded by a single gene, while both the human and mouse genomes contain 13 functional IFN-α genes

As opposed to H2N2 and H3N2, the NS1 proteins of 1918PV, HPAIV and some H1N1 viruses (except 1940-1957 and 1977-1990) block the activation of IRF3 and interferon-β transcription.

Kuo, R.L. et al. Influenza A virus strains that circulate in humans differ in the ability of their NS1 proteins to block the activation of IRF3 and interferon-β transcription. *Virology.* 408. 146-58 (2010).

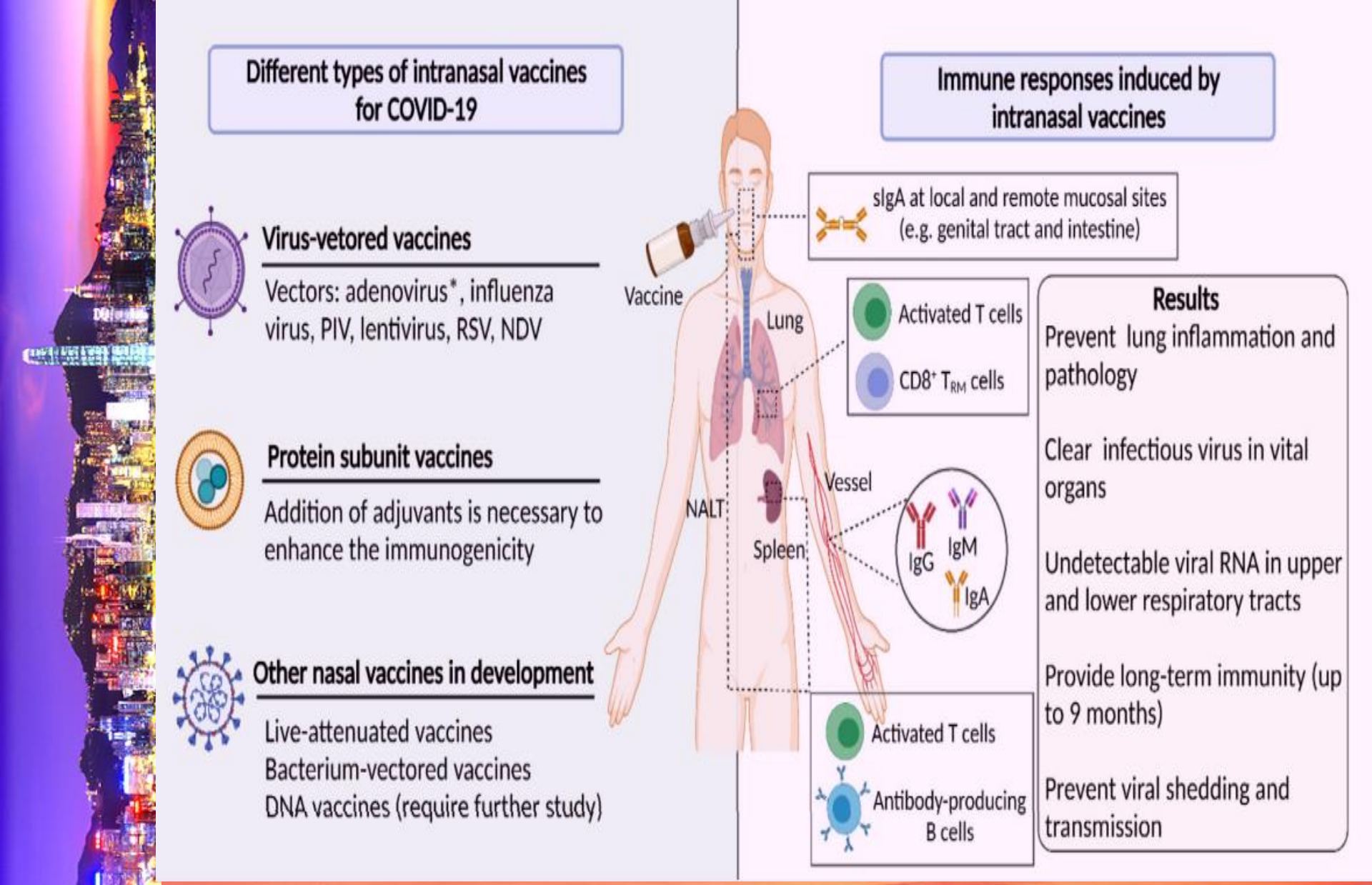

Alu A, Chen L, Lei H, Wei Y, Tian X, Wei X. Intranasal COVID-19 vaccines: From bench to bed. EBioMedicine. 2022 Feb;76:103841. doi: 10.1016/j.ebiom.2022.103841..

Live Attenuated Vaccines

Kaur SP, Gupta V. COVID-19 Vaccine: A comprehensive status report. *Virus Res*. 2020;288:198114.

DelNS1-SARS-CoV2-RBD (University of Hong Kong)

- This LAV is influenza-based vaccine strain with a deletion in the NS1 gene. It is re-organized to express the RBD domain of SARS-CoV-2 spike protein on its surface and, is cultivated in the chick embryo and/or Madin Darby Canine Kidney Cells (MDCK) cells. It is potentially more immunogenic than the wild type influenza virus and can be administered as a nasal spray
- This vaccine strategy has been selected as one of the five vaccine technologies by the Ministry of Science and Technology of China for further evaluation.

https://fightcovid19.hku.hk/hku-state-key-laboratory-for-emerging-infectious-diseases-joins-global-effort-to-develop-covid-19-vaccine/
https://cepi.net/news_cepi/cepi-partners-with-university-of-hong-kong-to-develop-covid-19-vaccine/

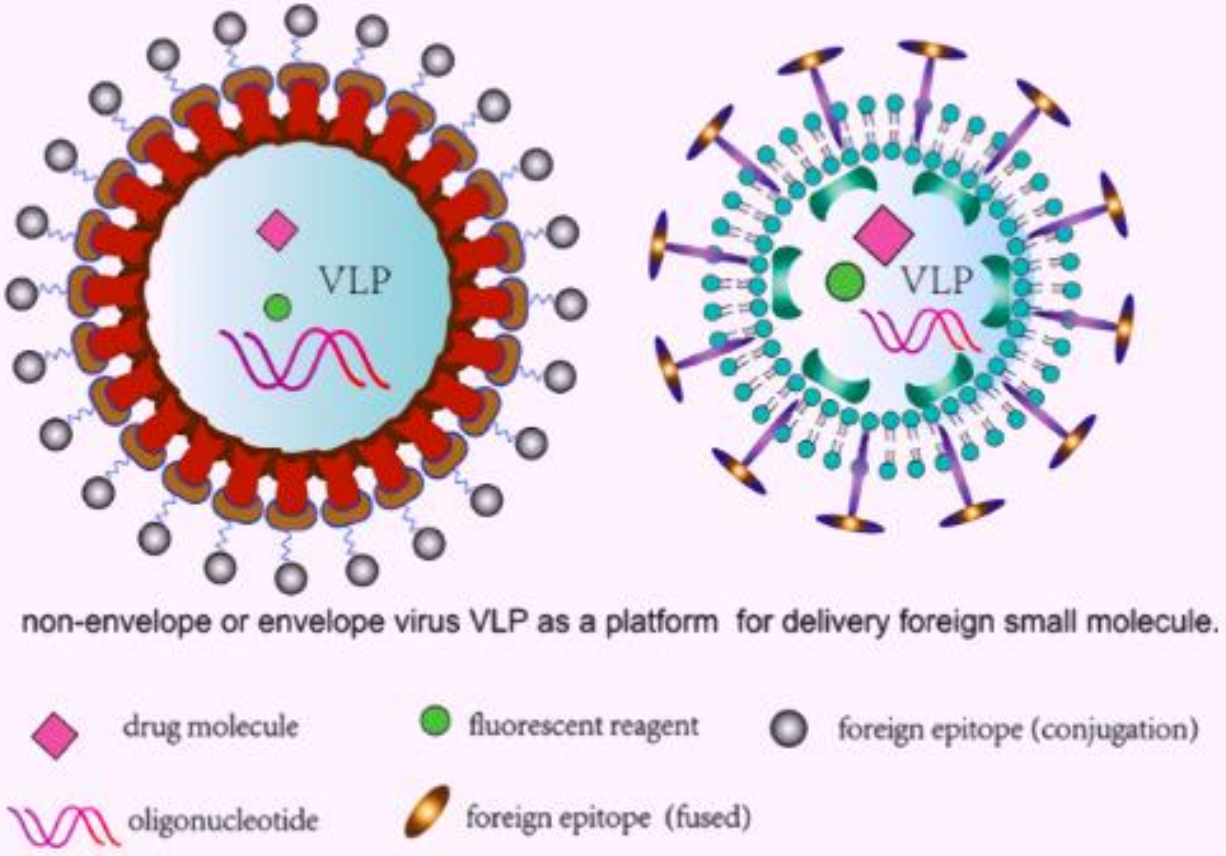

A schematic representation of assembly VLPs derived from enveloped or nonenveloped viruses. (Yan, 2015)

Virus Like Particle

https://www.creative-biolabs.com/sars-cov-virus-like-particles-vlps.html

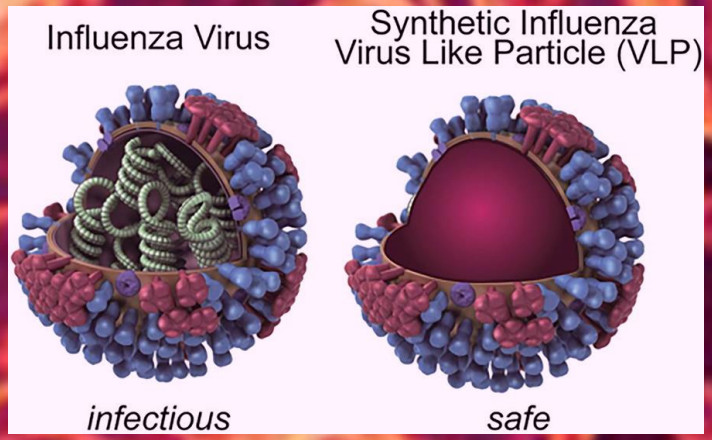

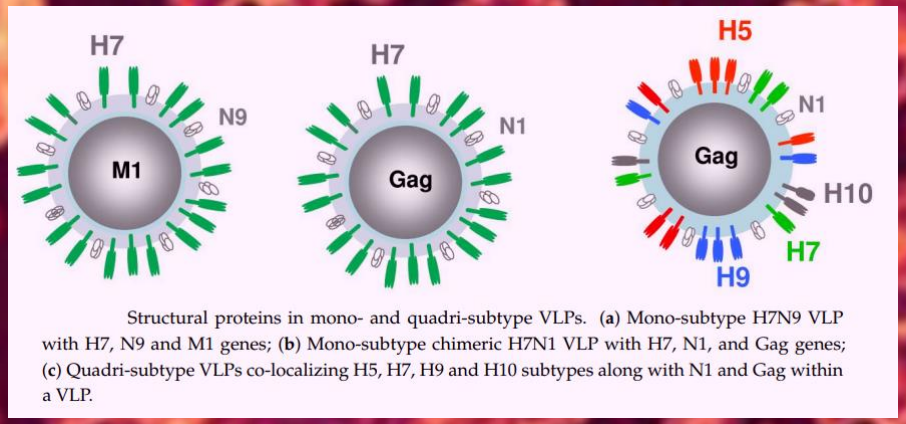

Structural proteins in mono- and quadri-subtype VLPs. (**a**) Mono-subtype H7N9 VLP with H7, N9 and M1 genes; (**b**) Mono-subtype chimeric H7N1 VLP with H7, N1, and Gag genes; (**c**) Quadri-subtype VLPs co-localizing H5, H7, H9 and H10 subtypes along with N1 and Gag within a VLP.

Influenza Virus-like Particles

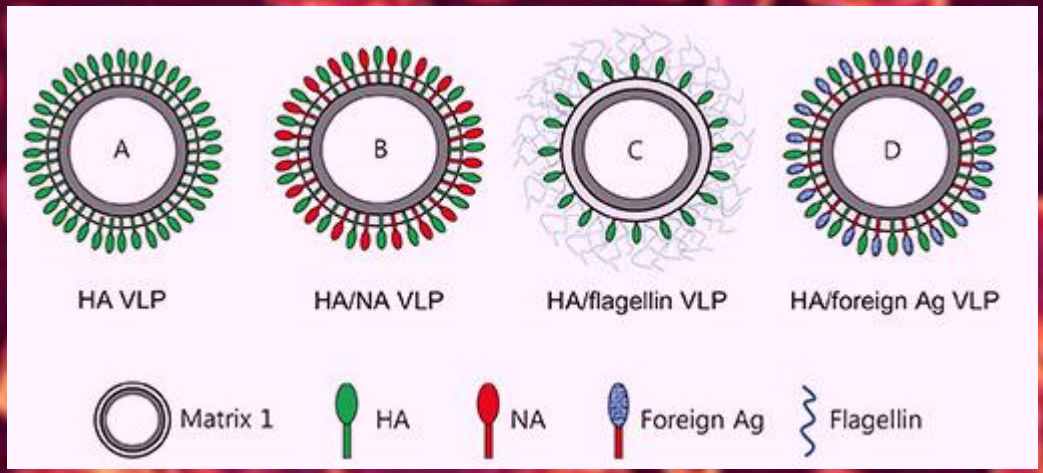

Virus-like particles mimic a natural virus in size, structure and surface protein but do not have the RNA necessary for infection. They trigger an immune response as if a natural infection takes place.

Sari-Ak D, Mol Biol. 2019;2025:213-226 Pushko P, Viruses. 2020;12(5):518. Clin Exp Vaccine Res. 2014 Jul;3(2):133-139.

Influenza Virus-like Particles

Vaccine platform using influenza VLP-based delivery of SARS-CoV-2 RBD protein in combination with cytokine adjuvants to develop hybrid vaccines.

Influenza virus-like particle-based hybrid vaccine containing RBD induces immunity against influenza and SARS-CoV-2 viruses Ramireddy Bommireddy, et a;l. bioRxiv 2022.02.01.478657;

Virus-like particles mimic a natural virus in size, structure and surface protein but do not have the RNA necessary for infection. They trigger an immune response as if a natural infection takes place.

VLP: a worthy platform to produce vaccine against SARS-CoV-2

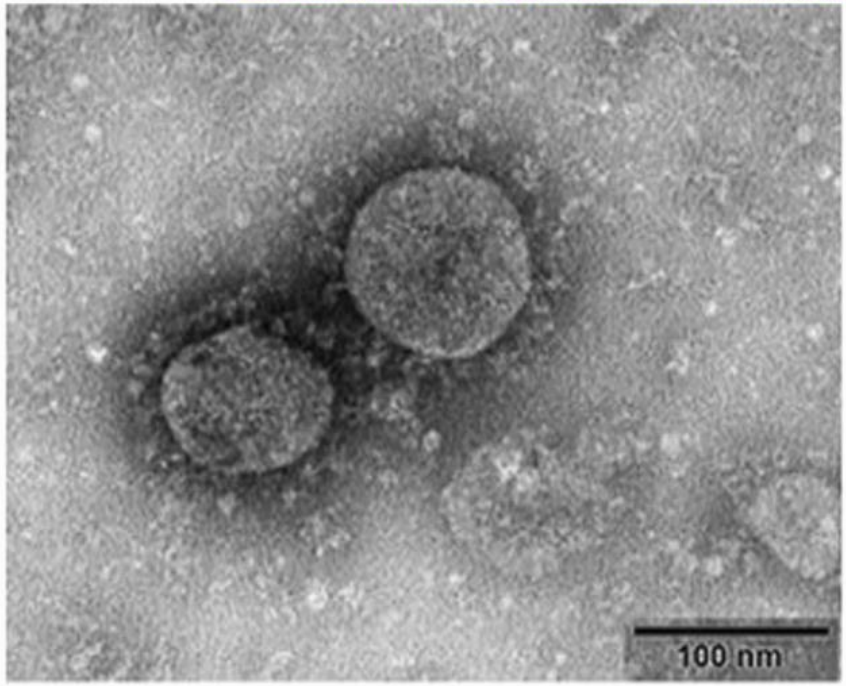

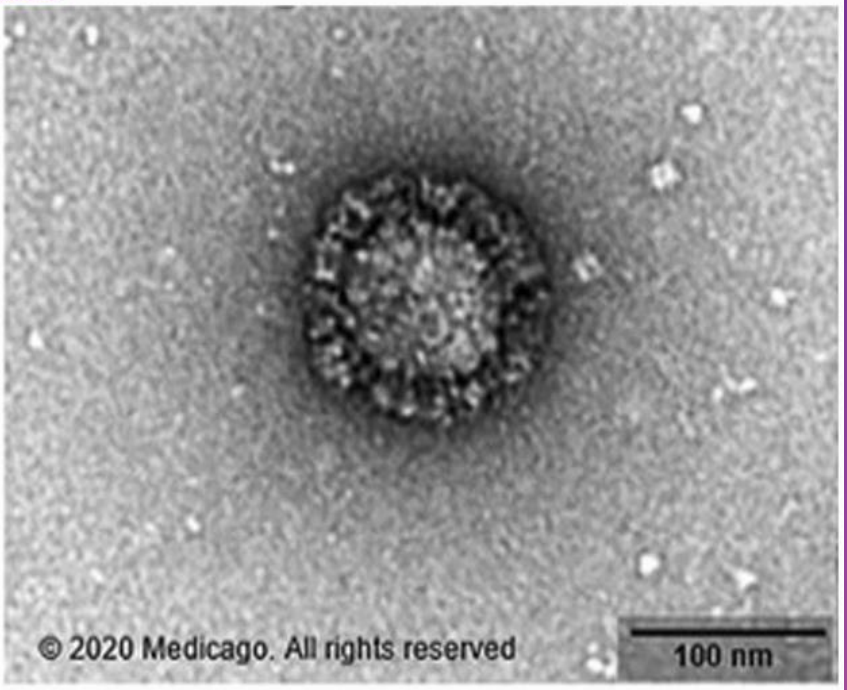

Comparison of SARS-CoV-2 VLP made by Medicago with wild-type SARS-CoV-2 (Ward et al., 2021) https://www.medicago.com/en/).

VLP (HA, NA, M1 protein)

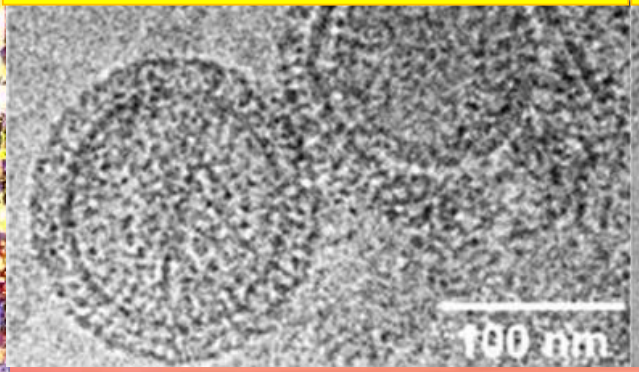

A/H3N2 influenza virus

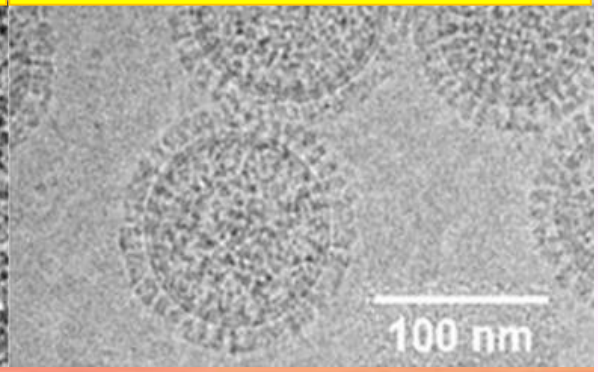

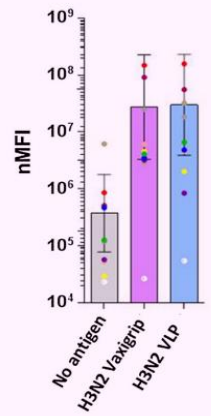

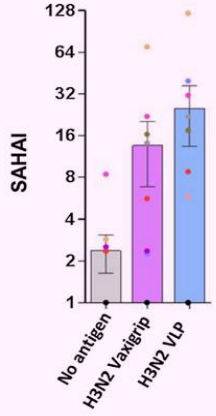

Hemmati, F., Hemmati-Dinarvand, M., Karimzade, M. et al. Plant-derived VLP: a worthy platform to produce vaccine against SARS-CoV-2. Biotechnol Lett 44, 45–57 (2022).
Buffin S, et al. Vaccine. 2019 Oct 31;37(46):6857-6867.

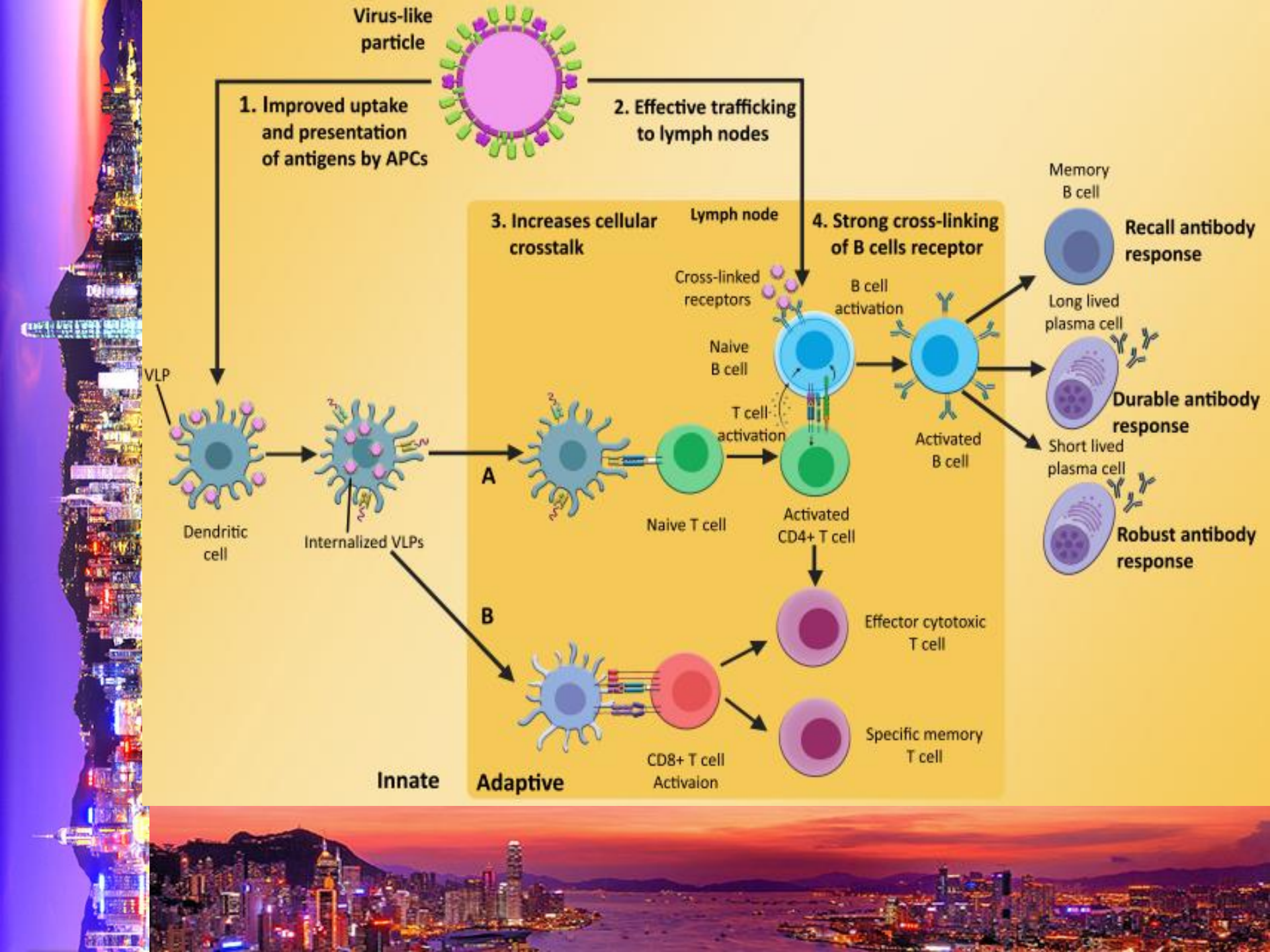
Virus-like particle
1. Improved uptake and presentation of antigens by APCs
2. Effective trafficking to lymph nodes
3. Increases cellular crosstalk
Lymph node
4. Strong cross-linking of B cells receptor
Cross-linked receptors
B cell activation
Naive B cell
T cell activation
Activated B cell
Memory B cell
Recall antibody response
Long lived plasma cell
Durable antibody response
Short lived plasma cell
Robust antibody response
VLP
Dendritic cell
Internalized VLPs
A
Naive T cell
Activated CD4+ T cell
B
Effector cytotoxic T cell
Specific memory T cell
CD8+ T cell Activaion
Innate
Adaptive

VLP vaccines

Non-infectious

Safe for immune-compromised individuals

Fast manufacturing process

More stable than other subunit vaccines

No allergens

High yield

No risk of mutation due to lack of genetic material

V S

Conventional vaccines

Reversion to virulent form

Toxicity

Lengthy formulation time

Stability issues

Risk of allergic response

Low yield

Mutation risks

Virus-like particle (VLP) is a self-assembled nanostructure incorporating key viral structural proteins. VLP resembles molecular and morphological features of authentic viruses but is non-infectious and non-replicating due to lack of genetic materials.

Virus-Like Particles: Revolutionary Platforms for Developing Vaccines Against Emerging Infectious Diseases Hasnat Tariq Front. Microbiol., 03 January 2022
Construction of SARS-CoV-2 Virus-Like Particles by Mammalian Expression System Ruodan Xu, et al. Front. Bioeng. Biotechnol., 30 July 2020

Expression Systems for VLP Production

Expression systems	Bacteria	Yeast	Insect cells	Mammalian cells	Plant cells
	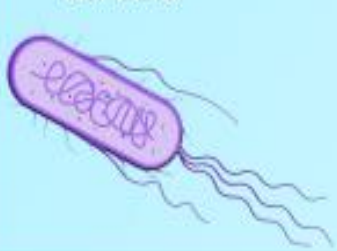			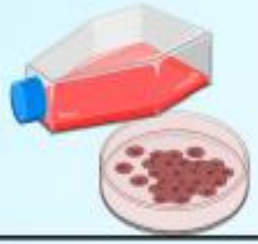	
Advantages	• Cost-effective • Scalable • Rapid growth • Easy manipulation • High-level expression • Genetic stability	• Low production cost • No endotoxins contamination • High-density fermentation • Support most protein folding	• Carry and deliver large amount of DNA • High protein expression • Support eukaryotic protein PTMs • Proper protein folding and assembly	• Perform proper folding, assembly, and PTMs of proteins	• Highly scalable • Cost-effective • Carry out N-glycosylation • High expression • Correct folding and assembly
Limitations	• Poor immunogenicity • Recombinant proteins lack PTMs • Protein solubility issues • Contamination by bacterial endotoxins • Inability to create di-sulfide bonds	• Vlp yield lower than E. coli • High mannose modification • Lack mammalian like PTMs	• Difficult to scale up • High production cost • Baculoviruse contamination • Simpler N-glycosylation than mammalian cells • Incomplete modification of proteins	• Require large-scale production facilities • Lengthy expression time • Low yield • Contamination by mammalian pathogens	• Low yield than mammalian cells • Technical and regulatory issues

Thank you for your attention

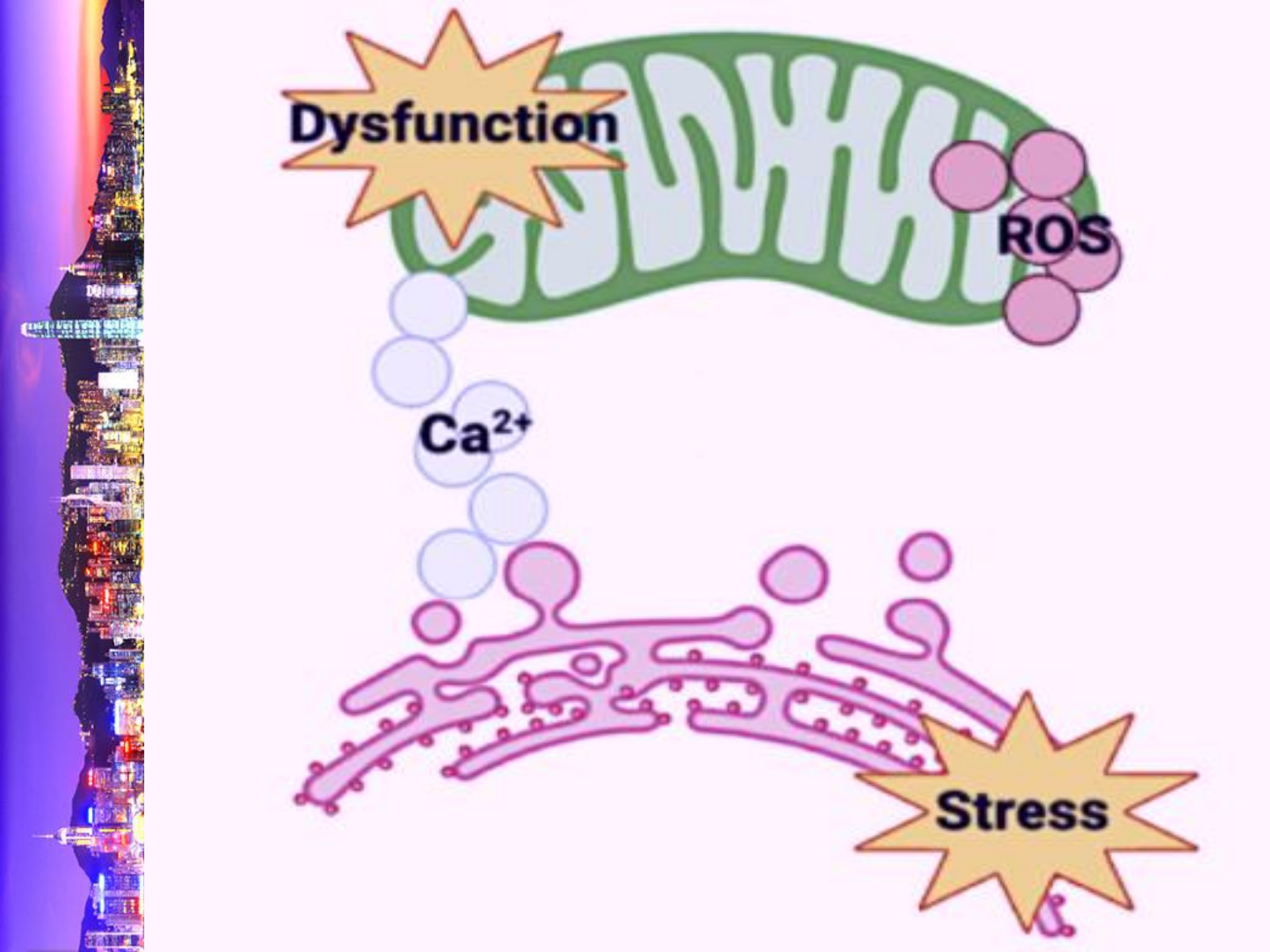
Dysfunction
ROS
Ca2+
Stress

Influenza Cytokine Dysregulation

IL-1β/IL18 => Ferritin

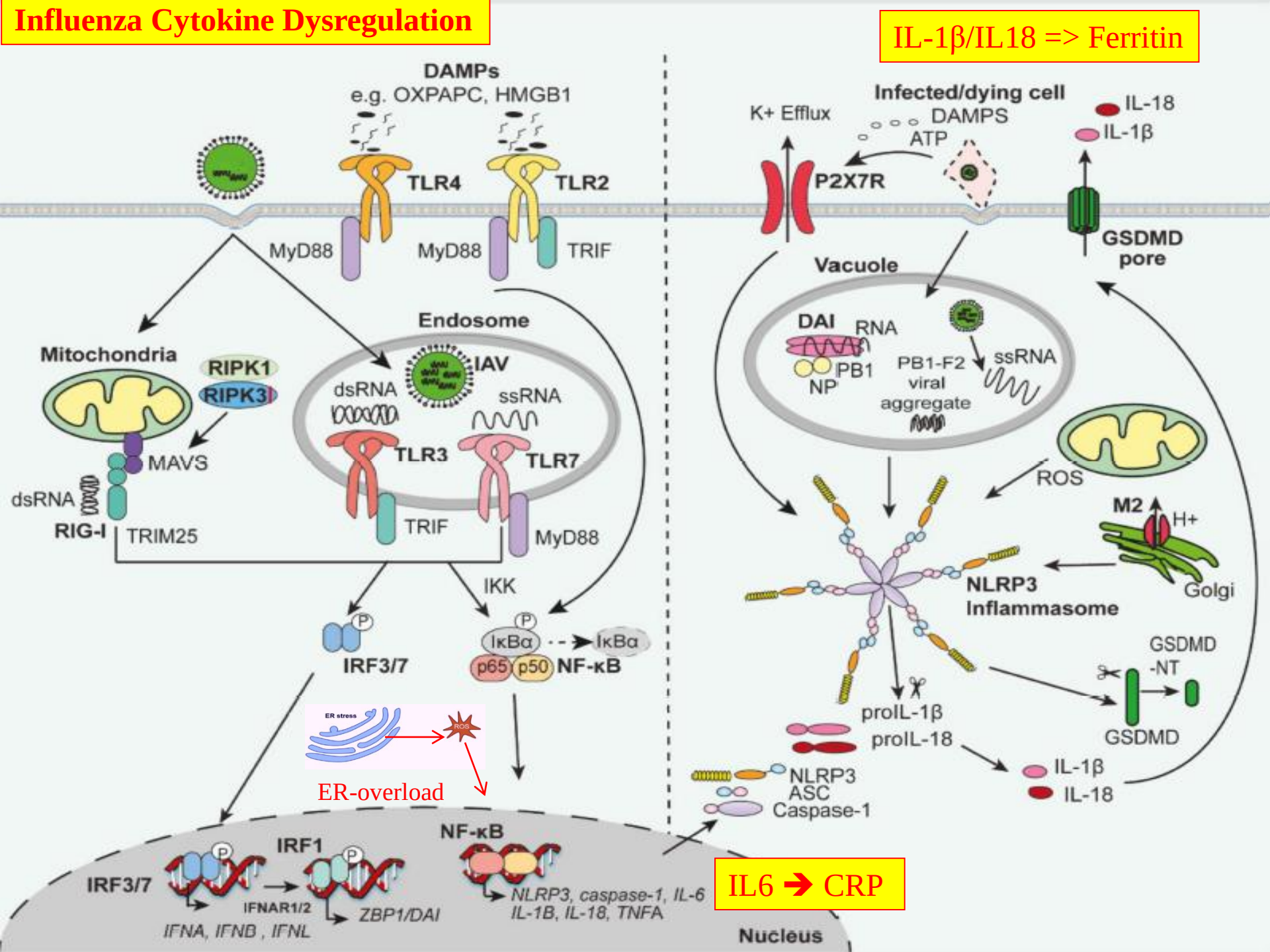

IL6 ➔ CRP

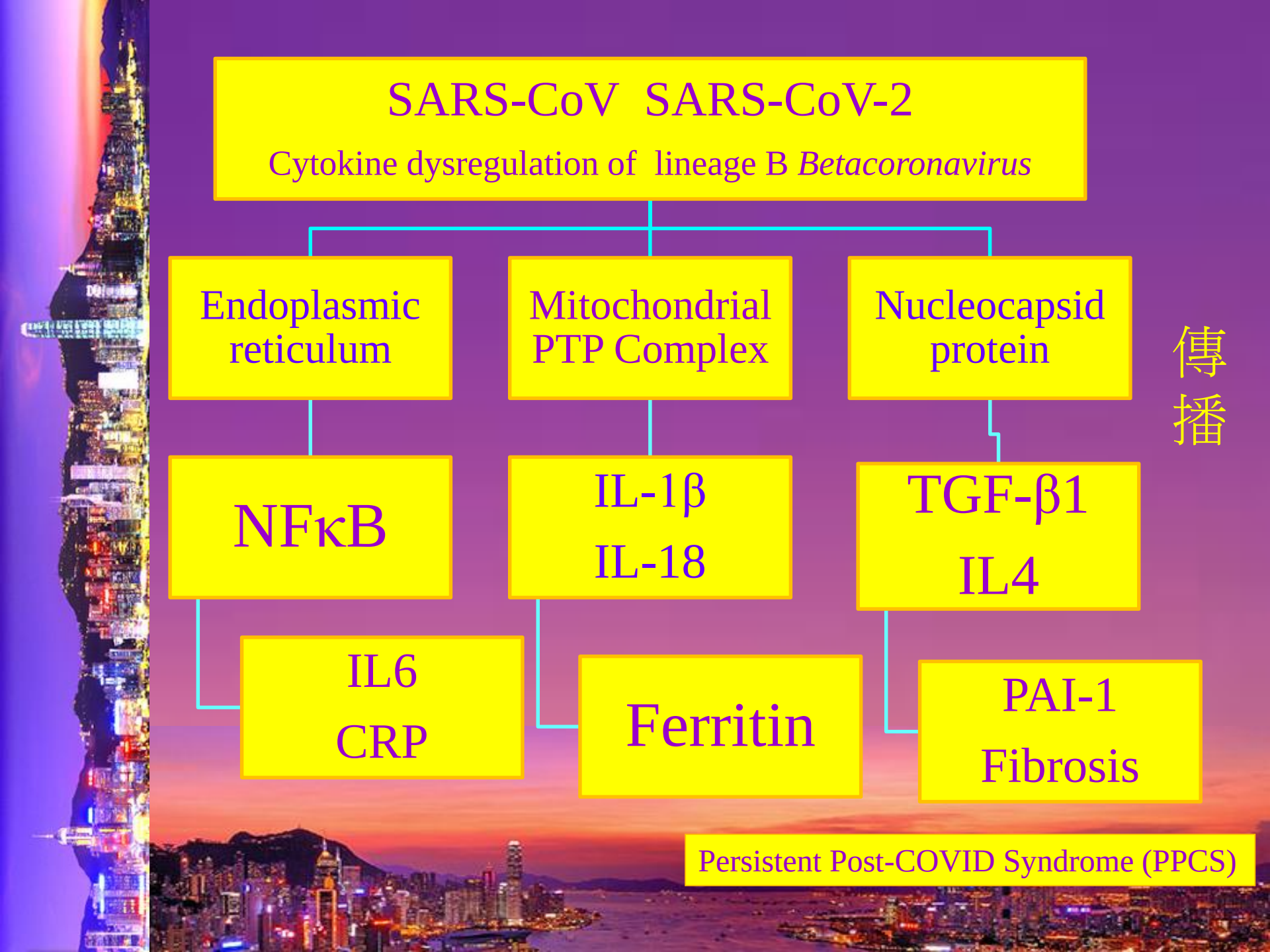
SARS-CoV SARS-CoV-2
Cytokine dysregulation of lineage B *Betacoronavirus*
Endoplasmic reticulum
Mitochondrial PTP Complex
Nucleocapsid protein
傳播
NFκB
IL-1β
IL-18
TGF-β1
IL4
IL6
CRP
Ferritin
PAI-1
Fibrosis
Persistent Post-COVID Syndrome (PPCS)

Steroid
High dose NAC
IVIG
Niacinamide
Zinc
? Cyclosporin A

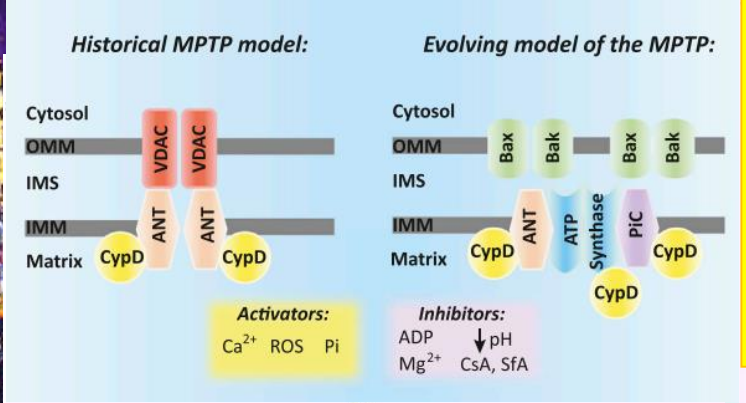

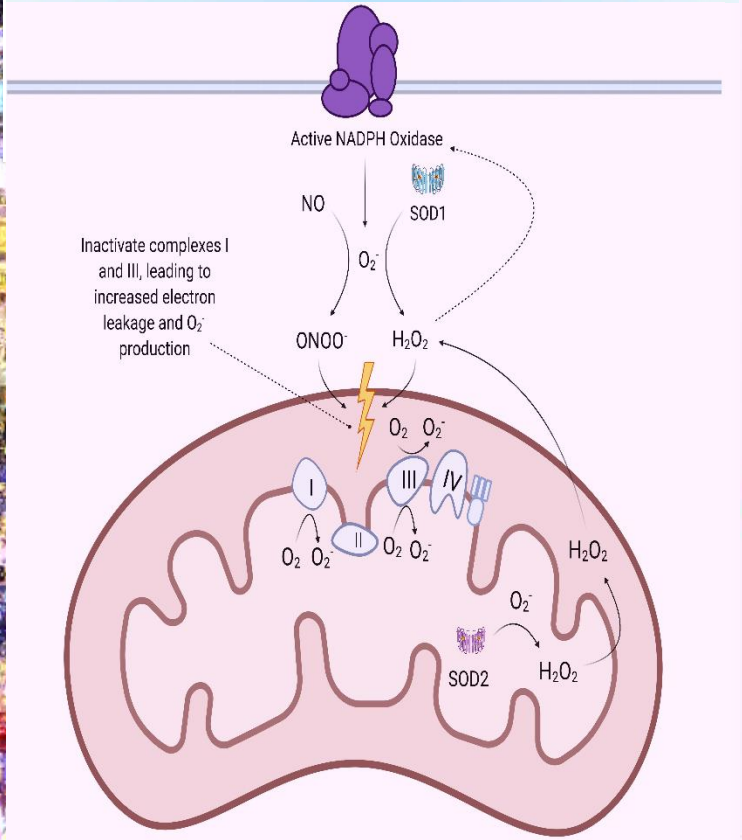

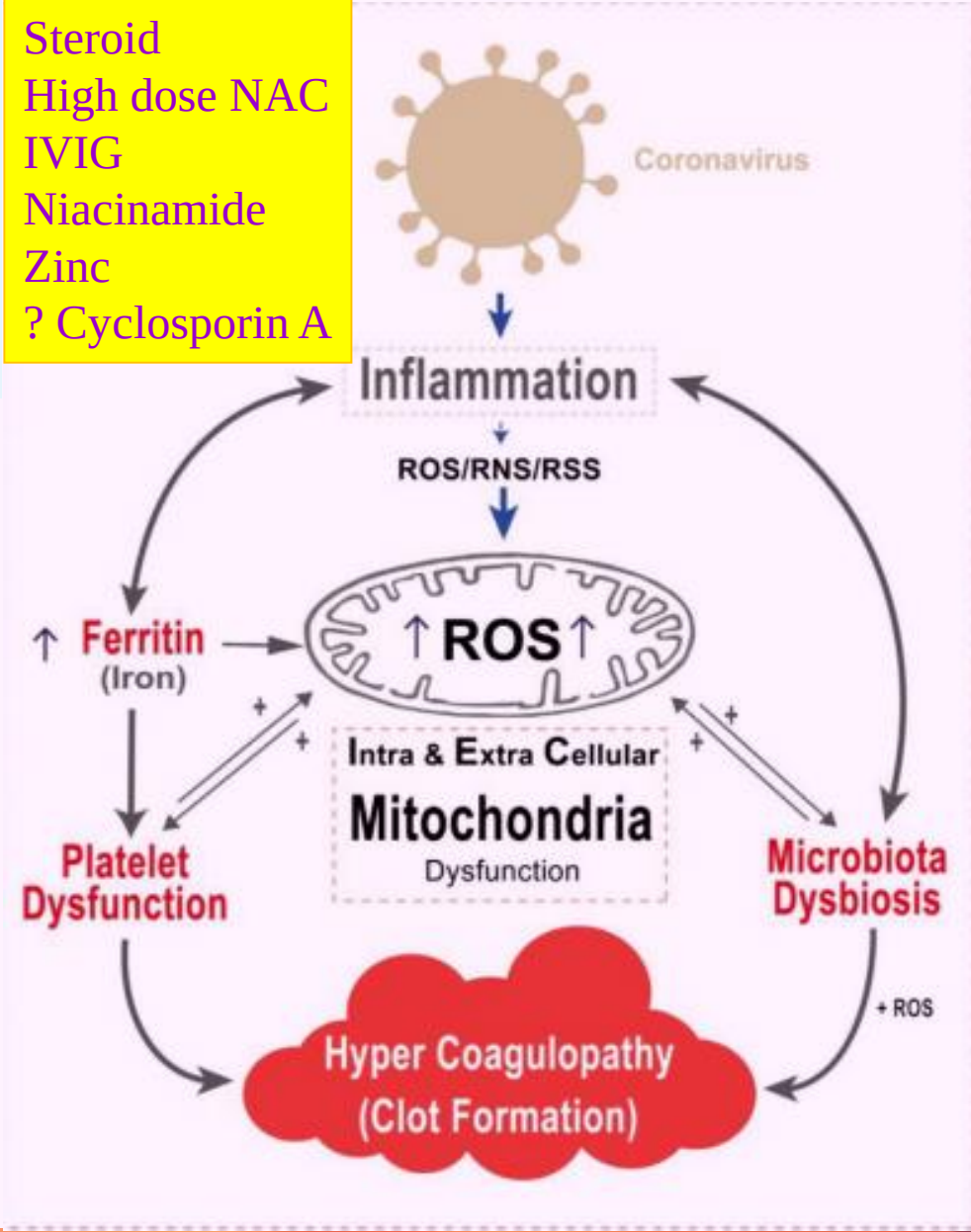

Saleh J, Peyssonnaux C, Singh KK, Edeas M. Mitochondria and microbiota dysfunction in COVID-19 pathogenesis. Mitochondrion. 2020 Sep;54:1-7.

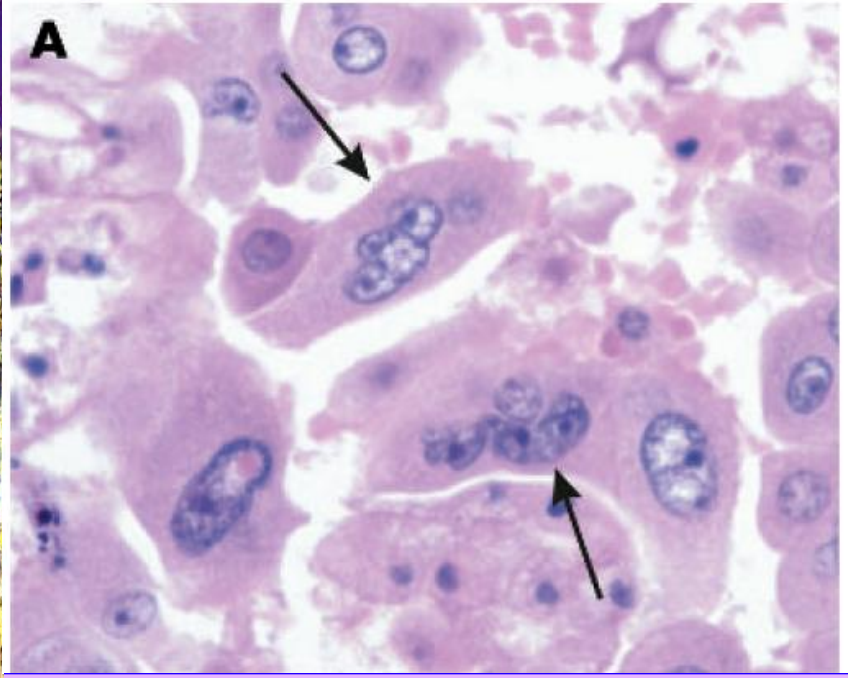

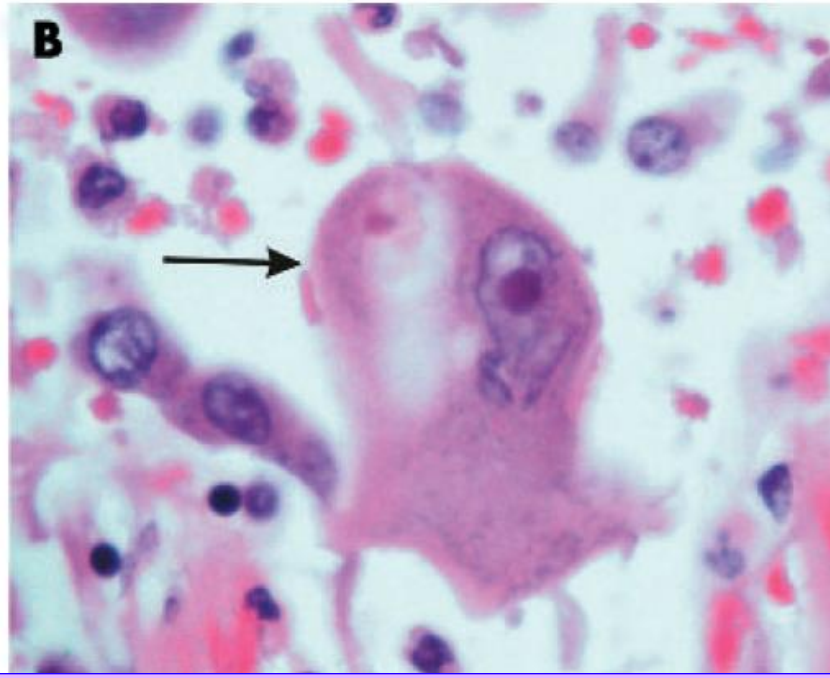

Summary of the pulmonary pathological features of patients with severe acute respiratory syndrome

	Patients						
	1	2	3	4	5	6	7
Atypical pneumocytes	+	+	+	+	+	+	+
Diffuse alveolar damage							
Pulmonary oedema	+++	+++	+++	+++	+++	+++	+++
Hyaline membrane	+	+++	+++	+++	++	++	++
Organising phase	+	+	++	++	++	++	++
Interstitial fibrosis	+	+	+	+	++	+++	++
BOOP-like	−	+	+	+	−	+	−
Pulmonary haemorrhage	−	−	++	−	+	++	−
Bronchopneumonic changes	−	+	+	−	−	+	−

+, mild; ++, moderate; +++, severe; −, not present.
BOOP-like, bronchiolitis obliterans organising pneumonia-like lesion.

J Clin Pathol. 2004 Mar; 57(3): 260–265.

Chin Med J (Engl). 2003 Sep;116(9):1283-7.

Dynamic changes in blood cytokine levels as clinical indicators in severe acute respiratory syndrome.

Beijing Group of National Research Project for SARS.

The mean concentration of serum **TGF-β1** in SARS patients was higher than that of the control group during all clinical courses. Although **TGF-β1** in serum decreased in remission and recovery stage in SARS patients, the average was still higher than that of the control group ($P < 0.01$).

Severe Acute Respiratory Syndrome-associated Coronavirus Nucleocapsid Protein Interacts with Smad3 and Modulates Transforming Growth Factor-β Signaling*

Received for publication, September 26, 2007, and in revised form, November 29, 2007 Published, JBC Papers in Press, November 30, 2007, DOI 10.1074/jbc.M708033200

Xingang Zhao[‡], **John M. Nicholls**[§], **and Ye-Guang Chen**[‡1]

From the [‡]*State Key Laboratory of Biomembrane and Membrane Biotechnology, Department of Biological Sciences and Biotechnology, Tsinghua University, Beijing 100084 and the* [§]*Department of Pathology, University of Hong Kong, Hong Kong, China*

SARS-CoV nucleocapsid (N) protein **inhibits apoptosis in favor of virus packaging and replication at the early stage of SARS development. N protein potentiates TGF-β1 induced PAI-1 expression leading to development of lung fibrosis at the late stage**. TGF-β downregulate the expression of extracellular matrix proteases and stimulate the expression of extracellular matrix protease inhibitors. PAI-1, which is the primary inhibitor of both tissue-type and urokinase-type plasminogen activator is a well established target of TGF-β via the Smad pathway and plays a pivotal role in TGF-β-promoted tissue fibrosis.

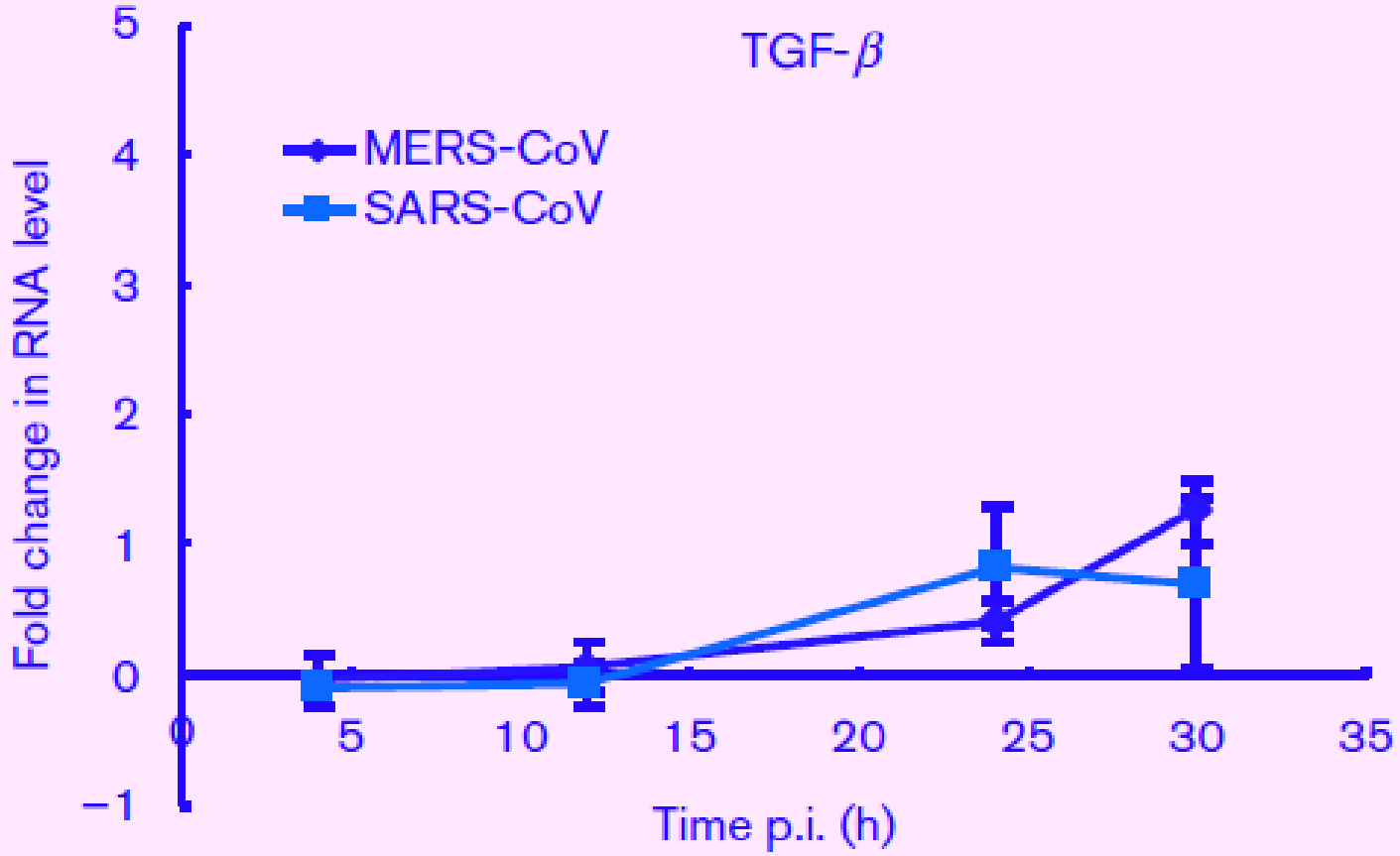

Journal of General Virology (2013), **94**, 2679–2690 DOI 10.1099/vir.0.055533-0

Delayed induction of proinflammatory cytokines and suppression of innate antiviral response by the novel Middle East respiratory syndrome coronavirus: implications for pathogenesis and treatment

Susanna K. P. Lau,[1,2,3,4] Candy C. Y. Lau,[4] Kwok-Hung Chan,[4] Clara P. Y. Li,[4] Honglin Chen,[1,2,3,4] Dong-Yan Jin,[5] Jasper F. W. Chan,[4] Patrick C. Y. Woo[1,2,3,4] and Kwok-Yung Yuen[1,2,3,4]

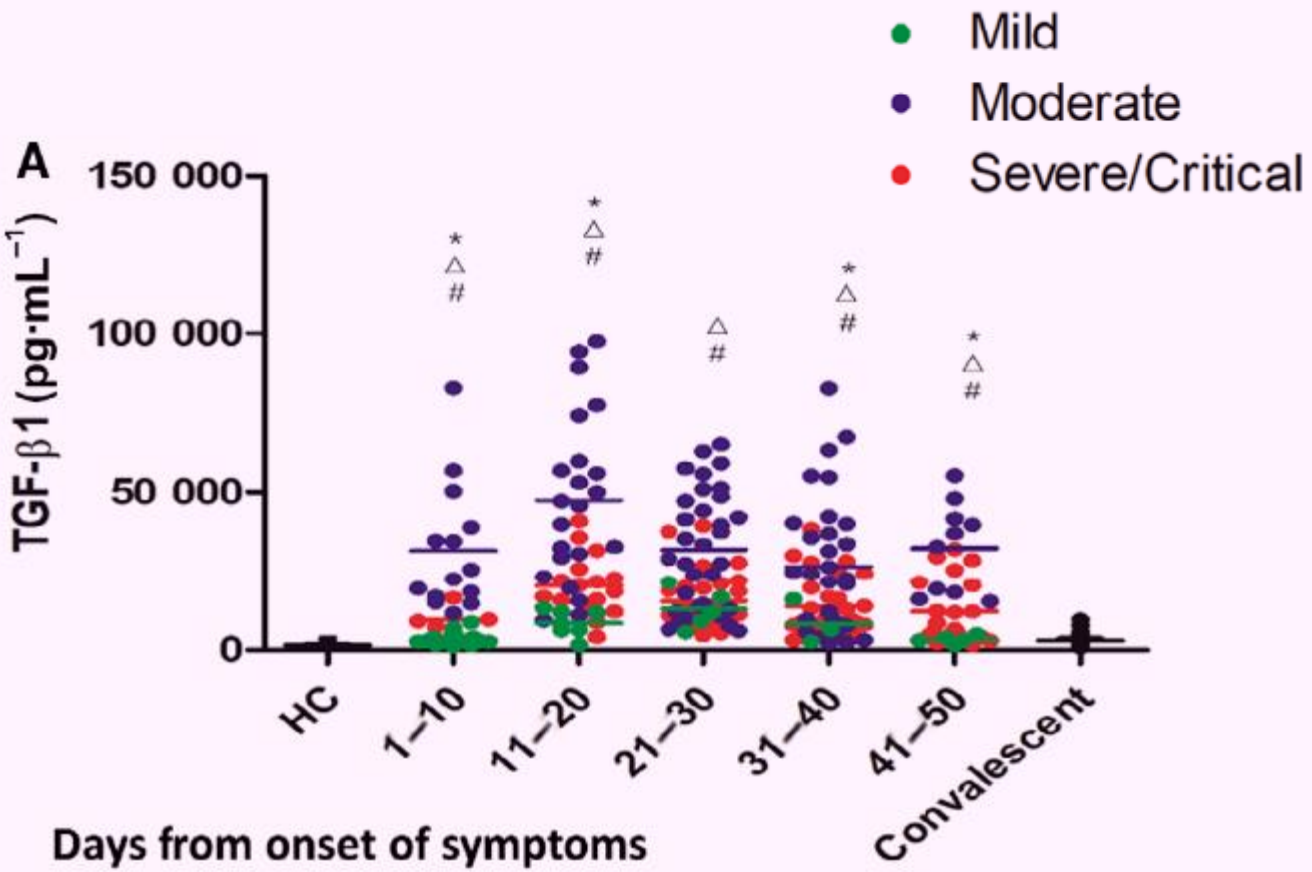

Mild	20	7	5	3	5	32
Moderate	14	22	32	30	10	
Severe	5	16	26	28	20	

Er-yi Wang et al.Serum levels of the IgA isotype switch factor TGF-β1 are elevated in patients with COVID-19 FEBS Letters Volume595, Issue13 July 2021

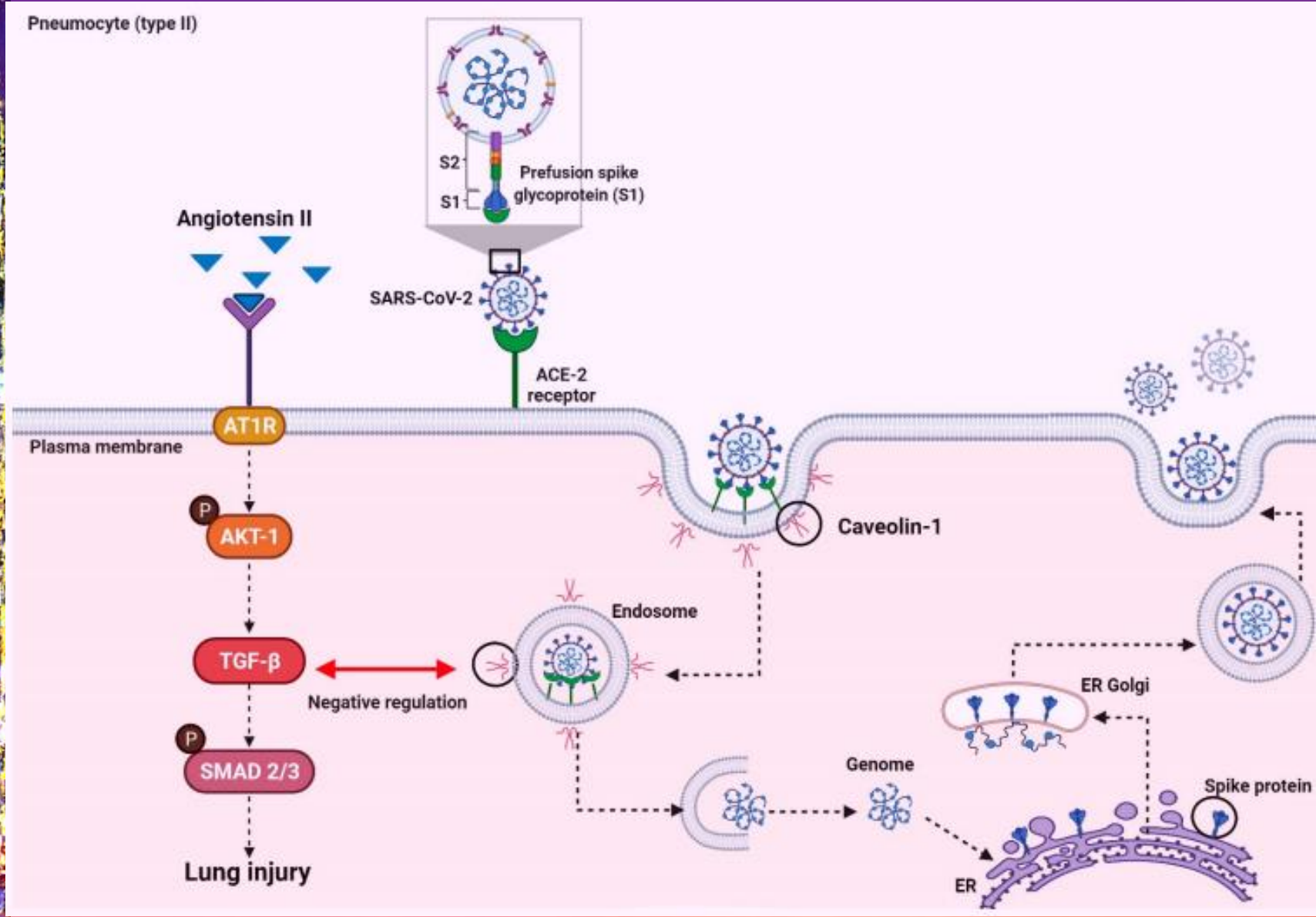

Vaz de Paula CB, et al. COVID-19: Immunohistochemical Analysis of TGF-β Signaling Pathways in Pulmonary Fibrosis. Int J Mol Sci. 2021 Dec 24;23(1):168

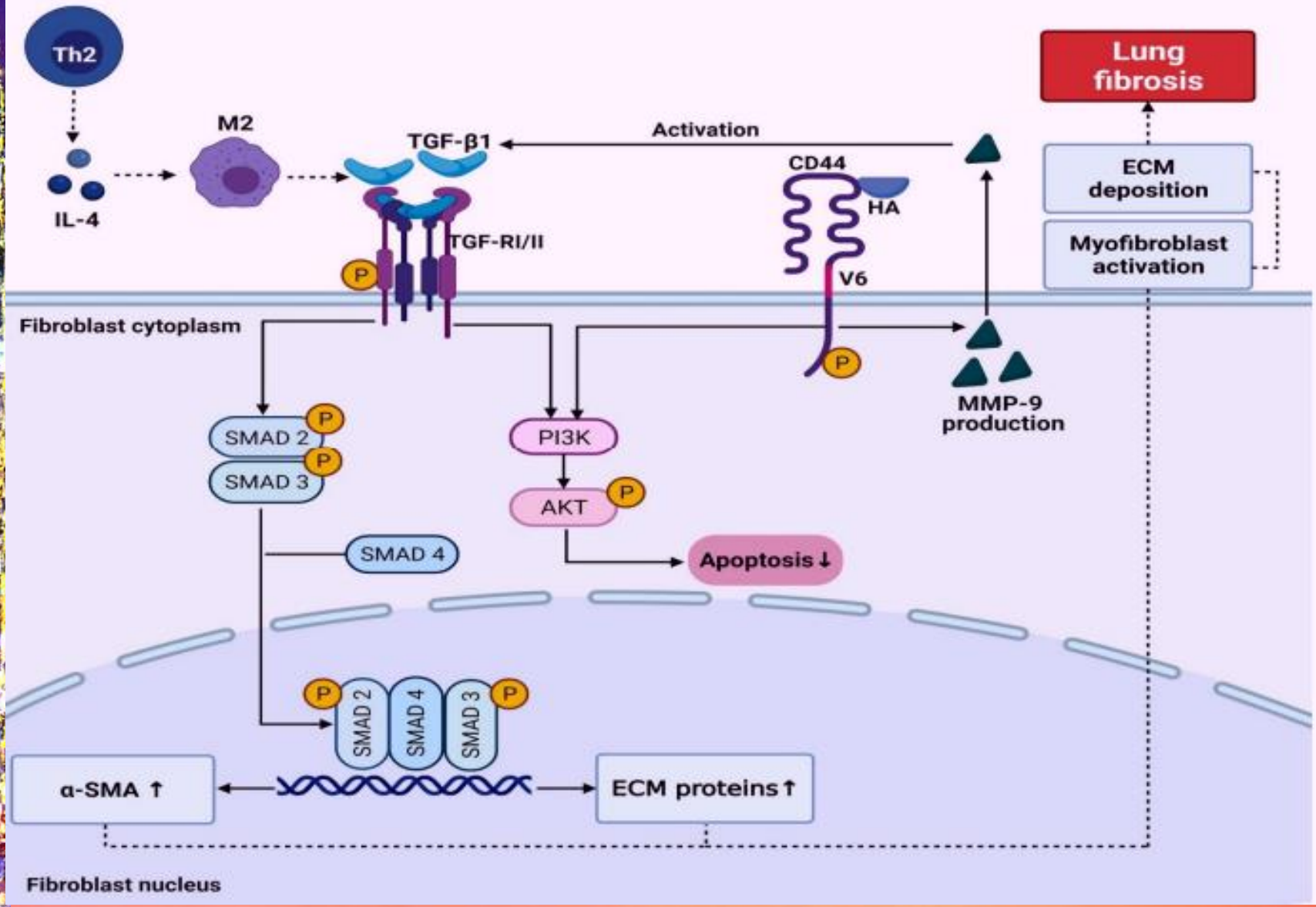

Vaz de Paula CB, et al. COVID-19: Immunohistochemical Analysis of TGF-β Signaling Pathways in Pulmonary Fibrosis. Int J Mol Sci. 2021 Dec 24;23(1):168.

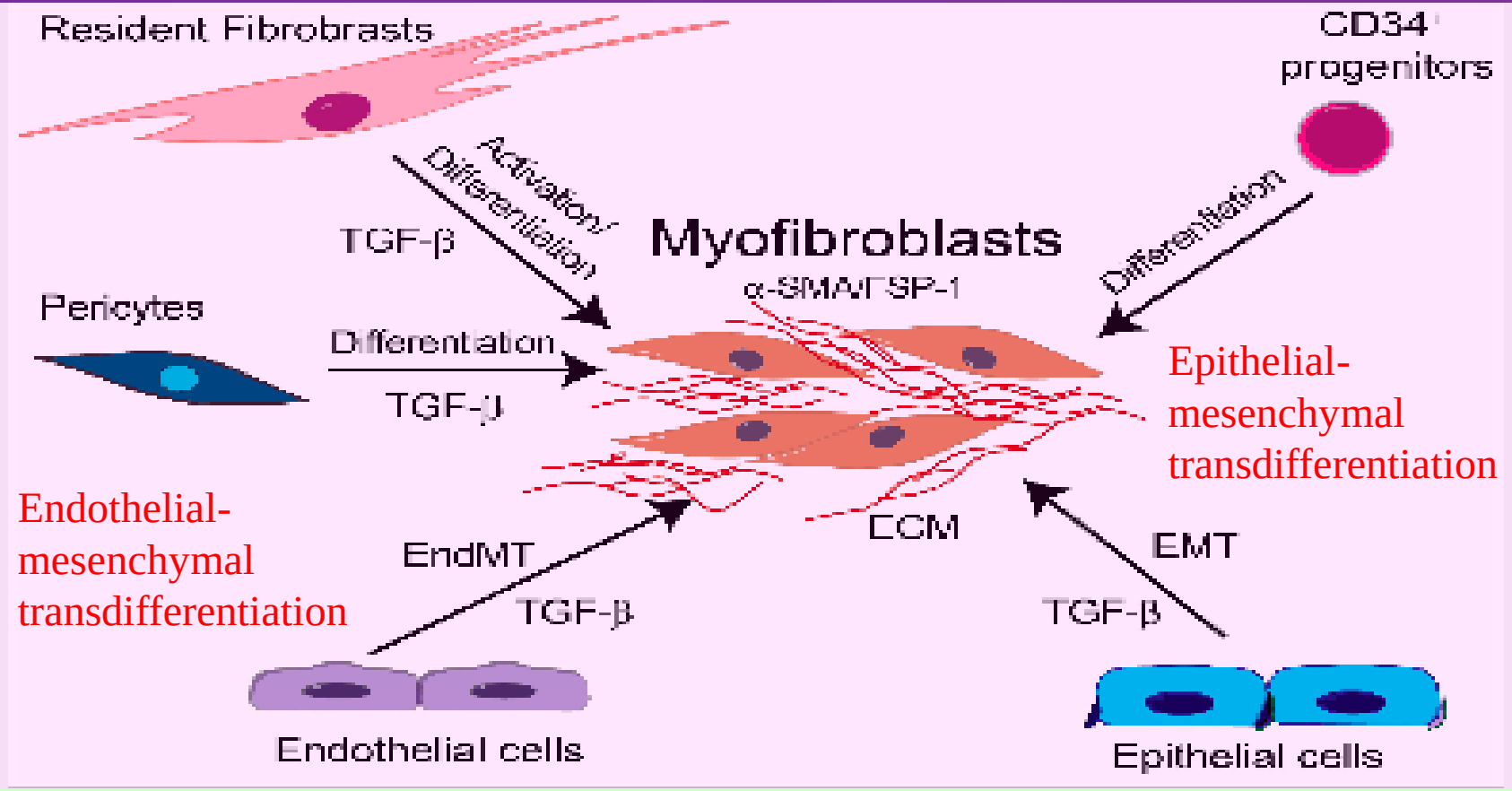

SARS-CoV-2 in severe COVID-19 induces a TGF-β-dominated chronic immune response that does not target itself Ferreira-Gomes et al. Nat Commun. 2021 Mar 30;12(1):1961

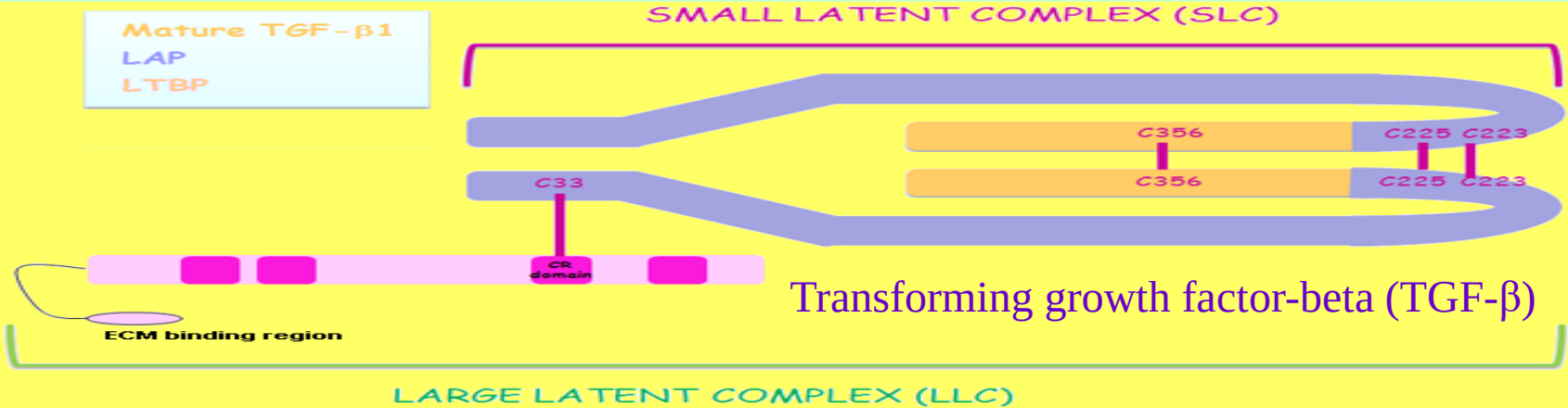

Transforming growth factor-beta (TGF-β)

TGF-β ? Role in Long COVID-19

- Before seroconversion in response to SARS-CoV-2 spike protein, peripheral plasmablasts display a type 1 interferon-induced gene expression signature; however, following seroconversion, plasmablasts lose this signature, express instead gene signatures induced by IL-21 and TGF-β, and produce mostly IgG1 and IgA1.
- In the sustained immune reaction from COVID-19 patients, plasmablasts shift to the expression of IgA2, thereby reflecting an instruction by TGF-β. Despite their continued presence in the blood, plasmablasts are not found in the lungs of deceased COVID-19 patients, nor does patient IgA2 binds to the dominant antigens of SARS-CoV-2.
- The results thus suggest that, in severe COVID-19, SARS-CoV-2 triggers a chronic immune reaction that is instructed by TGF-β, and is distracted from itself.

Ferreira-Gomes, M., *et al.* SARS-CoV-2 in severe COVID-19 induces a TGF-β-dominated chronic immune response that does not target itself. *Nat Commun* **12,** 1961 (2021).

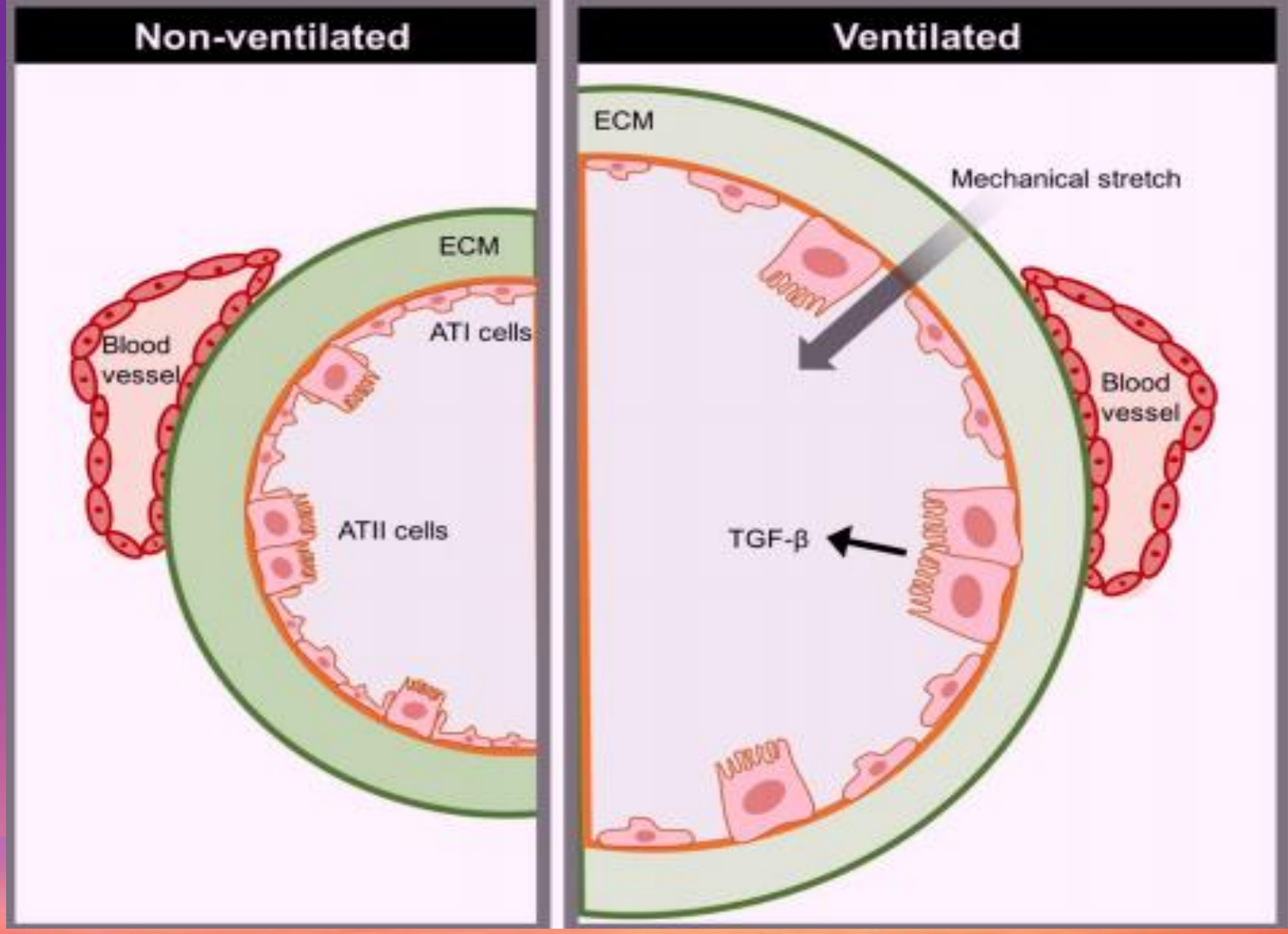

Oronsky B, Larson C, Hammond TC, Oronsky A, Kesari S, Lybeck M, Reid TR. A Review of Persistent Post-COVID Syndrome (PPCS). Clin Rev Allergy Immunol. 2021 Feb 20:1–9. doi: 10.1007/s12016-021-08848-3.

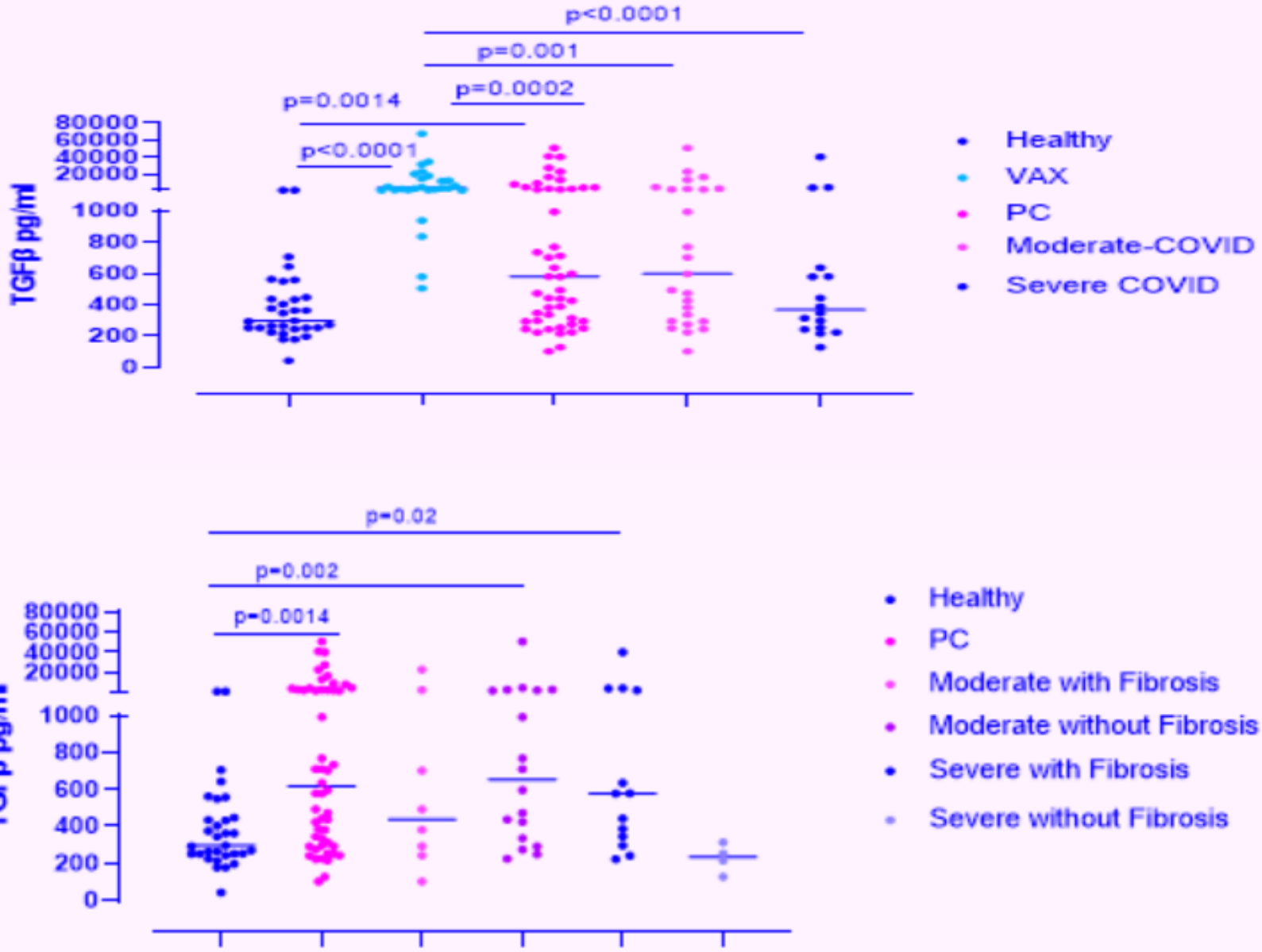

Post-COVID-19 Patients Who Develop Lung Fibrotic-like Changes Have Lower Circulating Levels of IFN-β but Higher Levels of IL-1α and TGF-β.

Colarusso C, et al. Biomedicines. 2021 Dec 17;9(12):1931.

Zinc

Enhanced re-epithelialization of respiratory epithelium

Pentoxifylline (NFkB/TNF-α inhibitor)

Transforming growth factor-beta (TGF-β)
Inhibit both fibroblast proliferation
Inhibit collagen synthesis

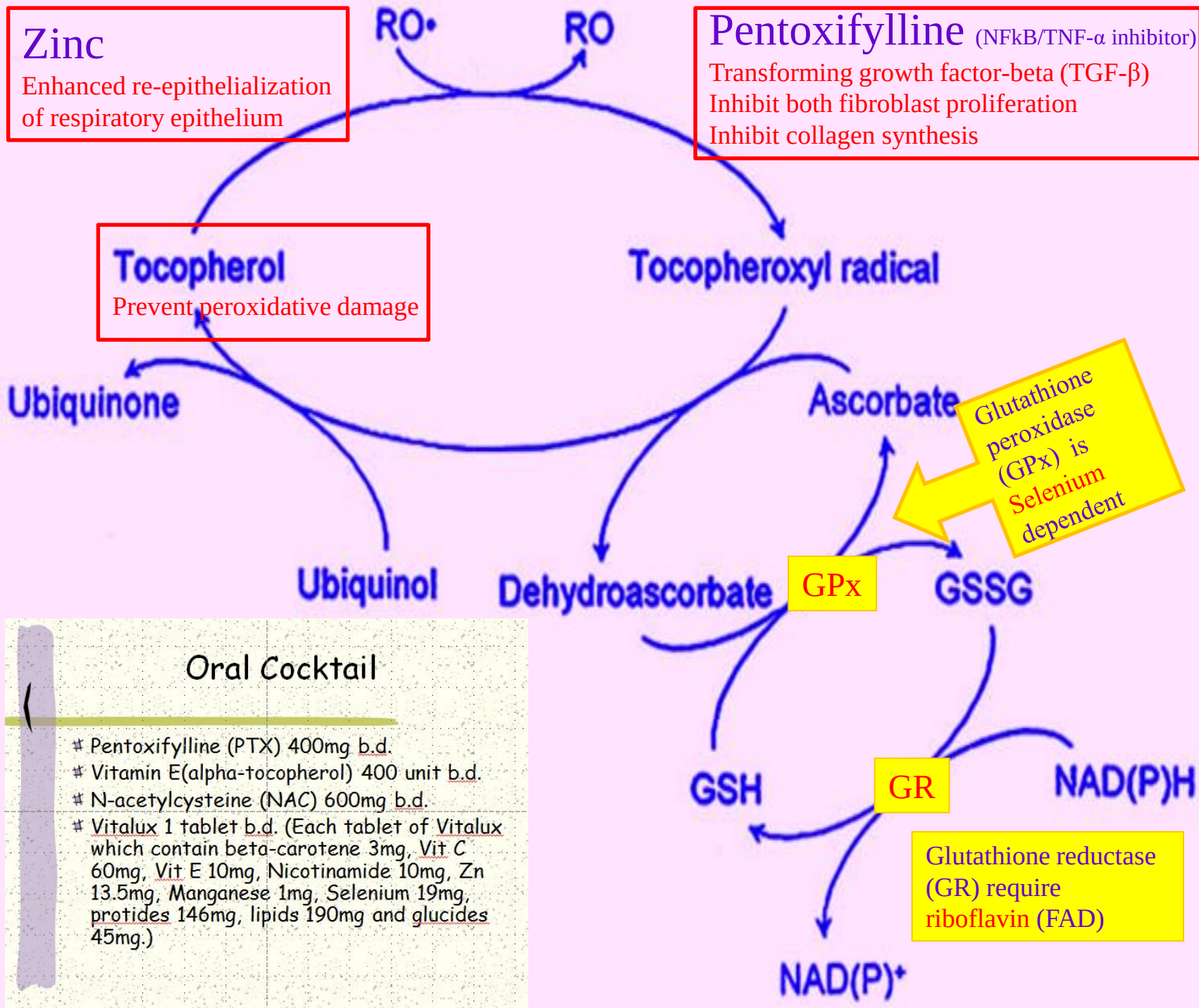

Oral Cocktail

- Pentoxifylline (PTX) 400mg b.d.
- Vitamin E(alpha-tocopherol) 400 unit b.d.
- N-acetylcysteine (NAC) 600mg b.d.
- Vitalux 1 tablet b.d. (Each tablet of Vitalux which contain beta-carotene 3mg, Vit C 60mg, Vit E 10mg, Nicotinamide 10mg, Zn 13.5mg, Manganese 1mg, Selenium 19mg, protides 146mg, lipids 190mg and glucides 45mg.)

Any Questions ?

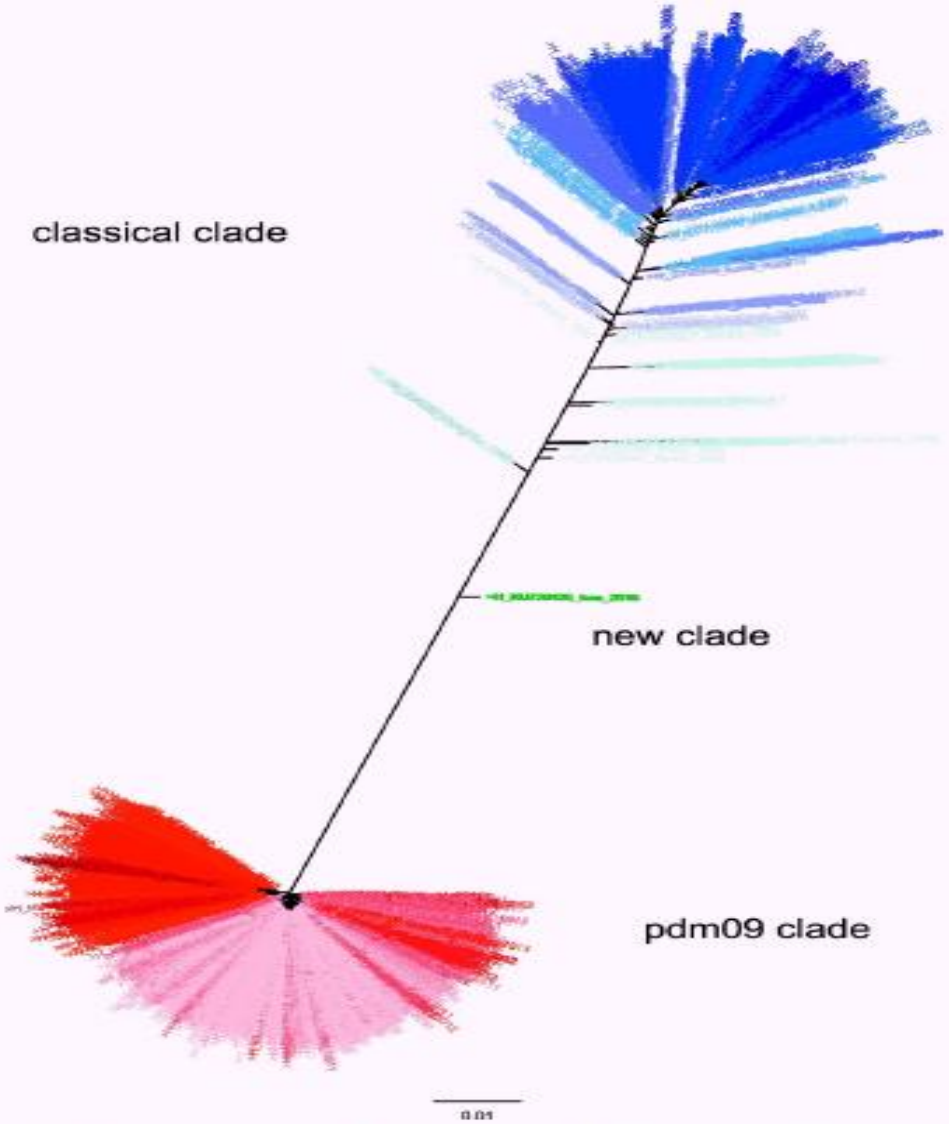

Fig. 1. Phylogenetic tree of HA genes in H1N1. The classical clade and the pdm09 clade are represented by blue and red, respectively. The new clade is green. Sequences in each clade isolated over time are coloured from light to dark.

We may be facing a new H1N1 influenza pandemic after COVID-19 panedmic

Novel antigenic shift in HA sequences of H1N1 viruses detected by big data analysis. Zhang R, Xu C, Duan Z. Infect Genet Evol. 2017:138-142.

Isolation And Quarantine Policy

ICU admission closely follow HSI case load except with a phase lag.

Confirmed HSI cases staying in ICU (from 27 Apr to 31 Oct 2009)

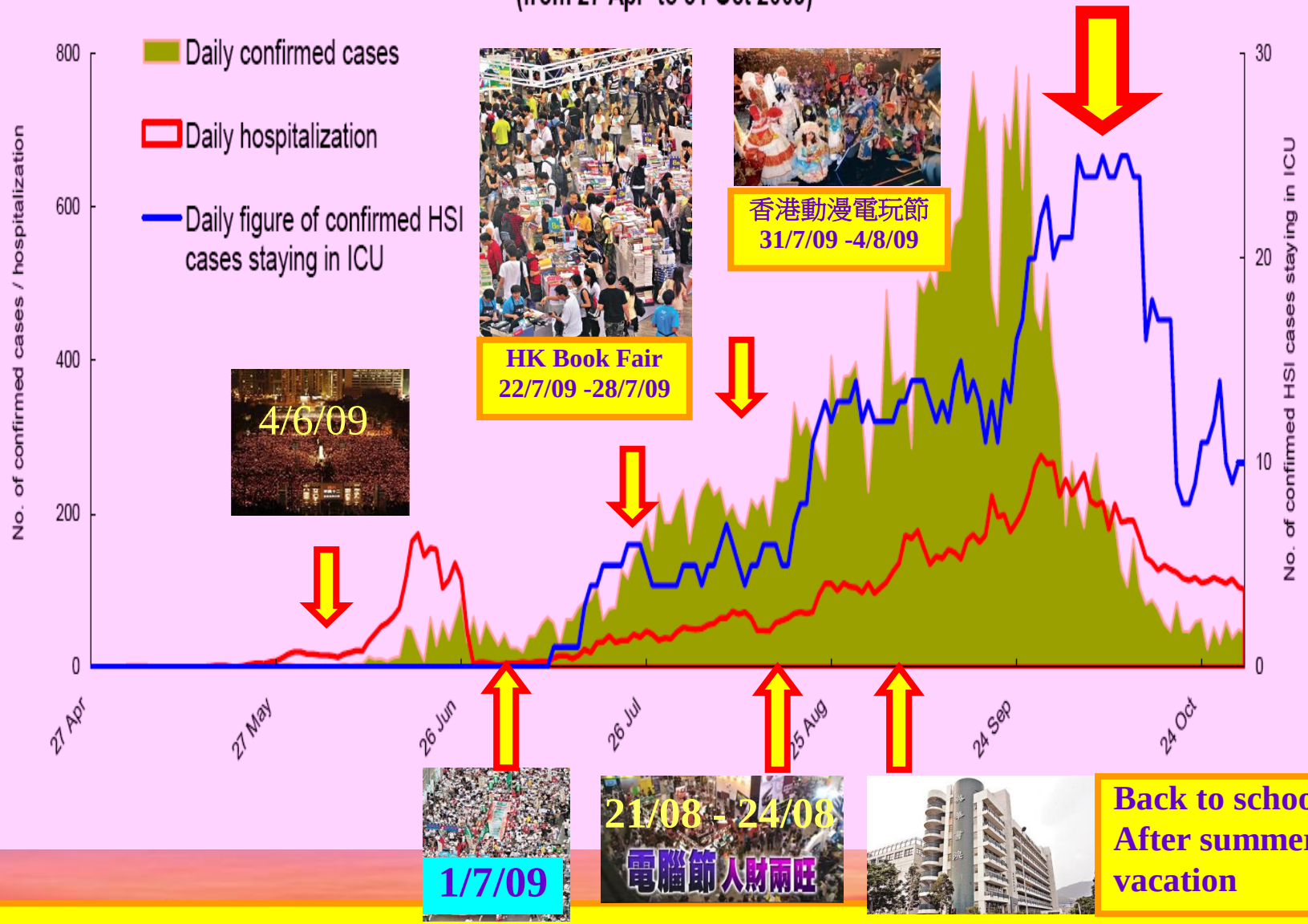

Disease Burden of novel H1N1 2009 to Hong Kong

First Wave ➔ Poor Mitigation Beyond Control of Government

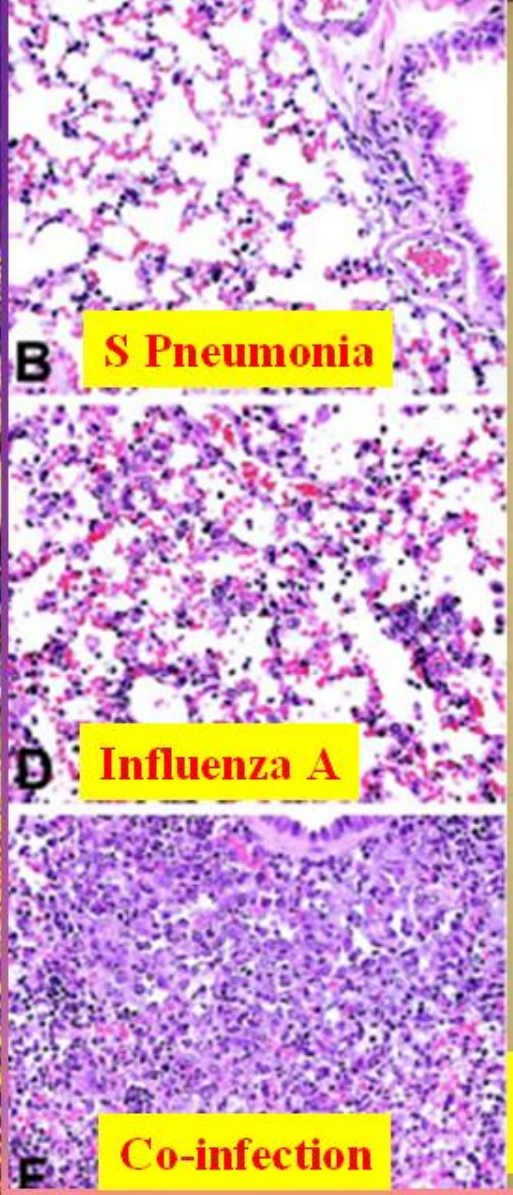
B
S Pneumonia
D
Influenza A
F
Co-infection

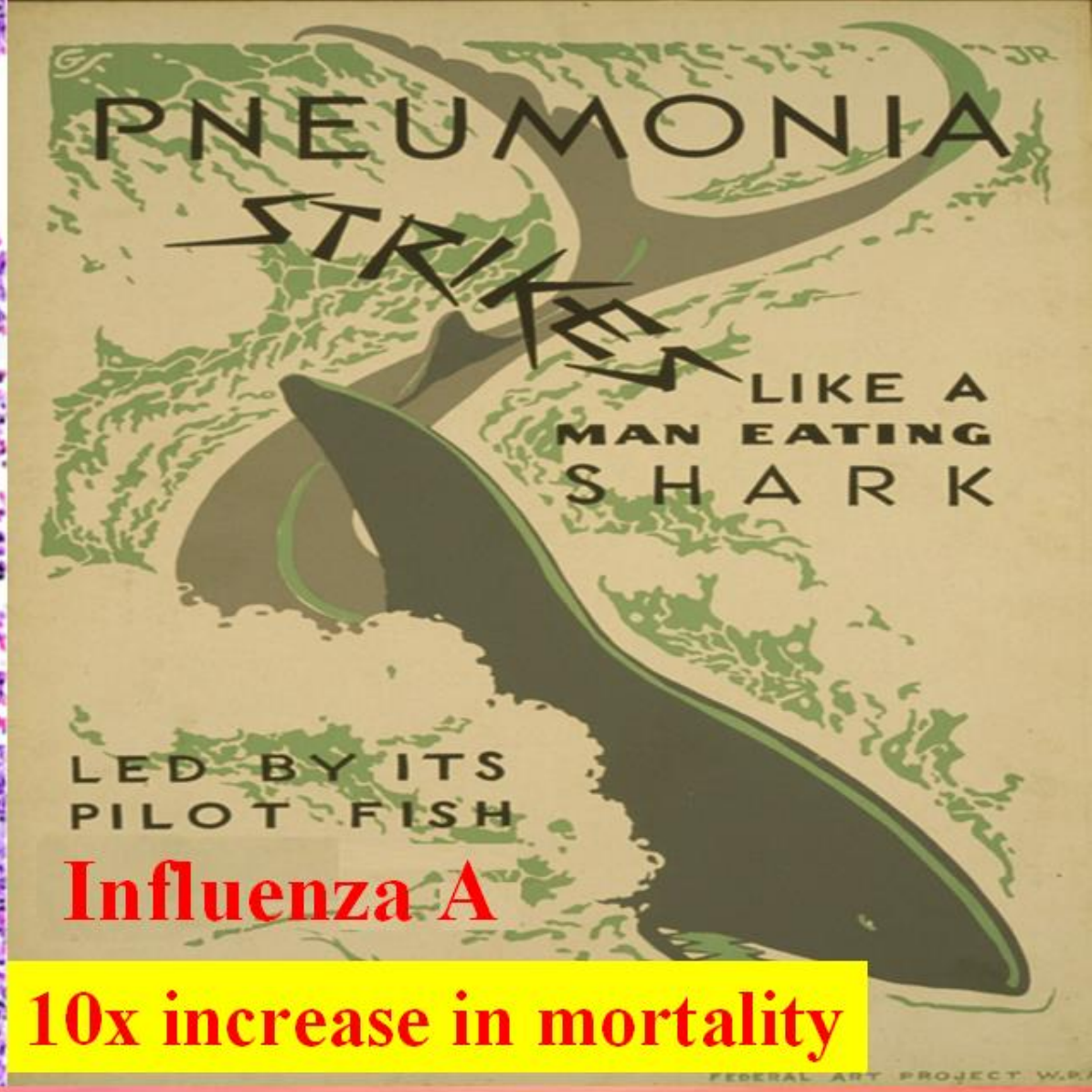
PNEUMONIA
STRIKES
LIKE A
MAN EATING
SHARK
LED BY ITS
PILOT FISH
Influenza A
10x increase in mortality
FEDERAL ART PROJECT W.P.A.

Hong Kong Childhood Immunisation Programme

AGE	Immunisation RECOMMENDED
Newborn	B.C.G. Vaccine Hepatitis B Vaccine - First dose
1 month	Hepatitis B Vaccine - Second dose
2 months	DTaP-IPV Vaccine - First Dose Pneumococcal Vaccine - First Dose
4 months	DTaP-IPV Vaccine - Second Dose Pneumococcal Vaccine - Second Dose
6 months	DTaP-IPV Vaccine - Third Dose Pneumococcal Vaccine - Third Dose Hepatitis B Vaccine - Third Dose
1 year	MMR Vaccine (Measles, Mumps & Rubella) - First Dose Pneumococcal Vaccine - Booster Dose
1 1/2 year	DTaP-IPV Vaccine - Booster Dose
Primary 1	MMR Vaccine (Measles, Mumps & Rubella) - Second Dose DTaP-IPV Vaccine - Booster Dose
Primary 6	dTap-IPV Vaccine - Booster Dose

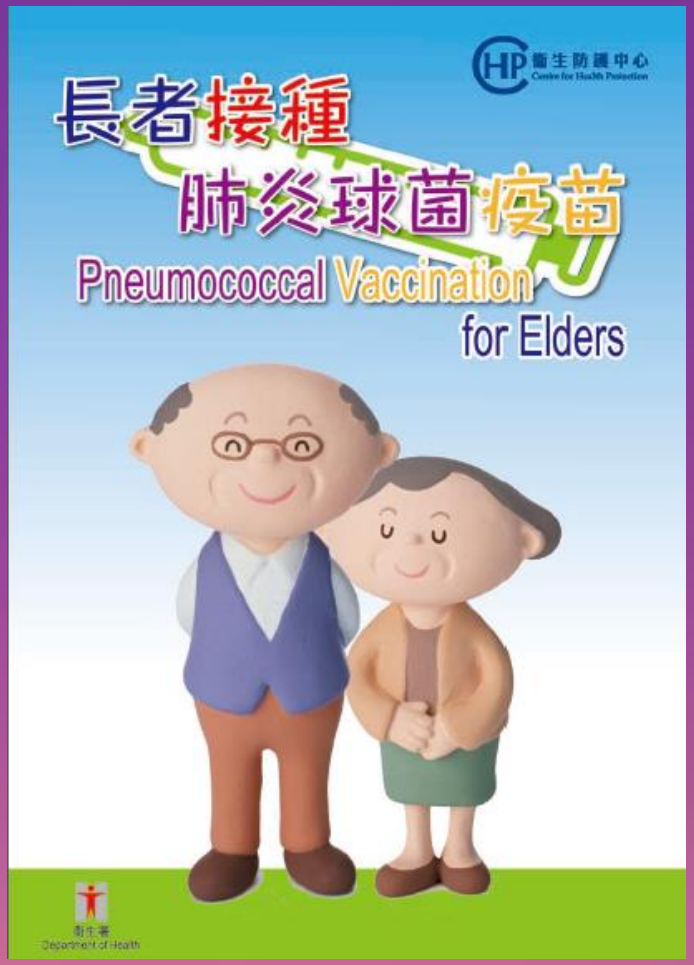

The Importance of Pneumococcal Vaccination

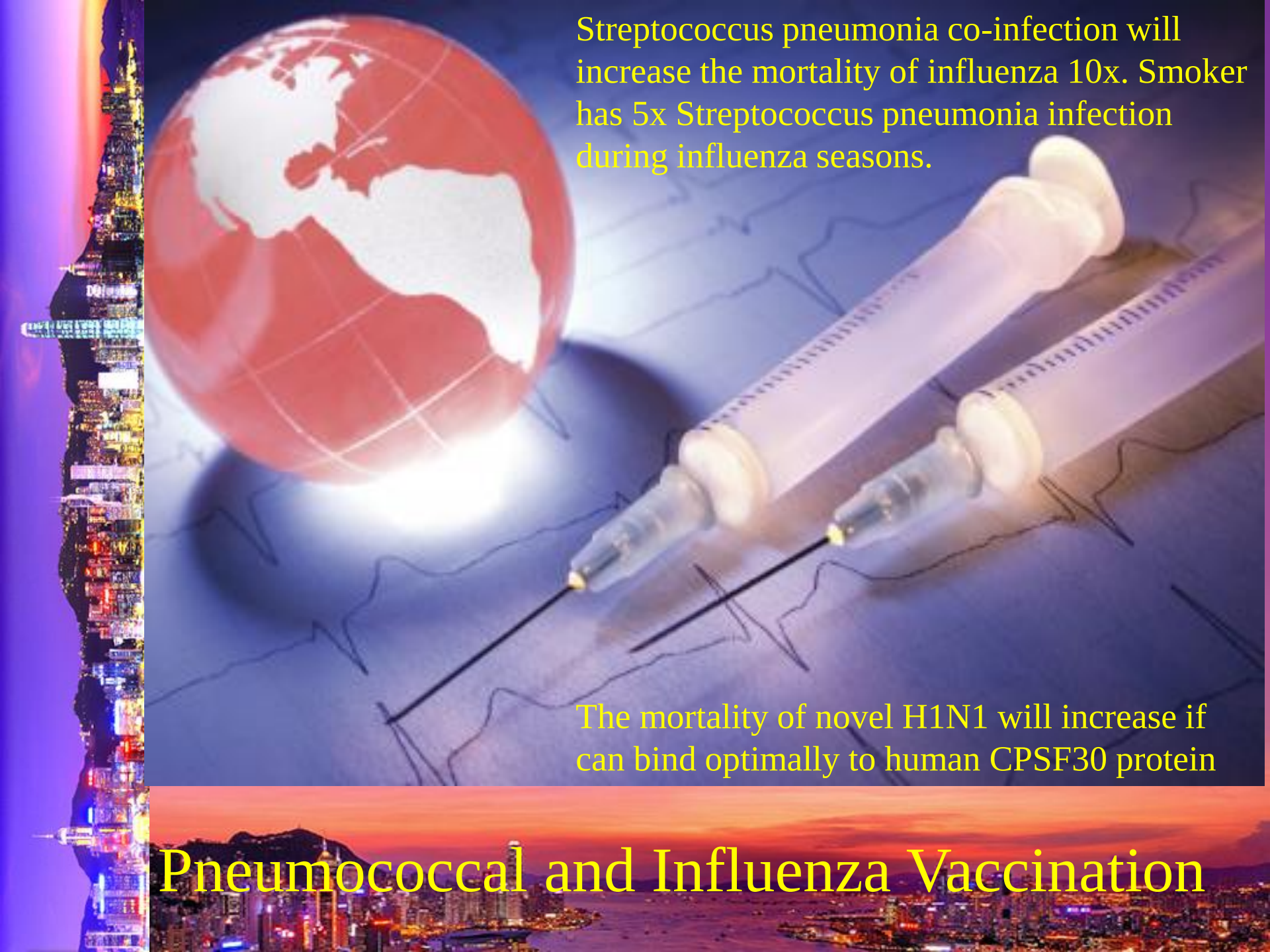

Streptococcus pneumonia co-infection will increase the mortality of influenza 10x. Smoker has 5x Streptococcus pneumonia infection during influenza seasons.

The mortality of novel H1N1 will increase if can bind optimally to human CPSF30 protein

Pneumococcal and Influenza Vaccination

fight the flu

use soap and water for 15-20 seconds

wash your hands

Thank you for your attention